MINISTRY OF EDUCATION AND SCIENCE UKRAINE

ODESSA I. I. MECHNIKOV NATIONAL UNIVERSITY

ФОТОЭЛЕКТРОНИКА

PHOTOELECTRONICS
INTER-UNIVERSITIES SCIENTIFIC ARTICLES

Founded in 1986

Number 24

ODESSA
ONU
2015

«PHOTOELECTRONICS»
№ 2 4 – 2 0 1 5

INTER-UNIVERSITIES SCIENTIFIC ARTICLES

Founded in 1986

Certificate of State Registration
KB № 15953

«ФОТОЭЛЕКТРОНИКА»
№ 24–2015

МЕЖВЕДОМСТВЕННЫЙ НАУЧНЫЙ СБОРНИК

Основан в 1986 г.

Свидетельство о Государственной регистрации
KB № 15953

UDC 621.315.592:621.383.51:537.221

The results of theoretical and experimental studies in problems of the semiconductor and micro-electronic devices physics, opto- and qantum electronics, quantum optics, spectroscopy and photophysics of nucleus, atoms, molecules and solids are presented in the issue. New directions in the photoelectronics, stimulated by problems of the super intense laser radiation interaction with nuclei, atomic systems and substance, are considered. Scientific articles «Photoelectronics» collection abstracted in ВИНИТИ and «Джерело»

Scientific articles «Photoelectronics» collection abstracted in ВИНИТИ and «ДЖЕРЕЛО»,and are in scientificmetric base INDEX COPERNICUS.

The issue is introduced to the List of special editions of the Ukrainian Higher Certification Com-mission in physics-mathematics and technical sciences.

For lecturers, scientists, post-graduates and students.

У збірнику наведено результати теоретичних і експериментальних досліджень з питань фізики напівпровідників та мікроелектронних приладів, опто- та квантової електроніки, квантової оптики, спектроскопії та фотофізики ядра, атомів, молекул та твердих тіл. Розглянуто нові напрямки розвитку фотоелектроніки, пов'язані із задачами взаємодії надінтенсивного лазерного випромінювання з ядром, атомними системами, речовиною.

Збірник включено до Переліку спеціальних видань ВАК України з фізико-математичних та технічних наук. Збірник «Photoelectronics» реферується у ВІНІТІ (Москва) та «Джерело» (Київ) і знаходиться у науковометричній базі INDEX COPERNICUS

Для викладачів, наукових працівників, аспіранітв, студентів

В сборнике приведены результаты теоретических и экспериментальных исследований по вопросам физики полупроводников и микроэлектронных приборов, опто- и квантовой электроники, квантовой оптики, спектроскопии и фотофизики ядра, атомов, молекул и твердых тел. Рассмотрены новые направ¬ления развития фотоэлектроники, связанные с задачами взаимодействия сверхинтенсивного лазерного излучения с ядром, атомными системами, веществом.

Сборник включен в Список специальных изданий ВАК Украины по физико-математическим и тех¬ническим наукам. Сборник «Photoelectronics» реферируется в ВИНИТИ (Москва) и «Джерело» (Киев) и находится в наукометричной базе INDEX COPERNICUS

Для преподавателей, научных работников, аспирантов, студентов

Address of editorial board:

Odessa I. I. Mechnikov National University 42, Pasteur str., Odessa, 65026, Ukraine
Information is on the site: http://phys.onu.edu.ua/journals/photoele/
http://experiment.onu.edu.ua/exp_ru/files/.

TABLE OF CONTENTS:

UDC 621.315.592

Yu. F. Vaksman, Yu. A. Nitsuk

I. I. Mechnikov Odesa National University
e-mail: nitsuk@onu.edu.ua

PHOTOCONDUCTIVITY AND PHOTOLUMINESCENCE OF ZnSe:Cr CRYSTALS IN THE VISIBLE SPECTRAL REGION

The photoconductivity and photoluminescence of ZnSe:Cr crystals in the visible spectra region are studied. The scheme of optical transitions within Cr2+ impurity centers is established. It is shown that the high-temperature impurity photoconductivity of ZnSe:Cr crystals is controlled by optical transitions of electrons from the 5T2(D) ground state to the higher levels of excited states of Cr2+ ions, with subsequent thermal activation of the electrons to the conduction band. Efficient excitation of intracenter luminescence of ZnSe:Cr crystals is attained with light corresponding to the region of intrinsic absorption in Cr2+ ions.

INTRODUCTION

Zinc selenide single crystals doped with chromium are promising materials for use as laser media. At present lasing in such crystals in the mid-infrared (IR) region is being extensively studied. On the basis of ZnSe:Cr crystals, lasers tunable in the wavelength range from 1.9–3 μm [1].

The transition elements, among them chromium, are thought to form centers that suppress luminescence in the visible spectral region. For this reason, the number of studies concerned with the effect of chromium ions on the optical properties of ZnSe in the visible region is rather limited. At the same time, the calculation of energy states of chromium impurity centers in ZnSe [2,3] suggests that radiative transitions with the photon energy close to the band gap of the semiconductor can really occur. In this context, the study of optical properties of ZnSe:Cr crystals in the visible spectral region presents a topical problem. In previous studies of optical absorption in the range 1.7–2.6 eV [3], we detected absorption bands defined by intracenter transitions in Cr^{2+} ions.

In this study, we analyze and identify the structure of the photoconductivity and photoluminescence (PL) spectra of ZnSe:Cr crystals in the visible spectral region. The photoconductivity and PL bands associated with transitions within chromium ions are observed.

The purpose of this study is to identify the photoconductivity and PL spectra in ZnSe:Cr crystals.

EXPERIMENTAL

The samples under study were fabricated by diffusion doping of initially pure ZnSe crystals with the Cr impurity. The undoped crystals were obtained by the technique of free growth on single crystal ZnSe substrate oriented in the (111) plane. The advantage of diffusion doping is that it is possible to vary the impurity concentration and profile. The procedure of doping and the studies of optical absorption in the crystals are described in detail elsewhere [3,4]. The chromium content in the crystals was determined from the change in the band gap as a function of the dopant concentration.

The photoconductivity spectra were recorded with the use of an MUM-2 monochromator. For the source of excitation light, we used a halogen lamp. The power of the light flux was kept constant by controlling the filament current of the lamp. For the photoconductivity measurements, ohmic indium contacts were deposited onto the crystals.

The PL spectra were recorded with the use of an ISP-51 prism spectrograph. The emission signal was detected with an FEU-100 photomultiplier.

The PL signal was excited with light-emitting diodes (LEDs), Edison Opto Corp., the emission

peaks of which corresponded to the wavelengths 400, 460, and 500 nm, and with an ILGI-503 nitrogen pulse laser emitting at the wavelength 337 nm.

ANALYSIS OF PHOTOCONDUCTIVITY SPECTRA

Figure 1 shows the photoconductivity spectra of the ZnSe:Cr crystals with different Cr concentrations.

The photoconductivity spectrum of the undoped crystal is shown in Fig. 1 for comparison. The undoped crystals exhibit a single photoconductivity band with a peak at 2.65 eV at 300 K (Fig. 1, curve 1). This band is due to interband optical transitions. On doping of the crystals with chromium, the band shifts to lower energies. As the Cr concentration is increased, the shift increases and corresponds to the change in the band gap determined from the optical absorption spectra in [3].

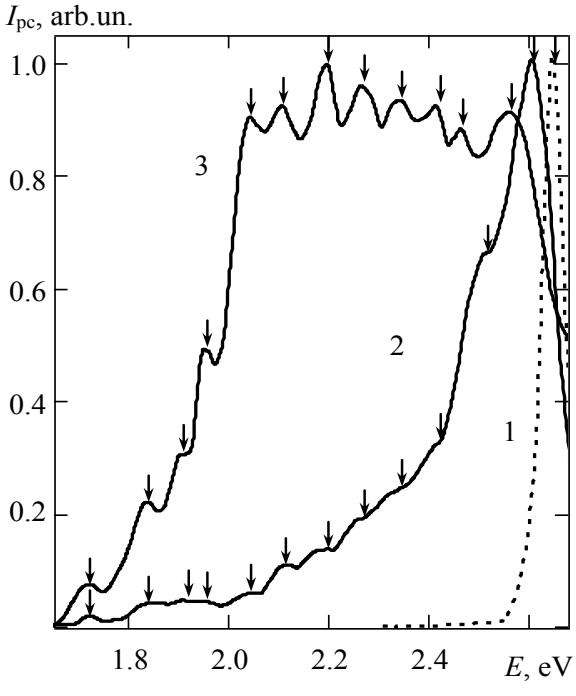

Fig.1. Photoconductivity spectra of (1) ZnSe and (2, 3) ZnSe:Cr crystals. The Cr dopant concentrations are [Cr] = (2) $2\cdot10^{18}$ and (3) $2\cdot10^{19}$ cm^{-3}.

Doping with chromium brings about the appearance of series photoconductivity bands in the range of photon energies from 1.7 to 2.6 eV (Fig. 1, curves 2, 3). As the Cr concentration is increased, the intensity of these bands increases. We observe well-defined bands at 1.74, 1.85, 1.92, 1.97, 2.04, 2.07, 2.14, 2.22, 2.31, 2.42 and 2.50 eV. The band at 2.50 eV changes its position as the Cr concentration is changed. The positions of other bands do not vary with increasing degree of doping.

At the temperature T = 77 K, only one interband photoconductivity band is observed in all of the crystals under study (Fig. 2, curve 1). As the temperature is elevated from 77 to 350 K, the impurity photoconductivity makes a weightier contribution to the spectrum (Fig. 2). We observed a similar effect previously in studying the photoconductivity of ZnSe crystals doped with Fe [5].

As the temperature is elevated from 300 to 350 K the 2.50 eV photoconductivity band shifts to lower photon energies by 20 meV. Such shift corresponds to the temperature change in the band gap of ZnSe. Other impurity photoconductivity bands do not change their position with temperature, suggesting that the corresponding transitions are of intracenter character. In addition, the position of the above mentioned bands agrees well with the position of optical absorption bands detected for these crystals previously. In [3] these absorption bands were attributed to intracenter optical transitions that occur within the Cr^{2+} ions. The above result suggests that these photoconductivity bands are due to the same optical transitions as those involved in optical absorption. The energies and identification of optical transitions are given in the table. The table summarizes the data obtained in studies of optical absorption [3], photoconductivity and luminescence.

The photoconductivity process in the crystals under study occurs in the manner briefly described below. The 2.50 eV photoconductivity band is associated with optical transitions from the $^5T_2(D)$ ground state of the Cr^{2+} ion into the conduction band. Comparison of the photon energy corresponding to the peak of this photoconductivity band with the energy position of the intrinsic photoconductivity peak for the crystals with the Cr concentration [Cr] = $2\cdot10^{18}cm^{-3}$ (2.60 eV) allows us to believe that the level of the ground state of the Cr^{2+} ion is 100 meV above the top of the valence band.

Energies of optical transitions in ZnSe:Cr crystals

Line No	Absorption		Photoconductivity, *E*, eV	Luminescence, *E*, eV	Stokes shift, E, meV
	E, eV[3]	Transition			
1	---	$^5T_2(D)\rightarrow{}^4T_1(F)+e^-_{c.b}$	2.5	---	---
2	2.6	$^5T_2(D)\rightarrow{}^1A_2(I)$	---	2.58	20
3	2.49	$^5T_2(D)\rightarrow{}^3T_2(D)$	---	2.46	30
4	2.41	$^5T_2(D)\rightarrow{}^1T_2(I)$	2.42	2.38	30
5	2.31	$^5T_2(D)\rightarrow{}^1A_1(G)$	2.31	2.30	20
6	2.22	$^5T_2(D)\rightarrow{}^1E(I)$	2.22	2.20	20
7	2.14	$^5T_2(D)\rightarrow{}^3T_1(F)$	2.14	2.12	20
8	2.07,2.04	$^5T_2(D)\rightarrow{}^3E(G)$	2.07,2.04	2.02	20
9	1.97	$^5T_2(D)\rightarrow{}^3A_2(F)$	1.97	1.95	20
10	1.92	$^5T_2(D)\rightarrow{}^1T_2(I)$	1.92	---	---
11	1.85	$^5T_2(D)\rightarrow{}^3T_2(G)$	1.85	1.81	40
12	1.74	$^5T_2(D)\rightarrow{}^3E(H)$	1.74	1.72	20
13	1.67	$^5T_2(D)\rightarrow{}^3T_2(F)$	---	1.62	50
14	1.58	$^5T_2(D)\rightarrow{}^3T_1(H)$	---	1.54	40
15	1.19	$^5T_2(D)\rightarrow{}^3T_2(H)$	---	1.16	30

The other photoconductivity bands are formed in a two-stage process. Initially, the intracenter optical transitions of electrons from the $^5T_2(D)$ ground state to the higher excited states of the Cr^{2+} ions (table) occur; then thermally activated transitions of these electrons to the conduction band are observed. As a result the local centers transit to the Cr^{3+} charged state. Later the Cr^{3+} centers trap electrons and the centers transit to their initial Cr^{2+} state.

It should be noted that the results of studies of the thermoelectric power are indicative of the electron photoconductivity of the ZnSe:Cr crystals.

ANALYSIS OF LUMINESCENCE PROPERTIES

The PL spectra were studied in the temperature range from 77 to 300 K. The PL spectra of undoped crystals excited with nitrogen laser radiation (λ =337 nm) at T = 77 K exhibit one emission band with peak at 2.77 eV (Fig. 2, curve 1). In our previous studies the 2.77 eV emission band was attributed to emission of excitons localized at neutral zinc vacancies [6].

Upon doping of the crystals with chromium, the excitonic emission bands shift to lower energies (Fig. 2, curve 2). The shift corresponds to the change in the band gap with the chromium concentration [Cr] in ZnSe, as determined in [3].

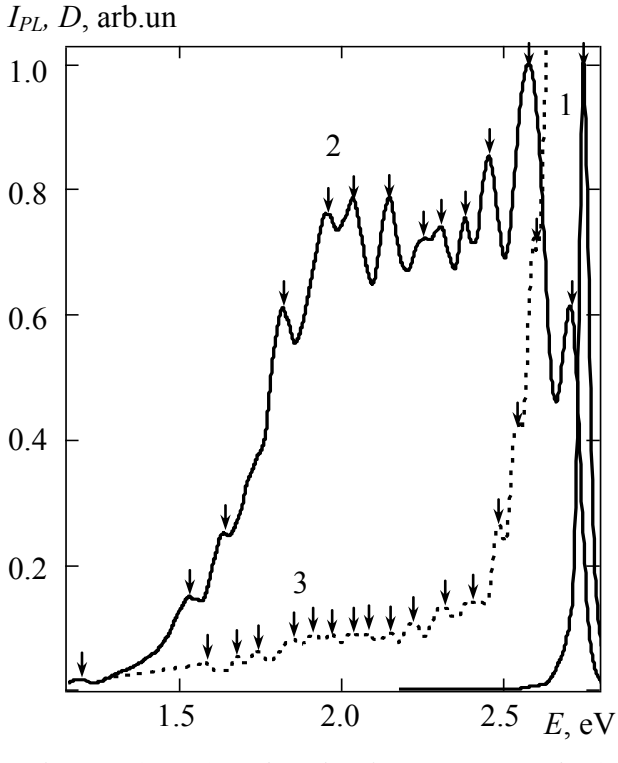

Fig. 2. (1, 2) Photoluminescence and (3) absorption spectra of (1) ZnSe and (2, 3) ZnSe:Cr crystals.

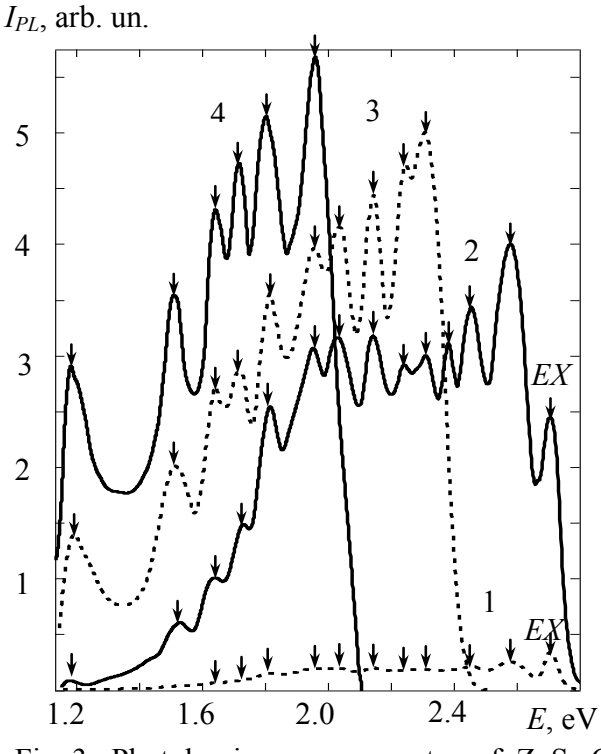

Fig. 3. Photoluminescence spectra of ZnSe:Cr crystals. E_{ex} =3.74 (1), 3.1 (2), 2.69 (3) and 2.25 eV (4).

Doping of the crystals with chromium brings about a series of long-wavelength emission lines with peaks at 1.16, 1.54, 1.62, 1.72, 1.81, 1.95, 2.02, 2.12, 2.20, 2.30, 2.38, 2.46, 2.58 (Fig. 2, curve 2). As the Cr concentration is increased, the intensity of these emission lines increases, whereas their position remains unchanged.

Figure 2 (curve 3) shows the absorption spectrum of the ZnSe:Cr crystals at T = 77 K. The spectrum involves lines that correlate with the emission lines observed in this study. As can be seen from the table, the Stokes shifts of the PL lines with respect to the corresponding absorption lines are in the range 10–50 meV.

It is established that the relative luminescence intensity of the ZnSe:Cr crystals heavily depends on the photon energy of excitation light (Fig. 3, curves 1–4).

Emission with the lowest intensity is excited with a nitrogen laser with the photon energy 3.67 eV. The highest emission intensity is attained on excitation with LEDs with the photon energy in the emission peak 2.69 and 2.25 eV (Fig. 3, curves 3, 4). This suggests that the band-to-band excitation of long-wavelength luminescence of the ZnSe:Cr crystals is inefficient. At the same time, under changes in the excitation photon energy, the position of emission peaks remains unchanged. It is also established that, as the excitation photon energy is lowered, the contribution of low-energy bands to the luminescence spectrum increases. This effect is typical of intracenter luminescence.

As the temperature is elevated from 77 to 300 K, the intensity of all emission lines decreases, while the positions of the peaks remain unchanged. Similar temperature behavior was observed for the corresponding absorption

lines. This suggests that the absorption and luminescence lines under study are due to intracenter optical transitions that occur within chromium ions.

CONCLUSIONS

1. It is shown that the high-temperature long-wavelength photoconductivity of the ZnSe:Cr crystals is controlled by intracenter optical ransitions within the Cr^{2+} ions and by subsequent thermally induced transitions of electrons from the levels of the excited Cr^{3+} states into the conduction band.

2. It is established that doping with iron gives rise to a series of emission lines in the visible spectral region. The luminescence bands detected for the ZnSe:Cr crystals are attributed to intracenter transitions in the Cr^{2+} ions.

3. Efficient excitation in impurity-related luminescence of the ZnSe:Cr crystals is attained with light corresponding to the region of intrinsic absorption in the Cr^{2+} ions.

REFERENCES

1. Moskalev I.S. Fedorov V.V., Mirov S.B. Tunable, single-frequency, and multi-watt continuous-wave Cr^{2+}:ZnSe Lasers // Optics express. – 2008. – V. 16, № 6. – P. 4145-4153.
2. Zunger A. Electronic structure of 3d-transition atom impurities in semiconductors // Solid State Physics. – 1986. – V.39. – P. 27674.
3. Ницук Ю.А. Энергетические состояния иона Cr^{2+} в кристаллах ZnSe// ФТП. – 2013. – Т. 47, В. 6. – С. 728-

731.
4. Ваксман Ю.Ф., Павлов В.В., Ницук Ю.А. Оптическое поглощение и диффузия хрома в монокристаллах ZnSe // ФТП. - 2005. - Т. 39, №4. - С. 401-404.
5. Ваксман Ю.Ф., Ницук Ю.А., Яцун В.В., Влияние примеси железа на люминесценцию и фотопроводимость кристаллов ZnSe в видимой области спектра // ФТП. – 2011. – Т. 45, В. 9. – С. 1171-1174.
6. Vaksman Yu. F., Nitsuk Yu. A., Purtov Yu. N., Shapkin P. V. Native and impurity defects in ZnSe:In single crystals prepared by free growth // Semiconductors. – 2001. – V.3. – P. 883-889.

This article has been received within 2015 .

UDC 621.315.592

Yu. F. Vaksman, Yu. A. Nitsuk

PHOTOCONDUCTIVITY AND PHOTOLUMINESCENCE OF ZnSe:Cr CRYSTALS IN THE VISIBLE SPECTRAL REGION

Abstract

The photoconductivity and photoluminescence of ZnSe:Cr crystals in the visible spectra region are studied. The scheme of optical transitions within Cr^{2+} impurity centers is established. It is shown that the high-temperature impurity photoconductivity of ZnSe:Cr crystals is controlled by optical transitions of electrons from the $^5T_2(D)$ ground state to the higher levels of excited states of Cr^{2+} ions, with subsequent thermal activation of the electrons to the conduction band. Efficient excitation of intracenter luminescence of ZnSe:Cr crystals is attained with light corresponding to the region of impurity absorption.

Key words: zinc selenide, diffusion doping, chromium impurity, photoconductivity, photoluminescence.

УДК 621.315.592

Ю. Ф. Ваксман, Ю. А. Ницук

ФОТОПРОВОДИМОСТЬ И ФОТОЛЮМИНЕСЦЕНЦИЯ КРИСТАЛЛОВ ZnSe:Cr В ВИДИМОЙ ОБЛАСТИ СПЕКТРА

Резюме

Исследована фотопроводимость и фотолюминесценция кристаллов ZnSe:Cr в видимой области спектра. Установлена схема оптических переходов, происходящих в пределах примесных центров Cr^{2+}.

Показано, что высокотемпературная фотопроводимость кристаллов ZnSe:Cr обусловлена оптическими переходами электронов из основного состояния $^5T_2(D)$ на более высокие возбужденные энергетические уровни иона Cr^{2+} с их последующей термической активацией в зону проводимости. Эффективное возбуждение внутрицентровой люминесценции кристаллов ZnSe:Cr осуществляется светом из области примесного поглощения.

Ключевые слова: селенид цинка, диффузионное легирование, примесь хрома, фотопроводимость, фотолюминесценция.

УДК 621.315.592

Ю. Ф. Ваксман, Ю. А. Ніцук

ФОТОПРОВІДНІСТЬ І ФОТОЛЮМІНЕСЦЕНЦІЯ КРИСТАЛІВ ZnSe:Cr У ВИДИМІЙ ОБЛАСТІ СПЕКТРУ

Резюме

Досліджено фотопровідність і фотолюмінесценцію кристалів ZnSe:Cr у видимій області спектру. Встановлено схему оптичних переходів в межах домішкових центрів Cr^{2+}.

Показано, що високотемпературна фотопровідність кристалів ZnSe:Cr обумовлена оптичними переходами електронів з основного стану $^5T_2(D)$ на більш високі збуджені енергетичні рівні іону Cr^{2+} з їх подальшою термічною активацією в зону провідності. Ефективне збудження внутрішньоцентрової люмінесценції кристалів ZnSe:Cr відбувається світлом з області домішкового поглинання іонів Cr^{2+}.

Ключові слова: селенід цинку, дифузійне легування, домішка хрому, фотопровідність, фотолюмінесценція.

UDC 539.182

A. V. Glushkov, A. V. Glushkov, V. B. Ternovsky, V. V . Buyadzhi, P. A. Zaichko, L. V. Nikova

Odessa State Environmental University, L'vovskaya str.15, Odessa-16, 65016, Ukraine
E-mail: dirac13@mail.ru

ADVANCED RELATIVISTIC ENERGY APPROACH TO RADIATION DECAY PROCESSES IN ATOMIC SYSTEMS

We consider the fundamental aspects of the advanced generalized energy approach to relativistic calculation of the radiative decay (transitions) probabilities in heavy neutral atomic systems and multicharged ions. The approach is based on the Gell-Mann and Low S-matrix formalism and the relativistic many-body perturbation theory (PT) with using the optimized one-quasiparticle representation and an accurate account of the relativistic and correlation. In relativistic case the Gell-Mann and Low formula expresses an energy shift through the electrodynamical scattering matrix including the interaction with as the laser field as the photon vacuum field. The last case is corresponding to definition of the traditional radiative transitions probabilities for atoms and ions.

1. Introduction

Accurate radiative decay widths and probabilities, oscillator strengths of atomic and ionic line transition are of a great interest for astrophysical analysis, laboratory, thermonuclear plasma diagnostics, fusion research, laser physics etc [1–160].

Spectral lines are usually characterized by their wavelength and oscillator strength. Typically, transition probabilities are known less accurately than wavelengths. Moreover, for many spectral lines of heavy atoms and especially multicharged ions the radiative transition probabilities are not reliably known at all. Radiative transition probabilities have been mainly determined from calculations and to a much smaller extent from experiment [1,2]. Many theoretical methods use techniques which include extensive configuration interaction or multi-configuration treatments [2-22]. The well known multi-configuration Hartree-Fock method (the relativistic effects are often taken into account in the Pauli approximation or Breit Hamiltonian etc) allowed to obtain the useful spectral data on light and not heavy atomic systems [8]. The multi-configuration (MC) Dirac-Fock (DF) method is the most reliable version of calculation for multielectron systems with a large nuclear charge. In these calculations the effects are taken into account practically precisely [3-17]. The calculation program of Desclaux (the Desclaux program, Dirac package) is compiled with proper account of the one- and two-particle relativistic, a finiteness of the nucleus size etc. In last decades a consistent quantum-electrodynamical (QED) techniques have been implemented to atomic theory calculations (look [17]). It should be given special attention to two very general and important computer systems for relativistic and QED calculations of atomic and molecular properties developed in the Oxford group and known as GRASP ("GRASP", "Dirac"; "BERTHA", "QED", "Dirac") (see [3–7] and references there). Besides, the well known density functional theory (DFT), relativistic coupled-cluster approach and model potential approaches in heavy atoms and ions should be mentioned too [18-24].

In order to determine the transition probabilities one usually uses usually a standard amplitude approach. Each of theoretical approaches to calculation of transition probabilities contains critical factors (configuration interaction or multiconfiguration treatment, spectroscopic coupling

schemes and relativistic corrections, exchange-correlation corrections convergence of probabilities results and of the dipole length and velocity forms, accuracy of transition energies etc) which need to be adequately taken care of to get reliable results.

The purpose of this paper is to review the fundamental ideas of the generalized relativistic energy approach to calculation of the radiative decay characteristics for atoms and multicharged ions, in particular, transition probabilities and oscillators strengths, line strengths etc. The bases of the energy approach to one-electron ions have been considered by Labzovsky et al [25]. Originally the energy approach to radiative and autoionization processes in multielectron atoms and ions has been developed by Ivanova-Ivanov et al [23,24] (the PC code "Superatom-ISAN"). More accurate, advanced version of the relativistic energy approach has been further developed in Refs. [26,27]). The energy approach is based on the Gell-Mann and Low S-matrix formalism combined with the relativistic perturbation theory (PT). In relativistic case the Gell-Mann and Low formula expressed an energy shift ΔE through the electrodynamical scattering matrix including interaction with as the photon vacuum field as a laser field. The first case is corresponding to determination of radiative decay characteristics for atomic systems. Earlier we have applied the corresponding generalized versions of the energy approach to many problems of atomic, nuclear and even molecular spectroscopy, including, cooperative electron-gamma-nuclear "shake-up" processes, electron-muon-beta-gamma-nuclear spectroscopy, spectroscopy of atoms in a laser field etc [28-34].

2. Relativistic energy approach to radiative decay processes

Generally speaking, the majority of complex atomic systems possesses a dense energy spectrum of interacting states with essentially relativistic properties. In the theory of the non-relativistic atom a convenient field procedure is known for calculating the energy shifts ΔE of degenerate states. This procedure is connected with the secular matrix *M* diagonalization [24-26]. In constructing *M,* the Gell-Mann and Low adiabatic formula for ΔE is used. A similar approach, using the Gell-Mann and Low formula with the electrodynamic scattering matrix, is applicable in a theory of relativistic atom; the approach is consistently electrodynamical. In contrast to the non-relativistic case, the secular matrix elements are already complex in the second order of the PT (first order of the interelectron interaction). Their imaginary parts are connected with the radiation decay (radiation) probability. The total energy shift of the state is usually presented in the form:

$$\Delta \mathrm{E} = \mathrm{Re}\,\Delta E + i\,\mathrm{Im}\,\Delta E \qquad \mathrm{Im}\,\Delta E = -\Gamma/2 \quad (1)$$

where Γ is interpreted as the level width, and the decay possibility $\mathrm{P} = \Gamma$.

In this approach, the whole calculation of the energies and decay probabilities of a non-degenerate excited state is reduced to the calculation and diagonalization of the complex matrix *M*. In the papers of different authors, the $\mathrm{Re}\,\Delta E$ calculation procedure has been generalized for the case of nearly degenerate states, whose levels form a more or less compact group. One of these variants has been previously [23,26] introduced: for a system with a dense energy spectrum, a group of nearly degenerate states is extracted and their matrix *M* is calculated and diagonalized. If the states are well separated in energy, the matrix *M* reduces to one term, equal to ΔE. The non-relativistic secular matrix elements are expanded in a PT series for the interelectron interaction.

The complex secular matrix *M* is represented in the form [23]:

$$M = M^{(0)} + M^{(1)} + M^{(2)} + M^{(3)}. \qquad (2)$$

where $M^{(0)}$ is the contribution of the vacuum diagrams of all order of PT, and $M^{(1)}$, $M^{(2)}, M^{(3)}$ those of the one-, two- and three- quasiparticle diagrams respectively. $M^{(0)}$ is a real matrix, proportional to the unit matrix. It determines only the general level shift. It is usually assumed $M^{(0)} = 0$. The diagonal matrix $M^{(1)}$ can be presented as a sum of the independent one-quasiparticle contributions. For simple systems (such as alkali atoms and ions) the one-quasiparticle energies can be taken from the experiment. Substituting these quantities into (2) one could have summarized all the

contributions of the one -quasiparticle diagrams of all orders of the formally exact relativistic PT. However, the necessary experimental quantities are not often available. The first two order corrections to $\mathrm{Re}\,M^{(2)}$ have been analyzed previously [23,35] using the Feynman diagrams technique.

The contributions of the first-order diagrams have been completely calculated. In the second order, there are two kinds of diagrams: polarization and ladder ones. The polarization diagrams take into account the quasiparticle interaction through the polarizable core, and the ladder diagrams account for the immediate quasiparticle interaction.

An effective form for the two-particle polarizable operator has been proposed in Ref. [28]; it has the following form:

$$V^{d}_{pol}(r_1 r_2) = X\left\{\int \frac{dr'\left(\rho_c^{(0)}(r')\right)^{1/3}\theta(r')}{|r_1 - r'|\cdot|r' - r_2|} - \right.$$
$$\left. - \int \frac{dr'\left(\rho_c^{(0)}(r')\right)^{1/3}\theta(r')}{|r_1 - r'|}\int \frac{dr''\left(\rho_c^{(0)}(r'')\right)^{1/3}\theta(r'')}{|r'' - r_2|}\Big/\left\langle\left(\rho_c^{(0)}\right)^{1/3}\right\rangle\right\},$$
$$\left\langle\left(\rho_c^{(0)}\right)^{1/3}\right\rangle = \int \boldsymbol{d}\ \left(\rho_c^{(0)}(r)\right)^{1/3}\theta(r), \qquad (3)$$
$$\theta(r) = \left\{1 + \left[3\pi^2\cdot\rho_c^{(0)}(r)\right]^{2/3}\Big/c^2\right\}^{1/2}$$

where ρ_c^0 is the core electron density (without account for the quasiparticle), X is numerical coefficient, c is the light velocity. The similar approximate potential representation has been received for the exchange polarization interaction of quasiparticles. Some of the ladder diagram contributions as well as some of the three-quasiparticle diagram contributions in all PT orders have the same angular symmetry as the two-quasiparticle diagram contributions of the first order. These contributions have been summarized by a modification of the central potential, which must now include the screening (anti-screening) of the core potential of each particle by the two others (look details in Refs. [23,26,35]). The additional potential modifies the one-quasiparticle orbitals and energies. Then the secular matrix can be approximated as follows: $M \sim \tilde{M}^{(1)} + \tilde{M}^{(2)}$, where $\tilde{M}^{(1)}$ is the modified one-quasiparticle matrix (diagonal), and $\tilde{M}^{(2)}$ the modified two-quasiparticle one. $\tilde{M}^{(1)}$ is calculated by substituting the modified one-quasiparticle energies), and $\tilde{M}^{(2)}$ by means of the first PT order formulae for $M^{(2)}$, putting the modified radial functions of the one-quasiparticle states in the radial integrals (look below)

Let us remind that in the QED theory the photon propagator D(12) plays the role of interparticle interaction. Naturally the analytical form of D(12) depends on the gauge, in which the electrodynamical potentials are written. In general, the results of all approximate calculations depended on the gauge. Naturally the correct result must be gauge invariant. The gauge dependence of the amplitudes of the photoprocesses in the approximate calculations is a well known fact and is in details investigated by Grant, Armstrong, Aymar, Luc-Koenig, Glushkov-Ivanov (look Refs. [1,3,26]). Grant has investigated the gauge connection with the limiting non-relativistic form of the transition operator and has formulated the conditions for approximate functions of the states, in which the amplitudes of the photoprocesses are gauge invariant. These results remain true in the energy approach because the final formulae for the probabilities coincide in both approaches.

3. Imaginary part of the secular matrix and transition probability

Within the relativistic energy approach the radiative processes are determined by the imaginary part of the interaction (1b) between the active quasiparticle and the electrodynamic vacuum of the electronic field. The presence of the polarizable core can be effectively accounted for by modification of (1b). This corresponds to a modification of the radiation transition operator in the traditional amplitude approach. A local form of the modified transition operator has been previously treated by Hibbert, Migdalec, Ivanova-Ivanov et al (look, for example, see Refs. [9,21,23,24,26]). An integral form of the additional polarization interaction, including the imaginary part, has been deduced on the base of the analysis of the second-order (the QED PT fourth order) polarization diagrams. In result one could take into account for the corresponding corrections to $\mathrm{Im}\,\Delta E$. The detailed description of the accounting for the correlation corrections of the PT high orders within the Green functions method (with the use of the Feynman diagram's technique) is given in Refs. [23,24, 34,35], where additional details can be found. The corresponding form of the polarizable operator is given below.

The probability is directly connected with imaginary part of electron energy of the system, which is defined in the lowest order of the PT as follows [23]:

$$\mathrm{Im}\,\Delta E = -\frac{e^2}{4\pi}\sum_{\substack{\alpha>n>f\\[\alpha<n\le f]}} V^{|\omega_{\alpha n}|}_{\alpha n\alpha n}, \tag{4}$$

where $\sum^{-}_{\alpha>n>f}$ for electron and $\sum^{-}_{\alpha<n\le f}$ for vacancy. The potential V is as follows:

$$V^{|\omega|}_{ijkl} = \iint dr_1 dr_2 \Psi^*_i(r_1)\Psi^*_j(r_2)\frac{\sin|\omega|r_{12}}{r_{12}}(1-\alpha_1\alpha_2)\Psi^*_k(r_2)\Psi^*_l(r_1) \tag{5}$$

The individual terms of the sum in (5) represent the contributions of different channels and a probability of the dipole transition is:

$$\Gamma_{\alpha_n} = \frac{1}{4\pi}\cdot V^{|\omega_{\alpha_n}|}_{\alpha_n\alpha_n} \tag{6}$$

The corresponding oscillator strength is defined as:

$$gf = \lambda_g^2\cdot\Gamma_{\alpha_n}/6.67\cdot10^{15}, \tag{7}$$

where g is the degeneracy degree, l is a wavelength in angstroms (Å). When calculating the matrix elements (5), one should use the angle symmetry of the task and write the corresponding expansion for $\sin|w|r_{12}/r_{12}$ on spherical harmonics as follows:

$$\frac{\sin|\omega|r_{12}}{r_{12}} = \frac{\pi}{2\sqrt{r_1 r_2}}\sum_{\lambda=0}^{\infty}(\lambda)J_{\lambda+1/2}(|\omega|r_1)J_{\lambda+1/2}(|\omega|r_2)P_\lambda(\cos\widehat{r_1 r_2}) \tag{8}$$

where J –is the Bessel function of first kind and (l) = 2l + 1. This expansion is corresponding to usual multipole expansion for probability of the radiative transition. Substitution of the expansion (11) to matrix element of interaction gives the following expression:

$$V^{\omega}_{1234} = [(j_1)(j_2)(j_3)(j_4)]^{1/2}\times \times\sum_{\lambda\mu}(-1)^{\mu}\begin{pmatrix} j_1 j_3 & \lambda\\ m_1 - m_3 & \mu\end{pmatrix}\times\mathrm{Im}\,Q_\lambda(1234) \tag{9}$$

$$Q_\lambda = Q^{\mathrm{Qul}}_\lambda + Q^{\mathrm{Br}}_\lambda. \tag{10}$$

where j_i are the entire single electron momentums, m_i – their projections; Q^{Cul}_λ and Q^{Br}_λ are connected with the Coulomb and Breit magnetic parts of the operator (1b). The total radiation width of the one-quasiparticle state is presented in the form:

$$\Gamma(\gamma) = -2\,\mathrm{Im}\,M^1(\gamma) = -2\sum_{\lambda nlj}(2j+1)\,\mathrm{Im}\,Q_\lambda\left(n_\gamma l_\gamma j_\gamma nlj\right)$$
$$Q_\lambda = Q^{Cul}_\lambda + Q^{Br}_\lambda. \tag{11}$$

The individual terms of the $\sum_{\eta lj}$ sum correspond to the partial contribution of the $n_\lambda l_\lambda j_\lambda \to nlj$ transitions; $\sum_\lambda$ is a sum of the contributions of the different multiplicity transitions. The detailed expressions for the Coulomb and Breit parts can be found in Refs. [23,35]. The imaginary part Q^{Cul}_λ contains the radial R_l and angular S_l integrals as follows (in the Coulomb units):

$$\begin{aligned}\mathrm{Im}\,Q^{\mathrm{Qul}}_\lambda(12;43) = Z^{-1}\,\mathrm{Im}\{&R_l(12;43)S_\lambda(12;43)+\\ &+R_\lambda(\tilde1 2;4\tilde3)S_\lambda(\tilde1 2;4\tilde3)+\\ &+R_\lambda(1\tilde2;\tilde43)S_\lambda(1\tilde2;\tilde43)+\\ &+R_\lambda(\tilde1\tilde2;\tilde4\tilde3)S_\lambda(\tilde1\tilde2;\tilde4\tilde3)\}\end{aligned} \tag{12}$$

In the non-relativistic limit there remains only the first term in (14) depending only on the large component $f(r)$ of the one-electron Dirac functions:

$$\begin{aligned}&\mathrm{Im}\,R_\lambda(12;43) = \frac{1}{2}(2\lambda+1)\pi X_\lambda(13)X_\lambda(24)\\ &X_\lambda(12) = \int dr\, r^{3/2} f_1(r) J^{(1)}_{\lambda+1/2}\left(r\alpha Z|\omega| f_2(r)\right)\end{aligned} \tag{13}$$

The angular coefficient has only a real part:

$$S_\lambda(1243) = \{\lambda l_1 l_3\}\{\lambda l_2 l_4\}\begin{pmatrix} j_1 & j_3 & \lambda\\ 1/2 & -1/2 & 0\end{pmatrix}\begin{pmatrix} j_2 & j_4 & \lambda\\ 1/2 & -1/2 & 0\end{pmatrix} \tag{14}$$

$\{\lambda l_1 l_3\}$ means that λ, l_1 and l_3 must satisfy the triangle rule and the sum $\lambda + l_1 + l_3$ must be an even number. The rest terms in (12) include the small components of the Dirac functions. The tilde designates that the large radial component f must be replaced by the small one g, and instead of $l_i, \tilde l_i = l_i - 1$ should be taken for $j_i < l_i$ and $\tilde l_i = l_i + 1$ for $j_i > l_i$. The Breit (magnetic) part can be expressed as follows:

$$Q^{Br}_\lambda = Q^{Br}_{\lambda,\lambda-1} + Q^{Br}_{\lambda,\lambda} + Q^{Br}_{\lambda,\lambda+1} \tag{15}$$

The corresponding imaginary part (15) is as follows:

$$\begin{aligned}\mathrm{Im}\,Q_\lambda^{\mathrm{Br}}(12;43) = Z^{-1}\,\mathrm{Im}\{&R_l\left(12;\widetilde{4}\widetilde{3}\right)S_\lambda\left(12;\widetilde{4}\widetilde{3}\right)+\\ &+R_\lambda\left(\widetilde{1}\widetilde{2};43\right)S_\lambda\left(\widetilde{1}\widetilde{2};43\right)+\\ &+R_\lambda\left(\widetilde{1}2;\widetilde{4}3\right)S_\lambda\left(\widetilde{1}2;\widetilde{4}3\right)+\\ &+R_\lambda\left(1\widetilde{2};4\widetilde{3}\right)S_\lambda\left(1\widetilde{2};4\widetilde{3}\right)\}\end{aligned} \tag{16}$$

The angular part S_λ^l has the form

$$S_\lambda^l\left(12;43\right)=\left(2\lambda+1\right)S_\lambda^l\left(13\right)S_\lambda^l\left(24\right)\left(-1\right)^{\lambda+l+1} \tag{17}$$

The total probability of a λ - pole transition is usually represented as a sum of the electric P_λ^E and magnetic P_λ^M parts. The electric (or magnetic) λ - pole transition $\gamma \to \delta$ connects two states with parities which by λ (or λ +1) units. In our designations:

$$P_\lambda^E(\gamma \to \delta) = 2(2j+1)Q_\lambda^E(\gamma\delta;\gamma\delta) \tag{18}$$

$$Q_\lambda^E = Q_\lambda^{Qul} + Q_{\lambda,\lambda-1}^{Br} + Q_{\lambda,\lambda+1}^{Br} \tag{19}$$

$$P_\lambda^M(\gamma \to \delta) = 2(2j+1)Q_\lambda^M(\gamma\delta;\gamma\delta) \tag{20}$$

$$Q_\lambda^M = Q_{\lambda,\lambda}^{Br} \tag{21}$$

In the numerical calculations the transition probability, as usually, is expanded to the series on the known parameter *aw* as follows:

$$\begin{aligned}&Q_\lambda^{Qul} \approx (\alpha\omega)^{(\lambda)},\ Q_{\lambda,\lambda-1}^{Br} \approx (\alpha\omega)^{\lambda},\\ &Q_{\lambda\lambda}^{Br} \approx (\alpha\omega)^{\lambda+3},\ Q_{\lambda,\lambda+1} \approx (\alpha\omega)^{\lambda+5}.\end{aligned} \tag{22}$$

In a case of the two-quasi-particle states (for example, this is a case of the Ne-like ions, where the excited state can be represented as stale with the two quasiparticles – electron and vacancy above the closed shells core $1s^22s^22p^6$) the corresponding probability has the following form (say, transition: $j_1 j_2[J] \to \bar{j}_1 j_2[\bar{J}]$):

$$P(\lambda \mid j_1 j_2[J], \bar{j}_1 j_2[\bar{J}]) = (\bar{J})\begin{Bmatrix}\lambda \ldots J \ldots \bar{J}\\ j_2 \ldots \bar{j}_1 \ldots j_1\end{Bmatrix} P(\lambda \mid 1\,\bar{1})(\bar{j}_1) \tag{23}$$

It should be noted that that all calculation is usually carried out in the *jj*-coupling scheme representation. The transition to the intermediate coupling scheme has been realized by diagonalization of the secular matrix. Indeed, only $\mathrm{Re}\,M$ should be diagonalized. The imaginary part is converted by means of the matrix of eigenvectors $\{C_{mk}\}$, obtained by diagonalization of $\mathrm{Re}\,M$:

$$\mathrm{Im}\,M_{mk} = \sum_{ij} C_{mi}^*\, M_{ij}\, C_{jk} \tag{24}$$

M_{ij} are the matrix elements in the *jj*-coupling scheme, and M_{mk} in the intermediate coupling scheme representation. This procedure is correct to terms of the order of $\mathrm{Im}\,M/\mathrm{Re}\,M$. Further let us also underline that the tedious procedure of phase convention in calculating the matrix elements of different operators is avoided in the energy approach, although the final formulae, of course, must coincide with the formulae obtained using the traditional amplitude method operating with the amplitudes of the processes. Therefore, the energy approach simplifies the analysis of complex atomic processes including processes with the interference of different kinds of channels (i.e. radiation and autoionization ones).

4. The one-quasiparticle optimized representation

The problem of the searching for the optimal one-electron representation is one of the oldest in the theory of multielectron atoms. Two decades ago Davidson had pointed the principal disadvantages of the traditional representation based on the self-consistent field approach and suggested the optimal "natural orbitals" representation. Nevertheless , there remain insurmountable calculational difficulties in the realization of the Davidson program (look, for example, Ref.[12]). One of the simplified recipes represents, for example, the DFT method [18,19].

Unfortunately, this method doesn't provide a regular refinement procedure in the case of the complicated atom with few quasiparticles (electrons or vacancies above a core of the closed electronic shells). For simplicity, let us consider now the one-quasiparticle atomic system (i.e. atomic system with one electron or vacancy above a core of the closed electronic shells). The multi-quasiparticle case doesn't contain principally new moments. In the lowest, second order, of the QED PT for the D*E* there is the only one-

quasiparticle Feynman diagram a (fig.1), contributing the ImDE (the radiation decay width).

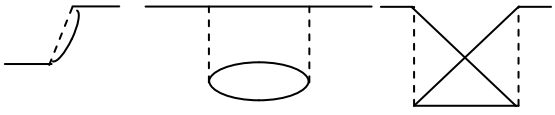

(a) (b) (c)

Figure 1. a: second other PT diagram contributing the imaginary energy part related to the radiation transitions; b and c: fourth order polarization diagrams.

In the next, the fourth order there appear diagrams, whose contribution into the ImDE account for the core polarization effects. This contribution describes collective effects and it is dependent upon the electromagnetic potentials gauge (the gauge non-invariant contribution). Let us examine the multielectron atom with one quasiparticle in the first excited state, connected with the ground state by the radiation transition. In the PT zeroth approximation one can use the one-electron bare potential:

$$V_N(r)+V_C(r), \qquad (25)$$

with $V_N(r)$ describing the electric potential of the nucleus, $V_C(r)$, imitating the interaction of the quasiparticle (initial or any other appearing in the real and virtual processes) with the core of closed shells.

The perturbation in terms of the second quantization representation reads as follows:

$$-V_C(r)\, y^+(r)\, y(r) \; - \; j_m(x)\, A^m(x). \qquad (26)$$

The core potential $V_C(r)$ is related to the core electron density $r_C(r)$ in a standard way. The latter fully defines the one electron representation. Moreover, all the results of the approximate calculations are the functionals of the density $r_C(r)$. Here, the lowest order multielectron effects, in particular, the gauge dependent radiative contribution for the certain class of the photon propagator gauge is treating. This value is considered to be the typical representative of the electron correlation effects, whose minimization is a reasonable criteria in the searching for the optimal one-electron basis of the PT. Besides, this procedure derives an undoubted profit in the routine spectroscopic calculations as it provides the way of the refinement of the atomic characteristics calculations, based on the "first principles" . Remember that the closeness of the radiation probabilities calculated with the alternative forms of the transition operator is commonly used as a criterion of the multielectron calculations quality. It is of special interest to verify the compatibility of the new optimization principle with the other requirements conditioning a "good" one-electron representation.

The imaginary part of the diagram a (fig.1) contribution has been presented previously as a sum of the partial contributions of *a-s* transitions from the initial state *a* to the final state *s* [26]:

$$\mathrm{Im}DE_a\,(\mathrm{a}) = \sum_S \; \mathrm{Im}\; DE\ (a\text{-}s;\ \mathrm{a}). \qquad (27)$$

Two fourth order polarization diagrams b,c (fig.1) should be considered further. The contributions being under consideration, are gauge-dependent, though the results of the exact calculation of any physical quantity must be gauge independent . All the non-invariant terms are multielectron by their nature.

Let us take the photon propagator calibration as follows:

$$D = D_T + CD_L,$$

$$D_T = d_{mn} / (k - k^2),$$
$$D_L = - k_m k_n / (k - k^2). \qquad (28)$$

Here C is the gauge constant; D_T represents the exchange of electrons by transverse photons, D_L that by longitudinal ones. One could calculate the contribution of the a,b,c diagrams (fig.1) into the Im DE taking into account both the D_T and D_L parts. The a diagram (fig.1) contribution into the Im DE related to the *a -s* transition reads as

$$-\frac{e^2}{8\pi}\iint \mathrm{d}r_1\mathrm{d}r_2 y_a^+(r_1)\, y_s^+(r_2)\mathrm{x}$$
$$\mathrm{x}\ \frac{1-\alpha_1\alpha_2}{} \sin(w_{as} r_{12}) y_a(r_2) y_s(r_1), \qquad (29)$$

for $D = D_T$ and

$$- \frac{e^2}{8\pi}\int\int \mathrm{d}r_1\,\mathrm{d}r_2\, y_a^+(r_1)\, y_s^+(r_2)\ \{[(1- a_1 n_{12} a_2 n_{12})/ r_{12}]\sin(w_{as} r_{12}) + w_{as}\,(1+ a_1 n_{12} a_2 n_{12})' \cos(w_{as} r_{12})\}\, y_a(r_2) y_s(r_1), \qquad (30)$$

for $D=D_{\mathrm{L}}$, where w_{as} is the a -s transition energy. According to the Grant theorem [1], the $D_{mn,\mathrm{L}}$ contribution vanishes, if the one-quasiparticle functions y_a , y_s satisfy the same Dirac equation. Nevertheless this term is to be retained when using the distorted waves approximation, for example. Another very important example represents the formally exact approach based on the bare Hamiltonian defined by its spectrum without specifying its analytic form [26,34]. Here the non-invariant contribution appears already in the lowest order. When calculating the forth order contributions some approximations are inevitable.

These approximations have been formulated in Refs.[26], where the polarization corrections to the state energies have been considered.

Let us consider the direct polarization diagram b (fig.1) as an example. After the some transformations the formal expression for the sought for value looks as

$$\mathrm{Im}\, E_{ninv}(\alpha - s \mid A_d) = -C\frac{e^2}{4\pi}\iiint\int dr_1 dr_2 dr_3 dr_4 \sum \Big(\frac{1}{\omega_{mn}+\omega_{\alpha_s}} + \frac{1}{\omega_{mn}-\omega_{\alpha_s}}\Big)\Psi_\alpha^+(r_1)\Psi_m^+(r_2)\Psi_s^+(r_3)\Psi_n^+(r_4)(1-\alpha_1\alpha_2)/r_{12}\cdot \{[(\alpha_3\alpha_4 - (\alpha_3 n_{34})(\alpha_4 n_{34}))/r_{34}\cdot \sin[\omega_{\alpha_n}(r_{12}+r_{34}) + \omega_{\alpha_n}\cdot \cos[\omega_{\alpha_n}(r_{12}+r_{34})](1+(\alpha_3 n_{34})(\alpha_4 n_{34}))]\}\Psi_m(r_3)\Psi_\alpha(r_4)\Psi_n(r_2)\Psi_s(r_1), \qquad (31)$$

and the upper continuum electron states; $m \pounds f$ indicates the finite number of states in the core and the states of the negative continuum (accounting for the electron vacuum polarization).

All the vacuum polarization and the self-energy corrections to the sought for values are omitted. Their numerical smallness compared with the other relativistic corrections to the different atomic characteristics had been verified by the numerous calculations. The renormalization procedure is not needed here. Nevertheless the second-order vacuum polarization and self-energy corrections can be additively added to the complex state energy. The remaining expression includes summation over the bound and upper continuum atomic states. To evaluate this sum, we use the analytic relation between the atomic electron Fermi level and the core electron density $r_{\mathrm{c}}(r)$, appropriate to the homogeneous nonrelativistic electron gas (the Tomas- Fermi approximation). Now the sum $\sum_{n>f,\ m<f}$ can be calculated analytically, its value becomes a functional of the core electron density. The resulting expression looks as the correction due to the additional nonlocal interaction of the active quasiparticle with the closed shells. Nevertheless, its calculation is reducible to the solving of the system of the ordinary differential equations (1-D procedure) [26]. The most important refinements can be introduced by accounting for the relativistic and the density gradient corrections to the Tomas- Fermi formula (see Refs. [23,26]). The same program is realized for other polarization diagrams. The minimization of the functional Im dE_{ninv} (b+c) leads to the integro-differential equation for the r_{c} (the DF or Dirac-Kohn-Sham-like equations for the electron density) that are numerically solved. In result we obtain the optimal one-quasiparticle representation, which is further used in calculation of the radiative (autoionization) transition characteristics (7)-(10).

5. Conclusion

We have considered the fundamental blocks of the generalized energy approach to relativistic calculation of the radiative decay (transitions) probabilities in heavy neutral atomic systems and multicharged ions. The approach is based on the Gell-Mann and Low S-matrix formalism and the gauge-invariant relativistic many-body perturbation theory (PT) with using the optimized one-quasiparticle representation and an accurate account of the relativistic and exchange-correlation effects. In relativistic case the Gell-Mann and Low formula expresses an energy shift ΔE through the electrodynamical scattering matrix including the interaction with the photon vacuum field. This case is corresponding to definition of the traditional radiative transitions probabilities for atoms and ions. Obviously, the same program can be realized in order to give adequate quantitative description of interaction of atomic systems

with a laser field and further computing the radiation emission and absorption lines parameters, the corresponding lines moments etc. [28,29].

References

1. W.Martin, NIST Spectra Database, version 2.0, NIST, Washington,2004; (http:// physics.nist.gov.asd); C. Moore, NBS Spectra Database, NBS, Washington, 1997.
2. A.Weiss, J.Quant.Spectr. Radiat.Transf. **18**, 481 (1997) ; Phys.Scripta. **T65**, 188(1999); M. Grance, Atomic Data. **5**, 185 (1993).
3. I.P. Grant, Relativistic Quantum Theory of Atoms and Molecules, Theory and Computation, Springer Series on Atomic, Optical, and Plasma Physics, vol. 40 (Springer, Berlin, 2007), p. 587–626
4. Relativistic Electronic Structure Theory, Series: Theoretical and Computational Chemistry Series., vol.11, part1, ed. P. Schwerdtfeger (Springer, 2002); vol.12, part2, ed. P. Schwerdtfeger (Springer, 2004);
5. S. Wilson, in Recent Advances in Theoretical Physics and Chemistry Systems, Series: Progress in Theoretical Chemistry and Physics, vol. 16, ed. by J. Maruani, S. Lahmar, S. Wilson, G. Delgado-Barrio (Springer, Berlin, 2007), p. 11-80.
6. K.L. Bell, K.A. Berrington, D.S.F. Crothers, A. Hibbert, K.T. Taylor, Bertha: 4-Component Relativistic Molecular Quantum Mechanics, in Supercomputing, Collision Processes, and Application, Series: Physics of Atoms and Molecules, (Kluwer, New York, 1999) pp. 213–224.
7. H.Jensen, T.Saue, L.Visscher with contr. by V.Bakken, E.Eliav, T. Enevoldsen, T.Fleig, O.Fossgaard, T.Helgaker, J.Laerdahl, C.Larsen, P. Norman, J.Olsen, M.Pernpointner, J.Pedersen, K.Ruud, P.Salek, J. van Stralen, J.Thyssen,O. Visser, T.Winther, DIRAC Code, a relativistic ab initio electronic structure program, Release DIRAC4.0.-2004; (http://dirac.chem.sdu.dk).
8. C.Froese-Fischer, Phys.Rev.A**39**, 963 (1999); C.Froese Fischer, G.Tachiev, Atom. Data Nucl. Data Tables. **87**, 1 (2004); C.Froese Fischer, G.Tachiev, A. Irimia, GAtom. Data Nucl. Data Tables. **92**, 607 (2006).
9. M.A.Klapish, Comp.Phys.Commun. **2**, 239 (1999); C.Laughlin, G.A. Victor, Adv. Atom. Mol. Phys. **25,** 163 (1998).
10. K. Cheng, Y. Kim, J. Desclaux, Atom. Data Nucl. Data Tabl. **24**, 11 (1999); P. Indelicato, J.P. Desclaux, Phys. Scripta T **46**, 110 (1993) ; B.Saha, S.Fritzsche, J.Phys. B: At. Mol. Opt. Phys.**38**, 1161 (2005).
11. J.Bieron, C.Froese-Fischer, S.Fritzsche, K. Pachucki, J.Phys.B:At.Mol.Opt. Phys. **37**, L305 (2004); J. Bieron, P. Pyykkö, P. Jonsson, Phys. Rev. A **71**, 012502 (2005); J. Bieron, P. Pyykkő, Phys. Rev. A **71**, 032502 (2005).
12. D.Feller, E.R.Davidson, J.Chem.Phys. **74**, 3977 (1991); K.Dietz, B.A.Heb, Phys.Scripta. **39**, 682 (1999).
13. W.R.Johnson, C.D.Lin, K.T.Cheng, Phys.Scr. **21**, 409 (1990); W.R.Johnson, J.Sapistein, S.Blundell, Phys.Rev.A**37**, 307 (1988); E. Luc-Koenig, A. Lyras, J.-M. Lecomte, M. Aymar, J.Phys. B: At. Mol. Opt. Phys. **30**, 5213 (1997).
14. V. Dzuba, V. Flambaum, P. Silvestrov, O. Sushkov, Phys. Rev. A **44**, 2828 (1991); V. Dzuba, V. Flambaum, M.S. Safranova, Phys. Rev. A **73**, 022112 (2006)
15. U.I. Safranova, M.S. Safranova, W. Johnson, Phys. Rev. A **71**, 052506 (2005); M.S. Safronova, W.R. Johnson, U.I. Safranova, T.Cowan, Phys. Rev.A.**74**, 022504 (2006).
16. P. Quinet, C. Argante, V. Fivet, C. Terranova1, A. V. Yushchenko, É. Biémont, Astrophys. Astron. **474**, 307 (2007) ; É. Biémont, V. Fivet, P. Quinet, J.Phys. B: At. Mol. Opt. Phys 37, 4193 (2004); O.Yu. Khetselius, Int. Journ.Quant. Chem. **109**, 3330 (2009); Phys.Scripta.

T135, 014023 (2009).
17. J.Sapirstein, K.T.Cheng, Phys. Rev. A 71, 022503 (2005); V.M.Shabaev, I.I.Tupitsyn, K.Pachucki, G.Plunien, and V.A.Yerokhin, Phys.Rev.A 72, 062105 (2005); V. Yerokhin, A.N. Artemyev, V.M. Shabaev, Phys. Rev. A **75**, 062501 (2007).
18. W. Kohn, L.J. Sham, Phys. Rev. A **140**, 1133 (1994); P. Hohenberg, W. Kohn, Phys. Rev. B **136**, 864 (1994); E.G. Gross, W. Kohn, Exchange-Correlation Functionals in Density Functional Theory (Plenum, New York, 2005).
19. The Fundamentals of Electron Density, Density Matrix and Density Functional Theory in Atoms, Molecules and the Solid State, Series: Progress in Theoretical Chemistry and Physics, vol. 14, eds. N. Gidopoulos and S. Wilson (Springer, Berlin, 2004), p.1.
20. E. Kaldor, E. Eliav, A. Landau, in Recent Advances in Relativistic Molecular Theory, ed. by K. Hirao and Y. Ishikawa (World Scientific, Singapore, 2004), p. 283.
21. A.Hibbert, Adv. Atom. and Mol. Phys.**18**, 309 (1982); A.Hibbert, J.E.Hansen// J.Phys. B: At. Mol. Opt. Phys. **27**, 3325 (1994); M.D.Kunisz, Acta Phys.Polon.A **62**, 285 (1992); J.Migdalek, Can.J.Phys. **54,** 130 (1996).
22. V.N. Ostrovsky, S.A.Sheynerman, Opt. Spectr. **67**, 16 (1989); E.K.Anderson, E.M.Anderson, Opt.Spectr. **54,** 955 (1983).
23. L.N.Ivanov, E.P.Ivanova, Atom.Data Nucl. Data Tabl. **24**, 95 (1999); L.N. Ivanov, V.S. Letokhov, Com.Mod. Phys.D.:At.Mol.Phys. **4**, 169 (1985); E.P. Ivanova, L.N. Ivanov, A.V. Glushkov, A. Kramida, Phys. Scripta **32**, 512 (1995); E.P. Ivanova, A.V. Glushkov, J. Quant. Spectr. Rad. Transfer. **36**, 127 (1986).
24. L.N. Ivanov, E.P. Ivanova, L. Knight, Phys. Rev. A **48,** 4365 (1993); E.P. Ivanova, A.V.Gulov, Atom.Dat.Nuc. Dat. Tabl. **49**, 1 (1991); E.P. Ivanova, I.P. Grant, J. Phys.B: At.Mol.Opt.Phys. **31**, 2871 (1998); E.P. Ivanova, N.A. Zinoviev, Quant. Electr. **29**, 484 (1999); Phys. Lett. A**274**, 239 (2001).
25. L.N. Labzovsky, JETP, **57**, 663 (1969); M.A.Braun, Yu.Yu.Dmitriev, L.N. Labzovsky, JETP. **57,** 2189 (1969); V.V.Tolmachev, Adv. Quant. Chem. **4**, 331 (1969).
26. A.V. Glushkov, L.N. Ivanov, E.P Ivanova, Autoionization Phenomena in Atoms, (Moscow University Press, Moscow, 1996) pp.152-164; A.V. Glushkov, L.N. Ivanov, Phys. Lett. A **170**, 33 (1992); A.V. Glushkov, L.N. Ivanov, Preprint of ISAN, AS N-1, Moscow-Troitsk, 1992); J. Phys. B: At. Mol. Opt. Phys. **26,** L379 (1999);
27. A.V. Glushkov, E.P. Ivanova, in: Spectroscopy of multicharged ions, ed. U.I.Safronova (Nauka, Moscow, 1996), p.5-195; A.V. Glushkov, S.V Malinovskaya, in: Many-body effects in atoms, ed. U.I.Safronova (Nauka, Moscow, 1998), pp.73-189
1. A.V. Glushkov, J. Appl. Spectr. **52,** 297 (1990); **56,** 13 (1992); **56,** 482 (1992); Opt. Spectr. **70**, 952 (1991); **71**, 395 (1991); **72,** 55 (1992); **72,** 542 (1992); JETP Lett. 55, 97 (1992); Russian Phys.J., **34,** 34 (1991); **35 ,** 3 (1992); S.V.Mali-novskaya, A.V.Glushkov, Russian Phys.J., **35**, 999 (1992).
28. A.V. Glushkov, O.Yu. Khetselius, A.V.Loboda, A.A.Svinarenko, in Frontiers in Quantum Systems in Chemistry and Physics, Series: Progress in Theoretical Chemistry and Physics, vol. 18, ed. by S. Wilson, P.J. Grout., J. Maruani, G. Delgado-Barrio, P. Piecuch (Springer, Berlin, 2008), pp.541-588; A.V. Glushkov, A.V.Loboda, J. Appl. Spectr. (Springer) **74**, 305 (2007).
29. A.V. Glushkov, O.Yu. Khetselius, S.V. Malinovskaya, in Frontiers in Quantum Systems in Chemistry and Physics, Series: Progress in Theoretical Chemistry and Physics, vol. **18**, ed. by S.Wilson, P.J.Grout, J. Maruani, G. Delgado-Barrio, P. Piecuch (Springer, Berlin, 2008), p. 523; Europ.Phys. Journ. ST **160**, 195

(2008); Molec. Phys. **106**, 1257 (2008).
30. A.V. Glushkov, O.Yu. Khetselius, L. Lovett, L., in: Advances in the Theory of Atomic and Molecular Systems Dynamics, Spectroscopy, Clusters, and Nanostructures. Series: Progress in Theoretical Chemistry and Physics, vol. **20**, ed. by P.Piecuch, J. Maruani, G. Delgado-Barrio, S. Wilson (Springer, Berlin, 2010), pp.125-172.
31. A.V. Glushkov, S.V. Malinovskaya, L.A.Vitavetskaya, Yu.V. Dubrovskaya, O.Yu. Khetselius, in: Recent Advances in Theoretical Physics and Chemistry Systems, Series: Progress in Theoretical Chemistry and Physics, vol. 15, ed. by J.-P. Julien, J. Maruani, D. Mayou, S. Wilson, G. Delgado-Barrio (Springer, Berlin, 2006), pp. 301-318.
32. A.V. Glushkov, O.Yu. Khetselius, A.A. Svinarenko, in: Advances in the Theory of Quantum Systems in Chemistry and Physics. Series: Progress in Theoretical Chemistry and Physics, vol. **22**, ed. by .Hoggan, E.Brandas, G. Delgado-Barrio, P.Piecuch (Springer, Berlin, 2012), pp.51-70.
33. A.V. Glushkov, V.D. Rusov, S.V. Ambrosov, A.V. Loboda, in New Projects and New Lines of Research in Nuclear Physics, ed. by G. Fazio and F. Hanappe (World Scientific, Singapore, 2003), p. 126-142; A.V. Glushkov, O.Yu. Khetselius, A.V. Loboda, E.P. Gurnitskaya, in Meson-Nucleon Physics and the Structure of the Nucleon, ed. by S. Krewald, H. Machner (IKP, Juelich, Germany), SLAC eConf C070910 (Menlo Park, CA, USA) **2**, 186 (2007); A.V.Glushkov, ibid. **2**, 111 (2007).
34. A.V. Glushkov, S.V. Ambrosov, A.V. Loboda, Yu.G. Chernyakova, O.Yu. Khetselius, A.A. Svinarenko, Nucl. Phys. A **734**S, 21 (2004); Glushkov, A.V., Ambrosov, S.V., Loboda, A.V., Gurnitskaya, E.P., Prepelitsa, G.P. Int. J. Quantum Chem. **104**, 562 (2005); A.V. Glushkov, S.V. Ambrosov, A.V. Loboda, E.P. Gurnitskaya, O.Yu. Khetselius, in Recent Advances in Theoretical Physics and Chemistry Systems, Series: Progress in Theoretical Chemistry and Physics, vol. 15, ed. by J.-P. Julien, J. Maruani, D. Mayou, S. Wilson, G. Delgado-Barrio (Springer, Berlin, 2006), pp. 285-300.
35. A.V. Glushkov, O.Yu. Khetselius, E.P. Gurnitskaya, A.V. Loboda, T.A. Florko, D.E. Sukharev, L. Lovett, in Frontiers in Quantum Systems in Chemistry and Physics, Series: Progress in Theoretical Chemistry and Physics, vol. 18, ed. by S. Wilson, P.J. Grout., J. Maruani, G. Delgado-Barrio, P. Piecuch (Springer, Berlin, 2008), p.501-522.
36. L.Curtis, Phys.Rev.A**35**, 2089 (1987); Phys.Rev.A **40**, 6958 (1989) ; Phys. Scripta. **43**, 137 (1991) ; Phys.Rev.A.**51,** 4574 (1995); Y.Li, G.Pretzler, E.E.Fill, Phys. Rev. A **52,** R3433–R3435 (1995); U.I.Safronova, T.M.Cowan, M.S. Safronova, J.Phys.B: At. Mol. Opt. Phys. **38**, 2741 (2005); Y.Ishikawa, J.M.Lopez, E.Trabert, Phys. Scripta. **79**, 025301 , (2009).

This article has been received within 2015

UDC 539.182

A. V. Glushkov, A. V. Glushkov, V. B. Ternovsky, V. V . Buyadzhi, P. A. Zaichko, L. V. Nikova

ADVANCED RELATIVISTIC ENERGY APPROACH TO RADIATION DECAY PROCESSES IN ATOMIC SYSTEMS

Abstract.

We consider the fundamental aspects of the generalized energy approach to relativistic calculation of the radiative decay (transitions) probabilities in heavy neutral atomic systems and multicharged ions. The approach is based on the Gell-Mann and Low S-matrix formalism and the relativistic many-body perturbation theory (PT) with using the optimized one-quasiparticle representation and an accurate account of the relativistic and correlation. In relativistic case the Gell-Mann and Low formula expresses an energy shift ΔE through the electrodynamical scattering matrix including the interaction with as the laser field as the photon vacuum field. The last case is corresponding to definition of the traditional radiative transitions probabilities for atoms and ions.

Key words: energy approach, atomic systems and multicharged ions, radiative transitions, Gell-Mann and Low S-matrix formalism

УДК 539.182

А. В. Глушков, В. Б. Терновский, В. В. Буяджи, П. А. Заичко, Л. В. Никола

РЕЛЯТИВИСТСКИЙ ЭНЕРГЕТИЧЕСКИЙ ПОДХОД К ОПИСАНИЮ ПРОЦЕССОВ РАДИАЦИОННОГО РАСПАДА В АТОМНЫХ СИСТЕМАХ

Резюме.

В работе рассмотрены фундаментальные аспекты обобщенного релятивистского энергетического подхода в релятивистской теории радиационных распадов (переходов) вероятностей в тяжелых нейтральных атомных системах и многозарядных ионов. Подход базируется на S-матричном формализма Гелл-Манна и Лоу и релятивистской многочастичных теории возмущений с выполнением оптимизированного одинквазичастинквого представления и аккуратным учетом релятивистских и корреляционных поправок. В релятивистском случае формула Гелл-Манна и Лоу выражает энергетический сдвиг через электродинамическую матрицу рассеяния, в том числе, с учетом взаимодействия как с полем лазерного излучения, так и полем фотонного вакуума. Последний случай соответствует определению традиционных вероятностей радиационных переходов для атомов и ионов

Ключевые слова: энергетический подход, атомные системы и многозарядные ионы, радиационные переходы, S-матричный формализм Гелл-Манна и Лоу

УДК 539.182

А. В. Глушков, В. Б. Терновський, В. В. Буяджи, П. О. Заїчко, Л. В. Нікола

РЕЛЯТИВІСТСЬКИЙ ЕНЕРГЕТИЧНИЙ ПІДХІД ДО ОПИСУ ПРОЦЕСІВ РАДІАЦІЙНОГО РОЗПАДУ В АТОМНИХ СИСТЕМАХ

Резюме.

У роботі розглянуті фундаментальні аспекти удосконаленого релятивістського енергетичного підходу в релятивістській теорії радіаційних розпадів (переходів) ймовірностей у важких нейтральних атомних системах і багатозарядних іонів. Підхід базується на S-матричному формалізму Гелл-Манна та Лоу і релятивістської багаточастинковій теорії збурень з імплементацією оптимізованого одинквазічастинквого представлення і акуратним урахуванням релятивістських і кореляційних поправок. У релятивістському випадку формула Гелл-Манна і Лоу виражає енергетичний зсув через електродинамічну матрицю розсіювання, в тому числі, з урахуванням взаємодії як з полем лазерного випромінювання, так й полем фотонного вакууму. Останній випадок відповідає визначенню традиційних ймовірностей радіаційних переходів для атомів та іонів

Ключові слова: енергетичний підхід, атомні системи і багатозарядні іони, радіаційні переходи, S-матричний формалізм Гелл-Манна та Лоу

UDC 539.186

P. O. Kondratenko[1], Yu. M. Lopatkin[2] , A. V. Glushkov and T. N. Sakun[1]

[1]National Aviation University, 1, Komarov Ave, 03680 Kiev, Ukraine
[2]Sumy State University, 2, Rimsky-Korsakov Street, 40007, Sumy, Ukraine
E-mail: nucsukh@mail.ru
[3] Odessa State Environmental University, 15, Lvovskaya str., 65016, Odessa, Ukraine

EXPERIMENTAL AND THEORETICAL STUDYING OF PHOTOCONDUCTIVITY OF POLYMERIC LAYERS WITH DYES

We present the results of the experimental and theoretical studying photoconductivity of polymer layers with the dyes. It's investigated photoconductivity of organic dyes in solid polymeric matrices with rectangular pulse excitation light. The obtained experimental data indicate on the quadratic (i.e. non-linear) relationship between photocurrent values that are obtained for two different levels of radiation intensities.

1. Introduction

To present time there are carried out numerous experimental and theoretical works data showing that the excitation relaxation processes in polymeric materials with different impurities do not prevent leakage of important science and practice processes in the highly excited states such as generation of carriers, photochemical and radiation-chemical processes [1-15]. Studying photo-conductivity of the polyacene linear crystals (anthracene, tetracene, pentatsen) showed that its high quantum efficiency is observed only under irradiation of the highly excited molecules when there is possible a birth of holes and free electrons.

In this paper we present the results of the experimental and theoretical studying photoconductivity of polymer layers with the dyes. It's investigated photoconductivity of organic dyes in solid polymeric matrices with rectangular pulse excitation light (methodics details in Refs. [3,4,6,7]). Initially, samples were kept at a constant high voltage (for most of them was taken U = 80 V) for some time until it is established steady dark current. Then through the transparent electrodes cell sample are radiated by a light from a mercury lamp, and a light had been focused so that the sample was evenly lit. The photocurrent appearance is recorded on the recorder and a photocurrent grew exponentially to a constant value i_c. Time of stationary photocurrent is dependent on dye concentration, nature of the polymer matrix, and presence of alkali in the layer, and equal one to a few min.

After the cessation of current lighting around the same time period reached its original value. Typical kinetics of the photocurrent growth and decline for most of the samples (PVP= polyvinylpyrrolidone; PVA= Polyvinyl acetate; PVC= Polyvinyl alcohol; PVE= Poliviniletylal) is shown in Fig.1.

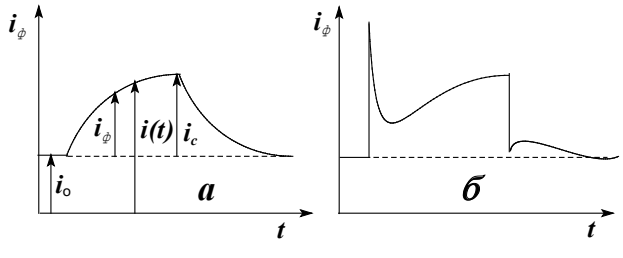

Figure 1. Time dependence of the photocurrent changing for solid solvents of rezazuryne: a) in polymers of PVP, PVA, PVC, b) in PVE (C = 10-3).

Kinetics of photoconductivity for PvE layer of rezazuryne (P = 10^{-3} mol/l) without alkali was somewhat complicated character. As it is shown in Fig. 1b, photocurrent model has two components (fast and slow) which are superimposed, giving the appearance of a complex curve. Quick component met in some other examples, and they have not helped to increase and sharp decline in photocurrent for the first time after turning on the light.

This component of the photocurrent disappears quickly, and for some samples it did not appear. Its rapid disappearance indicates that there are traps in the sample volume that capture electrons and holes, or carriers localized near the sample surface, creating an electrical double layer. As it is shown in Fig.1a, the growth photocurrent relaxation curve has exponential areas (i.e. relaxation occurs in a continuous lifetime on the considerable distance). To obtain quantitative information it is suggested that the increasing the photocurrent satisfies to the law:

$$i(t) = i_0 + i_c\left(1 - e^{-\frac{t}{\tau}}\right),$$

and

$$\tau = -\frac{t}{\mathrm{h}\left[1 - \frac{i(t) - i_0}{i_c}\right]}.$$

It is reasonable to portray the results in the coordinates , where

for a curve of the photo current increasing.).

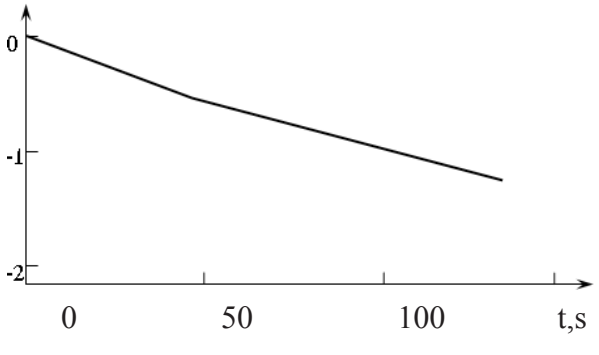

Figure 2. Kinetics of the photocurrent for rezazuryne in PVP (C = 10^{-3}mol/l in presence of the KOH) in the coordinates "t-ln(1-i_{ph}/i_c)

The exponential areas are plotted by the straight lines with a slope that determines τ, which is on the absolute value equal to the cotangent of the angle of the curve inclination (look Figure 2). Found lifetimes depending on the concentration rezazuryne polymer matrix and the presence of alkali are shown in Table. 1.

Table 1.

The lifetimes τ (s) in dependence on the rezazuryne concentration (C) in a polymer matrix and availability an alkalis KOH (light without filter).

Polimer	τ, s			
	Pure	C = 10^{-3}, KOH.	C = 10^{-3}, KOH	C = 10^{-4}, KOH
PVP	123	90	65	78
PVE	42	42	70	95
PVA	67	60	76	–

In Figures 3a,b,c we present the related changing photocurrent in polymers with different concentration of rezazuryne in dependence on a light intensity *I*.

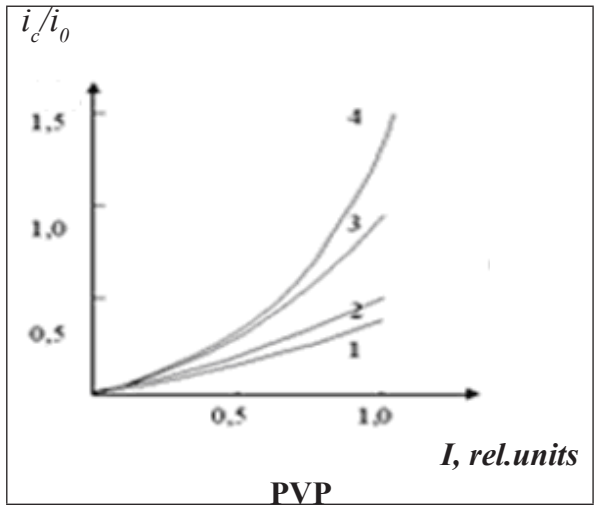

Figure 3a. The related changing photocurrent in polymers with different concentration of rezazuryne in dependence on a light intensity a) PVP (1 – C = 0; 2 – C = 10^{-4}, KOH; 3–C = 10^{-3}; 4 – C = 10^{-3}, KOH); n = i_c/i_o: 3(2), 3 (3), 4 (4);

Using the obtained kinetical curves of a photocurrent for all polymers with the rezazuryne concentration C=10^{-3} *mol/l* , it has been found the following relationship:

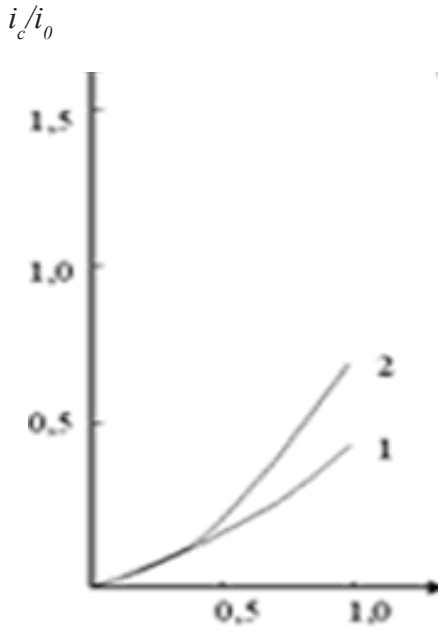

Figure 3b. The related changing photocurrent in polymers with different concentration of rezazuryne in dependence on a light intensity: b). PVE (1 – C = 10^{-4}, KOH; 2 – C = 10^{-3}, KOH); n = i_c/i_o: 2,5 (1), 4,2 (2);

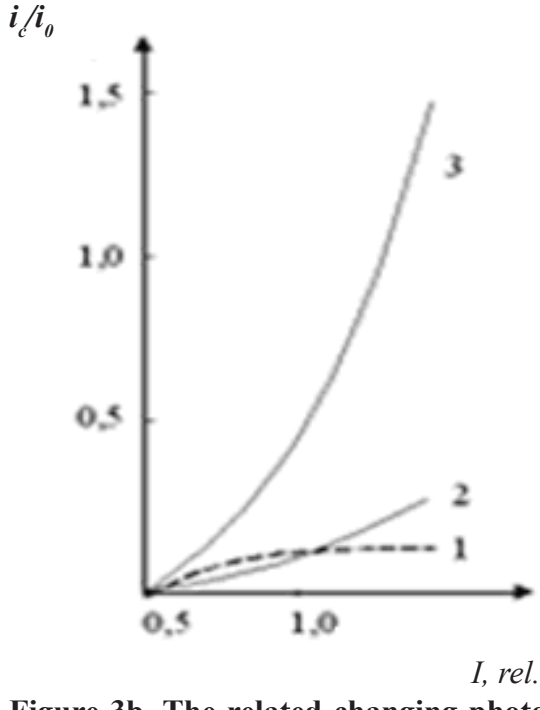

Figure 3b. The related changing photocurrent in polymers with different concentration of rezazuryne in dependence on a light intensity: c) PVA (1 – C = 0; 2 – C=10^{-3}; 3 – C =10^{-3}, KOH); n = i_c/i_o:3 (3,7).

$$\left(\frac{i_c}{i_0}\right)_{I=1} \Big/ \left(\frac{i_c}{i_0}\right)_{I=0,5} = 4,$$

where i_c is the value of a photocurrent under saturation; i_0 is the value of a dark current under some constant voltage.

In order to determine an influence of the dyes concentration on a photosensitivity of the polymer layer it is studied a dependence $i_{ph}/i_0 = f(t)$ for different concentrations of the rezazuryne (look Figure 4).

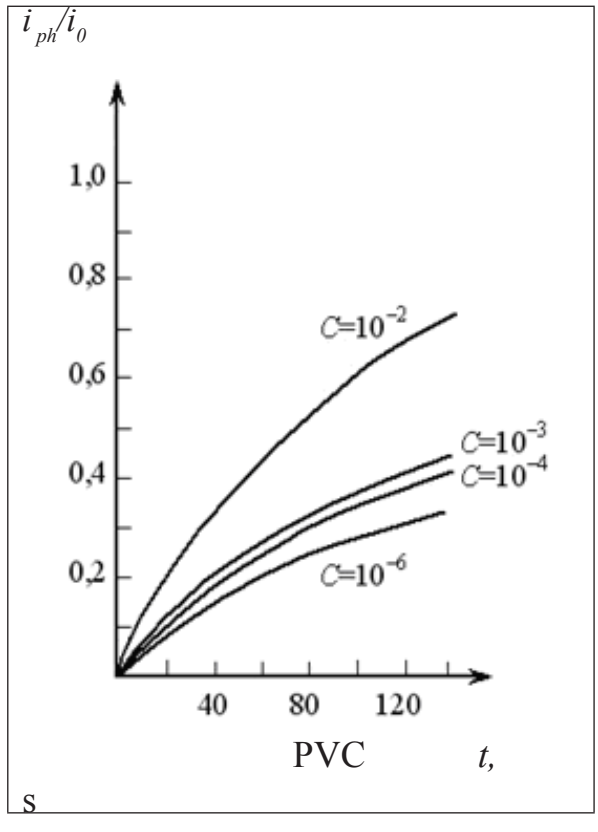

Figure 4a. Dependence $i_{ph}/i_0 = f(t)$ for different rezazuryne concentrations in matrix PVC

The obtained experimental data indicate on the quadratic (i.e. non-linear) relationship between photocurrent values that are obtained for two different levels of radiation intensities.

This phenomenon is characteristic for the two-quantum processes and confirms earlier obtained the results [5,6]. Note that when irradiated the sample through the filter UFS-1

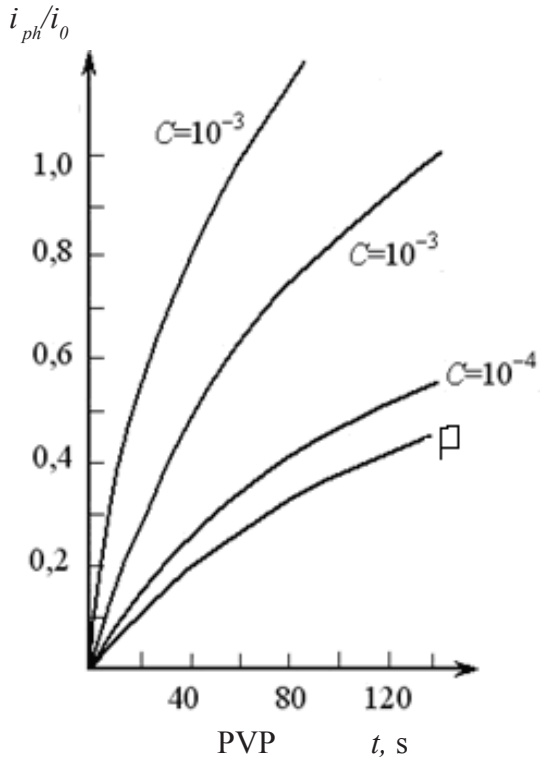

Figure 4b. Dependence $i_{ph}/i_0 = f(t)$ for different rezazuryne concentrations in matrix PVP (P- pure)

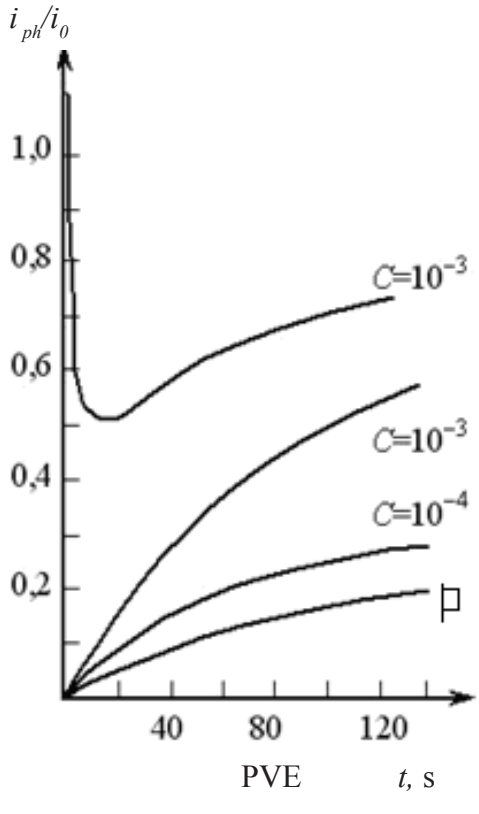

Figure 4c. Dependence $i_{ph}/i_0 = f(t)$ for different rezazuryne concentrations in matrix PVE (P- pure)

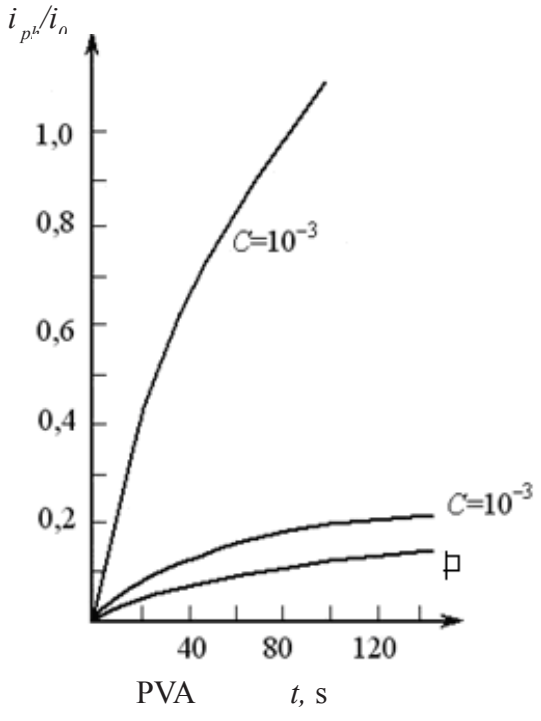

Figure 4d. Dependence $i_{ph}/i_0 = f(t)$ for different rezazuryne concentrations in matrix PVA (P- pure)

it is observed a linear dependence of a photocurrent on the intensity of exposure.

References

1. Kondratenko P.A., Photochemical action of light./ (Tutorial).- Kiev: Publishing center "Kyiv University".-2005.– 401P.
2. Turro N., Molecular Photochemistry.- M.:Mir, 1967-328P.
3. Kondratenko P.A., Lopatkin Yu.M, Sakun T.N., Relaxation Processes in Highly Excited Molecules of Resazurin // Physics and Chemistry of Solids -2007.-Vol.8,№1.-P.100-108
4. Kondratenko P.A.,.Lopatkin Yu.M, Sakun T.N., Spectroscopic properties of the resazurin in liquid and solid solutions// Physics and Chemistry of Solids.-2006.-Vol.7,N4. – P.695-700
5. Becker H.G.O., Hoffman G. Israel G. Ionische und radikalische Dediazonierungen von Aryldiazonium-salzen

ein Beispiel für wellenlan-genab-hängige Photoreaktionen // J. Prakt. Chem. – 1977. – Vol.319, N6. – P.1021-1030.
6. Kondratenko N.P., Kondratenko P.A., Sensitization sensitivity diazonium salts // Scientific Notes of the Dragomanov's NPU. Ser. Phys.-Math.- 2001. - C. 83-88.
7. Kondratenko P.A., Lopatkin Yu.M., Kondratenko N.P. // Molecules with a Xe-O type interfragmentary bond. Diazonium salts and azides. // Functional Materials. – 2002. –Vol.9, N4.- P.713-720
8. Siliņš EA. The electronic states of organic molecular crystals. – Riga: Zinatne.-1978.- 344p.
9. Onsager L., Initial recombination of ions // Physical Reviews. – 1938. – Vol.54. – P.554–557.
10. Kondratenko P.A., Lopatkin Yu.M., Single and double quantum processes in solid solutions of dyes//Physics and Chemistry of Solids.-2004.-Vol.5, № 3.-P.474-480.
11. Kondratenko P.A., Maksimyuk V.A., Tantsyura L.Y., Two-photon processes in the methylene blue in photo-thermoplastic environment//Chemical Physics.- 1983.- N7.-P.955-962.
12. Dewar M.J.S., Zoebisch E.G., Healy E.F., Stewart J.J.P., AM1: A new general quantum mechanical molecular model//J.Amer.Chem.Soc.-1985.-Vol. 107, N3.-P.3902-3909.
13. Dewar M.J.S., Thiel W., Ground states of molecules. 38. The MNDO method. Applications and parameters // J. Amer. Chem. Soc.–1977.-Vol.99,N15.-P.4899 – 4907.
14. Glushkov A.V., Kondratenko P.A., Lepikh Ya.I. , Fedchuk A.P., Svinarenko A.A., Lovett L., Electrodynamical and quantum - chemical approaches to modelling the electrochemical and catalytic processes on metals, metal alloys and semiconductors//Int. Journ. of Quantum Chem.-2009.-Vol.109,N14.-P.3473-3481.
15. Glushkov A.V., Fedchuk A.P., Kondratenko P.A., Lepikh Ya.I., Lopatkin Yu.M., Svinarenko A.A., The Green's functions and density functional approach to vibrational structure in the photoelectron spectra: Molecules of CH, HF// Photoelectronics.-2011.-Vol.20.-P. 58-62.
16. Velikodnaya V.V., Kondratenko P.A., Lopatkin Yu.M., Glushkov A.V. , Sakun T.N., Kovalenko O.A., Quantum chemical studying the trimethine cyanine dye structure and relaxation dynamics// Photoelectronics.-2014.-Vol.23.-P.112-118.

This article has been received within 2015

UDC 539.186

P. O. Kondratenko, Yu. M. Lopatkin, A. V. Glushkov, T. N. Sakun

EXPERIMENTAL AND THEORETICAL STUDYING PHOTOCONDUCTIVITY OF POLYMERIC LAYERS WITH DYES

Abstract.

We present the results of the experimental and theoretical studying photoconductivity of polymer layers with the dyes. It's investigated photoconductivity of organic dyes in solid polymeric matrices with rectangular pulse excitation light. The obtained experimental data indicate on the quadratic (i.e. non-linear) relationship between photocurrent values that are obtained for two different levels of radiation intensities.

Key words: polymer layers with dyes, photoconductivity

УДК 539.186

П. А. Кондратенко, Ю. М. Лопаткин, А. В. Глушков, Т. Н. Сакун

ЭКСПЕРИМЕНАТЛЬНОЕ И ТЕОРЕТИЧЕСКОЕ ИЗУЧЕНИЕ ФОТОПРОВОДИМОСТИ ПОЛИМЕРНЫХ СЛОЕВ С КРАСИТЕЛЯМИ

Резюме.

Представлены результаты экспериментального и теоретического изучения фотопроводимости полимерных слоев с красителями. Приведены результаты исследования фотопроводимости органических красителей в твердых полимерных матрицах со светом (импульс прямоугольной формы). Полученные экспериментальные данные показывают квадратичное (т.е. нелинейное) соотношение между значениями фототока, полученными для двух различных уровней интенсивности излучения.

Ключевые слова: полимерные слои с красителями, фотопроводимость

УДК 539.186

П. О. Кондратенко, Ю. М. Лопаткін, О. В. Глушков, Т. М. Сакун

ЕСПЕРИМЕНТАЛЬНЕ ТА ТЕОРЕТИЧНЕ ВИВЧЕННЯ ПОЛІМЕРНИХ ШАРІВ З БАРВНИКАМИ

Резюме.

Представлені результати експериментального та теоретичного вивчення фотопровідності полімерних шарів з барвниками. Наведено результати дослідження фотопровідності органічних барвників в твердих полімерних матрицях зі світлом (імпульс прямокутної форми). Отримані експериментальні дані показують квадратичне (тобто нелінійне) співвідношення між значеннями фототока, отриманими для двох різних рівнів інтенсивності випромінювання.

Ключові слова: полімерних шарів з барвниками, фотопроводимість

PACS: 71.24.+q; 78.55.Mb; 78.66.w; UDC 621.315.592

I. K. Doycho[1], S. A. Gevelyuk[1], E. Rysiakiewicz-Pasek[2]

PHOTOLUMINESCENCE OF TAUTOMERIC FORMS OF NANOPARTICLE ENSEMBLES OF DYES BASED ON THE 4-VALENCE STANNUM COMPLEXES IN POROUS SILICA GLASS

[1]I. I. Mechnikov National University of Odessa, Dvoryanska St., 2, Odessa, 65026, Ukraine
[2] Institute of Physics, Wrocław University of Technology, W.Wyspianskiego 27, 50-370 Wrocław, Poland

Luminescence of tautomeric forms of dyes based on the 4-valence stannum complexes was researched. Symmetry of photoluminescence spectra of different tautomeric forms relative to direction of reading of atom positions in the hydrazide fragment was found clockwise or anti clockwise. It was determined that the illumination of nanoparticle ensembles of dyes in A-type porous silica glass is always more intensive than in appropriate solution. It was shown that the luminescence intensity of tautomeric forms increases, if the substituent comes nearer to the coordination set irrespective of type and nature of substituent and type of coordination set. At the same time, change of illumination energy of tautomeric forms depends on both type and nature of substituent and coordination set. The results were explained by the development of inner surface of matrix and also by the features of atom disposition in dye molecule and by interaction between them.

1. INTRODUCTION

Interest to the dyes on base of the 4-valence stannum complexes is non-random, as far as it is known [1-3] that such dyes are most sensitive to the gas composition of environment, therefore they can be used for construction of gas sensors, used for the ecological monitoring [4]. It is a big group of dyes, which are close structurally and differ with some details of their molecular composition only. So arise an opportunity to research the influence of these details on the optical properties of dyes. Investigation of the mechanism of optical processes in such systems will make it possible to improve the luminescence efficiency of new nanostructures. It would give the opportunity to create new generation of microelectronic devices, such as new classes of luminophores and photosensitive optoelectronics elements, which would promote expansion of potential resources of optoelectronics.

It is known [5] that the dyes usually luminesce onle in the solutions, which provide formation of electron-vibration sublevels in the system, so its illumination is a result of transitions among them. We managed to find luminescence of nanoparticle ensembles of dyes formed in A-type porous silica glass. Illumination intensity of such system considerably exceeds luminescence intensity of appropriate solution.

The photoluminescence spectra of all the feasible tautomeric forms of dyes based on the 4valence stannum complexes with coordination sets of 2 types and with the substituent in hydrazide fragment of both nicotinoyl (HN^+) and benzoyl types were researched in the present paper. The last ones were of 2 sorts: hydroxyl (OH) and amine (NH_3). We studied 4-dimethylaminbenzaldehydes $\{SnCl_4ON\}$ and 2hydroxynaftaldegydes $\{SnCl_3O_2N\}$. Fig.1 shows the structural formulas of appropriate coordination sets (e.g., see [6]).

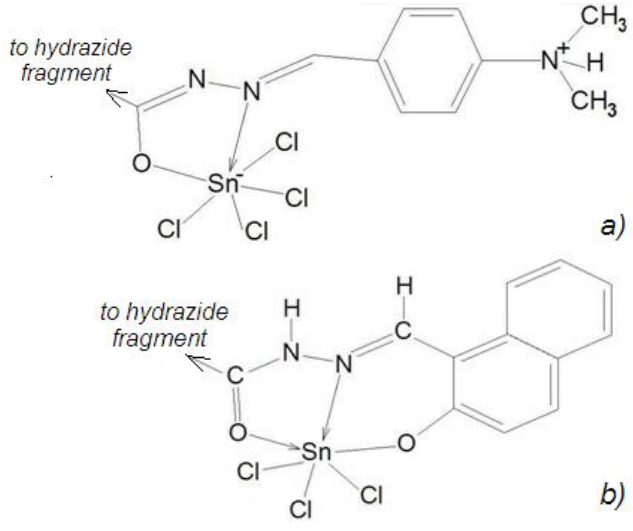

Fig. 1. Structural formulas of coordination sets of 4-dimethylaminbenzaldehydes (a) and 2hydroxynaftaldegydes (b) in the case of hydroxyl substituent. Loss of hydrogen atom on nitrogen atom occurs for providing electroneutrality for amine substituents

Hydrazide fragment represents usual benzene ring with substituent *(A)*. The substituent can be of nicotinoyl or benzoyl type. In the first case some nitrogen group incorporates into the benzene ring directly (i.e. in fact a substitution of carbon atom with nitrogen one takes place), in the second case one of the hydrogen atoms in some position of hydrazide fragment is substituted with hydroxyl or amine group. The isomeric dyes, which differ only in substituent *(A)* position relative to the hydrazide fragment, are called the dyes with different tautomeric forms. Substituent position in current tautomeric form is designated by number. The bond, connecting the hydrazide fragment with the coordination set, is market as «1». One indicates the other positions with the natural numbers anticlockwise from «2» to «6» by increase. Fig.2 shows the nicotinoyl substituent in position «5», and benzoyl one in position «3».

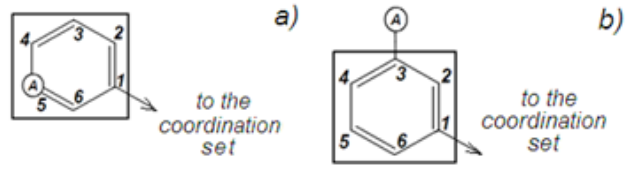

Fig. 2. Hydrazide fragment with constituent of nicotinoyl (a) and benzoyl (b) types

2. MATERIALS AND METHODS

The porous glass ***A*** is obtained from sodium boron-silicate glass. The glass is heated at the temperature of 763 K at 165 hours in order to separate phases rich in silica and sodium-boron. Then it is immersed in 0.5N hydrochloric acid and deionized water. The porosity determined from the mass decrement after etching was: 38%. The texture parameters of investigated glasses were determined by adsorption poroscopy method. The average diameter of pores was 30 nm, total average pore volume was 292 $mm^3\ g^{-1}$ and the average surface area was 54.7 $m^2\ g^{-1}$. The residual fine dispersed secondary silica gel presents in pores of glass after this chemical treatment.

Nanoparticle ensembles of dyes in porous silica glass were formed by soaking glass, embedding it directly into dimethylformamide (DMFA) solution of appropriate dye with concentration 1×10^{-3} gMole l^{-1}. We have selected particularly this solvent because it adsorbs the light in radiated range minimally, and so all dyes fluoresced most intensively in it. Storage duration of glass in the solution of each concrete dye was verified visually and usually formed more than 12 hours. After finish of soaking the specimen was exposed to low-temperature anneal that was necessary in order to provide sufficiently uniform space distribution of nanoparticles in glass.

Composition and structure of the investigated dyes were determined by the complex of spectroscopic and X-ray methods. Fig.1 and Fig.2 show these results.

Photoluminescence spectra were excited with UV laser LCS-DTL-374QT (wavelength λ=355 nm, power 15 mW) and were recorded by standard set-up [7].

3. EXPERIMENTAL RESULTS

Fig.3 shows photoluminescence spectra for three dyes on the basis of complexes, molecular structures of which are the most alike. They all have similar coordination set (depicted in Fig.1,*a),* shortened $\{SnCl_4\}$) and similar tautomeric form «2». They differ only in substituent. The spectra, marked with thick and dash line are for dyes with substituents of benzoil type OH or NH_3, correspondingly, and spectrum, marked with

thin line belongs to dye with substituent of nicotinoyl type NH^+. The left part of Fig.3 corresponds to solutions of the specified dyes in DMFA, and the right one – to ensemble of nanoparticles in porous matrix. One may see from the figure that similar dyes in porous matrix glow considerably more intensively than in solution.

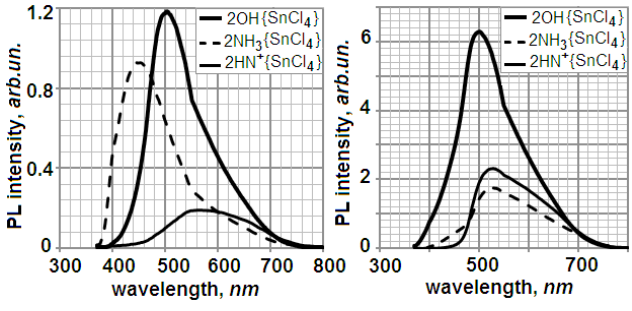

Fig. 3. Photoluminescence spectra for some dyes, which have similar molecular structure, in DMFA solution (on the left) and as nanopArticles ensemble in porous glass (on the right)

A comparison of the photoluminescence spectra of DFMA-solutions of dyes based on the 4-valence stannum complexes and ***A***-type silica porous glass matrixes, soaked in same solution, showed [8] that they have one maximum for all the considered dyes. These spectra only differ in glow intensity and spectral position of this maximum. Taking it into account and as the coordination set preserves its original for isomerous dyes with different tautomeric forms we have compared the histograms, which correspond with the intensity and maximum position of photoluminescence spectrum depending on the complex's tautomeric forms for further research.

Fig.4 shows the histograms of dependences of intensity and maximum position of photoluminescence spectra of dyes with benzoyl type hydroxyl (OH) substituent on its position in tautomeric form for the complexes with coordination sets $\{SnCl_4ON\}$ and $\{SnCl_3O_2N\}$. One can see that the glow intensity of nanoparticle ensemble of dye always exceeds the glow intensity of its solution. Dye with coordination set $\{SnCl_3O_2N\}$ illuminates more intensively both in solution and in porous matrix. However, the photoluminescence intensity for the dye with coordination set $\{SnCl_4ON\}$ increases almost sixfold by transition from solution to the nanoparticles ensemble, whereas for the dye with coordination set $\{SnCl_3O_2N\}$ it increases roughly threefold only.

One can see from histograms, which describe the change of luminescence maximum position, that all the photoluminescence spectra are hyperchromic ones by transition from solution to the nanoparticle ensemble irrespective of tautomeric form and coordination set for the dyes with benzoyl type

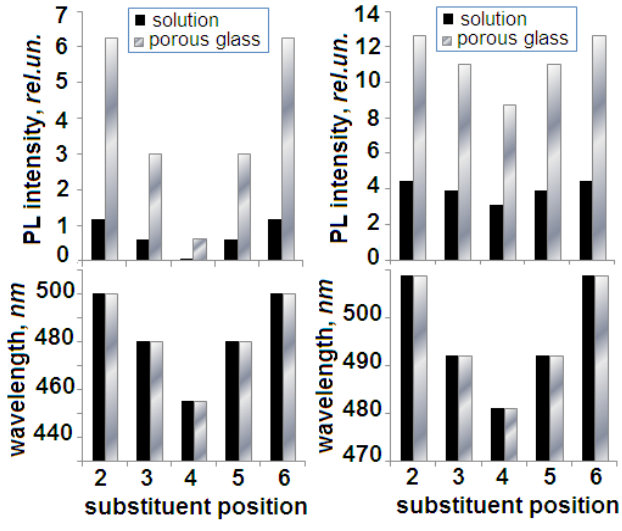

Fig. 4. Dependence of photoluminescence intensity and maximum position of its spectrum for dye with coordination set $\{SnCl_4ON\}$ (on the left) and $\{SnCl_3O_2N\}$ (on the right) on position of benzoyl type OH substituent in tautomeric form

hydroxyl (OH) substituent. We also can mark that the wavelength of illumination differs by the change of the coordination set insignificantly for each tautomeric form. In all the cases the illumination energy of current tautomeric form of dyes based on 2-hydroxynaftaldegyde $\{SnCl_3O_2N\}$ is a little less than of those based on 4dimethylaminbenzaldehyde $\{SnCl_4ON\}$. Besides, one can conclude from histograms that the illumination of dyes with tautomeric form «4», in which the substitutient is most distant from the coordination set in it, has maximal energy.

Fig.5 shows the histograms of dependences of intensity and maximum position of photoluminescence of dyes with benzoyl type amine (NH_3) substituent on it position in tautomeric form for the complexes with coordination sets $\{SnCl_4ON\}$ and $\{SnCl_3O_2N\}$. One can observe for such dyes the same regularity as for ones with hydroxyl substitu-

ent: illumination of nanoparticle ensemble of dye in the porous glass is more intensive than in its solution irrespective of tautomeric form. The illumination of dye with coordination set $\{SnCl_3O_2N\}$ in solution is about 2.5-fold fainter than that with coordination set $\{SnCl_4ON\}$, which has the same tautomeric form. Intensity of photoluminescence for the dye with coordination set $\{SnCl_3O_2N\}$ increases by almost ten times by transition from solution to the nanoparticle ensemble, whereas for the dye with coordination set $\{SnCl_3O_2N\}$ it increases less than 2-fold (while for the tautomeric form «4» it doesn't change practically in this case).

Researching change of maximum position of photoluminescence spectrum for dyes with benzoyl type amine (NH_3) substituent on its position in tautomeric form shows bathochromic shift of photoluminescence spectra for all tautomeric forms of dyes with coordination set $\{SnCl_4ON\}$ by transition from solution to the nanoparticle ensemble, whereas in the case of coordination set $\{SnCl_3O_2N\}$ they remain hyperchromic. Herewith the wavelength of illumination, when tautomeric form changes for the case of coordination set $\{SnCl_3O_2N\}$, changes to a very little degree (within 10 nm). Same effect occurs also for the solution of dyes with coordination set $\{SnCl_4ON\}$. However, wavelength of illumination changes more considerably (up to 50 nm) by transition to the nanoparticle ensemble in this case. Illumination of dyes with tautomeric form «4», in which substituent is the most distant from coordination set, also has maximal energy for this substitutient.

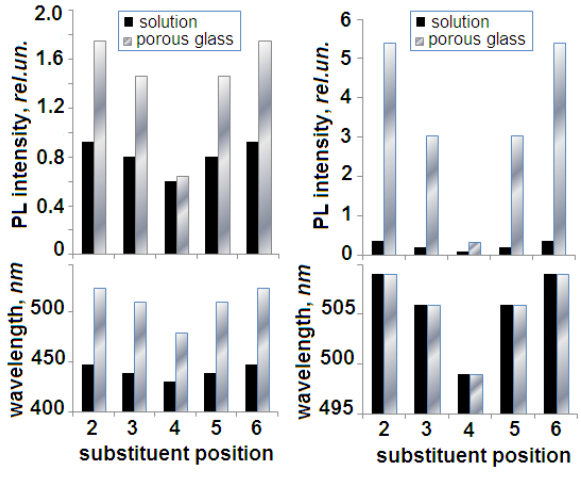

Fig. 5. Dependence of photoluminescence intensity and maximum position of its spectrum for dye with coordination set $\{SnCl_4ON\}$ (on the left) and $\{SnCl_3O_2N\}$ (on the right) on position of benzoyl type NH_3 substituent in tautomeric form

The dyes with nicotinoyl type amine (HN^+) substituent behave somewhat in a different way. Fig.6 shows that the histograms of dependences of photoluminescence intensity on the substitutient position in tautomeric form are very similar for both types of coordination sets for the dyes with such substitutient. In both cases the illumination intensity changes to a little degree for different tautomeric forms in solution, but by transition from solution to the nanoparticle ensemble it increases about by ten times (for the tautomeric form «4» this increment is a little less). The difference is only that the dyes based on 2-hydroxynaftaldegyde $\{SnCl_3O_2N\}$ glow about 4-fold more intensively than those based on 4dimethylaminbenzaldehyde $\{SnCl_4ON\}$.However quite notable difference in dependences of photoluminescence spectra of dyes with nicotinoyl type amine (HN^+) substituent on the substitutient position in tautomeric form deduces from histograms of change of maximum position of photoluminescence spectrum of dyes with such substituent as against similar spectra of dyes with benzoyl substituent. As distinct from dyes with benzoyl type substituents radiant energy decreases for these dyes when substituent moves away from coordination set (irrespective of its type), and thus it turns out to be minimum for tautomeric form «4». Besides, hypsochromic shift of photoluminescence spectra takes place for all tautomeric forms by transition from solution to nanoparticle ensemble for dyes on the basis of 4-dimethylaminbenzaldehyde $\{SnCl_4ON\}$, whereas spectra remain hyperchromic for the dyes on the basis of 2-hydroxynaftaldegyde $\{SnCl_3O_2N\}$ irrespective of tautomeric form.

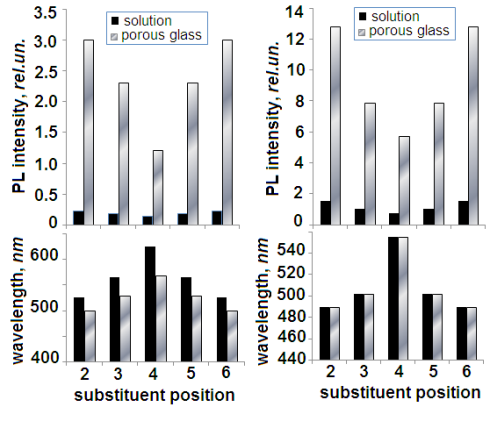

Fig. 6. Dependence of photoluminescence intensity and maximum position of its spectrum for dye with coordination set $\{SnCl_4ON\}$ (on the left) and $\{SnCl_3O_2N\}$ (on the right) on position of nicotinoyl type HN^+ substituent in tautomeric form

4. DISCUSSION

The nature of occurrence of nanoparticle ensemble glow in pores of porous silica glass is the same as in solution: luminescence occurs as consequence of transition between level, situated close to bottom of first excited dye molecule state, and set of electron-vibration sublevels of its ground state. Intensity of photoluminescence at that increases on the account of development of inner matrix surface and due to insignificant probability of aggregations' appearance because of presence of residual silica gel in pores of A-type matrix, it always exceeds intensity of glow of appropriate solution. The silica gel prevents aggregation of dye in big pores by covering the formed dye nanoparticles [9-10]. It is known [11-13] that aggregation would lead to dye bleaching. Effect of increasing of photoluminescence intensity of dye in porous glass takes place irrespective of type of their coordination set and tautomeric form of dyes based on 4-valence stannum complexes.

Invariability of photoluminescence spectra occurs relative to direction of reading of positions of atoms in hydrazide fragment clockwise or anti clockwise for tautomeric forms of all the dyes based of 4-valence stannum complexes both in solution and in the case of nanoparticle ensemble. That is, tautomeric forms with substituents in positions «2» and «6» or «3» and «5» turn out to be equivalent. This conclusion seems trivial at first, as all connections of benzoyl ring are equivalent. Nevertheless, on account of possible intramolecular hydrogen bondings the specified tautomeric forms are not necessarily equivalent. The obtained results show that intramolecular hydrogen bondings are not formed in the researched complexes for any coordination sets, tautomeric forms or substituents.

Glow intensity increases when substituent in hydrazide fragment moves closer to coordination set for all tautomeric forms both in dye solution and in its nanoparticle ensemble. This effect can be considered as direct consequence of symmetry of tautomeric forms relative to direction of reading of atom positions in hydrazide fragment. Indeed, as tautomeric forms are equivalent to substituents in positions «2» and «6» additional rotation symmetry occurs in dye molecule. It causes formation of additional electron rotational levels, fit for radiative transition.

In order to explain the dependence of dye radiative energy on substituent position in tautomeric form one should assume presence of two competing mechanisms in the system. One is connected with interaction of substituent with coordination set, and the other is connected with the degree of freedom of the substituent in relation to benzoyl ring of hydrazide fragment. Let us recall that at substitution nicotinoyl type substituent incorporates into benzoyl ring of hydrazide fragment, substituting carbon therein. At that no additional degree of freedom appears in the substituent. On account of interaction of substituent and coordination set some energy is radiated, and the closer the substituent to coordination set is, the higher the energy is. And that is why histogram, represented in the lower part of the Fig.6, shows that maximal radiative energy corresponds to tautomeric forms with the closest to coordination set substituent «2» (or «6»), and minimal energy corresponds to tautomeric form with the most distant from coordination set substituent «4», as one may see from maximum position of photoluminescence spectra. In the case of benzoyl substitution small hydrogen atom in benzoyl ring of hydrazide fragment is substituted by bulky group of atoms, which can vibrate relative to benzoyl ring. The further from coordination set benzoyl type substituent is, the more intensively it can vibrate, and the more electron-vibration states, fit for radiative transition, occur in the system, that, as follows from histograms shown in the lower part of Fig.4 and Fig.5, with a vengeance compensates losses, connected with substituent's moving away from coordination set. Thus, at benzoyl substitution maximal radiative energy corresponds to tautomeric form with maximally distant from coordination set substituent «4».

5. CONCLUSIONS

Illumination intensity of nanoparticle ensembles of dyes based on the 4-valence stannum complexes in the pores of porous silica glass is always more than illumination intensity of appropriate solution. Herewith the luminescence intensity of dyes of such type with hydroxyl substituent was always more than in case with the amine one.

Symmetry of photoluminescence spectra relative to clockwise or anti clockwise reading of

atom positions in the hydrazide fragment takes place for the tautomeric forms of all the dyes based on the 4-valence stannum complexes both in solution and for nanoparticle ensemble. Herewith the Illumination intensity increases if the substituent in the hydrazide fragment moves closer to the coordination set for all the tautomeric forms both in dye solution and in its nanoparticle ensemble. Probably this effect was connected with appearance of additional electron-rotational states, which would suit for radiative transition. It's a consequence of the degeneration due to abovementioned symmetry. At the same time, it was shown that the change of illumination energy of tautomeric forms depends on both type and nature of substituent and on coordination set.

Radiative energy at nicotinoyl substitution is minimal for the tautomeric form with substituent, which is most distant from coordination set. However, at benzoyl substitution radiative energy will be maximal for such tautomeric forms.

ACKNOWLEDGMENT

The authors express gratitude to associate professor of the Chair of General Chemistry and Polymers of I. I. Mechnikov National University of Odessa, Shmatkova N.V., for useful discussions during preparation of the present paper.

REFERENCES

1. Zhu C., Zheng H., Li D., Liand S., Xu J. Fluorescence quenching method for the determination of sodium dodecyl sulphate with near-infrared hydrophobic dye in the presence of Triton X-100 // Spectrochim. Acta A. – 2004. – V. 60. P. 3173-3179.
2. Zhu Ch-Q., Wu Yu-Q., Zheng H., Chen J-L., Li D-H., Li Sh-H., Xu J-G. Determination of nucleic acids by nearinfrared fluorescence quenching of hydrophobic thiacyanine dye in the presence of Triton X-100. // Anal. Sci. – 2004. – V. 20. P. 945-949.
3. Бордовский В.А., Жаркой А.Б., Кастро Р.А., Марченко А.В. Свойства и структура полимерных материалов, включающих четырёхвалентное олово // Известия РГПУ им. А.И. Герцена. – 2007. – № 38. С.41-50.
4. Oekermann T. Structure-directed electrodeposition of highly porous metal oxidefilms for dye-sensitized solar cells // Porous Glasses - Special Glasses (9th International Seminar, 1-5 September 2009, Wrocław-Szklarska Poręba, Polska). Abstracts. – Institute of Physics, Wrocław: 2009. P.6.
5. Klim O.V., Meshkovski I.K. Formation of mycrooptical elements in bulk of composition material on base of porous glass // Optica Applicata. – 2000. – V. 30, № 4. P.577-579.
6. Shmatkova N.V., Seifullina I.I., Doycho I.K., Gevelyuk S.A., Smyntyna V.A., Viter R.V. Size effects on photoluminescence spectra of nanoparticles of tin(IV) complexes with hydrazones of 4-dimethylaminobenzaldehyde in silica porous matrix // II-nd International conference «Applied physical-inorganic chemistry» – "DIP", Simferopil: 2013. P.197-198.
7. Gevelyuk S.A., Doycho I.K., Lishchuk D.V., Prokopovich L.P., Safronsky E.D., Rysiakiewicz-Pasek E., Roizin Ya.O. Linear extension of porous glasses with modified internal surface in humid environment // Optica Applicata. – 2000. – V. 30, № 4. P.605-611.
8. Шматкова Н.В., Сейфуллина И.И., Дойчо И.К., Гевелюк С.А., Витер Р.В. Фотолюминесценция наноразмерных частиц на основе комплексов Sn(IV) с гидразонами // X Всероссийская конференция с международным участием: «Спектроскопия координационных соединений». – Туапсе: 2013. С.140-142.
9. Tyurin O.V., Bercov Y.M., Zhukov S.O., Levitskaya T.F., Gevelyuk S.A., Doycho I.K., Rysiakiewicz-Pasek E. Dye aggregation in porous glass // Optica Applicata. – 2010. – V. 40, № 2. P.311-321.

10. Viter R.V., Geveluk S.A., Smyntyna V.A., Doycho I.K., Rysiakiewicz-Pasek E., Buk J., and Kordás K. Optical properties of nanoporous glass filled with TiO_2 nanostructures // Optica Applicata. – 2012. – V. 42, № 2. P.307-313.
11. Tyurin A.V., Churashov V.P., Zhukov S.A., Manchenko L.I., Levitskaya T.F., and Sviridova O.I. Interaction of Molecular and Polymolecular Forms of a Dye // Optics and Spectroscopy. – 2008. – V. 104, № 1. P.88-94.
12. Zhang H., Wang L., Jiang W. Label free DNA detection based on gold nanoparticles quenching fluorescence of Rhodamine B // Talanta. – 2011. – V. 85, № 1. P.725–729.
13. Kuznetsov K.A., Laptinska T.V., Mamayev Y.B. Triplen harmonics generation in J-aggeregated dyes in polymeric matrix // Quantum electronics. – 2004. – V. 34, № 10. P. 927-929.

This article has been received within 2015

UDC 621.315.592

I. K. Doycho, S. A. Gevelyuk, E. Rysiakiewicz-Pasek

PHOTOLUMINESCENCE OF TAUTOMERIC FORMSOF NANOPARTICLE ENSEMBLES OF DYES BASED ON THE 4-VALENCE STANNUM COMPLEXES IN POROUS SILICA GLASS

Summary

Luminescence of tautomeric forms of dyes based on the 4-valence stannum complexes was researched. Symmetry of photoluminescence spectra of different tautomeric forms relative to direction of reading of atom positions in the hydrazide fragment was found clockwise or anti clockwise. It was determined that the illumination of nanoparticle ensembles of dyes in A-type porous silica glass is always more intensive than in appropriate solution. It was shown that the luminescence intensity of tautomeric forms increases, if the substituent comes nearer to the coordination set irrespective of type and nature of substituent and type of coordination set. At the same time, change of illumination energy of tautomeric forms depends on both type and nature of substituent and coordination set. The results were explained by the development of inner surface of matrix and also by the features of atom disposition in dye molecule and by interaction between them.

Key words: photoluminescence, porous glass, dyes on base of stannum complexes, tautomeric forms, nanoparticle ensembles

UDC 621.315.592

І. К. Дойчо, С. А. Гевелюк, Е.Ришякевич-Пасек

ФОТОЛЮМІНЕСЦЕНЦІЯ ТАУТОМІРНИХ ФОРМ АНСАМБЛІВ НАНОЧАСТИНОК БАРВНИКІВ НА БАЗІ КОМПЛЕКСІВ 4-ВАЛЕНТНОГО СТАНУМУ В СЕРЕДИНІ ШПАРИСТИХ СИЛІКАТНИХ СТЕКОЛ

Резюме

Досліджено люмінесценцію таутомірних форм барвників на базі комплексів чотиривалентного стануму. Виявлено сіметрію спектрів фотолюмінесценції різних таутомірних форм відносно напрямку відліку позицій атомів у гідразидному фраґменті за стрілкою годинника або проти неї. Виявлено, що світіння ансамблю наночастинок барвника у шпаристому силікатному склі типу А є завжди більш інтенсивним, ніж у відповідному розчині. Продемонстровано, що інтенсивність люмінесценції таутомірних форм зростає, якщо замісник наближається до координаційного вузла, незалежно від типу і природи замісника и типу координаційного вузла. Натомість, змінення енергії випромінювання таутомірніх форм залежить як від типу замісника, тік і від його природи і координаційного вузла. Результати пояснено розгорнутістю внутрішньої поверхні матриці, а також особливостями розміщення атомів всередині молекули барвника та взаємодії між ними.

Ключові слова: фотолюмінесценція, шпаристі стекла, барвники на базі комплексів стануму, таутомірні форми, ансамблі наночастинок

UDC 621.315.592

И. К. Дойчо, С. А. Гевелюк, Е. Рысакеви-Пасек

ФОТОЛЮМИНЕСЦЕНЦИЯ ТАУТОМЕРНЫХ ФОРМ АНСАМБЛЕЙ НАНОЧАСТИЦ КРАСИТЕЛЕЙ НА ОСНОВЕ КОМПЛЕКСОВ 4-ВАЛЕНТНОГО ОЛОВА В ПОРИСТЫХ СИЛИКАТНЫХ СТЁКЛАХ

Резюме

Исследована люминесценция таутомерных форм красителей на основе комплексов четырёхвалентного олова. Обнаружена симметрия спектров фотолюминесценции разных таутомерных форм относительно направления отсчёта позиций атомов в гидразидном фрагменте по, либо против часовой стрелки. Установлено, что свечение ансамбля наночастиц красителя в пористом силикатном стекле типа А всегда интенсивнее, чем в соответствующем растворе. Показано, что интенсивность люминесценции таутомерных форм возрастает при приближении заместителя к координационному узлу, независимо от типа и природы заместителя и типа координационного узла. Вместе с тем, изменение энергии излучения таутомерных форм зависит как от типа заместителя, так и от его природы, и от координационного узла. Результаты объяснены развитостью внутренней поверхности матрицы, а также особенностями расположения атомов в молекуле красителя и взаимодействия между ними.

Ключевые слова: фотолюминесценция, пористое стекло, красители на основе комплексов олова, таутомерные формы, ансамбли наночастиц

UDC 541.13

G. P. Prepelitsa

Odessa State Environmental University, 15, Lvovskaya str., Odessa, Ukraine
Odessa National Polytechnical University, 1, Shevchenko av., Odessa, Ukraine
e-mail: quantpre@mail.ru

NEW NONLINEAR ANALYSIS, CHAOS THEORY AND INFORMATION TECHNOLOGY APPROACH TO STUDYING DYNAMICS OF THE THE ERBIUM ONE-RING FIBRE LASER

Within new non-linear analysis, chaos theory and information technology approach it is nu-merically investigated chaos dynamics generation in the erbium one-ring fibre laser (EDFL, 20.9mV strength, λ= 1550.190nm) with the control parameters: the modulation frequency f and dc bias voltage of the electro-optical modulator. It is shown that in depending upon f, V values there are realized 1-period f = 75MHz, V = 10V and f = 60MHz, V = 4V), 2-period (f = 68 MHz, V = 10V or f = 60MHz, V = 6V), chaotic (f = 64MHz, V = 10 V and f = 60MHz, V = 10V) regimes; there are calculated LE, correlation, embedding, Kaplan-York dimensions, Kolmogorov entropy and theoretically shown that chaos in the erbium fiber laser device is generated via intermittency by increasing the DC bias voltage and period-doubling bifurcation by reducing the modulation fre-quency.

1 Introduction

It is very known that a chaos is alternative of randomness and occurs in very simple deterministic systems. Although chaos theory places fundamental limitations for long-rage prediction (see e.g. [1-9]), it can be used for short-range prediction since ex facte random data can contain simple deterministic relationships with only a few degrees of freedom. Chaos theory establishes that apparently complex irregular behaviour could be the outcome of a simple deterministic system with a few dominant nonlinear interdependent variables. The past decade has witnessed a large number of studies employing the ideas gained from the science of chaos to characterize, model, and predict the dynamics of various systems phenomena (see e.g. [1-13]). The outcomes of such studies are very encouraging, as they not only revealed that the dynamics of the apparently irregular phenomena could be understood from a chaotic deterministic point of view but also reported very good predictions using such an approach for different systems.

In a modern quantum electronics and laser physics etc there are many systems and devices (such as multi-element semiconductors and gas lasers etc), dynamics of which can exhibit chaotic behaviour. These systems can be considered in the first approximation as a grid of autogenerators (quantum generators), coupled by different way [2,14,15]. In this paper we present an application of a new and advanced known non-linear analysis, chaos theory and information technology methods [1-20] to studying non-linear dynamics of the erbium one-ring fibre laser (EDFL, 20.9mV strength, λ= 1550.190nm) with the control parameters: the modulation frequency *f* and dc bias voltage of the electro-optical modulator. Technique of non-linear analysis includes a whole sets of new algorithms and advanced known methods such as the wavelet analysis, multi-fractal formalism, mutual information approach, correlation integral analysis, false nearest neighbour algorithm, Lyapunov exponent's (LE) analysis, and surrogate data method, neural networks prediction approach etc (see details in Refs. [1-34]).

2. Methods of studying dynamics of the laser systems

As used non-linear analysis, chaos theory and information technology methods to studying non-linear dynamics of the laser systems have been earlier in details presented [1-20] here we are limited only by the key ideas. As usually, we formally consider scalar measurements $s(n) = s(t_0 + n\Delta t) = s(n)$, where t_0 is the start time, Δt is the time step, and is n the number of the measurements. Packard et al. [18] introduced the method of using time-delay coordinates to reconstruct the phase space of an observed dynamical system. The direct use of the lagged variables $s(n + \tau)$, where τ is some integer to be determined, results in a coordinate system in which the structure of orbits in phase space can be captured. First approach to compute τ is based on the linear autocorrelation function. The second method is an approach with a nonlinear concept of independence, e.g. the average mutual information. Briefly, the concept of mutual information can be described as follows [5,7,13]. One could remind that the autocorrelation function and average mutual information can be considered as analogues of the linear redundancy and general redundancy, respectively, which was applied in the test for nonlinearity. If a time series under consideration have an n-dimensional Gaussian distribution, these statistics are theoretically equivalent as it is shown in Ref. [22].

The goal of the embedding dimension determination is to reconstruct a Euclidean space R^d large enough so that the set of points d_A can be unfolded without ambiguity. There are several standard approaches to reconstruct the attractor dimension (see, e.g., [1,7,23]), but let us consider in this study two methods only. The correlation integral analysis is one of the widely used techniques to investigate the signatures of chaos in a time series. The analysis uses the correlation integral, $C(r)$, to distinguish between chaotic and stochastic systems. To compute the correlation integral, the algorithm of Grassberger and Procaccia [23] is the most commonly used approach. According to this algorithm, the correlation integral is

$$C(r) = \lim_{N\to\infty} \frac{2}{N(n-1)} \sum_{\substack{i,j \\ (1\le i<j\le N)}} H\left(r - |\,\mathbf{y}_i - \mathbf{y}_j\,|\right) \qquad (1)$$

where H is the Heaviside step function with $H(u) = 1$ for $u > 0$ and $H(u) = 0$ for $u \le 0$, r is the radius of sphere centered on $\mathbf{y}_i$ or $\mathbf{y}_j$, and N is the number of data measurements. If the time series is characterized by an attractor, then the integral $C(r)$ is related to the radius r given by

$$d = \lim_{\substack{r\to 0 \\ N\to\infty}} \frac{\log C(r)}{\log r}, \qquad (2)$$

where d is correlation exponent that can be determined as the slop of line in the coordinates $\log C(r)$ versus $\log r$ by a least-squares fit of a straight line over a certain range of r, called the scaling region.

There are certain important limitations in the use of the correlation integral analysis in the search for chaos. To verify the results obtained by the correlation integral analysis, we use surrogate data method. The method of surrogate data [1,7,19] is an approach that makes use of the substitute data generated in accordance to the probabilistic structure underlying the original data. Advanced version is presented in [7-9].

The next step is computing the Lyapunov's exponents (LE). The LE are the dynamical invariants of the nonlinear system. A negative exponent indicates a local average rate of contraction while a positive value indicates a local average rate of expansion. In the chaos theory, the spectrum of LE is considered a measure of the effect of perturbing the initial conditions of a dynamical system. Note that both positive and negative LE can coexist in a dissipative system, which is then chaotic. Since the LE are defined as asymptotic average rates, they are independent of the initial conditions, and therefore they do comprise an invariant measure of attractor. In fact, if one manages to derive the whole spectrum of the LE, other invariants of the system, i.e. Kolmogorov entropy and attractor's dimension can be found. The Kolmogorov entropy, K, measures the average rate at which information about the state is lost with time. An estimate of this measure is the sum of the positive LE. The inverse of the Kolmogorov entropy is equal to an average predictability.

Estimate of dimension of the attractor is provided by the Kaplan and Yorke conjecture. There are a few approaches to computing the LE.

One of them computes the whole spectrum and is based on the Jacobi matrix of system [27]. In the case where only observations are given and the system function is unknown, the matrix has to be estimated from the data. In this case, all the suggested methods approximate the matrix by fitting a local map to a sufficient number of nearby points.

In our work we use the method with the linear fitted map proposed by Sano and Sawada [27] added by the neural networks algorithm [7-10]. To calculate the spectrum of the LE from the amplitude level data, one could determine the time delay τ and embed the data in the four-dimensional space.

3. Chaotic elements in dynamics of the erbium one-ring fibre laser: Some illustrations and conclussions

Here we present results of the quantitative studying a chaotic dynamics in the erbium one-ring fibre laser with the control parameters: the modulation frequency *f* and dc bias voltage of the electro-optical modulator. Feng and et al. [35] have observed experimentally generate chaos in dynamics in the erbium one-ring fibre laser (laser parameters: the initial strength of 20.9 mV, 1550.190 nm wavelength) with added electro-optical modulator made from crystal LiNbO3.

In the first series of measurements (Exp.1) the constant bias voltage was maintained at 10V, the frequency modulation control parameter *f* was *f* = 64-75MHz. In figure 1 there are listed the measured time-series of the output voltage V_{out} dependence on the frequency modulation by Feng and et al. [35] : Up fig. - *f* = 75 MHz (1-period state), Middle fig.- *f* = 68MHz (2-period state), Down fig.- *f* = 64MHz (chaos).

In a second series of measurements (Exp 2.) by Feng and et al. [35] the frequency modulation was kept at the value of 60 MHz, and the constant bias voltage V was varied from 4V till 10V.

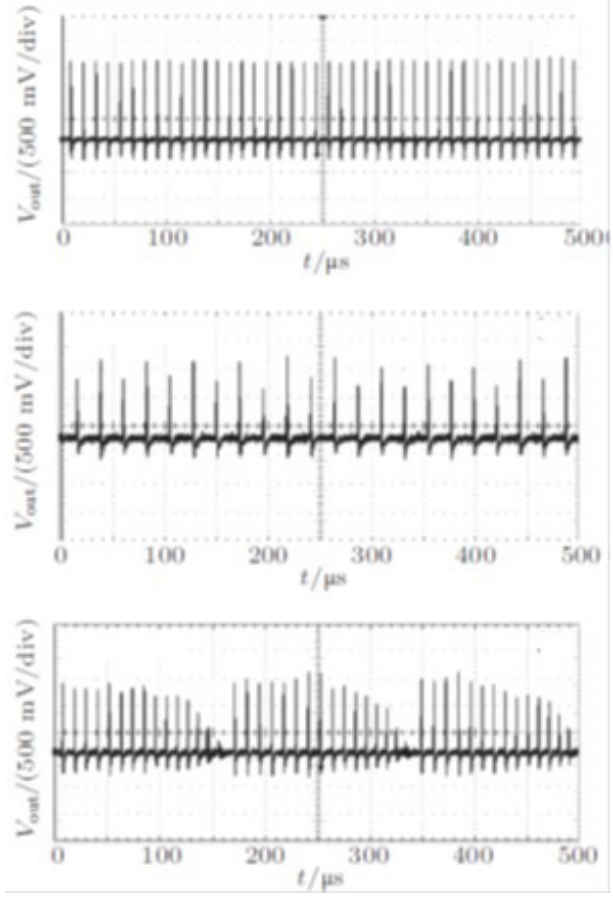

Figure 1. The temporal dependence of V_{out} upon f : Up fig. - f = 75 MHz (1-period state), Middle fig.- f = 68MHz (2-period state), Down fig.- f = 64MHz (chaos).

The theoretical examination shows that depending on the values of *f, V* the laser device is in the one-period (*f* = 75 MHz, *V* = 10V or *f* = 60MHzs, *V* = 4V), two-period (*f*= 68MHz, *V* = 10V or *f* = 60MHz, *V* = 6V), chaotic (*f* = 64MHz, *V* = 10V or f = 60MHz, *V*=10V) states.

Further we have calculated the LE values, correlation dimension, the Kaplan- York dimension, the Kolmogorov entropy and other quantities for two measured temporal series on the above descrinbed methods and algorithms. In table 1 we present the computed values of the Lyapunov's exponents LE λ_1–λ_4 in the descending order and the Kaplan- York dimension, the Kolmogorov entropy for two series of measurements.

Table 1.

Numerical parameters of the chaotic regime in the the erbium one-ring fibre laser with the control parameters: the modulation frequency f and dc bias voltage of the electro-optical modulator: □$_1$□□$_4$ are the Lyapunov exponents in descending order, d_L the Kaplan- York dimension; K – Kolmogorov entropy (our data)

Series	λ1	λ2	λ3
Exp I	0.168	0.0212	-0.223
Exp II	0.172	0.0215	-0.220
Series	λ4	d_L	Kentr
Exp I	-0.323	2.85	0.19
Exp II	-0.318	2.88	0.19

In whole application of the non-linear analysis, chaos theory and information technology methods [7-18] to studying non-linear dynamics of the erbium one-ring fibre laser (EDFL, 20.9mV strength, λ= 1550.190nm) with the control parameters: the modulation frequency *f* and dc bias voltage of the electro-optical modulator shows that there is a chaos in the erbium fiber laser device, generated via intermittency by increasing the DC bias voltage and the period-doubling bifurcation scenario by reducing the frequency modulation.

References

1. H.Abarbanel, R.Brown, J.Sidorowich and L.Tsimring, Rev.Mod.Phys. (1993) 5, 1331.
2. A.Vedenov, A.Ezhov and E. Levchenko, in Non-linear waves. Structure and bi-furcations, ed. by A. Gaponov-Grekhov and M. Rabinovich, (Nauka, Moscow, 1987), pp.53-69.
3. M. Gutzwiller, Chaos in Classical and Quantum Mechanics (N.-Y., Springer, 1990), 720 p.
4. E. Ott, Chaos in dynamical systems, (Cambridge: Cambridge Univ.Press, 2002), 490p.
5. R. Gallager, Information theory and reliable communication (N.-Y.,Wiley, 1986).
6. D. Ullmo, Rep. Prog. Phys. 71, 026001 (2008).
7. A.V. Glushkov, Modern theory of a chaos, (Odessa, Astroprint, 2008), 450p.
8. G.P. Prepelitsa, Nonlinear dynamics of quantum and laser systems with elements of a chaos// Photoelectronics.-2014.-Vol.23.-P.96-106.
9. A. Glushkov, O. Khetselius, S. Brusentseva, P. Zaichko and V. Ternovsky, in Adv. in Neural Networks, Fuzzy Systems and Artificial Intelligence, Series: Recent Adv. in Computer Engineering, vol. 21, ed. by J.Balicki (WSEAS, Gdansk, 2014), pp.69-75.
10. A. Glushkov, A. Svinarenko, V. Buyadzhi, P. Zaichko and V. Ternovsky, in: Adv. in Neural Networks, Fuzzy Systems and Artificial Intelligence, Series: Recent Adv. in Computer Engineering, vol.21, ed. by J.Balicki (WSEAS, Gdansk, 2014), pp.143-150.
11. A.V. Glushkov, O.Yu. Khetselius, A.A. Svinarenko, G.P. Prepelitsa, Energy approach to atoms in a Laser Field and Quantum Dynamics with Laser Pulses of Different Shape, In: Coherence and Ultrashort Pulsed Emission, ed. by F.J. Duarte (Intech, Vienna, 2011), 101-130.
12. A.V. Glushkov, V.N. Khokhlov, I.A. Tsenenko, Atmospheric teleconnection patterns: wavelet analysis, Nonlin. Proc. in Geophys. 11, 285 (2004).
13. A.V. Glushkov, V.N. Khokhlov, N.S. Loboda, N.G. Serbov, K. Zhurbenko, Stoch. Environ. Res. Risk Assess. (Springer) 22, 777 (2008).
14. V.N. Khokhlov, A.V. Glushkov, N.S. Loboda, Yu.Ya. Bunyakova, Atm. Environment (Elsevier) 42, 7284 (2008).
15. A. Glushkov, Y. Bunyakova, A. Fedchuk, N. Serbov, A. Svinarenko and I. Tsenenko, Sensor Electr. and Microsyst. Techn. 3(1), 14 (2007).
16. A.V. Glushkov, V. Kuzakon, V. Ternovsky and V. Buyadzhi, in: Dynamical Systems Theory, vol.T1, ed by J. Awrejcewicz, M. Kazmierczak, P. Olejnik, and J. Mrozowski (Lodz, Polland, 2013), P.461-466.
17. A.V.Glushkov, G. Prepelitsa, A. Svinarenko and P. Zaichko, in:

Dynamical Systems Theory, vol.T1, ed by J. Awrejcewicz, M. Kazmierczak, P. Olejnik, and J. Mrozowski (Lodz, Polland, 2013), pp.P.467-487.
18. A.V.Glushkov, O.Yu.Khetselius, S.V. Brusentseva, P.Zaichko, V.B. Ternovsky, In: Advances in Neural Networks, Fuzzy Systems and Artificial Intelligence, Series: Recent Advances in Computer Engineering, Ed. J.Balicki.(Gdansk, World Sci.Pub.).-2014.-Vol.21.-P.69-75.
19. E. N. Lorenz, Journ. Atm. Sci. 20, 130 (1963).
20. N. Packard, J. Crutchfield, J. Farmer and R. Shaw, Phys.Rev.Lett. 45, 712 (1988).
21. M. Kennel, R. Brown and H. Abarbanel, Phys.Rev.A. 45, 3403 (1992).
22. F. Takens in: Dynamical systems and turbulence, ed by D. Rand and L. Young (Springer, Berlin, 1981), pp.366–381
23. R. Mañé, in: Dynamical systems and turbulence, ed by D. Rand and L. Young (Springer, Berlin, 1981), pp.230–242.
24. M. Paluš, E.Pelikán, K. Eben, P. Krejčíř and P. Juruš, in: Artificial Neural Nets and Genetic Algorithms, ed. V. Kurkova (Springer, Wien, 2001), pp. 473-476.
25. P. Grassberger and I. Procaccia, Physica D. 9, 189 (1983).
26. J. Theiler, S. Eubank, A. Longtin, B. Galdrikian, J. Farmer, Phys.D. 58, 77 (1992).
27. A. Fraser and H. Swinney, Phys Rev A. 33, 1134 (1986).
28. J. Havstad and C. Ehlers, Phys.Rev.A. 39, 845 (1989).
29. M. Sano and Y. Sawada, Phys Rev.Lett., 55, 1082 (1995).
30. T. Schreiber, Phys.Rep. 308, 1 (1999).
31. H. Schuste, Deterministic Chaos: An Introduction (Wiley, N.-Y., 2005), 312 p.
32. A. Glushkov, G. Prepelitsa, S. Dan'kov, V. Polischuk and A. Efimov, Journ. Tech. Phys. 38, 219 (1997).
33. A.G. Vladimirov and E.E. Fradkin, Optics and Spectr. 67, 219 (1989).
34. S.P. Kuznetsov and D.I. Trubetskov, Izv. Vuzov. Ser. Radiophys. 48, 1 (2004).
35. C. Feng, F. Yu-Ling, Y. Zhi-Hai, F.Jian, S.Yuan-Chao, Z. Yu-Zhu Chin. Phys. B. 21, 100504 (2013).

This article has been received within 2015

UDC 541.13

G. P. Prepelitsa

NEW NONLINEAR ANALYSIS, CHAOS THEORY AND INFORMATION TECHNOLOGY APPROACH TO STUDYING DYNAMICS OF THE QUANTUM GENERATOR AND LASER SYSTEMS

Abstract

Within new non-linear analysis, chaos theory and information technology approach it is numerically investigated chaos dynamics generation in the erbium one-ring fibre laser (EDFL, 20.9mV strength, l= 1550.190nm) with the control parameters: the modulation frequency f and dc bias voltage of the electro-optical modulator. It is shown that in depending upon f, V values there are realized 1-period f = 75MHz, V = 10V and f = 60MHz, V = 4V), 2-period (f = 68 MHz, V = 10V or f = 60MHz, V = 6V), chaotic (f = 64MHz, V = 10 V and f = 60MHz, V = 10V) regimes. There are calculated the Lyapunov's exponents, correlation, embedding, Kaplan-York dimensions, Kolmogorov entropy. Theoretically it is shown that a chaos in the erbium fiber laser device is generated via intermittency by increasing the DC bias voltage and period-doubling bifurcation by reducing the modulation frequency.

Keywords: laser system, dynamics, chaos, nonlinear analysis

УДК 541.13

Г. П. Препелиця

НОВЫЙ ПОДХОД НА ОСНОВЕ НЕЛИНЕЙНОГО АНАЛИЗА, ТЕОРИИ ХАОСА И ИНФОРМАЦИОННЫХ ТЕХНОЛОГИЙ К ИЗУЧЕНИЮ ДИНАМИКИ КВАНТОВЫХ ГЕНЕРАТОРОВ И ЛАЗЕРНЫХ СИСТЕМ

Резюме.

На основе нового похода, включающего методы нелинейного анализа, теории хаоса и информационных технологий численно исследована динамика генерации хаоса в эрбиевом одно-кольцевом волоконном лазере (EDFL, 20.9mV, l= 1550.190nm) с управляющими параметрами: частотой модуляции *f* и постоянным напряжением смещения электрооптического модулятора. Показано, что в зависимости от *f, V* в системе реализуются одно-периодный (*f* = 75MHz, V = 10V and *f* = 60MHz, V = 4V), 2-периодный (*f* = 68 MHz, V = 10V or *f* = 60MHz, V = 6V), и хаотический (*f* = 64MHz, V = 10 V and *f* = 60MHz, V = 10V) режимы. Теоретически определены показатели Ляпунова, размерности вложения, Каплана-Йорка, энтропия Колмогорова и др. Теоретически показано, что хаос в эрбиевом волоконном лазере генерируется посредством перемежаемости при увеличения напряжения смещения постоянного тока и через бифуркации удвоения периода при уменьшения частоты модуляции.

Ключевые слова: лазерная система, динамика, хаос, нелинейный анализ

УДК 541.13

Г. П. Препелиця

НОВИЙ ПІДХІД НА ОСНОВІ НЕЛІНІЙНОГО АНАЛІЗУ, ТЕОРІЇ ХАОСУ ТА ІНФОРМАЦІЙНИХ ТЕХНОЛОГІЙ ДО ВИВЧЕННЯ ДИНАМІКИ КВАНТОВИХ ГЕНЕРАТОРІВ І ЛАЗЕРНИХ СИСТЕМ

Резюме.

На основі нового походу, що включає методи нелінійного аналізу, теорії хаосу та інформаційних технологій, чисельно досліджена динаміка генерації хаосу в ербієвому одно-кільцевому волоконному лазері (EDFL, 20.9mV, l = 1550.190nm) з керуючими параметрами: частотою модуляції *f* і постійною напругою зміщення електрооптичного модулятора. Показано, що залежно від *f, V* в системі реалізуються одно-періодний (*f* = 75MHz, V = 10V and *f* = 60MHz, V = 4V), 2-періодний (*f* = 68 MHz, V = 10V or *f* = 60MHz, V = 6V) і хаотичний (*f* = 64MHz, V = 10 V and *f* = 60MHz, V = 10V). Теоретично визначені показники Ляпунова, кореляційна розмірність, розмірності вкладення, Каплана-Йорка, ентропія Колмогорова та ін. Теоретично показано, що хаос в ербієвому волоконному лазері генерується за допомогою переміжаємості при збільшенні напруги зсуву постійного струму і скрізь біфуркації подвоєння періоду при зменшення частоти модуляції..

Ключові слова: лазерна система, динаміка, хаос, нелінійний аналіз

UDC 539.184

I. N. Serga

Odessa State Environmental University, 15, Lvovskaya str., Odessa, Ukraine
e-mail: nucserga@mail.ru

RELATIVISTIC THEORY OF SPECTRA OF PIONIC ATOMS: RADIATION TRANSITION PROBABILITIES

A new theoretical approach to the description of spectral parameters pionic atoms in the excited states with precise accounting relativistic, radiation and nuclear effects is applied to the study of radiation parameters of transitions between hyperfine structure components. As an example of the present approach presents new data on the probabilities of radiation transitions between components of the hyperfine structure transitions 5g-4f, 5f-4d in the spectrum of pionic nitrogen are presented and it is performed comparison with the corresponding theoretical data by Trassinelli-Indelicato

1. Introduction

Our work is devoted to the further application of earlier developed new theoretical approach [1-3] to the description of spectra and different spectral parameters, in particular, radiative transitions probabilities for pionic atoms in the excited states with precise accouting relativistic, radiation. Here problem to be solved is estimate of the hyperfine structure components transitions probabilities. As it was indicated earlier [1-3] nowadays investigation of the pionic and at whole the exotic hadronic atomic systems represents a great interest as from the viewpoint of the further development of atomic and nuclear spectral theories as creating new tools for sensing the nuclear structure and fundamental pion-nucleus strong interactions [1-15]. It is, above all, the strong pion-nucleon interaction, new information about the properties of nuclei and hadrons themselves and their interactions with the nucleus of the measured energy X-rays emitted during the transition pion spectrum of the atom. That is, optics and spectroscopy of pion atoms already in the electromagnetic sector is extremely valuable area of research that provide unique data for different areas of physics. It should be emphasized that the theory of pion spectra of atoms are highly excited, even in the electromagnetic sector (ie short-range strong pion-N interaction

neglects little) is extremely complex and at present, despite the known progress remains very poorly developed. It is about the fundamental theoretical problems describing relativistic atoms considering nuclear, radiation effects, and a completely insufficient spectral data for pion atoms. While determining the properties of pion atoms in theory is very simple as a series of H such models and more sophisticated methods such combination chiral perturbation theory (TC), adequate quantitative description of the spectral properties of atoms in the electromagnetic pion sector (not to mention even the strong interaction sector) requires the development of High-precision approaches, which allow you to accurately describe the role of relativistic, nuclear, radiation QED (primarily polarization electron-positron vacuum, etc.). pion effects in the spectroscopy of atoms.

The most popular theoretical models are naturally (pion is the Boson with spin 0, mass:

$$m_{\pi^-} = 139.57018 \text{ МэВ},$$
$$r_{\pi^-} = 0.672 \pm 0.08 \text{ fm}$$

based on the using the Klein-Gordon-Fock equation, but there are many important problems connected with accurate accounting for as pion-nuclear strong interaction effects as QED radiative corrections (firstly, the vacuum polarization effect etc.). This topic has been a subject of intensive theoretical and experimental interest (see [1-16]). The perturbation theory expansion on the physical; parameter αZ is usually used to take into account the radiative QED corrections, first of all, effect of the polarization of electron-positron vacuum etc. This approximation is sufficiently correct and comprehensive in a case of the light pionic atoms, however it becomes incorrect in a case of the heavy atoms with large charge of a nucleus Z.

The more correct accounting of the QED, finite nuclear size and electron-screening effects for pionic atoms is also very serious and actual problem to be solved more consistently in comparison with available theoretical models and schemes. At last, a development of the comprehensive theory of hyperfine structure and computing radiative transitions probabilities between its components is of a great interest and importance in a modern theory of the pionic atom spectra.

2. Theory

The basic topics of our theoretical approach have been earlier presented [1-3], so here we are limited only by the key elements. Naturally, the relativistic dynamic of a spinless boson (pion) particle is described by the Klein-Gordon-Fock (KGF) equation. As usually, an electromagnetic interaction between a negatively charged pion and the atomic nucleus can be taken into account introducing the nuclear potential A_ν in the KG equation via the minimal coupling $p_\nu \rightarrow p_\nu - qA_\nu$. The relativistic wave functions of the zeroth approximation for pionic atoms are determined from the KGF equation [1]:

$$m^2c^2\Psi(x) = \{\frac{1}{c^2}[i\hbar\partial_t + eV_0(r)]^2 + \hbar^2\nabla^2\}\Psi(x) \quad (1)$$

where *h* is the Planck constant, c the velocity of the light and the scalar wavefunction $\Psi_0(x)$ depends on the space-time coordinate x = (ct,r).

Here it is considered a case of a central Coulomb potential (V_0(r),0). Then the standard stationary equation looks as:

$$\{\frac{1}{c^2}[E + eV_0(r)]^2 + \hbar^2\nabla^2 - m^2c^2\}\varphi(x) = 0 \quad (2)$$

where E is the total energy of the system (sum of the mass energy mc^2 and binding energy ε_0). In principle, the central potential V_0 should include the central Coulomb potential, the radiative (in particular, vacuum-polarization) potential as well as the electron-screening potential in the atomic-optical (electromagnetic) sector. Surely, the full solution of the pionic atom energy especially for the low-excited state requires an inclusion the pion-nuclear strong interaction potential. However, the main problem considered here is computing the radiative transitions probabilities between components of the hyperfine structure for sufficiently high states, when the strong pion-nuclear interaction is not important from the quantitative viewpoint. However, if a pion is on the high orbit of the atom, the strong interaction effects can not be accounted because of the negligible value.

The next step is accounting the nuclear finite size effect or the Breit-Rosenthal-Crawford-Schawlow one. In order to do it we use the widespread Gaussian model for nuclear charge distribution. The advantages of this model in comparison with usually used models such as for example an uniformly charged sphere model and others had been analysed in Ref. [1-]. Usually the Gauss model is determined as follows:

$$\rho(r|R) = \left(4\gamma^{3/2}/\sqrt{\pi}\right)\exp\left(-\gamma r^2\right), \quad (3)$$

where $\gamma = 4\pi/R^2$, R is an effective radius of a nucleus.

In order to take into account very important radiation QED ceffects we use the radiative potential from the Flambaum-Ginges theory [15]. In includes the standard Ueling-Serber potential and electric and magnetic form-factors plus potentials for accounting of the high order QED corrections such as:

$$\Phi_{rad}(r) = \Phi_U(r) + \Phi_g(r) + \Phi_f(r) + .$$
$$+ \Phi_l(r) + \frac{2}{3}\Phi_U^{high-order}(r) \quad (4)$$

where

$$\Phi_U^{high-order}(r) = -\frac{2\alpha}{3\pi}\Phi(r)\frac{0.092Z^2\alpha^2}{1+(1.2\sqrt{2}\,r/r_C)^4}.$$

$$\Phi_l(r) = -\frac{B(Z)}{e}Z^4\alpha^5 m^2 e^{-Z/a_B} \qquad (5)$$

Here e – a proton charge and universal function $B(Z)$ is defined by expression: $B(Z)=0.074+0.35Z\alpha$.

At last to take into account the electron screening effect we use the standard procedure, based on addition of the total interaction potential SCF potential of the electrons, which can be determined within the Dirac-Fock method by solution of the standard relativistic Dirac equations. It should be noted however, that contribution of theses corrections is practically zeroth for the pionic nitrogen, however it can be very important in transition to many-electron as a rule heave pionic atoms.

As we are planning to consider the radiative transitions in heavy pionic atoms in future, this block is remained in our approach.

Further in order to calculate probabilities of the radiative transitions between energy level of the pionic atoms we have used the well known relativistic energy Ivanova-Ivanov approach (look [17-19] and Refs. in [16], which is used for computing probabilities.

The expression for the energy of the hyperfine splitting (magnetic part of) the energy levels of the atom in the pion:

$$E_1^{nlF} = \frac{\mu_I\mu_N e\mu_0\hbar c^2}{4\pi\left(E_0^{nl}-\left\langle nl\left|V_0(r)\right|nl\right\rangle\right)}\times$$

$$\times\left[\frac{F(F+1)-I(I+1)-l(l+1)}{2I}\right]\left\langle nl\left|r^{-3}\right|nl\right\rangle \qquad (6)$$

Here $\mu_N = e\hbar/2m_pc$; other notations are standard. In a consistent precise theory it is important allowance for the contribution to the energy of the hyperfine splitting of the levels in the spectrum of the pion atom due to the interaction of the orbital momentum of the pion with the quadrupole moment of the atomic nucleus. The corresponding part can be presented as follows [3]:

$$< LIFM\left|W_Q\right|LIFM >= \Delta + BC(C+1) \qquad (7)$$

where

$$C=F(F+1)-L(L+1)-I(I+1), \qquad (8)$$

$$B = -\frac{3}{4}\frac{e^2Q}{I(2I-1)}\frac{(\gamma\cdot L\|\eta_2\|\gamma\cdot L)}{\sqrt{L(L+1)(2L-1)(2L+1)(2L+3)}} \qquad (9)$$

$$\Delta = \frac{e^2Q(I+1)}{(2I-1)}\frac{(\gamma\cdot L\|\mu_2\|\gamma\cdot L)L(L+1)}{\sqrt{L(L+1)(2L-1)(2L+1)(2L+3)}} \qquad (10)$$

Here L – is orbital moment of pion, F is a total moment of an atom.

3. Results and conclusions

As example of application of the presented approach, in table 1 we present the data on radiative transition probabilities (in s^{-1}) for hyperfine transitions 5g-4f in the spectrum of the pion nitrogen): Th1- data by Trassinelli-Indelicato; Th2- our data. In theory by Trassinelli-Indelicato (look, for example, [4])

it has been used the standard atomic spectroscopy amplitude scheme when the transitions energies and probabilities are calculated in the known degree separately. At the same time this computing within the relativistic energy approach is performed more correctly and self-consistently (look details in [16] and multiple references therein).

Table 1.

Radiative transition probabilities (in s^{-1}) for hyperfine transitions 5g-4f in the spectrum of the pion nitrogen: Th1- data by Trassinelli-Indelicato; Th2- our data

F-F'	T.I : P (5g-4f)	T.II : P (5g-4f)
5-4	7.13×10^{13}	7.04×10^{13}
4-3	5.47×10^{13}	5.41×10^{13}
4-4	5.27×10^{13}	5.23×10^{13}
3-2	4.17×10^{13}	4.12×10^{13}
3-3	0.36×10^{13}	0.34×10^{13}
3-4	0.01×10^{13}	0.009×10^{13}

In table 2 we present our data for radiative transition probabilities (in s^{-1}) for hyperfine transitions 5f-4d in the spectrum of the pion nitrogen: our data

Table 2.

Radiative transition probabilities (in s^{-1}) for hyperfine transitions 5f-4d in the spectrum of the pion nitrogen: our data

F-F'	Our data (5f-4d)
4-3	4.57×10^{13}
3-2	3.16×10^{13}
3-3	2.98×10^{13}
2-1	2.13×10^{13}
2-2	2.25×10^{13}
2-3	0.01×10^{13}

In whole, the computed radiative transition probabilities values for considered transitions between hyperfine structure components in the spectrum of the pion within theory by Trassinelli-Indelicato and ours demonstrate physically reasonable agreement. , however our values are a little lower. This fact can be explained by difference in the computing schemes and different level of accounting for nuclear finite size, QED and other effects (look details [1-3,20,21]). In any case the data obtained can be considered as sufficiently accurate ones and used in the corresponding applications, indicated in the introduction. There is a great interest the detailed studying the radiative transitions parameters for the heavy pionic toms especially in the Rydberg states. This topic will be considered by us in the next publications.

References

1. Serga I.N., Electromagnetic and strong interactions effects in X-ray spectroscopy of pionic atoms// Photoelectronics.-2011.-Vol.20.-P.109-112.
2. Serga I.N., Dubrovskaya Yu.V., Kvasikova A.S., Shakhman A.N., Sukharev D.E., Spectroscopy of hadronic atoms: Energy shifts// Journal of Physics: C Ser.-2012.- Vol.397.-P.012013.
3. Serga I.N., Relativistic theory of spectra of pionic atoms with account of the radiative corrections: hyperfine structure// Photoelectronics.-2014.-Vol.23.-P.171-175.
4. Deslattes R., Kessler E., Indelicato P., de Billy L., Lindroth E. , Anton J., Exotic atoms//Rev. Mod. Phys. -2003.-Vol.75.-P.35-70; Indelicato P., Trassinelli M., From heavy ions to exotic atoms// arX-iv: physics.-2005.-V1-0510126v1.-16P.
5. Backenstoss G., Pionic atoms//Ann. Rev.Nucl.Sci.-1970.-Vol.20-P.467-510
6. Menshikov L I and Evseev M K, Some questions of physics of exotic atoms// Phys. Uspekhi.2001-Vol. 171.-P.150-184.
7. Mitroy J., Ivallov I.A., Quantum defect theory for the study of hadronic atoms// J. Phys. G: Nucl. Part. Phys.-2001.-Vol.**27.-P.**1421–1433
8. Lyubovitskij V., Rusetsky A., πp atom in ChPT: Strong energy-level shift// Phys. Lett.B.-2000.-Vol.494.-P.9-13.
9. Schlesser S., Le Bigot E.-O., Indelicato P., Pachucki K., Quantum-electro-dynamics corrections in pionic hydrogen // Phys.Rev.C.-2011.-Vol.84.-P.015211 (8p.).
10. Sigg D., Badertscher A., Bogdan M. et al, The strong interaction shift and width of the ground state of pionic hydrogen// Nucl. Phys. A.-1996.-Vol.609.-P.269-309.
11. Gotta D., Amaro F., Anagnostopoulos D., Conclusions from recent pionic–atom experiments//Cold Antimatter Plasmas and Application to Fundamental Physics, ed. Y.Kania and Y.Yamazaki (AIP).-2008.-Vol.CP1037.-P.162-177.
12. Gotta D., Amaro F., Anagnostopoulos D., Pionic Hydrogen//Precision Physics of Simple Atoms and Molecules, Ser. Lecture Notes in Physics (Springer, Berlin / Heidelberg).-2008.-Vol.745.-P.165-186

13. Deloff A., Fundamentals in Hadronic Atom Theory, Singapore: World Scientific, 2003.-352P.
14. Serga I.N., Dubrovskaya Yu.V., Kvasikova A.S., Shakhman A.N., Sukharev D.E., Spectroscopy of hadronic atoms: Energy shifts// Journal of Physics: C Ser.-2012.- Vol.397.-P.012013.
15. Flambaum V.V., Ginges J.S.M., Radiative potential and calculation of QED radiative corrections to energy levels and electromagnetic amplitudes in many-electron atoms //Phys.Rev.-2005.-Vol.72.-P.052115 (16p).
16. Glushkov A.V., Relativistic quantum theory. Quantum mechanics of atomic systems, Odessa: Astroprint, 2008.-700P.
17. Ivanov L.N.,Ivanova E.P., Extrapolation of atomic ion energies by model potential method: Na-like spectra/ // Atom.Data Nucl .Data Tab.-1979.-Vol.24.-P.95-121.
18. Glushkov A.V., Ivanov L.N., Ivanova E.P., Radiation decay of atomic states. Generalized energy approach// Autoionization Phenomena in Atoms.- M.: Moscow State Univ.-1986.
19. Glushkov A.V., Ivanov L.N. Radiation decay of atomic states: atomic residue and gauge non-invariant contributions // Phys. Lett.A.-1992.-Vol.170.-P.33-38.
20. Pavlovich V.N., Serga I.N., Zelentsova T.N., Tarasov V.A., Mudraya N.V., Interplay of the hyperfine, electroweak and strong interactions in heavy hadron-atomic systems and x-ray standards status// Sensor Electronics and Microsyst. Techn.-2010.-N2.-P.20-26.
21. Serga I.N., Relativistic theory of spectra of pionic atoms with account of the radiative and nuclear corrections// Photoelectronics.2013.-Vol.22.-P.84-92

This article has been received within 2015

UDC 539.184

I. N. Serga

RELATIVISTIC THEORY OF SPECTRA OF PIONIC ATOMS WITH ACCOUNT OF THE NUCLEAR AND RADIATIVE CORRECTIONS: RADIATIVE TRANSITION PROBABILITIES

Abstract.

A new theoretical approach to the description of spectral parameters pionic atoms in the excited states with precise accounting relativistic, radiation and nuclear effects is applied to the study of radiation parameters of transitions between hyperfine structure components. As an example of the present approach presents new data on the probabilities of radiation transitions between components of the hyperfine structure transitions 5g-4f, 5f-4d in the spectrum of pionic nitrogen are presented and it is performed comparison with the corresponding theoretical data by Trassinelli-Indelicato.

Keywords: relativistic theory, hyperfine structure, pionic atom, radiative transitions

УДК 539.184

И. Н. Серга

РЕЛЯТИВИСТСКАЯ ТЕОРИЯ СПЕКТРОВ ПИОННЫХ АТОМОВ С УЧЕТОМ ЯДЕРНЫХ И РАДИАЦИОННЫХ ПОПРАВОК: ВЕРОЯТНОСТИ РАДИАЦИОННЫХ ПЕРЕХОДОВ

Резюме.

Новый теоретический подход к описанию спектральных параметров пионных атомов в возбужденном состоянии с учетом релятивистских, радиационных эффектов применен к изучению параметров радиационных переходов между компонентами сверхтонкой структуры. В качестве примера применения представленного подхода, представлены новые данные о вероятности радиационных переходов между компонентами сверхтонкой структуры переходов 5g-4f, 5f-4d в спектре пионного азота и проведено сравнение с соответствующими теоретическими данными Trassinelli-Indelicato.

Ключевые слова: релятивистская теория, сверхтонкая структура, пионный атом, радиационные переходы

УДК 539.184

І. М. Сєрга

РЕЛЯТИВІСТСЬКА ТЕОРІЯ СПЕКТРІВ ПІОННИХ АТОМІВ З УРАХУВАННЯМ ЯДЕРНИХ ТА РАДІАЦІЙНИХ ПОПРАВОК: ЙМОВІРНОСТІ РАДІАЦІЙНИХ ПЕРЕХОДІВ

Резюме.

Новий теоретичний підхід до опису спектральних параметрів піонних атомів у збудженому стані з урахуванням релятивістських, радіаційних ефектів на основі рівняння Клейна-Гордона-Фока застосовано до вивчення параметрів радіаційних переходів між компонентами надтонкої структури. Як приклад застосування представленого підходу, представлені нові дані про ймовірностей радіаційних переходів між компонентами надтонкої структури переходів 5g-4f, 5f-4d в спектрі піоного азоту і проведено порівняння з відповідними теоретичними даними Trassinelli-Indelicato.

Ключові слова: релятивістська теорія, надтонка структура, піоний атом, радіаційні переходи

PACS: 78.30.-j; 78.67.-n

V. S. Grinevich, L. M. Filevska

Odesa Mechnikov National University, ul. Dvoryanska 2, Odesa, 65082 Ukraine, E-mail: grinevich@onu.edu.ua, tel. +38-048-7317403

RAMAN SCATTERING IN NANOSCALE TIN DIOXIDE

The Raman scattering spectra peculiarities are analyzed for nanosized samples of tin dioxide using the authors' own research and the available literature. The presented results show the series of differences in RS spectra in the nanoobjects in comparison with the bulk material. The principle peculiarities comprise: the broadening of peaks, the spectra 'washing-out' (the notable dispersion presence), the peaks shifting to the short waves part from the basic positions, the new lines appearance which are not specific for the bulk SnO2. The principle reason for the deviations is quantum-size effect of the spatial confinement for phonons. The oxygen vacancies notably influence the shape and intensity of RS spectra for studied materials. New bands in the low-frequency part of the spectrum are conditioned by the nanoparticles' normal vibrations.

INTRODUCTION

Metal oxides are the active components in many modern electronic devices [1,2]. There are enough comprehensive reviews devoted to the properties of tin dioxide [2], and to other transparent conductive oxides [1].

Chemical and electrical properties of tin dioxide in the nanocrystalline state strongly depend on the particle size [2,3]. The defectiveness of the subsurface layers, caused by the decrease of crystallites grains, influences the electronic processes in them. This leads both to the appearance of surface vibration modes in the Raman scattering (RS) and in the infrared absorption (IR). At the same time the temperature of the material's reduction by hydrogen decreases and the intercrystalline barriers also influence the charge transport. The Raman spectroscopy is one of the most sensitive methods for the materials science investigations, therefore the nanosized tin dioxide being studied by this method gives plenty of information, especially in the field of its application in electronics.

The present work comprises the comparison of several sources from the available data together with the authors' results on the RS in nanosize tin dioxide.

GENERAL STATE IN RAMAN STUDIES OF NANOSIZE TIN DIOXIDE

Raman scattering (RS) for bulk SnO_2 rutile structure crystals was studied in detail by the authors [4]. Tin dioxide has six atoms in the unit cell, which resulted in 18 branches of vibration modes: 3 acoustic and 15 optical ones. Authors of [5] mentioned, that Raman active modes for SnO_2 rutile are: E_g 476 cm^{-1}, A_{1g} 638 cm^{-1}, B_{2g} 782 cm^{-1}, and B_{1g} 123 cm^{-1}. The last mode is weakly registered, as it has low scattering intensity.

The authors [5] studied SnO_x nanoparticles produced by gas-phase condensation and by "in-flight" sintering using Raman spectroscopy. They identified different vibration states of the rutile crystal phase of bulk SnO_2 particles and of substoichiometric SnO_x of different sizes (5, 10, 20 nm). Raman spectra for different sizes of particles are shown in Figure 1 [5].

As soon as the oxygen content in $SnO_{1.5}$ particles was significantly lower than in the bulk SnO_2, it was supposed a higher density of oxygen vacancies in the samples. The weak modes A_{1g} and B_{2g} are present only for particles' spectra in comparison with the similar modes in the bulk SnO_2. The E_g mode, can be registered only in a bulk SnO_2 sample, the B_{2g} mode is of very weak intensity exists at 747 cm^{-1} for 10 nm and 5 nm

thick samples. Furthermore, the two bands of 275 cm^{-1} and 515 cm^{-1} were observed only in nanocrystalline samples but not in bulk ones. Two possible interpretations are applicable: the band 275 cm^{-1} can be defined as B_{1g} mode and 515 cm^{-1} as A_{2g} mode. Although the both modes are inactive in RS for bulk sample and can't be detected in the rutile lattice, the authors [5] believe that the reduced lattice symmetry caused by the low oxygen stoichiometry make these transitions possible. The band 515 cm^{-1} is most likely connected with surface phonon states, similar to those previously detected by authors [6].

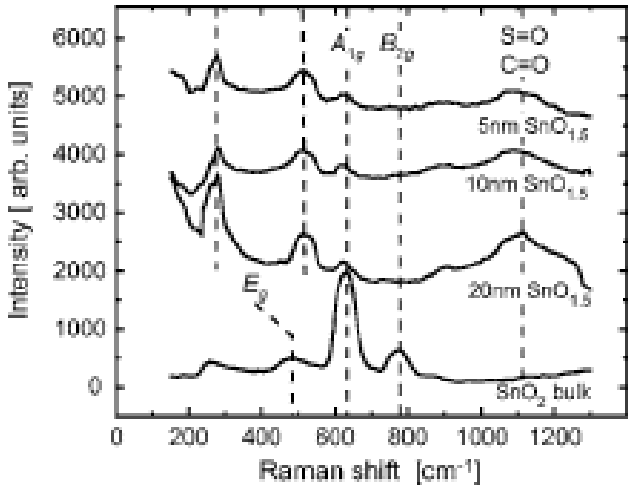

Fig. 1. Raman spectra for $SnO_{1.5}$ nanoparticles of different diameters [6].

Analyzing the entire Raman spectrum for the SnO_2 nanoparticles of 3 to 100 nm [7] they showed that the state of disorder and size of nanoparticles strongly affect the vibration properties of this material. The nanoparticles' sizes decrease is associated with the classical SnO_2 modes shifting and broadening. The correspondence between Raman bands and nanoparticles' sizes are well described by the spatial correlation model, at least for particles bigger than 8-10 nm. The decreasing of grain size leads to the appearance of two bands in the high frequency part of the spectrum. It is suggested that these bands appear due to the contribution of non-stoichiometric surface layer with different symmetry that SnO_2. The measured thickness of this layer is ~ 1.1 nm that is two or three unit cells size. The bands corresponding to the vibration of spherical as a whole nanoparticles appear in the low-frequency part of spectrum.

Raman spectra in the SnO_2- nanorods of different diameters obtained by redox reaction at different growth conditions were measured at room temperature by the authors [8]. The low-frequency Raman peaks were initially registered in the work. It was found that low frequency peaks were shifted to the higher frequency region with nanorods' diameter decreasing. The low frequency peaks' size dependence in SnO_2 nanorods may be caused by surface modes. Raman peaks detected in SnO_2 nanorods differ in depending on wavelengths of the excitation light (514.5 nm and 785 nm), thus, spectral line broadening is observed and the line shape becomes asymmetric. Moreover, some IR- active modes turned into the Raman-active ones, which is caused by such type of order breach as local defects in the crystal lattice and oxygen vacancies in thinner nanorods, which ones are formed as nanorods at the reducing of their diameter to 15 nm or less.

Authors [8], detected 3 categories of peaks: 1st: Low-frequency peaks in the interval of 30 – 100 cm^{-1} were located at 33.8; (34.9); 45.7; (51.9); 57.4; and 73.6 cm^{-1}. 2nd: Classic SnO_2 modes were located at 113.2 (114.6); 472.9 (472.4); 630.4 (630.1); and 768.5 (770.6) cm^{-1}, corresponding to modes B_{1g}, E_g, A_{1g}, and B_{2g} in the bulk SnO_2. 3rd: Abnormal peaks in the range 100-850 cm^{-1} were located at the 157.9; (156.3); 247.4; 392.8; 430.4; 602.1; 711.6 cm^{-1}. Symmetrical and thin Raman peak line in the bulk material broadens and became asymmetrical for the studied SnO_2 nanorods.

Raman peaks for low frequencies interval may be related to the elastic vibrations of nanorods itself, i.e., with existing of confined acoustic- phonon modes in the nanorodes. In [8] it was shown that the wave numbers of the Raman shift for both vibration modes are proportional to the sound velocity and inversely proportional to the nanorods' diameter *d*, i.e., low-frequency peaks are shifted to higher frequencies with nanorods diameter reduction.

As it is shown in [8] the less strictness of the selection rules (k = 0) with increasing disorder or size reduction explains the appearance of anomalous peaks in the range 100-850 cm^{-1} in nanorods samples of a smaller diameter. Infrared modes may turn into weak, but active Raman ones if structural changes are caused by the disorder and

size effects. The peak at 247.4 cm^{-1} corresponds to the IR-active E_u(2)TO, a peak at 430.4 cm^{-1} - IR-active E_u(3)LO, and peaks at 392.8 , 602.1 and 711.6 cm^{-1} - silent A_{2g}, IR-active E_u(l)TO A_{2u}LO modes, respectively. These modes are low active in Raman sense and were observed in other works due to structural distortion caused by local disorder in the crystal lattice and oxygen vacancies. Oxygen vacancies stimulate a non-stoichiometric SnO_x increase on the surface and may also be responsible for IR-active modes appearance. In the nanorods of SnO_2 studied in [8], the atomic ratio of tin to oxygen in the samples with IR-active peaks, is 1.44 (compared to 1.86 ratio for bigger size samples without IR-active modes) which indicates the presence of oxygen vacancies on the nanorods surfaces. The peaks of one and the same mode are different in different papers; the authors [8] explained this by specific microstructures of SnO_x nanorods samples. The peaks 601 and 300 cm^{-1} are stimulated by IR-active E_u(l) TO and $E_u(\upsilon_2)$TO, modes respectively. Nature of the peak at 157.9 (156.3) cm^{-1} stays not evident. It may be caused by sircumnuclear modes as the Raman spectrum reflects the single-phonon density of states.

The diameters of the nanorods in samples A and B, studied in [8], averaged at 15 ± 3 and 22 ± 2 nm respectively. The authors registered the Raman line peak's broadening and its shape asymmetry. As the samples A and B have different diameters, then the surface area to volume ratio for A is more. Moreover, the XPS results showed that samples A have more oxygen vacancies on the surface of the nanorods than samples B, which is mainly responsible for the IR- active modes. Thus, samples A have six IR-active modes and the samples B none. The Lamb theory application to the Raman experiments showed that some surface first-order modes can not be detected under these experimental conditions. Perhaps that forbidden phonon mode for the first order Raman scattering can be Raman active in the second-order Raman scattering due to the less strictness of the selection rules k = 0.

The investigation of RS spectra in tin dioxide crystallites with their sizes 4 nm and 25 nm (Figure 2) is presented in [3].

As it can be seen at the figure, the Raman spectra for different crystallites' size differ sharply. This agrees well with the results of previous studies and is a result of the selection rules violations for nanocrystalline objects due to the large number of surface atoms influence, which contribute to the Raman spectra. Nanocrystalline tin dioxide RS with a crystallites size of ~25nm containing vibration modes E_g, A_{1g} and B_{2g}, were registered by [8] in nanorods and are specific for rutile structure SnO_2.

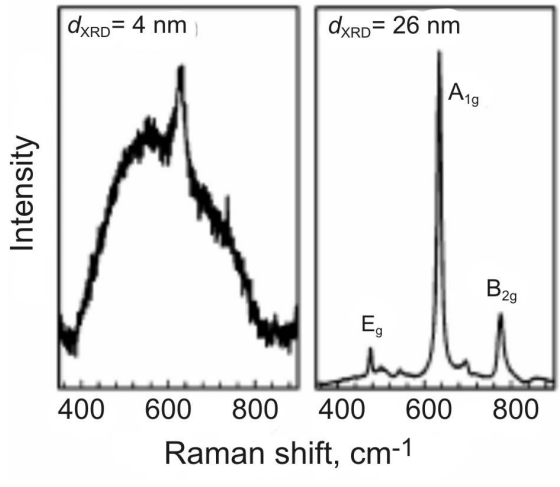

Fig. 2. Raman spectra of tin dioxide with different crystallites size [4].

It was established, that both in TiO_2, and in SnO_2 films with small nanocrystallites sizes the similar quantum size RS effect has place due to violations of phonon momentum conservation principle [9]. Manifestation of the essential role of boundary phonons which contribution increases with nanocrystal size reduction is notable for the first-order Raman scattering due to the whole Brilloin zone phonons involvement in the scattering. Both the dispersion dependence of vibration modes frequencies and half-width intensities for the corresponding peaks in this case leads to a decrease in intensity, to the broadening and the Raman scattering bands shift. For nanocrystalline TiO_2 samples depending on the size of nanocrystallites, the position and the half-width of the Raman lines together with their intensity in the low- and the high-frequency parts of the spectrum seriously varies which is considered by the authors [10] as the spatial restriction of phonons' confinement.

However, as the authors [5, 7, 11] show, the Raman scattering is also influenced both by bound-

ary phonons capture and by deviations from oxygen stoichiometry. When the ratio of O/Ti<2, the short-wave shift of the peaks E_g, the significant broadening of the lines and their intensity change also have place.[9,12]. Moreover, it was found that the most noticeable changes in the Raman spectrum are observed at small deviations from stoichiometry.

The authors [13] also showed a simple link between particle size and the peculiarities of Raman spectra of TiO_2 aerogels by analyzing the evolution of the peaks 142 and 630 cm^{-1}, in dependence on the morphology. Since the regularities of the phonon dispersion for anatase are not known, the authors used a similar dispersion for rutile. At the same time it was shown that there is good agreement between particle size estimated using their model and detected by the X-ray diffraction.

METHODS FOR THE FILMS' PREPARATION AND OF RESEARCH

The films' preparation methods are based on sol-gel technique modified by a polymer (polyvinyl acetate) application and is given in [14]. Bis(acetylacetonato)dichlorotin (BADCT) was used as a tin dioxide precursor [15]. The tin dioxide layers were formed after the 500 – 600 C annealing of the mixed solution of the polymer and precursor in acetone deposited on the glass substrate.

The tin dioxide layer's surface morphology was investigated by the industrial Atom Force microscope (AFM) NT-MDT-206. The measurements were fulfilled by a siliceous probe with a nominal radius ~10 nm (the production firm NT-MDT).

The Raman spectra were excited by He-Ne laser with 632 nm wavelength. Since the samples were thin films on glass substrates the authors enhanced the response by means of directing the laser beam on the film in a sliding mode. The monochromator MDR-23 (LOMO) output was registered by a PC method.

RESULTS AND DISCUSSION

The Raman spectra were studied for the films, obtained from the solution of 5% precursor and 0.1% polymer. Nanosized films structure is confirmed by the surface morphology studies. The AFM image of the sample surface morphology is given at Fig. 3.

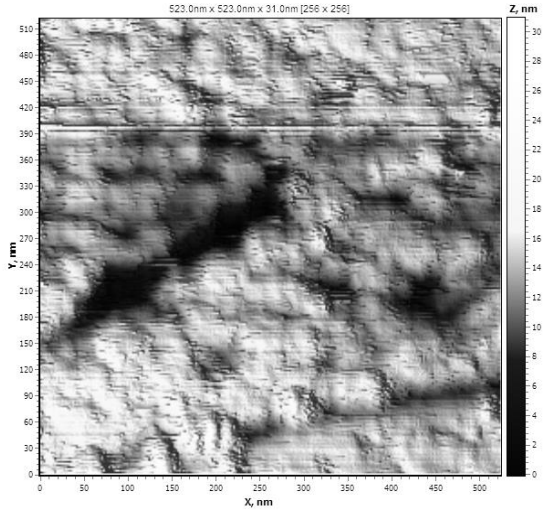

Fig. 3. AFM image of the surface morphology for tin dioxide investigated film.

The resulting RS spectra for the low-frequency region of the nanoscopic tin dioxide layers are not fully legible and asymmetrical. The peaks broadening and their asymmetry may, similar to other researchers, also be the result of selection rules violations for nanocrystalline objects due to the considerable number of surface atoms contribution to the Raman spectra. The surface morphology studies showed the nanoclusters presence in the films. This also allows one to connect the asymmetry in the Raman spectra with size effects and to comment it in the frames of the spatial phonons confinement. Figures 4(a) and 4(b) show the Raman scattering results in tin dioxide films obtained using polymers.

In the range of up to 100 cm^{-1} at least one phonon was registered at 25 cm^{-1} (Stokes region), and in the anti-Stokes region - at 34.9 cm^{-1}. The same peak was registered in [8] and it is connected with the normal vibrations of SnO_2 nanorods. Consequently, also in our case, this peak may contribute as a vibration of nanoparticle as a whole. Stokes peak has a value different from reported in the literature, as nanostructures of our samples differ from the samples of other researchers. The clusters in our films, according to the AFM image (Fig. 3), have a quasi spherical shape.

The interval 100-200 cm^{-1} contains three types

of phonons scattering in the left (a) and in the right parts of the spectrum, and at the same time have the noticeable absence of symmetry in the bands' positions: 97.78, 115.5, 166.7 cm^{-1} and in corresponding them 102.3, 112.39, 165.2 cm^{-1}.

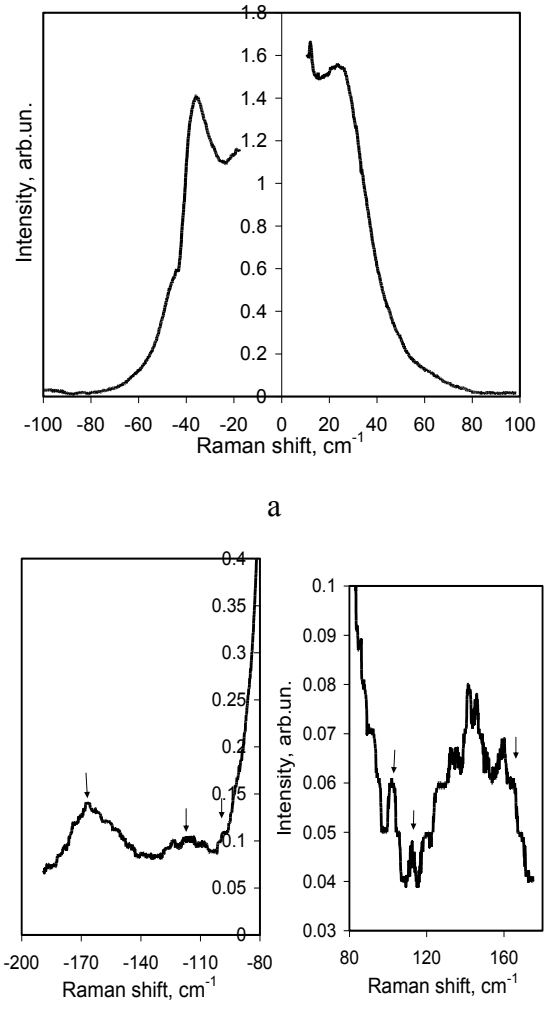

Fig. 4 (a and b). Raman spectra in the tin dioxide films produced using the polymers: a) in the range of 0-100 cm^{-1}; b) in the range of 100-200 cm^{-1} in the anti-Stokes and Stokes regions.

Two of the pointed bands are registered in [8]. The band 115,5 (112,39) cm^{-1}, evidently corresponds to the classical SnO_2 B_{1g}, mode and the band 166,7 (165,2) cm^{-1} is close to the circumnuclear mode 157,9 cm^{-1}, which is also detected in [8]. Such type asymmetry was observed also in [8] where authors studied the Raman scattering in nanoscopic rods of tin dioxide. In the said work the asymmetry of the spectra was influenced by the dimensional limitations in two directions. Basing on the surface morphology investigations at the Fig.3 and in [14], where nanostructured clusters were registered in these films, the Raman spectra asymmetry was also connected with size effects. As it is shown in [8] for nanorods of SnO_2, this asymmetry can be explained by phonons confinement.

However, the Raman shift of the peaks and their broadening in the investigated films can be attributed to another reason. This reason may be the stoichiometric deviation of the film composition, namely, the presence of oxygen vacancies. As it was shown in [11] for titanium dioxide films, the significant changes of this type spectra were observed at small deviations from stoichiometry. The majority researchers of nanostructured tin dioxide reported about oxygen vacancies as the basic defect in the material, defining their optical, electrical and adsorption properties.

CONCLUSION

The RS results presented in the work for the nanoscale tin dioxide showed the similar type of the Raman spectra deviations registered in nanosized material and in bulk crystalline tin dioxide for all studies.

The principal deviations in RS spectra were: the peaks broadening, not full legibility of the spectra (the presence of the noticeable dispersion), and their short waves shift from the basic positions, and the appearance of the new bands which are not specific for the bulk tin dioxide.

One of the main reasons for the said deviations is the effect of the spatial phonons confinement. At the same time the oxygen vacancies essentially influence the shape and intensity of the RS spectra in the investigated material.

The new bands presence in the low frequency part is considered to be due to the nanoparticles vibrations as a whole.

REFERENCES

1. D. S. Ginley, H. Hosono, D. C. Paine, *Handbook of Transparent Conductors*, Springer, New York (2010).
2. M. Batzill, U. Diebold. The surface and materials science of tin oxide // *Prog-*

ress in Surface Science, **79**, pp. 47-154 (2005).
3. M.N. Rumyantseva. *Chemical modification and sensory properties of nanocrystalline tin dioxide*, Authoref. diss ... dokt.him.nauk, Moscow, 46 p (2009) in Russian.
4. R.S. Katiyar, P. Dawson, M.M. Hargreave, G.R. Wilkinson, Dynamics of the rutile structure. III. Lattice dynamics, infrared and the Raman spectra of SnO_2 // *J. Phys. C Solid State Phys.* **4**, pp. 2421-2431(1971). doi: 10.1088/0022-3719/4/15/027.
5. C. Meier, S. Luttjohann, VG Kravets, H. Nienhaus, A. Lorke, P. Ifeacho, H. Wiggers, Ch. Schulz, M. K. Kennedy and F. E. Kruis. Vibrational and defect states in SnOx nanoparticles // *J. of Appl. Phys.* **99** 113108-6 p. (2006).
6. K. N. Yu, Y. Xiong, Y. Liu, and C. Xiong, Microstructural change of nano-SnO_2 grain assemblages with the annealing temperature // *Phys. Rev. B,* **55**, pp. 2666-2671(1997).
7. A. Direguez, A. Romano-Rodrrıguez , A. Vil`a, and J.R. Morante, The complete Raman spectrum of nanometric SnO_2 particles // *J. of Appl. Phys.* **90**(3) pp. 1550-1557 (2001) DOI: 10.1063/1.1385573.
8. Y.-K. Liu, Y. Dong, G.H. Wang, Low frequency and abnormal Raman spectrum in SnO_2 Nanorods // *Chan.Phis. Lett.*, **21**(1) pp. 156-159 (2004).
9. WF Zhang, Y.L. He, M.S. Zhang, Z. Yin, Q. Chen. Raman scattering study on anatase TiO_2 nanocrystals // *J. Phys. D: Appl.Phys.*, **33,** pp. 912-916 (2000).
10. D. Bersani, P.P. Lottici. Phonon confinement effects in the Raman scattering by TiO_2 nanocrystals. *Appl. Phys. Lett.*, **72**(1), pp. 912-916 (1998).
11. T.S. Busko, O.P. Dimitrenko, N.P. Kulish, N.M. White, N.V. Vityuk, A.M. Eremenko, N.P. Smirnova, V.V. Shlapatskaya, Optical properties of radiation-sensitized TiO_2 films with anatase structure // *Problems of Atomic Science and Technology, Series: Physics of Radiation Damage and Radiation Materials*, **92** (2), pp. 43-47 (2008) in Russian.
12. J.C. Parker, R.W. Siegel. Calibration of the Raman spectrum to the oxygen stoichiometry of nanophase TiO_2 // *Appl. Phys. Lett.*, **57**(9) pp. 943-945(1990).
13. S. Kelly, F.H. Pollak, M. Tomkiewiez, Raman spectroscopy as a morphological probe for TiO_2 aerogels // *J.Phys. Chem. B,* **101,** pp. 2730-2734(1997).
14. L.N. Filevskaya, V.A. Smyntyna, V.S. Grinevich Morphology of nanostructured SnO2 films prepared with polymers employment // *Photoelectronics*, 15, pp. 11-14 (2006).
15. B. Ulug, H.M. Türkdemir, A. Ulug, O. Büyükgüngör, M.B. Yücel, V.A. Smyntyna, V.S. Grinevich, L.N. Filevskaya. Structure, spectroscopic and thermal characterization of bis(acetylacetonato) dichlorotin(IV) synthesized in aqueous solution// Ukrainian chemical journal. – 2010. –76, №7. – P. 12-17.

This article has been received within 2015

PACS: 78.30.-j; 78.67.-n

V. S. Grinevich, L. M. Filevska

RAMAN SCATTERING IN NANOSCALE TIN DIOXIDE

Summary

The Raman scattering spectra peculiarities are analyzed for nanosized samples of tin dioxide using the authors' own research and the available literature. The presented results show the series of differences in RS spectra in the nanoobjects in comparison with the bulk material. The principle peculiarities comprise: the broadening of peaks, the spectra 'washing-out' (the notable dispersion presence), the peaks shifting to the short waves part from the basic positions, the new lines appearance which are not specific for the bulk SnO_2. The principle reason for the deviations is quantum-size effect of the spatial confinement for phonons. The oxygen vacancies notably influence the shape and intensity of RS spectra for studied materials. New bands in the low-frequency part of the spectrum are conditioned by the nanoparticles' normal vibrations.

Key words: Raman scattering, tin dioxide, nanoscale effect.

PACS: 78.30.-j; 78.67.-n

В. С. Гріневич, Л. М. Філевська

КОМБІНАЦІЙНЕ РОЗСІЮВАННЯ В НАНОРОЗМІРНОМУ ДІОКСИДІ ОЛОВА

Резюме

На основі власних досліджень авторів і аналізу наявної літератури в роботі розглянуті особливості спектрів комбінаційного розсіювання в нанорозмірних зразках двоокису олова. Показаний ряд відмінностей спектрів КР нанооб'єктів від таких для об'ємних матеріалів. Принципові особливості включають розширення піків, зміщення їх від основних положень, розмиття спектрів (присутність помітної дисперсії), появу нових смуг, які нехарактерні для об'ємного SnO_2. Основна причина відхилень - квантово- розмірний ефект просторового обмеження фононів. Суттєвим є вплив вакансій кисню на форму та інтенсивність спектрів комбінаційного розсіяння в досліджуваних матеріалах. Нові смуги в низькочастотній частині спектру обумовлені власними коливаннями наночастинок.

Ключові слова: комбінаційне розсіювання, діоксид олова, нанорозмірний ефект.

PACS: 78.30.-j; 78.67.-n

В. С. Гриневич, Л. Н. Филевская

КОМБИНАЦИОННОЕ РАССЕЯНИЕ В НАНОРАЗМЕРНОМ ДИОКСИДЕ ОЛОВА

Резюме

На основании собственных исследований авторов и анализа имеющейся литературы в работе рассмотрены особенности спектров комбинационного рассеяния в наноразмерных образцах двуокиси олова. Показан ряд отличий спектров КР в нанообъектах от таковых в объемных материалах. Принципиальные особенности включают в себя уширение пиков, смещение их от основных положений, размытие спектров (присутствие заметной дисперсии), появление новых полос, которые нехарактерны для объемного SnO_2. Основная причина отклонений - квантово-размерный эффект пространственного ограничения фононов. Существенно влияние вакансий кислорода на форму и интенсивность спектров КР в изучаемых материалах. Новые полосы в низкочастотной части спектра обусловлены собственными колебаниями наночастиц.

Ключевые слова: комбинационное рассеяние, диоксид олова, наноразмерный эффект.

UDC 539.135

Yu. V. Dubrovskaya, O. Yu. Khetselius, A. V. Ignatenko and D. E. Sukharev

Odessa National Polytechnical University, 1, Shevchenko av., Odessa, Ukraine
Odessa State Environmental University, 15, Lvovskaya str., Odessa, Ukraine
e-mail: nucdubr@mail.ru

RELATIVISTIC AND NONRELATIVISTIC APPROACHES IN THEORY OF PERMITTED BETA-RANSITIONS: AN EFFECT OF ATOMIC FIELD ON FERMI AND INTEGRAL FERMI FUNCTIONS VALUES

Within a new optimized gauge-invariant Dirac-Fock approach it is considered a problem of computing the permitted beta transition probabilities and estimating a quality of computing the Fermi and integral Fermi functions in dependence upon the type of the atomic self-consistent field. It is shown that for small and middle values for the nuclear charge (Z <40) the difference between data obtained from other methods is low (hundredths of %). At the large Z (till Z~ 95; for example the beta decay 241Pu-241Am) calculation in a case of the HFSrel field gives 0.5% lower value for F, and respectively in a case of the GIDF field - 0.8%, compared with the non-relativistic HFSnerel value. This difference is explained by an effect of the squeezing for relativistic orbitals.

1. Introduction

In this paper we go on studying a contribution of different factors which make an influence on the permitted beta decay characteristics and consider a quality of computing the Fermi function and integral Fermi function in our consistent relativistic approach and alternative theoretical methods. Computing the b decay characteristics is traditionally of a great interest that is strengthened due to the new experimental studies of the b decay for a number of nuclei [1-10]. A number of experimental and theoretical papers appeared where the different aspects of the b decay theory and accounting for different factors are considered. Naturally the important topic is problem to get the renewed data about the neutrino mass from the beta decay spectra shape. An exact value of the half-decay period for the whole number of heavy radioactive nuclei is important for standardisation of data about their properties.

Disagreement between different experimental data regarding the b-decay in heavy radioactive nuclei is provided by different chemical environment radioactive nucleus. For example, such disagreement in data on the half-decay period for the ^{241}Pu (see, for example, ref. [1,5,8,9]) is explained in some papers by special beta decay channel. The beta particle in this channel does not transit into free state, but it occupies the external free atomic level. Above important questions of theort one could note the following effects too: a). an influence of choice of atomic field model on the numerical characteristics of the beta decay, especially, it concerned the permitted beta transitions; b). changing electron wave functions as solutions of the corresponding quantum mechanical equations because of the changing atomic electric field and a difference in the valence shells occupation numbers in different chemical substances; c). A changing up limit of integration under calculating the Fermi integral function in different chemical substances [1,6].

As a rule, special tables [9] for the Fermi function and integral Fermi function are used for computing the beta spectrum shape. In ref. [9] calculation scheme is based on the non-relativistic Hartree-Fock-Slater approach, but the finite size of nucleus is taken into account. In paper [4] the relativistic Dirac-Fock (DF) method was used. Note that the DF approach is the most wide spread method of calculation, but, as a rule, the corresponding orbitals basis's are not optimized. Some problems are connected with correct definition of the nuclear size effects, QED corrections etc. We are applying below our gauge invariant DF (GIDF) type approach [11-17] for computing the permitted beta transition probabilities and estimating a quality of computing the Fermi and integral Fermi functions in dependence upon the type of the atomic self-consistent field.

2. Method

The details of our approach have been presented earlier (see, for example, [10,11,17,18]), here we are limited by the key ideas. As it is well known a distribution of the b particles on energy in the permitted transitions is as follows [9]:

$$dW_\beta(E)/dE = \frac{1}{2\pi^3} G^2 \cdot F(E,Z) \times \\ \times E \cdot p \cdot (E_0 - E)^2 \cdot |M|^2 \ . \qquad (1)$$

Here G is the weak interaction constant; E and $p=(E^2-1)^{1/2}$ are an entire energy and pulse of beta particle; $E_0=1+(E_{bn}/m_e c^2)$, E_{bn} is the boundary energy of β-spectrum; |M| is a matrix element, which is not dependent upon an energy in a case of the permitted β- transitions. The key elements of the beta-decay theory for computing the b decay shape and decay half period are the Fermi function and integral Fermi function. The Fermi function F and integral Fermi function f are defined as follows:

$$F(E,Z) = \frac{1}{2p^2}(g_{-1}^2 + f_{+1}^2), \qquad (2a)$$

$$f(E_0,Z) = \int_1^{E_0} F(E,Z) \cdot E \cdot p \cdot (E_0 - E)^2 dE. \qquad (2b)$$

Here f_{+l} and g_{-l} are the relativistic electron radial functions; the indexes $\pm l=c$, where $c=(l-j)/(2j+1)$.

Two schemes of calculation are usually used: i). the relativistic electron radial wave functions are calculated on the boundary of the spherical nucleus with radius R_0 (it has done in ref. [4]); ii). the values of these functions in the zero are used (see ref.[9]).

The normalisation of electron radial functions f_i and g_i provides the behaviour of these functions for large values of radial valuable as follows:

$$g_i(r) \rightarrow r^{-1}[(E+1)/E]^{1/2} \sin(pr + d_l), \qquad (3a)$$

$$f_i(r) \rightarrow r^{-1}(i/|i|)\,[(E-1)/E]^{1/2} \cos(pr + d_l) \qquad (3b)$$

An effect of interaction in the final state between beta electron and atomic electrons with an accuracy to $(aZ/v)^2$ is manifested and further accounted for in the first non-vanishing approximation [8]. This contribution changes the energy distribution of the beta electron on value and is derived in Ref. [1].

As method of calculation of the relativistic atomic fields and electron wave functions, we have used the GIDF approach [10,11]. The potential of Dirac equation includes also the electric and polarization potentials of a nucleus (the gaussian form of charge distribution in the nucleus was used).

All correlation corrections of the PT second and high orders (electrons screening, particle-hole interaction etc.) are accounted for [5]. The GIDF equations for N-electron system are written and contain the potential:

$$V(r) = V(r|nlj) + V_{ex} + V(r|R),$$

which includes the electrical and polarization potentials of the nucleus. The part V_{ex} accounts for exchange inter-electron interaction. The optimization of the orbital basis's is realized by iteration algorithm within gauge invariant QED procedure (look its application in the beta-decay theory [5]). Approach allows calculating the continuum wave functions, taking into account fully an effect of exchange of the continuum electron with

electrons of the atom. Note that this is one of the original moments of the paper. Another original moment is connected with using the consistent QED gauge invariant procedure for optimization of the electron functions basis's. Numerical calculation and analysis shows that used methods allow getting the results, which are more precise in comparison with analogous data, obtained with using non-optimized basis's. The details of the numerical procedure are presented in ref. [11-17].

3. Results and conclusions

The results of computing the atomic field effect of the Fermi function F values (HFS_{nonrel}, GIDF) are listed in Table 1.As the test parameter it is used the parameter:

$$\Delta_2 = \{[F^{rel}_{DIDF} (E, Z)/ F^{nonrel}_{HFS} (E, Z)]-1\}\cdot 100\%,$$

де F^{nonrel}_{HFS} is calculated in the Hartree-FockSlater (HFS) model atomic field (Harston-Pyper,1986), F^{rel}_{DIDF} – GIDF (our data). It is very inmportant to note that difference between data obtained by relativistic methods: GIDF and relativistic HFS is not significant (fractions of present) for the little and middle values of the nuclear charge Z.

Table 1

An influence of the atomic field model on the Fermi function F (E, Z) values: Δ_2 (%)

E_{kin}, keV	Z=20	Z=63	Z=95
10	-0,08	-0,24	-0,79
50	-0,06	-0,23	-0,77
100	+0,04	-0,18	-0,68
500	+0,13	-0,14	-0,61

Nevertheless, for larger Z (till Z =95) the HFS_{rel} calculation gives the value F which is less on 5% in comparison with the corresponding non-relativistic HFS_{nonrel} . For our approach this value is 0,8%. We suppose that this fact is connected with the effect of relativistic squeeze of the orbitals. In this case, the wave function (continuum) is to a greater extent screened from the charge of the atomic nucleus by a relativistic field of atomic electrons than the corresponding non-relativistic one. Further we present the results of computing function F for choosing different definitions of cited function. In the first case, the calculation of the F function is carried out using values electron wave functions on the boundary of the nucleus, in the second case - through the squares of the amplitudes of radial expansion of the wave functions $f^2_{+1}(0) + g^2_{-1}(0)$ when r→0. Here the test parameter is as follows:

$$\Delta_3 = \{[F (E, Z, R=0)) /$$

$$/F (E, Z, R=R_0]-1\}\cdot 100\%,$$

where F (E, Z, R = R0) – the function Fermi calculated the values of the wave functions on the boundary of the nucleus; F (E, Z, R = 0) - the Fermi function values calculated through the squares of the amplitudes of radial expansion of the wave functions $f^2_{+1}(0) + g^2_{-1}(0)$ when r→0. The corresponding results are presented in Table 2.

Table 2

The difference Δ_3 (%) between values of the Fermi function F (E, Z) for different definitions F (E, Z): HFS – (Band et al, 1986,2006), GIDF – our data.

E_{kin}, keV	Z=20		Z=63 GIDF	Z=95	
	HFS	GIDF		HFS	GIDF
0,1	1,35	1,39	12,72	33,9	36,8
1,0	1,37	1,42	12,84	34,1	37,2
50	1,38	1, 45	12,95	34,2	37,6
500	1,50	1,58	13,10	35,5	39,88

With the growing difference in Z values of the F function significantly increase. Similarly, the same situation takes a place with changing the integral Fermi function. In the transition from the first f definition to the second definition of the f function increases for decays:

i). ^{33}P-^{33}S (E_{bound}=249keV),^{35}S-^{35}Cl (E_{bound} =167keV) на 2-4%,

ii). ^{63}Ni-^{63}Cu (E_{bound} =65,8 keV)- на 5%,

iii). ^{155}Eu-^{155}Gd (E_{bound} =140,7 keV)-12%,

iv). ^{241}Pu-^{241}Am (E_{bound} =20,8 keV)-32%.

In literature there are different points of view on the correctness of a determination of the *F* function . We confirm more consistent and corrected definition of the *F* function through the squares of the amplitudes of radial expansion of the wave functions $f^2_{+1}(0) + g^2_{-1}(0)$ when r→0. An important issue is concerned with an area of the formation of $f(E_{bound}, Z)$.

The standard test parameter is as follows:

$$y = \int_0^x F(E,Z)\, Ep\, (E_0 - E)^2\, dE \Big/ \int_0^{E_0} F(E,Z)\, Ep\, (E_0 - E)^2\, dE$$

Ine Table 3 we present our estimates of the forming area for the integral Fermi function *f*

Table 3

The forming area for the integral Fermi function f (our estimates): t=x/E_{bound}

E_{bound} keV	β-decay	*y*, %			
		t=0,3	0,5	0,7	0,9
20,8	^{241}Pu→^{241}Am	67	89	99	100
39,4	^{106}Ru→^{106}Rh	66	88	98	100
65,8	^{63}Ni→^{63}Cu	65	87	97	100
140,7	^{155}Eu→^{155}Gd	63	84	96	100
167,4	^{35}S→^{35}Cl	58	81	95	100
249	^{33}P→^{33}S	53	78	93	100
257	^{45}Ca→^{45}Sc	52	77	91	100

Therefore, we have carried out the detailed quantitative impact assessment of the Fermi function F (E, Z) for a number permitted by beta-decays in dependence upon the choice of an atomic field in a few calculated methods such as HFS, HFS with taking into account the relativistic corrections in the Breit-Pauli approximation and our relativistic optimized DF one. It is shown that for small and middle values for the nuclear charge (Z <40) the difference between data obtained from other methods is low (hundredths of %). At the large Z (till Z~ 95; for example the beta decay ^{241}Pu-^{241}Am) calculation in a case of the HFS_{rel} field gives 0.5% lower value for F, and respectively in a case of the GIDF field - 0.8%, compared with the non-relativistic HFS_{nerel} value. This difference is in our opinion, explained by an effect of the squeezing for relativistic orbitals. In this case, the wave function (of continuum) is to a greater extent screened from the charge of the atomic nucleus by relativistic field of atomic electrons than by corresponding not- relativistic field.

References

1. Glushkov A.V., Khetselius O.Yu., Lovett L., Electron-b-nuclear spectroscopy of atoms and molecules and chemical environment effect on the b-decay parameters// Advances in the Theory of Atomic and Molecular Systems Dynamics, Spectroscopy, Clusters, and Nanostructures. Series: Progress in Theoretical Chemistry and Physics, Eds. Piecuch P., Maruani J., Delgado-Barrio G., Wilson S. (Berlin, Springer).-2009.-Vol. 20.-P. 125-172.
2. Tegen R., Beta decay of the free neutron and a (near) degenerate neutrino mass//Nucl.Phys.A.-2002.-Vol.706.-P.193-202.
3. Izosimov I. N., Kazimov A. A., Kalinnikov V. G., Solnyshkin A. A. and Suhonen J., Beta-decay strength measurement, total beta-decay energy determination and decay-scheme completeness testing by total absorption gamma-ray spectroscopy// Phys. Atom. Nucl.-2004.-Vol. 67, N10.-1876-1882.
4. Kopytin I. V., Karelin K. N., and Nekipelov A. A. Exact inclusion of the coulomb field in the photobeta decay of a nucleus and problem of bypassed elements// Phys. Atom. Nucl.-2004.-Vol. 67, N8.-P.1429-1441.

5. Band I.M., Listengarten M.A., Trzhaskovskaya M.B., Possibility of beta decay in model of atom of the Hartree-Fock-Dirac and influence of chemical composition on the beta decay// Izv. AN USSR.-1987.-Vol.51,N11.-P.1998-200
6. Glushkov A.V., Laser- electron-b-nuclear spectroscopy of atomic and molecular systems and chemical environment effect on the b-decay parameters: Review //Photoelectronics.-2010.-N19.-P.28-42.
7. Karpeshin F.,Trzhaskovskaya M.B., Gangrskii Yu.P.,Resonance Internal Conversion in Hydrogen-Like Ions // JETP.-2004.-Vol.99, N2.-P.286-289.
8. Kaplan I., Endpoint energy in the molecular beta spectrum, atomic mass defect and the negative $m_{\nu_e}^2$ puzzle// J.Phys.G.: Nucl.Part.Phys.-1997.-Vol.23.-P.683-692.
9. Drukarev E.G., Strikman M.I., Final state interactions of beta electrons and related phenomena// JETP.-1986. – Vol.64(10).-P.1160-1168.
10. Gelepov B.C., Zyryanova L.N., Suslov Yu.P. Beta processes.-Leningrad: Nauka, 1972.-372p.
11. Malinovskaya S.V., Dubrovskaya Yu.V., Vitavetskaya L.A., Advanced quantum mechanical calculation of the beta decay probabilities// Low Energy Antiproton Phys. (AIP).-2005.-Vol.796.-P.201-205.
12. Malinovskaya S.V., Dubrovskaya Yu.V., Zelentzova T.N., The atomic chemical environment effect on the b decay probabilities: Relativistic calculation// Kiev University Bulletin. Series Phys.-Math.–2004.-№4 .-C.427-432.
13. Glushkov A.V., Malinovskaya S.V., Dubrovskaya Yu.V., Sensing the atomic chemical composition effect on the b decay probabilities // Sensor Electr. & Microsyst. Techn.-2005.-N1.-P.16-20.
14. Dubrovskaya Yu.V., The atomic chemical environment and beta electron final state interaction effect on beta decay probabilities// Photoelectronics.-2005.-N14.-P.86-88.
15. Dubrovskaya Yu.V., The beta electron final state interaction effect on beta decay probabilities// Photoelectronics.-2006 .-N15.-P.92-94.
16. Turin A.V., Khetselius O.Yu.,. Dubrovskaya Yu.V, The beta electron final state interaction effect on beta decay probabilities for ^{42}Se nucleus within relativistic Hartree-Fock approach//Photoelectronics.-2007.-N16.-P.120-122..
17. Dubrovskaya Yu.V., Atomic chemical composition effect on the beta decay probabilities//Photoelectronics.-Vol.22.-P.124-129.
18. Dubrovskaya Yu.V., Sukharev D.E., Vitavetskaya L.A., Relativistic theory of the beta decay: Environment and final state interaction effects// Photoelectronics.-2011.-Vol.20.-P.113-116

This article has been received within 2015

UDC 539.135

Yu. V. Dubrovskaya, O. Yu. Khetselius, A. V. Ignatenko, D. E. Sukharev

RELATIVISTIC AND NONRELATIVISTIC APPROACHES IN THEORY OF PERMITTED BETA-RANSITIONS: AN EFFECT OF ATOMIC FIELD ON FERMI AND INTEGRAL FERMI FUNCTIONS VALUES

Abstract.

Within a new optimized gauge-invariant Dirac-Fock approach it is considered a problem of computing the permitted beta transition probabilities and estimating a quality of computing the Fermi and integral Fermi functions in dependence upon the type of the atomic self-consistent field. It is shown that for small and middle values for the nuclear charge (Z <40) the difference between data obtained from other methods is low (hundredths of %). At the large Z (till Z~ 95; for example the beta decay ^{241}Pu-^{241}Am) calculation in a case of the HFS_{rel} field gives 0.5% lower value for F, and respectively in a case of the GIDF field - 0.8%, compared with the non-relativistic HFS_{nerel} value. This difference is explained by an effect of the squeezing for relativistic orbitals.

Key words: the probability of beta decay, the Fermi function, model of the atomic field

УДК 539.135

Ю. В. Дубровская, О. Ю. Хецелиус, А. В. Игнатенко, Д. Е. Сухарев

РЕЛЯТИВИСТСКИЙ И НЕРЕЛЯТИВИСТСКИЙ ПОДХОДЫ В ТЕОРИИ РАЗРЕШЕННЫХ БЕТА-ПЕРЕХОДОВ: ВЛИЯНИЕ ВИДА АТОМНОГО ПОЛЯ НА ЗНАЧЕНИЯ ФУНКЦИИ ФЕРМИ И ИНТЕГРАЛЬНОЙ ФУНКЦИИ ФЕРМИ

Резюме.

В новой оптимизированной калибровочно-инвариантной теории Дирака-Фоку рассмотрена проблема вычисления вероятности разрешенных бета переходов и оценки качества вычисления функции Ферми и интегральной функции Ферми в зависимости от типа атомной поля. Проведена детальная количественная оценка влияния выбора атомного поля, генерируемого в методах Хартри-Фока-Слэтера, Хартри-Фока-Слэтера с учетом релятивистских поправок в приближении Брейта-Паули ($ХФС_{рел}$) и авторской версии оптимизированного метода Дирака-Фока (ОДФ) на функцию Ферми $F(E, Z)$ для ряда разрешенных бета распадов. Показано, что для малых и средних значений заряда ядра (Z <40) разница данных, полученных на основе всех методов является незначительной (сотые доли %). При больших Z (двигаясь к Z = 95; ^{241}Pu-^{241}Am) расчет в поле $ХФС_{рел}$ дает на 0,5% меньшую величину для F, а в поле ОДФ на 0.8%, по сравнению с нерелятивистским значением $ХФС_{нерел}$, что связано с эффектом релятивистского сжатия орбиталей.

Ключевые слова: вероятность бета распада, функция Ферми, модель атомного поля.

УДК 539.135

Ю. В. Дубровська, О. Ю. Хецеліус, Г. В. Ігнатенко, Д. Є. Сухарев

РЕЛЯТИВІСТСЬКИЙ І НЕРЕЛЯТІВІСТСКИЙ ПІДХОДИ В ТЕОРІЇ ДОЗВОЛЕНИХ БЕТА- ПЕРЕХОДІВ: ВПЛИВ ВИДУ АТОМНОГО ПОЛЯ НА ЗНАЧЕННЯ ФУНКЦІЇ ФЕРМІ І ІНТЕГРАЛЬНОЇ ФУНКЦІЇ ФЕРМІ

Резюме.

У новій оптимізованої калібрувально-інваріантній теорії Дірака-Фоку розглянута проблема обчислення ймовірності дозволених бета переходів, оцінки якості обчислення функції Фермі і інтегральної функції Фермі в залежності від типу атомної поля. Проведена докладна кількісна оцінка впливу вибору атомного поля, генеруємого у методах Хартрі-Фока-Слетеру, Хартрі-Фока-Слетеру з врахуванням релятивістських поправок у наближенні Брейта-Паулі ($ХФС_{рел}$) і авторської версії оптимізованого методу Дірака-Фоку (ОДФ) на функцію Фермі *F(E,Z)* для ряду дозволених бета розпадів. Показано, що для малих і середніх значень заряду ядра ($Z<40$) різниця даних, отриманих на основі всіх методів є незначною (соті долі %). При більших Z (рухуючись до $Z=95$; ^{241}Pu-^{241}Am) розрахунок у полі $ХФС_{рел}$ дає на 0,5% меншу величину для *F*, а в полі ОДФ на 0.8%, у порівнянні з нерелятивістським значенням $ХФС_{нерел}$, що пов'язано з ефектом релятивістського стиснення орбіталей.

Ключові слова: імовірність бета розпаду, функція Фермі, модель атомного поля

UDC 539.184

O. Yu. Khetselius, T. A. Florko, A. V. Smirnov, Yu. Ya. Bunyakova

Odessa State Environmental University, 15, Lvovskaya str., Odessa, Ukraine
Odessa National Politechnical University, 1, Shevchenko av., Odessa, Ukraine
e-mail: nuckhet@mail.ru

HYPERFINE STRUCTURE PARAMETERS OF THE MERCURY Hg ISOTOPES: CONSISTENT NUCLEAR-QED THEORY

It is presented the consistent theoretical nuclear-QED approach to estimating parameters of the hyperfine structure and electric quadrupole moment of the mercury isotope 201Hg. Analysis of the data shows that an account of the interelectron correlation effects is crucial in the calculation of the hyperfine structure parameters and therefore the conventional methods such as the method of Dirac-Fock (single configuration approximation) as well as their generalized versions with the limited accounting the exchange-correlation effects do not give a sufficiently high accuracy.

1. Introduction

Development of a new effective nuclear schemes and technologies for sensing different nuclear properties, studying the properties of heavy isotopes is of a great importance in the modern atomic, nuclear physics and technologies [1-3]. Among the most important problems one could mention the studying of nuclei, which are available in the little quantities (for example, the lanthanides isotopes, radioactive nuclei far of the stability boundary), search of the super dense nuclei and its sensing, laser governing by parameters of the proton and other beams and sensing their characteristics etc [1-17]. Such possibilities are provided by the modern laser methods and technologies (see, for example, [1,2]).

A high sensibility and resolution ability of laser spectroscopy methods allows investigating the characteristics of nuclei available in the little quantities, heavy isotopes. As an example (see ref. [1-6]) one can mention the CERN technical device for studying the short-lived nuclei which are obtained on the mass-separator in the line with synchrocyclotrone on 600 MeV (ISOLDE apparatus [1]). The shocking results have been obtained in studying of the odd neutron-deficit non-stable isotopes of $^{182\text{-}190}$Hg. The intensity of the ion beams of these isotopes with life time 1-60 min was 10^7-10^9 ions/s. Under excitation of fluorescence by dye pulsed laser radiation the second harmonics of radiation was tuning to region of 2537A and the measurement of the hyperfine structure for this line of Hg was carried out during 1-2 min disposing about 10^8 of the mercury isotope atoms. During transition from nucleus ^{186}Hg to nucleus ^{185}Hg it has been discovered the sharp changing of the middle square of the nuclear radius which is interpreted as sharp changing of the nuclear form (increasing of nonsoherity and electric quadrupole moment) during decreasing the neutrons number. In refs. [17-25] (see also [4,5]) we have developed new effective theoretical atomic method with possibility of advancing corresponding nuclear technology for sensing different parameters, including the hyperfine structure ones, for heavy isotopes and elements available in the little quantities. It is based on experimental receiving the isotope beams on the CERN ISOLDE type apparatus (see detailed description in [1,3,4]) and the précised theoretical and laser spectroscopy empirical estimating the hyperfine structure parameters, nuclear magnetic and electric moments of isotopes. We carried out

sensing and estimating the hyperfine structure (HFS) parameters, magnetic and electric moments of a nucleus for ^{235}U, and others. The HFS calculation theory is based on developed earlier gauge-invariant QED PT formalism with an precise account for exchange-correlation (inter electron interaction corrections), nuclear and QED effects and nuclear relativistic mean field (RMF) theory. New theory has been called as the nuclear-QED PT [26]. Here we present the results of advanced studying the hyperfine structure parameters and electric quadrupole moment a nucleus for the mercury isotopes, namely ^{201}Hg.

Following, [24,25], let us also remind that the accurate measurements of the hyperfine structure parameters for a whole number of heavy isotopes (e.g. [1,6,16]) not only provide the possibility for testing the quantum electrodynamics (QED) in strong fields, but also sensing the hyperfine structure parameters of spectra for heavy atomic systems, electric charge and magnetic moment distributions inside the nucleus [5-10]. Theoretical calculations fulfilled during the last several years apart from the basis Fermi-Breit relativistic contributions also include the magnetic dipole moment distribution inside the nucleus (Bohr-Weisskopf effect) and radiative QED corrections (e.g. [1-6]). In calculations of the heavy ions the well known multi-configuration (MC) Dirac-Fock (DF) approach is widely used (e.g.[14-20]).

2. Theoretical approach to calculating hyperfine structure parameters

Let us describe the key moments of the theoretical scheme. Full details of the whole method of calculating the hyperfine structure constants can be found in [4,5,17-24]. The wave electron functions zeroth basis is found from the Dirac equation solution with potential, which includes the core ab initio potential, electric, polarization potentials of nucleus. All correlation corrections of the second and high orders of PT (electrons screening, particle-hole interaction etc.) are accounted for [17]. The concrete nuclear model is used as described below. A quantitative estimate of the nuclear moments demands realistic proton single-particle wave functions which one could obtain by employing the RMF model of a nucleus. Though we have no guaranty that these wave-functions yield a close approximation to nature, the success of the RMF approach supports our choice (e.g.[26]). These wave functions do not suffer from known deficiencies of other approaches, e.g., the wrong asymptotics of wave functions obtained in a harmonic oscillator potential. The RMF model has historically been designed as a renormalizable meson-field theory for nuclear matter and finite nuclei. The realization of nonlinear self-interactions of the scalar meson led to a quantitative description of nuclear ground states. As a self-consistent mean-field model (for a comprehensive review see Ref. [25]), its ansatz is a Lagrangian or Hamiltonian that incorporates the effective, in-medium nucleon-nucleon interaction. Recently self-consistent models have undergone a reinterpretation which explains their quantitative success in view of the facts that nucleons are composite objects and that the mesons employed in RMF have only a loose correspondence to the physical meson spectrum [25-28]. RMF models are effective field theories for nuclei below an energy scale of 1GeV, separating the long- and intermediate-range nuclear physics from short-distance physics, involving, i.e., short-range correlations, nucleon form factors, vacuum polarization etc, which is absorbed into the various terms and coupling constants.

As it is indicated in refs.[27] the strong attractive scalar (*S:* -400 MeV) and repulsive vector (*V:* +350 MeV) fields provide both the binding mechanism ($S + V$: -50 MeV) and the strong spin-orbit force ($S - V$: -750 MeV) of both right sign and magnitude. In our calculation we have used so called NL3 (c.f.[25]), which is among the most successful parametrizations available.

The scheme of accounting for the finite size effect is in details described in ref. [17]. Here we only note that if the point-like nucleus possesses by some central potential $W(R)$ then transition to potential of the finite nucleus is realized by substitution $W(r)$ on

$$W(r|R) = W(r)\int_0^r dr\, r^2 \rho(r|R) + \int_r^\infty dr\, r^2 W(r)\rho(r|R) .$$

In our case the Coulomb potential for spherically symmetric density $\rho(r|R)$ is:

$$V_{nucl}(r|R) = -((1/r)\int_0^r dr' r'^2 \rho(r'|R) + \int_r^\infty dr' r' \rho(r'|R)$$

Further the standard Dirac-Fock -like equations for a multi-electron system {core-*nlj*} are solved. Formally they fall into one-electron Dirac equations for the orbitals *nlj* with potential:

$$V(r)=2V(r|SCF)+V(r|nlj)+V_{ex}+V(r|R).$$

It includes the electrical and polarization potentials of a nucleus with a finite size. The part V_{ex} accounts for exchange inter-electron interaction. The exchange effects are accounted for in the first two PT orders by the total inter-electron interaction [17]. The core electron density is defined by iteration algorithm within QED procedure [4]. The radiative QED (the self-energy part of the Lamb shift and the vacuum polarization contribution) are accounted for within the QED formalism [4,25]. The hyperfine structure constants are defined by the radial integrals of the known type (e.g. [29,17]):

$$A=\{[(4,32587)10^{-4}Z^2cg_I]/(4c^2-1)\}$$

$$\int_0^\infty drr^2 F(r)G(r)U(1/r^2, R)$$

$$B=\{7.2878\ 10^{-7}\ Z^3Q/[(4c^2-1)I(I-1)\}$$

$$\int_0^\infty drr^2 [F^2(r)+G^2(r)U(1/r^2, R)\ ,$$

Here I is a spin of nucleus, g_I is the Lande factor, Q is a quadruple momentum of nucleus; radial integrals are calculated in the Coulomb units (=3,57 $10^{20}Z^2m^{-2}$; = 6,174 $10^{30}Z^3m^{-3}$). Radial parts F and G of two components of the Dirac function for electron, which moves in the potential are defined by solution of the Dirac equations (PT zeroth order). The other details can be found in refs. [17-25].

3. Estimating the hyperfine structure parameters and conclusions

Earlier we have studied the hyperfine structure of spectra for the elements Be, C, Al, U, which have above cited rare, cosmic isotopes. Here we present advanced data (the Superatom package [4,5] is used) on the HFS parameters and quadrupole electric moment for the ^{201}Hg.

In Table 1 there are listed the experimental and calculated values of the nuclear electric quadrupole moment Q (mb) for ^{201}Hg (from [5,6,23,26]. The calculations were performed on the basis of the non-correlated DF, in the many approximation of DF (MCDF), taking into account the Breit and QED corrections, as well as on the basis of our method (the RMF model for the charge distribution in a nucleus).

Table 1

The values of the nuclear electric quadrupole moment Q (mb) for mercury

Q (мб)	Method	Reference	Год
383,1	At-Nucl	Our work	2013
380,5	Atomic	Glushkov et al	2006
387 (6)	Atomic	Pyykko et al	2005
347	Nuclear	Fornal et al	2001
(43)	Atomic	Ulm et al	1988
385	Muonic	Gunther et al	1983
(40)	Muonic	Hahn et al	1979
485	Muonic	Hahn et al	1979
(68)	Solid	Edelstein-	1975
386	Atomic	Pound	1960
(49)	Atomic	McDermott	1959
267	Atomic	etal	1957
(37)	Solid	Murakawa	1954
390	Atomic	Blaise-	1935
(20)		Chantrel	
455		Dehmelt et al	
(40)		Schuler-	
420		Schmidt	
500			
(50)			
600			
500			

As can be seen, the value of the moment of Q, obtained by us, in the best agreement with the data obtained by a group of Ulm. Comparison of the results of calculations in the framework of our method and the DF (the single-and many-approximation based on the Breit and QED corrections) shows that our values of the constants A are in better agreement with experiment than the DF.

In Table 2 there are listed the experimental and calculated values of the hyperfine constants (in MHz) for the $^3P_1$ state of the neutral mercury atom [5,6,23,26]. Analysis of the data shows that an account of the interelectron correlation effects is crucial in the calculation of the hyperfine structure parameters and therefore the conventional methods such as the method of DF (of single approximation) as well as the method with the limited accounting the exchange-correlation effects do not give a sufficiently high accuracy.

Table 2

Experimental and Calculations meaning of the nuclear electric quadrupole moment Q (mb) for ^{201}Hg and the HFS constants (MHz) for the $^3P_1$ state of the neutral atom of mercury ^{201}Hg

Method	*Q* (mb)	*A* (MHz)	*B* (MHz)
DF	478,13	-4368,266	---
MCDF (Breit+QED)	386,626	-5470,810	---
RMBT	380, 518	-5460, 324	-286,512
This work: EXC	-92,980	-1161,242	-58,478
This work: Breit-QED	-2,582	-20,384	-1,002
This work Total.	380, 518	-5458,420	-283,313
Experiment	Table 1	-5454,569 (0,003)	-280,107 (0,005)

Note: EXC- exchange-correlation contribution;

Analysis shows that a precise agreement between theory and experiment can be reached by means accounting for not only the relativistic and exchange-correlation effects, but the radiative QED corrections, the nuclear effects of Bohr-Weisskopf, Breit-Rosenthal-Crawford-Schawlow etc too.

References

1. Letokhov V.S., Non-linear selective photoprocesses in atoms and molecules.-Moscow: Nauka, 1987.-380P.
2. Klaft I.,Borneis S., Engel T., Fricke B., Grieser R., Huber G., Kuhl T., Marx D., Neumann R., Schroder S., Seelig P., Volker L. Precision laser spectroscopy of ground state hyperfine splitting of H-like $^{209}Bi^{82+}$//Phys.Rev.Lett.-1994.-Vol.73.-P.2425-2427.
3. Glushkov A.V., Relativistic and correlation effects in spectra of atomic systems.-Odessa: Astroprint, 2006.-400P.
4. Glushkov A.V., Khetselius O.Yu., Ambrosov S.V., Loboda A.V., Gurnitskaya E.P., QED calculation of heavy ions with account for the correlation, radiative and nuclear effects// Recent Adv. in Theor. Phys. and Chem. Systems (Springer). -2006.-Vol.15.-P.285-300.
5. Glushkov A.V., Khetselius O.Yu., Ambrosov S.V., Loboda A.V., Chernyakova Yu.G., Svinarenko A.A., QED calculation of the superheavy elements ions: energy levels, radiative corrections and hfs for different nuclear models// Nucl. Phys.A.: Nucl.and Hadr. Phys. –2004.-Vol.734.-P.21-28.
6. Freeman A.J., Frankel R.H., Hyperfine interactions.-N-Y.: Plenum, 1987.-340P.
7. Nagasawa T., Haga A., Nakano M., Hyperfine splitting of hydrogenlike atoms based on relativistic mean field theory// Phys.Rev.C.-2004.-Vol.69.-P. 034322:1–10.
8. Tomaselli M, Kuhl T., Nortershauser W., Borneis S., Dax A., Marx D, Wang H, Fritzsche S., Hyperfine splitting of hydrogenlike thallium//Phys. Rev.A-2002.-Vol.65.-P.022502.
9. Tomaselli M., Kuhl T., Seelig P., Hol-

brow C. and Kankeleit E., Hyperfine splittings of hydrogenlike ions and the dynamic-correlation model for one-hole nuclei// Phys.Rev.C.-1998.-Vol.58, N3.-P.1524-1534.
10. Tomaselli M., Schneider S.M., Kankeleit E., Kuhl T., Ground state magnetization of ^{209}Bi in a dynamic-correlation model// Phys.Rev.C.-1995.-Vol.51, N6.-P.2989-2997.
11. Benczer-Koller N., The role of magnetic moments in the determination of nuclear wave functions of short-lived excited states//J.Phys.CS.-2005.-Vol.20.-P.51-58.
12. Bieron J., Pyykko P., Degree of accuracy in determining the nuclear electric quadrupole moment of radium//Phys. Rev. A.-2005.-Vol.71.-P.032502-1-8.
13. Derevianko A., Porsev S.G., Dressing lines and vertices in calculations of matrix elements with the coupled-cluster method and determination of Cs atomic properties//Phys.Rev. A.-2005.-Vol.71.-P.032509.
14. Safronova M.S., Johnson W.R., Safronova U.I., Excitation energies, hyperfine constants, E1,E2,M1 transition rates and lifetimes of $6s^2nl$ states in TlI and PbII //Phys.Rev.A.-2005.-Vol.71.-P. 052506.
15. Martensson A.M., Gouch D.S., Hanaford P., Relativistic coupled-cluster approach to hyperfine structure of Tl atom//Phys. Rev.A.1993-.-Vol.49.-P.3351-3360.
16. Martensson A.M., Magnetic moment distributions in Tl nuclei// Phys. Rev. Lett.-1995.-Vol.74.-P.2184-2188.
17. Khetselius O.Yu., Hyperfine structure of atomic spectra.-Odessa: Astropritn, 2008.-210P.
18. Khetselius O.Yu., Relativistic perturbation theory calculation of the hyperfine structure parameters for some heavy-element isotopes// Int. Journ. of Quantum Chemistry.-2009.-Vol.109.-N14.-P. 3330-3335
19. Khetselius O.Yu., Gurnitskaya E.P., Sensing the electric and magnetic moments of a nucleus in the N-like ion of Bi // Sensor Electr. and Microsyst. Techn.-2006.-N3.-P.35-39.
20. Khetselius O.Yu., Gurnitskaya E.P., Sensing the hyperfine structure and nuclear quadrupole moment for radium// Sensor Electr. and Microsyst. Techn.-2006.-N2.-P.25-29.
21. Glushkov A.V., Khetselius O.Yu., Gurnitskaya E.P., Florko T.A., Sensing of nuclei available in little quantities by means of laser spectroscopy of hyperfine structure for isotopes: new theoretical scheme (U ,Hg) // Sensor Electr. and Microsyst. Techn.-2007.-N3.-P.21-26.
22. Khetselius O.Yu., On possibility of sensing nuclei of the rare isotopes by means of laser spectroscopy of hyperfine structure// Sensor Electr. and Microsyst. Techn.-2007.-N4.-P.11-16.
23. Khetselius O.Yu.,Hyperfine structure of energy levels for isotopes ^{73}Ge, ^{75}As, ^{201}Hg// Photoelectronics.-2007.-N16.-P.129-132.
24. Khetselius O.Yu., Hyper fine structure of radium// Photoelectronics.-2005.-N14.-P.83-85.
25. Khetselius O.Yu., Hyperfine structure parameters of the heavy isotopes: Consistent nuclear-QED theory // Photoelectronics.-2013.-N22.-P.146-152.
26. Khetselius O.Yu., Quantum structure of electroweak interaction in heavy finite ermi-systems.-Odessa: Astroprint, 2011.
27. Serot B. D., Advances in Nuclear Physics Vol. 16: The Relativistic Nuclear Many Body Problem/ Serot B. D., Walecka J. D.-Plenum Press, New York, 1986.
28. Burvenich T.J., Evers J., Keitel C.H., Dynamic nuclear Stark shift in superintense laser fields// Phys.Rev.C.-2006.-Vol.74.-P.044601-1-044601-10.
29. Dikmen E., Novoselsky A., Vallieres

M., Shell model calculation of low-lying states of ^{110}Sb// J.Phys.G.: Nucl. Part.Phys.-2007.-Vol.34.-P.529-535.
30. Sobel'man I.I. Introduction to theory of atomic spectra.-Moscow: Nauka.-1977.
31. Radtsig A.A.,Smirnov B.M., Parameters of atoms and ions. – Moscow,1986.

This article has been received within 2015

UDC 539.184

O. Yu. Khetselius, T. A. Florko, A. V. Smirnov, Yu. Ya. Bunyakova

HYPERFINE STRUCTURE PARAMETERS OF THE HEAVY ISOTOPES: CONSISTENT NUCLEAR-QED THEORY

Abstract.

It is presented the consistent theoretical nuclear-QED approach to estimating parameters of the hyperfine structure and electric quadrupole moment of the mercury isotope ^{201}Hg. Analysis of the data shows that an account of the interelectron correlation effects is crucial in the calculation of the hyperfine structure parameters and therefore the conventional methods such as the method of Dirac-Fock (single configuration approximation) as well as their generalized versions with the limited accounting the exchange-correlation effects do not give a sufficiently high accuracy.

Key words: hyperfine structure, heavy isotopes, nuclear-QED approach

УДК 539.184

О. Ю. Хецелиус, Т. А. Флорко, А. В. Смирнов, Ю. Я. Бунякова

ПАРАМЕТРЫ СВЕРХТОНКОЙ СТРУКТУРЫ ІЗОТОПОВ Hg В РАМКАХ ПОСЛЕДОВАТЕЛЬНОЙ ЯДЕРНО-КЭД ТЕОРИИ

Резюме.

Рассмотрен последовательный теоретический ядерно-КЭД подход к оценке параметров сверхтонкой структуры и электрического квадрупольного момента ядра изотопа ^{201}Hg. Анализ данных показывает, что учет межэлектронных корреляционных эффектов имеет критически важное значение при расчете параметров сверхтонкой структуры и, следовательно, применение к задаче традиционных методов типа метода Дирака-Фока (в одно- конфигурации приближении), а также его обобщенных версий с ограниченным учетом обменного корреляционных эффектов не дает возможности достичь достаточно высокой точности описания искомых свойств.

Ключевые слова: сверхтонкая структура, тяжелые изотопы, ядерно-КЭД теория

УДК 539.184

О. Ю. Хецелиус, Т. О. Флорко, А. В. Смірнов, Ю. Я. Бунякова

ПАРАМЕТРИ НАДТОНКОЇ СТРУКТУРИ ІЗОТОПІВ Hg В РАМКАХ ПОСЛІДОВНОЇ ЯДЕРНО-КЕД ТЕОРІЇ

Резюме.

Розглянуто послідовний теоретичний ядерно-КЕД підхід до оцінки параметрів надтонкої структури та електричного квадрупольного моменту ядра ізотопу ^{201}Hg. Аналіз даних показує, що урахування між електронних кореляційних ефектів має вирішальне значення при розрахунку параметрів надтонкої структури і, отже, застосування до задачі традиційних методів типу методу Дірака-Фока (в одно-конфігураційному наближенні), а також його узагальнених версій з обмеженим урахуванням обмінно-кореляційних ефектів не дає можливості досягнути достатньо високої точності опису шуканих властивостей. .

Ключові слова: надтонка структура, важкі ізотопи, ядерно-КЕД теорія

UDC 625.315.592

V. A. Borschak. Ie. V. Brytavskyi, M. I. Kutalova

Odessa I. I. Mechnikov National University,
Dvoryanskaya str., 2, Odessa, 65082, Ukraine
Phone: +380(48)7266356, Fax: +380(48)7233461, e-mail: borschak_va@mail.ru

INVESTIGATION OF CHEMICAL AND PHASE COMPOSITION OF CdS-Cu2S SENSORIC LAYERS

A set of studies aimed at clarifying the deviation from the stoichiometry of CuxS compound during the formation and followed over time to establish the characteristics of changes in the chemical composition of the heterojunction components were carried out. The question of relationship between optoelectrical properties of heterostructures and distribution of stoichiometry in the layer of copper sulfide is open, informative and very important for the practical implementation of the developed sensor. Electrochemical analysis and study by X-ray diffraction for large samples set were conducted

Key words: nonideal heterojunction, image sensor, phase composition, XRD

Introduction

Development of technologies for the synthesis of thin film semiconductor materials led to a wide range of application of opto-mechanical and electrical properties of the instrument in the field of electronics, such as further study actively used in the technological aspect Semiconductor is important. In particular among these compounds are attracted interest for modeling the properties and development of various applications applied heterostructures on the cadmium sulfide (CdS) and copper sulfide (Cu_2S), which can serve as the core material photodetectors for use in optical communication devices, particularly in the infrared region spectrum.

In addition, some marked prospects of these nonideal heterostructures in devices fixation ray images [1]. Another area of application material CdS-Cu2S moving towards the development of new gas-chemical sensors [2]. It describes the main advantages of these prototypes sensors: selective gas detection sensitivity and modes of operation at low temperatures.

Thus one of the characteristics of photosensitive heterostructures on the CdS-Cu_2S is the instability of photovoltaic parameters during operation. Eventually decrease circuit voltage and short circuit current, ie the sensor signal with the same levels of photoexcitation decreases in service. Consequently, there is a degradation over time as heterojunction photovoltaic, which can be associated with changes in both the structure element and component properties of films of transition. It is this negative phenomenon becomes an obstacle and a problem with the possible use of these heterostructures for practical applications in sensorics. However, none of the technologies used, does not get photocells released (without the involvement of special protection) from degradation.

It was discovered experimentally [3-5] that chemical methods of sulfide copper-based substitution reaction on the surface of cadmium sulfide lead to the formation of nonstoichiometric compounds Cu_xS. Depending on the reaction conditions the value of x can vary from 1 to 2. It is known that at room temperature phase are more stable sulfide copper halkotsyt - Cu_2S; dyurlit - $Cu_{1.96}S$; dihenyt - $Cu_{1.8}S$; anilit - $Cu_{1.75}S$; kovelit - CuS. Typically, between different phases form a solid solution. Each phase can be deviations from stoichiometry, which causes changes in physical

properties such as crystal lattice parameters, optical and electrical steel. [4] These property changes can be used for determination of bulk samples, and for variations in the properties of sensors based heterostructures CdS-CuS [6]. In the case of thin films and small amount of test material the use of direct techniques of chemical analysis is very complicated.

X-ray diffractometry analysis

Using electrochemical analysis to clarify the mechanisms change with time stoichiometry layer CuS actually proved inconclusive due to the presence of layers simultaneously studied a number of phases with different concentrations of Cu. So for samples that have undergone degradation caused by changing the chemical composition of copper sulfide layer in the electrochemical reduction reaction involved once all steps to separate phases and potential recovery due to varying phase, almost impossible, because they are imposed on the initial section of the recovery.

So for more information on changing the stoichiometry and phase composition distribution layer CuxS studied sensory structures under its degradation over time used the method of phase diffraction analysis [8]. It was involved X-ray diffractometer D8 Advance (Bruker AXS) with emission lines Cu K (wavelength 1.54183 Å, the working potential of the cathode Ua 40 kV, Ia cathodic current 40 mA).

We used scanning modes geometrically symmetric and scanning with a sliding beam falling (GIXRD). In the latter case the angle recorded at the value 0.5, diffraction pattern measured in the range of 20 to 80 mode step scanning step size 0.04, while fixing signal for 5 seconds. Processing and analysis of diffraction spectra was carried out using software Bruker-AXS EVA (11.0.0.3), for modeling spectrograms and further define the parameters studied layers used program Bruker-AXS TOPAS 3.0. Features component composition were studied using pattern database Joint Committee on Powder Diffraction Standards (JCPDS) [8].

For separation of the diffraction peaks due to the different layers of compounds present in the sample, ie contact layer SnO_2, base area and upper CdS films Cu_xS, and in some cases - the upper contact layer Cu or Au, diffraction scans were conducted separately for samples with only a layer of cadmium sulfide, for samples with predeposited on the substrate layer and SnO_2 sample formed with a layer of copper sulfide.

Results and discussion

Radiometric research base layer samples of CdS on a glass substrate with pre-deposited layer of tin oxide allowed to identify distinct diffraction peaks corresponding to these compounds. For spectrum in CdS was the most appropriate JCPDS-41-1049 file corresponding hexagonal lattice of CdS and the constant = 4.14092 Å, p = 6.7198 Å (Fig. 1). According to the comparative pattern JCPDS 41-1049, clear peaks were observed reflections for the crystallographic planes of the following indexes: (100) (002) (101) (102) (110) (103) (112) (004) (203) (114) (105).

During the analysis for each of the superimposed diffraction patterns obtained from the database directory JCPDS, corresponding to potentially available connections and fixed convergence in positions of diffraction peaks experimental data directory [8]. Used comparatives files related to sulfur, copper, oxygen, chlorine (could partly be in bed with incomplete substitution reaction), oxygen (possible oxidation of copper sulfide oxygen atmosphere): JCPDS 33-490 (Cu_2S), JCPDS 29-0578 ($Cu_{1.96}S$), JCPDS 34-0660 ($Cu_{31}S_{16}$), JCPDS 30-0502 ($Cu_{1.92}S$), JCPDS 41-0959 ($Cu_{1.81}S$), JCPDS 23-0958 (Cu_7S_4), JCPDS 06-0464 (CuS), JCPDS 44 -4750 (CuCl), JCPDS 36-5511 (Cu_2O). An example of a typical type of distribution relative intensities of the diffraction peaks of the diffraction angle obtained during scanning newly made and old samples CdS-Cu_xS, presented at ryc. 3, which also marked the position of peaks for compounds of hexagonal CdS and various phases of Cu_xS. Thus was the comparative analysis of the diffraction pattern in terms of identifying compounds present in the samples of all ages. The new samples were detected the possible presence of these copper sulfide phases: Cu_2S, $Cu_{1.96}S$, $Cu_{1.92}S$, Cu_7S_4.

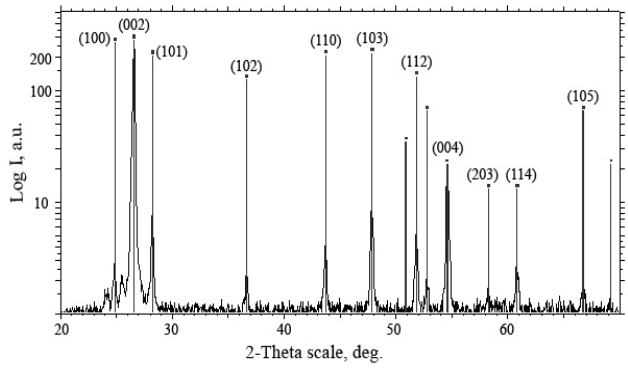

Fig. 1. Diffraction peaks for CdS layer on a glass substrate obtained by sputtering elektrohidrodynamichnoho. Marked provisions peaks for hexagonal CdS and the corresponding crystallographic indexes according to Comparative File JCPDS 41-1049.

For older specimens observed a wide range of diffraction peaks that meet the following phases: Cu_2S, $Cu_{1.96}S$, , CuS. Peaks corresponding to the compounds CuCl and Cu_2O, were not found.

After counting all the relevant peak was obtained comparative table, which indicated the number of peaks of each phase Cu_xS for a new sample and the sample aged 3 years. Evident differences in the composition of new and old sensory elements. This indicates the presence of the process of gradual change in the phase composition of copper sulfide layer, and thus likely outflow of copper from the compound Cu_xS over time. This process may be responsible for changing the stoichiometric Cu_2S layer heterojunction CdS-Cu_2S.

It is known [9] that copper atoms in the crystal lattice have the ability to form CdS acceptor centers that may compensate donor impurities initially present in the base layer. Also listed copper diffusion process along the borders of microcrystalline grains can cause the base effect bypass area. Note that in the investigated heterostructures reliably observed change stoichiometric copper sulfide layer svitlopohlynayuchoho emergence of a number of phases CuhS. Available for the process paths are: oxidation Cu_2S to Cu_2O by oxygen, electric Cu_2S decomposition with the release of free copper atoms and diffusion of copper into the crystal lattice Cu_2S CdS lattice as free atoms and formation of complexes.

Conclusion

Used diffractometry research methodology significantly helped to establish the existence of a number of phases in the non-stoichiometric copper sulfide layer and to make a comparative analysis of the phase distribution for samples of different ages and varying degrees of degradation. It was demonstrated that used in this paper methods of analysis phase composition of copper sulfide layers give unambiguous characterization of the degree of degradation with time sensor samples due to diffusion of copper atoms from the layer to the base layer Cu_xS-CdS.

References

1. V.A. Smyntyna. Sensor based on a non-ideal heterojunction to indicate X-ray images / V.A. Smyntyna, V.A. Borschak, M.I. Kutalova, N.P. Zatovskaya, A. P. Balaban // Semiconductor Physics, Quantum Electronics & Optoelectronics. – 2004. – V. 7. - N 2. - P. 222-223.
2. A. Galdikas. Room-temperature-functioning ammonia sensor based on solid-state Cu_xS films / A. Galdikas, A. Mironas, V. Strazdiene, A. Setkus, I. Ancutiene, V. Janickis // Sensors and Actuators. – 2000. - B 67. – P. 76–83.
3. B. Lepley. Copper diffusion and photovoltaic mechanisms at Cu-CdS contact / B. Lepley, P.H. Nguyen, C. Boutrit and S. Ravelet // J. Phys. D: Appl. Phys. – 1999. – V. 12. – P. 1917-1928
4. K. Moitra. Degradation of the performance of Cu_2S/CdS solar cells due to a two-way solid state diffusion process / K. Moitra, S. Deb // Solar Cells. – 1993. – no. 9. - P. 215-228.
5. H.C. Hsieh. The effect of Cu diffusion in CuS/CdS heterojunction solar cells / H.C. Hsieh // J. Appl. Phys. – 1999. - v. 53. - P. 1727-1733.

6. V. A. Borschak. Dependence of Conductivity of an Illuminated Nonideal Heterojunction on External Bias / V. A. Borschak, V. A. Smyntyna, E. V. Brytavskyi, A. P. Balaban, and N. P. Zatovskaya // Semiconductors. – 2011. - V. 45, no. 7. - P. 894–899.
7. E. Castel. Determination electrochimique de].a ccmposition des couches minoes de sulfure de cuivre non stoechidrétrique / E. Castel and J . Vedel // Analysis. – 1999. – V. 3, No 9. – P. 487-490.
8. В.И. Пунегов. Динамическая дифракция в слоисто-неоднородных системах / В. И. Пунегов // Письма в ЖТФ. – 1994. – Т. 20, в. 2. – С. 25-29
9. Katsuhito Shima. Diffusion of Copper in Cadmium Sulfide Single Crystals / Katsuhito Shima // Jpn. J. Appl. Phys. – 1999. – V. 15. – P. 195-197

This article has been received within 2015

UDC 625.315.592

V. A. Borschak, Ie. V. Brytavskyi, M. I. Kutalova

MODELLING OF RAPID STAGE DECAY OF SIGNAL OF OPTICAL SENSOR BASED ON HETEROSTRUCTURE CdS-Cu_2S

Summary. A set of studies aimed at clarifying the deviation from the stoichiometry of Cu_xS compound during the formation and followed over time to establish the characteristics of changes in the chemical composition of the heterojunction components were carried out. The question of relationship between optoelectrical properties of heterostructures and distribution of stoichiometry in the layer of copper sulfide is open, informative and very important for the practical implementation of the developed sensor. Electrochemical analysis and study by X-ray diffraction for large samples set were conducted.

Key words: nonideal heterojunction, image sensor, phase composition, XRD

УДК 625.315.592

В. А. Борщак, Є. В. Бритавський, М. І. Куталова

МОДЕЛЮВАННЯ ШВИДКОЇ ФАЗИ СПАДУ СИГНАЛУ ОПТИЧНОГО СЕНСОРУ НА ОСНОВІ ГЕТЕРОСТУКТУРИ CdS-Cu_2S

Анотація. Робота присвячена комплексу досліджень, направлених на з'ясування відхилень від стехіометрії сполуки Cu_xS при її формуванні та з подальшим плином часу для встановлення особливостей зміни хімічного складу компонентів гетеропереходу. Враховуючи, що питання про зв'язок ступеню та розподілу стехіометрії в шарі сульфіду міді з оптоелектричними властивостями гетероструктури є відкритим, інформативним та надзвичайно важливим для

практичного впровадження розробленого сенсору, для великої вибірки зразків були проведені електрохімічний аналіз та дослідження методом рентгенівської дифрактометрії.

Ключові слова: неідеальний гетероперехід, сенсор зображень, фазовий склад, рентгеноструктурний аналіз

УДК 625.315.592

В. А. Борщак, Е. В. Бритавский, М. И. Куталова

МОДЕЛИРОВАНИЕ БЫСТРОЙ ФАЗЫ СПАДА СИГНАЛА ОПТИЧЕСКОГО СЕНСОРА НА ОСНОВЕ ГЕТЕРОСТРУКТУРЫ CdS-Cu_2S

Аннотация

Работа посвящена комплексу исследований, направленных на выяснение отклонений от стехиометрии соединения Cu_xS при формировании и с последующим течением времени для установления особенностей изменения химического состава компонентов гетероперехода. Учитывая, что вопрос о связи степени и распределения стехиометрии в слое сульфида меди с оптоелектрическими свойствами гетероструктуры является открытым, информативным и чрезвычайно важным для практического внедрения разработанного сенсора, для большой выборки образцов были проведены электрохимический анализ и исследования методом рентгеновской дифрактометрии.

Ключевые слова: неидеальный гетеропереход, сенсор зображений, фазовый состав, рентгеноструктурный анализ

UDC 539.182

A. V. Glushkov, V. B. Ternovsky, S. V. Brusentseva, A. V. Duborez, Ya. I. Lepich

Odessa National Maritime Academy, Odessa, 4, Didrikhsona str., Odessa, Ukraine
e-mail: quantign@mail.ru

Odessa State Environmental University, 15, Lvovskaya str., Odessa, Ukraine

NONLINEAR DYNAMICS OF RELATIVISTIC BACKWARD-WAVE TUBE IN SELF-MODULATION AND CHAOTIC REGIME

It has been performed quantitative modelling, analysis, forecasting dynamics relativistic backward-wave tube (RBWT) with accounting relativistic effects (γ_0= 1.5-6.0), dissipation (factor D), a presence of space charge etc. There are computed the temporal dependences of the normalized field amplitudes (power) in a wide range of variation of the controlling parameters which are characteristic for distributed relativistic electron-waved self-vibrational systems: electric length of an interaction space N, bifurcation parameter proportional to (~current I) Pirse one J and relativistic factor γ_0. The computed temporal dependence of the field amplitude (power) Fmax in a good agreement with theoretical estimates and experimental data by Ginzburg etal (IAP, Nizhny Novgorod) with using the pulsed accelerator "Saturn". The analysis techniques including multi-fractal approach, methods of correlation integral, false nearest neighbour, Lyapunov exponent's, surrogate data, is applied analysis of numerical parameters of chaotic dynamics of RBWT. There are computed the dynamic and topological invariants of the RBWT dynamics in auto-modulation(AUM)/chaotic regimes, correlation dimensions values (3.1; 6.4), embedding, Kaplan-York dimensions, Lyapunov's exponents (+,+) Kolmogorov entropy. There are constructed the bifurcation diagrams with definition of the dynamics self-modulation/ chaotic areas in planes, namely, "J-γ_0", "D-J".

1. Introduction

As it is well known in the modern electronics, photoelectronics etc there are many physical systems (the backward-wave tubes, multielement semiconductors and gas lasers, different radiotechnical devices etc), which can manifest the elements of chaos and hyperchaos in their dynamics (c.f.[1-32]). The key aspect of studying the dynamics of these systems is analysis of the dynamical characteristics. Chaos theory establishes that apparently complex irregular behaviour could be the outcome of a simple deterministic system with a few dominant nonlinear interdependent variables. The past decade has witnessed a large number of studies employing the ideas gained from the science of chaos to characterize, model, and predict the dynamics of various systems phenomena (c.f.[1-16]). The outcomes of such studies are very encouraging, as they not only revealed that the dynamics of the apparently irregular phenomena could be understood from a chaotic deterministic point of view but also reported very good predictions using such an approach for different systems.

The backward-wave tube is an electronic device for generating electromagnetic vibrations of the superhigh frequencies range. In refs.[3-16] there have been presented the temporal dependences of the output signal amplitude, phase portraits, statistical quantifiers for a weak chaos arising via period-doubling cascade of self-modulation and for developed chaos at large values of the dimensionless length parameter. The authors of [3-16] solved the different versions of system of equations of nonstationary nonlinear theory for the O type backward-wave tubes with and without account of the spatial charge, without energy losses etc. It has been shown that the finite-dimension strange attractor is responsible for chaotic regimes in the backward-wave tube.

In our work it has been performed quantitative modelling, analysis, forecasting dynamics relativistic backward-wave tube (RBWT) with accounting relativistic effects (g_0= 1.5-6.0), dissipation, a presence of space charge etc. There are computed the temporal dependences of the normalized field amplitudes (power) in a wide range of variation of the controlling parameters which are characteristic for distributed relativistic electron-waved self-vibrational systems: electric length of an interaction space N, bifurcation parameter proportional to (~current *I*) Pirse one and relativistic factor g_0. There is computed a temporal dependence of the field amplitude (power) F_{max} in a good agreement with theoretical estimates and experimental data by Ginzburg etal (IAP, Nizhny Novgorod) with using the pulsed accelerator "Saturn".

2. Method

As the key ideas of our technique for nonlinear analysis of chaotic systems have been in details presented in refs. [17-32], here we are limited only by brief representation. The first important step is a choice of the model of the RBWT dynamics. We use the standard non-stationary theory [3-6], however, despite the cited papers we take into account a numver of effects, namely, influence of space charge, dissipation, the waves reflections at the ends of the system and others [12,13]. Usually relativistic dynamics is described system of equations for unidimensional relativistic electron phase $\theta(\zeta,\tau,\theta_0)$ (which moves in the interaction space with phase q_0 (q_0Î[0; 2p]) and has a coordinate z at time moment t) and field $E(x,t) = \mathrm{Re}[\varepsilon(x,t)\exp[i\omega_0 t - i\beta_0 x]$

unidimensional complex amplitude $F(\zeta,\tau) = \tilde{E}/(2\beta_0 UC^2)$ as follows [240, 249]:

$$\partial^2\theta/\partial\zeta^2 = -L^2\gamma_0^3[(1+\frac{1}{2\pi N}\partial\theta/\partial\zeta)^2 - \beta_0^2]^{3/2}\times$$

$$\times \mathrm{Re}[F\exp(i\theta)], \quad , \qquad (1)$$

$$\partial F/\partial\tau - \partial F/\partial\zeta = -L\tilde{I} \quad , \quad \tilde{I} = -\frac{1}{\pi}\int_0^{2\pi} e^{-i\theta}d\theta_0$$

with the boundary and initial conditions:

$$\theta|_{\zeta=0} = \theta_0 \, , \; \partial\theta/\partial\zeta\,|_{\zeta=0} = 0$$

$$F|_{\zeta=1} = 0 \, , F|_{\tau=0} = F^0(\zeta)$$

In is important to note that the system studied has a few controlling parameters which are characteristic for distributed relativistic electron-waved self-vibrational systems: electric length of an interaction space N, bifurcation parameter proportional to (~current *I*) Pirse one $L = 2\pi CN/\gamma_0$ (here C- is the known Piers parameter, $C = \sqrt[3]{I_0K_0/(4U)}$,and I_0 is a constant beam current component, U - accelerating voltage, K - resistance of copupling of the slowing down system) and relativistic factor $\gamma_0 = (1-\beta_0^2)^{-1.2}$

Since processes resulting in the chaotic behaviour are fundamentally multivariate, it is necessary to reconstruct phase space using as well as possible information contained in the dynamical parameter *s*(*n*), where *n* the number of the measurements. Such a reconstruction results in a certain set of *d*-dimensional vectors y(*n*) replacing the scalar measurements. Packard et al. [19] introduced the method of using time-delay coordinates to reconstruct the phase space of an observed dynamical system. The direct use of the lagged variables *s*(*n* + t), where t is some integer to be determined, results in a coordinate system in which the structure of orbits in phase space can be captured. Then using a collection of time lags to create a vector in *d* dimensions,

$$\mathrm{y}(n) = [s(n),\, s(n+\mathrm{t}),\, s(n+2\mathrm{t}),\, \ldots,\, s(n+(d\text{-}1)\mathrm{t})], \qquad (1)$$

the required coordinates are provided. In a nonlinear system, the *s*(*n* + *j*t) are some unknown nonlinear combination of the actual physical variables that comprise the source of the measurements. The dimension *d* is called the embedding dimension, d_E. According to Mañé and Takens [24,25], any time lag will be acceptable is not terribly useful for extracting physics from data. If t is chosen too small, then the coordinates s(n + jt) and s(n + (j + 1)t) are so close to each other in numerical value that they cannot be distinguished from each other. Similarly, if t is too large, then s(n + jt) and s(n + (j + 1)t) are completely independent of each other in a statistical sense. Also, if t is too small or too large, then the correlation

dimension of attractor can be under- or overestimated respectively. The autocorrelation function and average mutual information can be applied here. The first approach is to compute the linear autocorrelation function:

$$C_L(\delta) = \frac{\frac{1}{N}\sum_{m=1}^{N}[s(m+\delta)-\bar{s}][s(m)-\bar{s}]}{\frac{1}{N}\sum_{m=1}^{N}[s(m)-\bar{s}]^2}, \qquad \bar{s} = \frac{1}{N}\sum_{m=1}^{N} s(m) \tag{2}$$

and to look for that time lag where C_L(d) first passes through zero (see [18]). This gives a good hint of choice for t at that $s(n + j\mathrm{t})$ and $s(n + (j + 1)\mathrm{t})$ are linearly independent. a time series under consideration have an n-dimensional Gaussian distribution, these statistics are theoretically equivalent as it is shown by Paluš (see [15]). The general redundancies detect all dependences in the time series, while the linear redundancies are sensitive only to linear structures. Further, a possible nonlinear nature of process resulting in the vibrations amplitude level variations can be concluded.

The goal of the embedding dimension determination is to reconstruct a Euclidean space R^d large enough so that the set of points d_A can be unfolded without ambiguity. In accordance with the embedding theorem, the embedding dimension, d_E, must be greater, or at least equal, than a dimension of attractor, d_A, i.e. $d_E > d_A$. In other words, we can choose a fortiori large dimension d_E, e.g. 10 or 15, since the previous analysis provides us prospects that the dynamics of our system is probably chaotic. However, two problems arise with working in dimensions larger than really required by the data and time-delay embedding [5,6,18]. First, many of computations for extracting interesting properties from the data require searches and other operations in R^d whose computational cost rises exponentially with d. Second, but more significant from the physical point of view, in the presence of noise or other high dimensional contamination of the observations, the extra dimensions are not populated by dynamics, already captured by a smaller dimension, but entirely by the contaminating signal. In too large an embedding space one is unnecessarily spending time working around aspects of a bad representation of the observations which are solely filled with noise. It is therefore necessary to determine the dimension d_A.

There are several standard approaches to reconstruct the attractor dimension (see, e.g., [3-6,15]). The correlation integral analysis is one of the widely used techniques to investigate the signatures of chaos in a time series. The analysis uses the correlation integral, $C(r)$, to distinguish between chaotic and stochastic systems. To compute the correlation integral, the algorithm of Grassberger and Procaccia [10] is the most commonly used approach. If the time series is characterized by an attractor, then the integral $C(r)$ is related to the radius r given by

$$d = \lim_{\substack{r\to 0 \\ N\to\infty}} \frac{\log C(r)}{\log r}, \tag{3}$$

where d is correlation exponent that can be determined as the slop of line in the coordinates log $C(r)$ versus log r by a least-squares fit of a straight line over a certain range of r, called the scaling region. If the correlation exponent attains saturation with an increase in the embedding dimension, the system is generally considered to exhibit chaotic dynamics. The saturation value of correlation exponent is defined as the correlation dimension (d_2) of attractor.

The Lyapunov exponents are the dynamical invariants of the nonlinear system. In a general case, the orbits of chaotic attractors are unpredictable, but there is the limited predictability of chaotic physical system, which is defined by the global and local Lyapunov exponents.

A negative exponent indicates a local average rate of contraction while a positive value indicates a local average rate of expansion. In the chaos theory, the spectrum of Lyapunov exponents is considered a measure of the effect of perturbing the initial conditions of a dynamical system. Since the Lyapunov exponents are defined as asymptotic average rates, they are independent of the initial conditions, and therefore they do comprise an invariant measure of attractor. In fact, if one manages to derive the whole spectrum of Lyapunov exponents, other invariants of the system, i.e. Kolmogorov entropy and attractor's dimension can be found. The Kolmogorov entropy, K, measures the average rate at which information about

the state is lost with time. An estimate of this measure is the sum of the positive Lyapunov exponents. The inverse of the Kolmogorov entropy is equal to the average predictability. There are several approaches to computing the Lyapunov exponents (see, e.g., [5,6,18]). One of them [18] is in computing the whole spectrum and based on the Jacobin matrix of the system function [14].

3. Results

As input, the following parameters were taken: the energy of electrons - 150keV, starting current of 7A composed impedance connection 0,5W , length of interaction space - 0,623m, the average radius waveguides - 1,38sm period corrugating - 1,73sm radius of the electron beam - 0,67sm. The dynamic model (2.6) has been implemented in two ways considering the effects of space charge and without and with (unlike in [5]) the effect of slowing the loss of energy in the system (at the ends of reflection and some other factors discussed more etc.). As bifurcation parameter actually is $J = \ell\ |Z|(2\beta_0^2 m^2)$, where Z - resistance connection, I - beam current, $\beta_0 = v_0 / c$, v_0 - the initial velocity of the electrons, the parameter space charge $Q = Ieg(m\ \omega^2 b)$, transverse wave number $g = \omega(c\beta_0\gamma_0)$, k-harmonic and space charge density $q_k = (1/\pi)\int_0^{2\pi} e^{-k\theta} d\theta_0$, coefficient of reduction space charge $f_k^0 = 0.55$. To factor in the expression for the normalized dissipation parameter has been fixed D = 8Db. In figure 1 we list the relevant theoretical simulation test results in non-stationary processes RBWT at injection currents: (a) - 55A, (b) - 90A, (c) - 120A.

At current 7A it is set stationary mode that with increasing value of current strength transited to the periodic automodulation (I = 30A, on our data, the period of T_a = 7,3ns; experimental value [14b]: 8ns), and then when I = 55A it is realized the chaotic auto-modulation mode (fig 1a). By increasing the amount of current to 75A there is the quasi-periodical auto-modulation (period 13.8 ns) and, finally, when the current value is more than 100A it's realized essentially chaotic regime. Note that reset of the quasi-periodic auto-modulation mode can be explained by an effect of space charge.

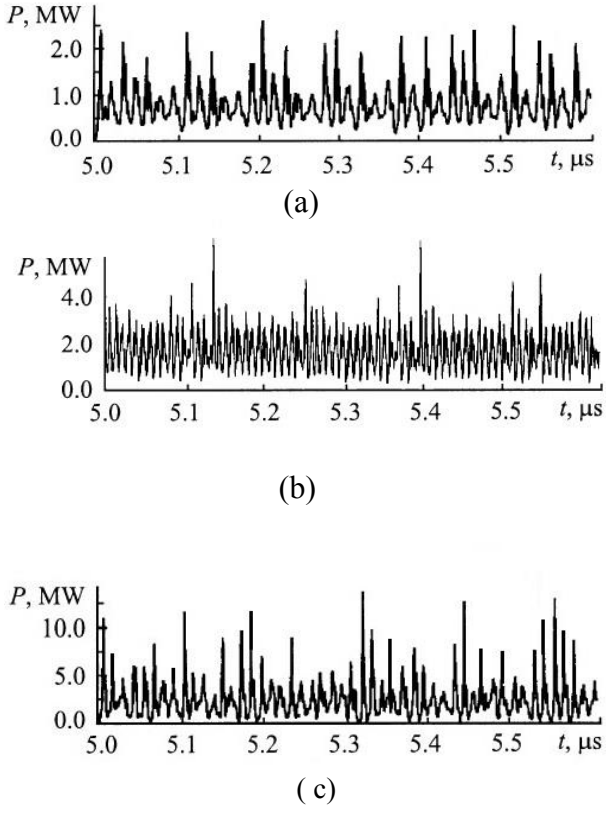

Figure 1. Theoretical results for the temporal dependence of power of the RBWT at the injection currents: (a)-55A, (b)-90A, (c) - 120A.

The similar theoretical estimates (however without the dissipation effect) and experiment results data have been obtained by Ginsburg et al. [5b]. Let us note that all results are in a physically reasonable agreement with each other.

Fig. 2 (a) shows the results of our computing the autocorrelation function, and Fig. 2b) - the average mutual information.

In fig.3 there is listed the relationship between the correlation exponent and embedding dimension of the temporal series (line 1), the mean values of variables replacement (line 2) and the implementation of one replacement (line 3). Columns errors indicate minimum values exponential correlation among all variables substituted. In Fig. 4 we presents data of estimating the embedding dimension based on the algorithm of false nearest neighbours for points of the original data series (line 1), the mean values of surrogate data (2), and one surrogate realization (3).

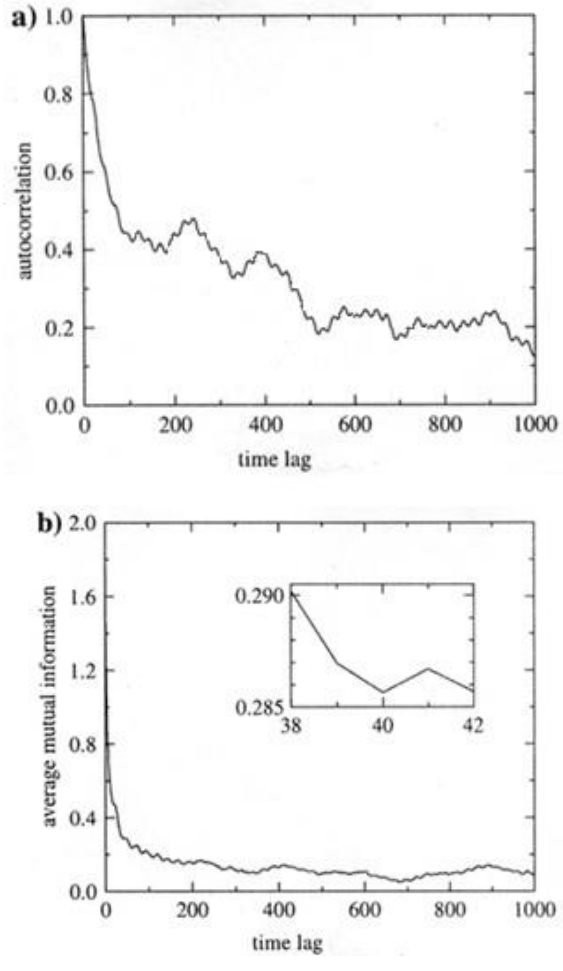

Figure 2. The autocorrelation function, (a) and the average mutual information (b).

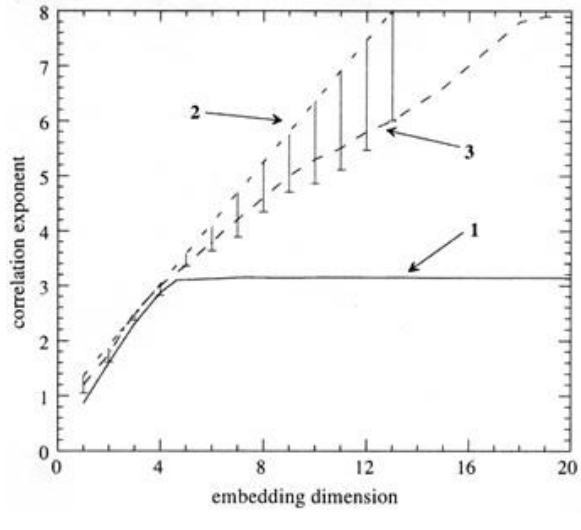

Figure 3. The relationship between the correlation exponent and embedding dimension of the temporal series (line 1), the mean values of variables replacement (line 2) and the implementation of one replacement (line 3).

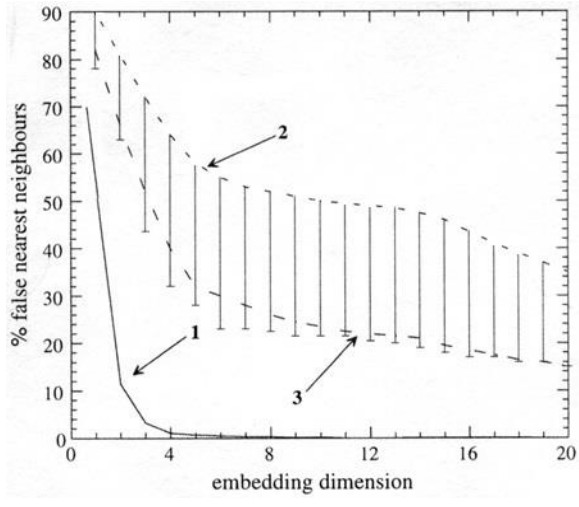

Fig. 4 we presents data of estimating the embedding dimension based on the algorithm of false nearest neighbours for points of the original data series (line 1), the mean values of surrogate data (2), and one surrogate realization (3).

Next in the table 1 we list our data on . the correlation dimension d_2, embedding dimension, determined on the basis of false nearest neighbours algorithm (d_N) with percentage of false neighbours (%). calculated for different values of lag **t** according to the analysis of two series fig1a (I - chaos) and fig.1c (II - hyperchaos).

Table 1

Correlation dimension d_2, embedding dimension, determined on the basis of false nearest neighbours algorithm (d_N) with percentage of false neighbours (%) calculated for different values of lag t

Chaos (I)			Hyperchaos (II)		
τ	d_2	(d_N)	τ	d_2	(d_N)
60	3.6	5 (5.5)	67	7.2	10 (12)
6	3.1	4 (1.1)	10	6.3	8 (2.1)
8	3.1	4 (1.1)	12	6.3	8 (2.1)

In Table 2 we list our computing data on the Lyapunov exponents (LE), the dimension of the Kaplan-York attractor, the Kolmogorov entropy K_{entr}. For studied series there are the positive and negative LE values. he resulting dimension Kaplan York in both cases are very similar to the correlation dimension (calculated by the algorithm by Grassberger-Procachia).

Table 1

The Lyapunov exponents (LE), the dimension of the Kaplan-York attractor, the Kolmogorov entropy K_{entr}. (our data)

Chaos	λ_1	λ_2	λ_3	λ_4	K
(I)	0.261	0.0001	–0.0004	–0.528	0.26
(II)	0.514	0.228	0.0000	–0.0002	0.74

Further, in Fig.5 we present the firstly obtained original (continuous line) and predicted (dotted line) dependences of power in the chaos mode (I): (a) - without energy loss effect, (b) - taking into account the effect of loss. order to estimate reliability (success) of prediction model [13-15] we have computed the correlation coefficient (r) between actual and

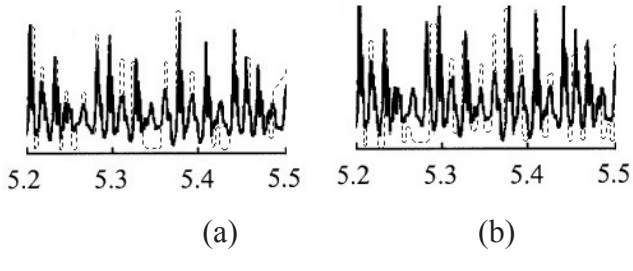

Figure 5. Original (continuous line) and predicted (dotted line) dependences of power in the chaos mode (I): (a) - without energy loss effect, (b) - taking into account the effect of loss

prognostic rows ranked to a number of the neighbours (NN). In this case, the mean forecast error was (σ = 1.9) for time series (chaos mode). In addition, usually to account for a forecast error one should take into account the noise level in the studied time series. For this purpose the methodology by Hu et al (see [13] was used.

Importantly, the above-described physical mechanism of changing different modes in the RBWT dynamics due an increasing a current value and the bifurcation parameter J corresponds to certain value relativistic factor, namely γ_0= 1,3.

More important is the analysis of the RBWT nonlinear dynamics in the plane «relativistic factor – bifurcation parameter.» Actually in this context a three-parametric relativistic nonlinear dynamics is fundamentally different from processes in non-relativistic BWT dynamics. In fig.6 we list a chart that shows the quantitative limits of auto-modulation (line I) in the plane of parameters: bifuracation parameter J - relativistic factor γ_0. Note that the second line (line II) limits the area where there is a twist particles and used theoretical model works. A characteristic feature of the chart is the presence of so-called effect of «beak», which is based on relativistic factor goes far deeper automodulation area. Firstly this effect was predicted in [3-6]. In essentially relativistic limit (see. Fig. 7) the frequency of auto-modulation falls by about half. Obviously, that all of the above characteristics is much more complicated compared to the dynamics of non-relativistic dynamics.

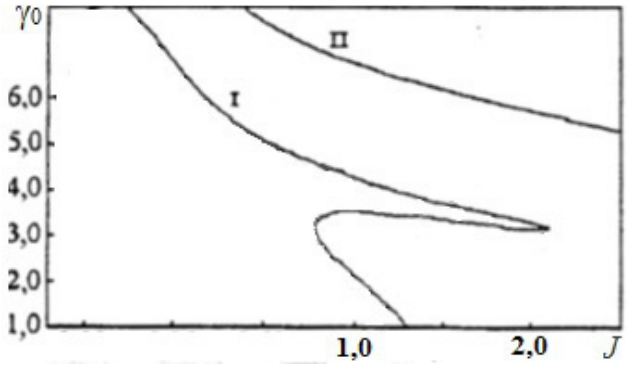

Figure 6. The limits of automodulation (line I) on the plane of parameters: “bifurcation parameter - relativistic factor”

So, we believe that a chaos in the RBWT dynamics should be called by relativistic chaos phenomenon.

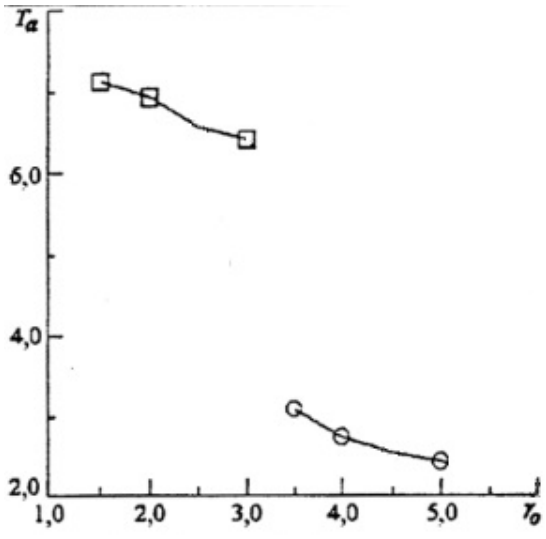

Figure 7. The dependence of the frequency of auto-modulation upon relativistic factor

Conclusions

In this work we have performed quantitative modelling, analysis, forecasting dynamics relativistic backward-wave tube (RBWT) with accounting relativistic effects (γ_0= 1.5-6.0), dissipation, a presence of space charge, reflection of waves at the end of deceleration system etc. There are computed the temporal dependences of the normalized field amplitudes (power) in a wide range of variation of the controlling parameters which are characteristic for distributed relativistic electron-waved self-vibrational systems: electric length of an interaction space N, bifurcation parameter proportional to (~current *I*) Pirse one *L*(*J*): 2.7-3.9 and relativistic factor g_0=1.5-6.0). There are computed the dynamic and topological invariants of the RBWT dynamics in auto-modulation/chaotic regimes, correlation dimensions values (3.1; 6.4), embedding, Kaplan-York dimensions, Lyapunov's exponents (LE:+,+) Kolmogorov entropy. There are firstly constructed the bifurcation diagrams with definition of the dynamics self-modulation/chaotic areas in planes: «J-γ_0», «D-J». It is shown that for moderately small γ_0 ~ 1.3 transition to chaos is realized through a sequence of the period doubling bifurcations, but with the growth of the g_0 dynamics significantly complicates with interchange of quasi-harmonical/ chaotic regimes (incl. discovery of a "beak" effect on the chart, sharp fall of automodulation period at γ_0~4), emergence of highly-d chaotic attractor, which evolves at a much complicated scenario. Firstly on basis of chaos-cybernetic approach with a new wavelet-expansion predicted paths algorithm it is realized forecasting the temporal evolution of chaotic dynamics for RBWT at different values of J, g_0 taking into account the effects of relativity, influence of space charge, dissipation and shown that in a case of low-attractor dynamics (chaotic auto-modulation) the predicted series well rebuilt the empirical data (correlation coefficient between predicted and real rows ranked among the neighbours number ~ 0.97), which is the first indication of the possibility of a new quantitative evolution prediction direction in studying relativistic microwave electronics devices.

References

1. Ott E. Chaos in dynamical systems. Cambridge: Cambridge Univ.Press, 2002.-490p.
2. Glushkov A.V., Prepelitsa G.P., Khetselius O.Yu., Kuzakon V.M., Solyanikova E.P., Svinarenko A.A., Modeling of interaction of non-linear vibrational systems on basis of temporal series analyses (application to semiconductor quantum generators)// Dynamical Systems - Theory and Applications.-2011.-P.BIF-110 (8p.).
3. Trubetskov D.I., Anfinogentov V.G., Ryskin N.M., Titov V.N., Khramov A.E., Complex dynamics of electron microwave devices (nonlinear non-stationary theory from nonlinear dynamics)//Radioengineering. -1999. – Vol.63. -P.61-68.
4. Ginsburg H. S., Kuznetsov S.P., Fedoseyev T.N. etal, Theory of transients in relativistic BWO// Izv. Vuzov. Ser. Radiophys.-1978.-T.21.- C.1037-1052.
5. Ginzburg N.S., Zaitsev N.A., Ilyakov E., Kulagin V.I., Novozhilov Yu., Rosenthal P., Sergeev V., Chaotic generation in backward wave tube of the megawatt power level// Journ. Of Techn.Phys.--2001-Vol.71.-P.73-80.
6. Kuznetsov S.P., Trubetskov D.I., Chaos and hyper-chaos in the backward wave

tube// Izv. Vuzov. Ser. Radiophys.-2004.-Vol.XLVII.-P.383-399.
7. Kuznetsov S.P., Nonlinear dynamics of backward-wave tube: Self-modulation, multistability and control// Izv. Vuzov. Ser. Applied non-linear dinamics.-2006-Vol.14.-P.3-35.
8. Zheng X., Tanaka K., Minami K., Granatstein V., Experimental study of a high-power backward-wave oscillator operating far from upper cutoff//Journ. of Phys.Soc.of Japan. - 1998. - Vol. 67. - No. 4. - P. 1466-1472.
9. Chang T., Chen S., Bamett L., Chu K., Characterization of stationary and non-stationary behavior in gyrotron oscillators//Phys.Rev.Lett.-2001.-Vol. 87.-P.321-325.
10. Levush B., Antonsen T.,Bromborsky A., Lou W., Relativistic backward wave oscillator: theory and experiment/ // Phys.Fluid-1992.-V.B4-P. 2293-2299.
11. Levush B., Antonsen T.M., Bromborsky A., Lou W.R., Carmel Y., Theory of relativistic backward wave oscillator with end reflections/ IEEE Trans, on Plasma Sci.-1992.-Vol.20..-P.263-280.
12. Glushkov A.V., Kuzakon V.M., Ternovsky V.B., Buyadzhi V.V., Dynamics of laser systems with absorbing cell and backward-wave tubes with elements of a chaos/ // Dynamical Systems Theory Eds. J. Awrejcewicz, M. Kazmierczak, P. Olejnik, J, Mrozowski (Lodz).-2013.-Vol.T1.-P.461-466.
13. Ternovsky V.B., Prepelitsa G.P., Buyadzhi V.V., Non-linear analysis of chaotic self-oscillations in backward-wave tube//Photoelectronics.-2013.-Vol.22.-P.103-107
14. Glushkov A.V., Khetselius O.Y., Ternovsky V.B., Brusentseva S.V., Zaichko P.A., Studying interaction dynamics of chaotic systems within a non-linear prediction method: application to neurophysiology// Advances in Neural Networks, Fuzzy Systems and Artificial Intelligence, Series: Recent Advances in Computer Engineering, Ed. J.Balicki. (World Sci. Pub.).-2014.-Vol.21.-P.69-75.
15. Glushkov A.V., Svinarenko A.A., Buyadzhi V.V., Ternovsky V.B., Zaichko P.A., Chaos-geometric attractor and quantum neural networks approach to simulation chaotic evolutionary dynamics during perception process/ // Advances in Neural Networks, Fuzzy Systems and Artificial Intelligence, Series: Recent Advances in Computer Engineering, Ed. J.Balicki.(World Sci. Pub.).-2014.-Vol.21.-P.143-150.
16. Ternovsky V.B., Geometry and Dynamics of a Chaos: Modelling non-linear processes in relativistic backward-wave tubes chain//Proceedings of Int. Geometry Center".-2014.-Vol.7,N3.-P. 79-86.
17. Abarbanel H., Brown R., Sidorowich J., Tsimring L., The analysis of observed chaotic data in physical systems// Rev Modern Phys.-1993.-Vol.65.-P.1331–1392.
18. Kennel M., Brown R., Abarbanel H., Determining embedding dimension for phase-space reconstruction using geometrical construction//Phys. Rev.A.-1992.-Vol.45.-P.3403–3411.
19. Packard N., Crutchfield J., Farmer J., Shaw R., Geometry from a time series//Phys Rev Lett.-1988.-Vol.45.-P.712–716.
20. Havstad J., Ehlers C., Attractor dimension of nonstationary dynamical systems from small data sets//Phys Rev A.-1989.-Vol.39.-P.845–853.
21. Gallager R.G., Information theory and reliable communication, Wiley, New York.-1986.
22. Grassberger P., Procaccia I., Measuring the strangeness of strange attractors// Physica D.-1983.-Vol.9.-P.189–208.
23. Fraser A., Swinney H., Independent coordinates for strange attractors from mutual information// Phys Rev A.-1986.-Vol.33.-P.1134–1140.
24. Takens F., Detecting strange attractors in turbulence//Lecture notes in mathematics (Springer).-1981.-N.898.-P.366–381

25. Mañé R., On the dimensions of the compact invariant sets of certain non-linear maps// Lecture notes in mathematics (Springer).-1981.-N898.-P.230–242
26. Sano M., Sawada Y., Measurement of Lyapunov spectrum from a chaotic time series// Phys. Rev.Lett.-1985.-Vol.55.-P.1082–1085
27. Sivakumar B., Chaos theory in geophysics: past, present and future//Chaos, Solitons & Fractals.-2004.-Vol.19.-P.441–462.
28. Theiler J., Eubank S., Longtin A., Galdrikian B., Farmer J., Testing for nonlinearity in time series: The method of surrogate data// Physica D.-1992.-Vol.58.-P.77–94.
29. Glushkov A.V., Khokhlov V.N., Tsenenko I.A. Atmospheric teleconnection patterns: wavelet analysis// Nonlin. Proc. in Geophys.-2004.-V.11.-P.285-293.
30. Glushkov A.V., Khokhlov V.N., Svinarenko A.A., Bunyakova Yu.Ya., Prepelitsa G.P., Wavelet analysis and sensing the total ozone content in the Earth atmosphere: MST "Geomath"// Sensor Electr. and Microsyst.Techn.-2005.-N3.-P.43-48.
31. Glushkov A.V., Khokhlov V.N., Loboda N.S., Bunyakova Yu.Ya., Short-range forecast of atmospheric pollutants using non-linear prediction method// Atm. Environment (Elsevier).-2008.-Vol.42.-P. 7284–7292.
32. Rusov V.D., Glushkov A.V., Prepelitsa G.P., et al, On possible genesis of fractal dimensions in turbulent pulsations of cosmic plasma- galactic-origin rays-turbulent pulsation in planetary atmosphere system//Adv. Space Res.-2008.-Vol42.-P.1614-1617.

This article has been received within 2015

UDC 517.9

A. V. Glushkov, V. B. Ternovsky, S. V. Brusentseva, A. V. Duborez, Ya. I. Lepich

NON-LINEAR DYNAMICS OF RELATIVISTIC BACKWARD-WAVE TUBE IN SELF-MODULATION AND CHAOTIC REGIME

Abstract.

It has been performed quantitative modelling, analysis, forecasting dynamics relativistic backward-wave tube (RBWT) with accounting relativistic effects (g_0= 1.5-6.0), dissipation (factor D), a presence of space charge etc. There are computed the temporal dependences of the normalized field amplitudes (power) in a wide range of variation of the controlling parameters which are characteristic for distributed relativistic electron-waved self-vibrational systems: electric length of an interaction space N, bifurcation parameter proportional to (~current *I*) Pirse one *J* and relativistic factor g_0. The computed temporal dependence of the field amplitude (power) F_{max} in a good agreement with theoretical estimates and experimental data by Ginzburg etal (IAP, Nizhny Novgorod) with using the pulsed accelerator "Saturn". The analysis techniques including multi-fractal approach, methods of correlation integral, false nearest neighbour, Lyapunov exponent's, surrogate data, is applied analysis of numerical parameters of chaotic dynamics of RBWT. There are computed the dynamic and topological invariants of the RBWT dynamics in auto-modulation(AUM)/chaotic regimes, correlation dimensions values (3.1; 6.4), embedding, Kaplan-York dimensions, Lyapunov's exponents (+,+) Kolmogorov entropy. There are constructed the bifurcation diagrams with definition of the dynamics self-modulation/chaotic areas in planes, namely, "J-g_0», «D-J».

Key words: relativistic backward-wave tube, chaos, non-linear methods

УДК 517.9

А. В. Глушков, В. Б. Терновский, С. В. Брусенцева, А. В. Дуборез, Я. И. Лепих

НЕЛИНЕЙНАЯ ДИНАМИКА РЕЛЯТИВИСТСКОЙ ЛАМПЫ ОБРАТНОЙ ВОЛНЫ В АВТОМОДУЛЯЦИОННОМ И ХАОТИЧЕСКОМ РЕЖИМАХ

Резюме.

Приведены результаты моделирования, анализа и прогноза динамики процессов в релятивистской лампе обратной волны (РЛОВ) с учета релятивистских эффектов (g_0= 1,5-6,0), диссипации (фактор D), наличия пространственного заряда и т.д. Вычислены временные зависимости нормированной амплитуды поля (мощности) в широком диапазоне изменения управляющих параметров, которые характерны для распределенных релятивистских электронно-волновых автоколебательных систем: электрическая длина пространства взаимодействия N, бифуркационный параметр, пропорциональный силе тока, J и релятивистский фактор g_0. Вычисленная зависимость амплитуды поля (мощности) Fmax находится в хорошем согласии с теоретическими оценками и данными эксперимента Гинзбурга и др. (ИПФ, Нижний Новгород) с использованием импульсного ускорителя «Сатурн». Техника нелинейного анализа, которая включает мультифрактальний подход, методы корреляционных интегралов, ложных ближайших соседей, экспонент Ляпунова, суррогатных данных, использованная для анализа численных параметров хаотических автоколебательных режимов в РЛОВ. Рассчитаны динамические и топологические инварианты динамики РЛОВ в автомодуляционном и хаотическом режимах, корреляционная размерность, размерности вложения (3.1; 6.4), Каплан-Йорка, показатели Ляпунова (+, +), энтропия Колмогорова и построены бифуркационные диаграммы с определением областей автомодуляции и хаоса , в частности, «J-g_0», «D-J».

Ключевые слова: релятивистская лампы обратной волны, хаос, нелинейные методы

УДК 517.9

О. В. Глушков, В. Б. Терновський, С. В. Брусенцева, А. В. Дуборез, Я. І. Лепіх

НЕЛІНІЙНА ДИНАМІКА РЕЛЯТИВІСТСЬКОЇ ЛАМПИ ЗВЕРНЕНОЇ ХВИЛІ В АВТОМОДУЛЯЦІЙНОМУ ТА ХАОТИЧНОМУ РЕЖИМАХ

Резюме.

Наведеныірезультати моделювання, аналізу і прогнозу динаміки процесів в релятивістської лампі зворотної хвилі (РЛЗХ) з урахуванням релятивістських ефектів (g_0= 1,5-6,0), дисипації (фактор D), наявності просторового заряду і т.і. Обчислені часові залежності нормованої амплітуди поля (потужності) в широкому діапазоні зміни керуючих параметрів, які характерні для розподілених релятивістських електронно-хвильових автоколивальних систем: електрична довжина простору взаємодії N, біфуркаційний параметр, пропорційний силі струму, J і релятивістський фактор g_0. Обчислена залежність амплітуди поля (потужності) Fmax знаходиться в хорошому злагоді з теоретичними оцінками і даними експерименту Гінзбурга та ін. (ІПФ,

Нижній Новгород) з використанням імпульсного прискорювача «Сатурн». Техніка нелінійного аналізу, яка включає мультіфрактальний підхід, методи кореляційних інтегралів, хибних найближчих сусідів, експонент Ляпунова, сурогатних даних, використана для аналізу чисельних параметрів хаотичних автоколивальних режимів у РЛЗХ. Розраховані динамічні та топологічні інваріанти динаміки РЛОВ в автомодуляціонном і хаотичному режимах, кореляційна розмірність, розмірності вкладення (3.1; 6.4), Каплан-Йорка, показники Ляпунова (+, +), ентропія Колмогорова і побудовані біфуркаційні діаграми з визначенням областей автомодуляції і хаосу, зокрема, «J-g_0», «D-J».

Ключові слова: релятивістська лампи зворотної хвилі, хаос, нелінійні методи

UDC 539.84

T. B. Tkach

Odessa State Environmental University, 15, Lvovskaya str., Odessa, Ukraine
e-mail: quantper@mail.ru

QUANTUM DEFECT APPROXIMATION IN THEORY OF RADIATIVE TRANSITIONS IN SPECTRUM OF Li-like CALCIUM

The combined relativistic quantum defect approximation and relativistic many-body perturbation theory with the zeroth order optimized approximation are applied to studying the Li-like calcium oscillator strengths of radiative transitions from ground state to the Rydberg states. New element in our scheme is an implementation of optimized relativistic quantum defect approximation to an energy approach frames. Comparison of calculated oscillator strengths with available theoretical and experimental (compillated) data is performed and a number of oscillator strengths are presented firstly.

1. Introduction

This paper goes on our work on studying radiative transitions characteristics in the multicharged ions on the basis of the combined relativistic quantum defect approximation [1,2] and relativistic many-body perturbation theory with the zeroth order optimized approximation [3].

Let us remind (look, for example, [1,2]) that the spectral data for highly ionized atoms has a fundamental importance in many fields of atomic physics (spectroscopy, spectral lines theory), plasma physics and chemistry, laser physics and quantum electronics, astrophysics and laboratory, thermonuclear plasma diagnostics and in fusion research.

There have been sufficiently many reports of calculations and compilation of energies and oscillator strengths for the Li-like ions and other alkali-like ions (see, for example, [1–23]). Particularly, Martin and Wiese have undertaken a critical evaluation and compilation of the spectral parameters for Li-like ions (Z=3-28) [4,5]. The results of the high-precision non-relativistic calculations of the energies and oscillator strengths of $1s22s_j1s22p$ for Li-like systems up to $Z = 50$ are presented in Refs. [12-20]. The Hylleraas-type variational method and the $1/Z$ expansion method have been used. Chen Chao and Wang Zhi-Wen [15] listed the nonrelativistic dipole-length, -velocity, -acceleration oscillator strengths for 1s22s–1s22p transitions of LiI isoelectronic sequence calculated within a full core plus correlation method with using multiconfiguration interaction wave functions. Fully variational nonrelativistic Hartree-Fock wave functions were used by Bièmont in calculating 1s2n2L (n<8=s,p,d,f; 3<Z<22) Li-like states [18].

In many papers the Dirac-Fock (DF) method, model potential, quantum defect approximation in the different realizations have been used for calculating the energies and oscillator strengths of the Li-like and similar ions (see Refs.[4-9,19-30]). The consistent QED calculations of the energies, ionization potentials, hyperfine structure constants for the Li-like ions are performed in Refs. [18,19]. However, for Li-like ions with higher Z, particularly, for their high-excited (Rydberg) states, there are not enough precise data available in literatures.

In this paper the combined relativistic quantum defect approximation (QDA) and relativistic many-body perturbation theory with the zeroth order optimized approximation are applied to studying

the Li-like calcium oscillator strengths of radiative transitions from ground state to the Rydberg states. New element in our scheme is an implementation of optimized relativistic quantum defect approximation to an energy approach frames. Comparison of calculated oscillator strengths with available theoretical and experimental (compillated) data is performed and a number of oscillator strengths are presented firstly.

2. Relativistic energy approach to atom in a strong laser field: Multiphoton resonances

As the detailed presentation of our version of the relativistic quantum defect approximation is in , for example, Ref. [1,2], here we present only the key elements. The relativistic energy approach in gauge-invariant form is presented in many books, articles (look [5-7,3]). Within an energy approach the imaginary part of electron energy shift of an atom is directly connected with the radiation transition probability. The total energy shift of the state is usually presented as (see, for example, [5,6] and also [3]):

$$\mathrm{DE} = \mathrm{ReDE} + \mathrm{i}\, G/2 \qquad (1)$$

where G is interpreted as the level width and decay possibility $P = G$. The imaginary part of electron energy of the system, which is defined in the lowest PT order as [3]:

$$\mathrm{Im}\Delta E(B) = -\frac{e^2}{4\pi} \sum_{\substack{\alpha>n>f \\ [\alpha<n\le f]}} V^{|\omega_{\alpha n}|}_{\alpha n \alpha n}, \qquad (2)$$

where $\sum_{\alpha>n>f}$ for electron and $\sum_{\alpha<n\le f}$ for vacancy. The matrix element is determined as follows:

$$V^{|\omega|}_{ijkl} = \iint dr_1 dr_2 \Psi^*_i(r_1)\Psi^*_j(r_2) \frac{\sin|\omega| r_{12}}{r_{12}}(1-\alpha_1\alpha_2)\Psi^*_k(r_2)\Psi^*_l(r_1) \qquad (3)$$

The separated terms of the sum in (3) represent the contributions of different channels and a probability of the dipole transition is:

$$\Gamma_{\alpha_n} = \frac{1}{4\pi} \cdot V^{|\omega_{\alpha_n}|}_{\alpha_n \alpha_n} \qquad (4)$$

The corresponding oscillator strength: $gf = \lambda_g^2 \cdot \Gamma_{\alpha n} / 6.67 \cdot 10^{15}$, where g is the degeneracy degree, l is a wavelength in angstrems (Å). Under calculating the matrix elements (3) one should use the angle symmetry of the task and write the expansion for potential $\sin|w|r_{12}/r_{12}$ on spherical functions and this expansion corresponds to usual multipole one for radiative probability. Substitution of expansion (5) to matrix element of interaction gives [5,6]:

$$V^{\omega}_{1234} = [(j_1)(j_2)(j_3)(j_4)]^{1/2} \times \times \sum_{\mu} (-1)^{\mu} \begin{pmatrix} j_1 & j_3 & \lambda \\ m_1 & -m_3 & \mu \end{pmatrix} \times \mathrm{Im}[Q^{Qul}_{\lambda} + Q^{B}_{\lambda}] \qquad (5)$$

where j_i is the total single electron momentum, m_i – the projections; Q^{Qul}_{λ} is the Coulomb part of interaction, Q^{Br}_{λ} - the Breit part. The Coulomb part Q^{Qul}_{λ} is expressed in terms of radial integrals R_l, angular coefficients S_l. The Breit interaction part is defined by similar way (see [3]). The relativistic wave functions are calculated by solution of the Dirac equation with the potential, which includes the "outer electron- ionic core" potential and polarization potential [3]. The calibration of the single model potential parameter has been performed on the basis of the special ab initio procedure within relativistic energy approach (see also [5-7]). In Ref.[6] the lowest order multielectron effects, in particular, the gauge dependent radiative contribution Im dE_{ninv} for the certain class of the photon propagator calibration is treated. This value is considered to be the typical representative of the electron correlation effects, whose minimization is a reasonable criterion in the searching for the optimal one-electron basis of the relativistic many-body PT. The minimization of functional Im dE_{ninv} leads to integral-differential equation that can be solved using one of the standard codes. Therefore, it provides the construction of the optimized 1-particle representation and thus optimized relativistic model potential ORMP

scheme [6]. The same procedure is used in generalization of the relativistic QDA. Usually, the most exact version of the QDA is provided by using the empirical data in order to determine the quantum defect values for different state.

The above described approach allows to generalize the QDA and get a new ab initio optimized QDA scheme, satisfying a principle of minimization for the gauge dependent radiative contributions to Im dE_{ninv} for the certain class of the photon propagator calibration. A relativistic quantum defect is usually defined as (see, for example, [3]:

$$\mu_\chi(E_n) = n - \nu_n + \gamma - |\chi|, \qquad (6)$$

where χ is he Dirac quantum number, and

$$\gamma = \sqrt{\chi^2 - (\alpha z)^2}\,,$$

$$\nu_n = \frac{z\varepsilon}{\lambda},$$

$$\lambda = \sqrt{-E_n(1+\varepsilon)}\,,$$

$$\varepsilon = 1 + \alpha^2 E_n\,. \qquad (7)$$

In the non-relativistic limit (i.e. the fine structure constant $\alpha \to 0$) expression (7) transfers to the well known non-relativistic expression for quantum defect:

$$\mu_l^{NR}(E_n) = n - n^* = n - \frac{z}{\sqrt{-2E_n}}\,, \qquad (8)$$

where n is the principal quantum number, n^* is an effective quantum number, E_n is an electron energy and z is a charge of a core (ion).

3. Results and conclusions

We applied the above described approach to calculating the energies and oscillator strengths of transitions in spectra of the Li-like calcium (Z=12). All calculation is performed on the basis of the numeral code Superatom. There are considered the radiative transitions from ground state to the Rydberg states, particularly, $2s_{1/2} - np_{1/2,3/2}$ (n=3-12). ASome preliminary data were listed in [1]. As usually, to test the obtained results, we compare our data on the oscillator strengths values for some Li-like ions with the known theoretical and compillated data [8-18]. In table 1 we present the our oscillator strengths values (OQDA) for the $2s_{1/2} - np_j$ (n=3-12, j=1/2,3/2) transitions in spectrum of the Li-like Ca^{17+}.

Table 1

Oscillator strengths values (OQDA) for the $2s_{1/2} - np_j$ (n=3-12, j=1/2,3/2) transitions in spectrum of the Li-like Ca^{17+}

Transition	Exp	QDA	DF
$2s_{1/2}$–$3p_{1/2}$	0.123	–	–
$2s_{1/2}$–$3p_{3/2}$	0.241	–	–
$2s_{1/2}$–$4p_{1/2}$	–	–	–
$2s_{1/2}$–$8p_{1/2}$	–	2.54[a]	2.53[a]
$2s_{1/2}$–$9p_{1/2}$	–	1.74[a]	1.73[a]
$2s_{1/2}$–$10p_{1/2}$	–	1.24[a]	1.24[a]
$2s_{1/2}$–$11p_{1/2}$	–	0.919[a]	0.916[a]
$2s_{1/2}$–$12p_{1/2}$	–	0.70[a]	0.698[a]
$2s_{1/2}$–$13p_{1/2}$	–	0.546[a]	0.54[a]
Transition	MBP	Our1	Our2
$2s_{1/2}$–$3p_{1/2}$	0.126	0.120	0.121
$2s_{1/2}$–$3p_{3/2}$	0.246	0.237	0.238
$2s_{1/2}$–$4p_{1/2}$	–	0.028	0.029
$2s_{1/2}$–$8p_{1/2}$	–	2.52	2.52
$2s_{1/2}$–$9p_{1/2}$	–	1.75	1.75
$2s_{1/2}$–$10p_{1/2}$	–	1.24	1.24
$2s_{1/2}$–$11p_{1/2}$	–	0.91	0.91
$2s_{1/2}$–$12p_{1/2}$	–	0.70	0.70
$2s_{1/2}$–$13p_{1/2}$	–	0.55	0.55

In Table 1 we list also the corresponding results on oscillator strengths obtained by computing within the standard QDA, Dirac-Fock (DF) by Zilitis and some experimental data by Martin-Weiss [1,4,8]. The QDA oscillator strengths

data become more exact with the growth of the principal quantum number. At the same time the accuracy of the DF data may be decreased. The agreement between the Martin-Weiss data and our results (our 1 and Our 2 are corresponding to two different gauges of a photon propagator or at usual amplitude approach language length and velocity forms of transition operator) is physically reasonable. The closeness of oscillator strength values proves a gauge invariance principle conservation in the radiative transition probabilities scheme.

References

1. Tkach T.B., Optimized relativistic model potential method and quantum defect approximation in theory of radiative transitions in spectra of multicharged ions//Photoelectronics (Ukraine-Italy).-2012.-N21.-P.22-27.
2. Khetselius O.Yu., Florko T.A., Svinarenko A.A., Tkach T.B., Radiative and collisional spectroscopy of hyperfine lines of the Li-like heavy ions and Tl atom in an atmosphere of inert gas// Physica Scripta (IOP, London). – 2013. – Vol.T153 – P.014037.
3. Glushkov A.V., Relativistic quantum theory. Quantum, mechanics of atomic systems. – Odessa: Astroprint, 2008. – 700P.
4. Martin G.A. and Wiese W. L., Tables of critically evaluated oscillator strengths for lithium isoelectronic sequence// Journ. of Phys. Chem. Ref. Data. – 1976. – Vol.5. – P.537-570.
5. Ivanov L.N., Ivanova E.P., Extrapolation of atomic ion energies by model potential method: Na-like spectra// Atom. Dat. Nuc. Dat.Tab. – 1979. – Vol.24. – P.95-121.
6. Glushkov A.V., Ivanov L.N., Ivanova E.P., Generalized energy approach in relativistic theory of atom// Autoionization Phenomena in Atoms. – M.: Moscow State Univ. – 1986.
7. Glushkov A.V., Ivanov L.N. Radiation Decay of Atomic States: atomic residue and gauge non-invariant contributions // Phys.Lett.A. – 1992. – Vol.170,N1. - P.33-38.
8. Zilitis V.A., Determination of the energies and oscillator strengths of Li-like ions//Opt. Spectr.-1983.-Vol.55.-P.215-218.
9. Froese Fischer C., Breit–Pauli energy levels, lifetimes, and transition probabilities for the beryllium-like to neon-like sequences//Atom.Dat.Nucl. Dat. Tabl.-2004.-Vol.87.-P.1–184.
10. Barnett R., Johnson E., Lester W.Jr., Quantum Monte Carlo determination of the lithium 2S-2P oscillator strength: Higher precision//Phys. Rev. A.-1995.-Vol.51.-P. 2049-2052.
11. Zong-Chao Yan and Drake G.W.F., Theoretical lithium 2S-2P and 2P-3D oscillator strengths//Phys. Rev. A.-1995.-Vol.52.-P.R4316-4319.
12. Lianhua Qu, Zhiwen Wang and Baiwen Li, Theory of oscillator strength of the lithium isoelectronic sequence//J. Phys. B: At. Mol. Opt. Phys.-1998.-Vol.31.-P.3601-3612.
13. Khetselius O.Yu, Relativistic perturbation theory calculation of hyperfine structure parameters for some heavy-element isotopes//Int. Journ. Quant. Chem.-2009.-Vol.109.-P.3330-3335.
14. Chen Chao, Wang Zhi-Wen, Oscillator strengths for 2s2–2p2P transitions of lithium isoelectronic sequence NaIX-CaXVIII// Com.Theor.Phys.-2005.-Vol.43.-P.305-312.
15. Hu Mu-Hong, Wang Zhi-Wen, Oscillator strengths for 2S–nP transitions of lithium isoelectronic sequence from Z = 11 to 20//Chinese Phys. B.-2009.-Vol.18.-P.2244-2258.
16. Bièmont E., Theoretical oscillator strengths in lithium isoelectronic sequence (3<Z<22)// Astr. and Astrophys Suppl. Ser.-1977.-Vol.27.-P. 489-494.
17. Zhi-Wen Wang and Ye Li , Calculations of the transition energies and oscillator

strengths for Cu^{26+} ion// Journ. of Atom. Mol. Sci.- 2010.- Vol.1.-P. 62-67.
18. Yerokhin V., Artemyev A., Shabaev V.M., QED treatment of electron correlation in Li-like ions//Phys.Rev.A.-2007.-Vol.75.-P.062501.
19. Ivanova E.P., Glushkov A.V. Theoretical investigation of spectra of multicharged ions of F-and Ne-like isoelectronic sequences//J.Quant.Spectr.Rad. Tr.-1986.-Vol.36.-P.127-145.
20. Ivanova E.P., Grant I.P., Oscillator strength anomalies in Ne isoelectronic sequence with applications to X-ray laser modeling//J.Phys.B.-1998.-Vol.31.-P.2871-2883.
21. Schweizer W., Faßbinder P. and Gonzalez-Ferez R., Model potentials for alkali metal atoms and Li-like ions 1999 Atom. Dat.Nucl.Dat.Tabl.-1999.-Vol.72.-P.33-55
22. Zelentsova T.N., Perelygina-Tkach T.B., Thermal photoionization of the Rydberg atoms by the blackbody radiation: New relativistic approach// Sensor Electr. and Microsyst. Techn.-2009.-N4.-P.5-11.
23. Malinovskaya S., Glushkov A., Khetselius O., Perelygina-Tkach T., Svinarenko A., etal Generalized energy approach to calculating electron collision cross-sections for multicharged ions in plasma: Debye model//Int. Journ.Quant. Chem.-2011.-Vol.111.-P.288-296.

This article has been received within 2015

UDC 539.84

T. B. Tkach

QUANTUM DEFECT APPROXIMATION IN THEORY OF RADIATIVE TRANSITIONS IN SPECTRUM OF Li-like CALCIUM

Abstract.

The combined relativistic quantum defect approximation and relativistic many-body perturbation theory with the zeroth order optimized approximation are applied to studying the Li-like calcium oscillator strengths of radiative transitions from ground state to the Rydberg states. New element in our scheme is an implementation of optimized relativistic quantum defect approximation to an energy approach frames. Comparison of calculated oscillator strengths with available theoretical and experimental (compillated) data is performed and a number of oscillator strengths are presented firstly.

Key words: quantum defect approximation, oscillator strengths, radiative transition, Li-like calcium

УДК 539.84

Т. Б. Ткач

ПРИБЛИЖЕНИЕ КВАНТОВОГО ДЕФЕКТА В ТЕОРИИ РАДИАЦИОННЫХ ПЕРЕХОДОВ В СПЕКТРЕ Li-ПОДОБНОГО КАЛЬЦИЯ

Резюме.

Комбинированный релятивистский метод модельного потенциала и метод теории возмущений с оптимизированным 1-частичным нулевым приближением использованы для вычисления энергий и сил осцилляторов радиационных переходов из основного состояния в низколежащие и ридберговские состояния в спектрах Li-подобных ионов. Основная особенность нового подхода заключается в имплементации оптимизированного релятивистского приближения модельного потенциала (квантового дефекта) в рамки энергетического подхода. Выполнен анализ и сравнение полученных данных для сил осцилляторов с имеющимися теоретическими и экспериментальными данными.

Ключевые слова: квантового дефекта приближение, силы осцилляторов, радиационные переходы, Li-подобный кальций

УДК 539.84

Т. Б. Ткач

НАБЛИЖЕННЯ КВАНТОВОГО ДЕФЕКТУ В ТЕОРІЇ РАДІАЦІЙНИХ ПЕРЕХОДІВ У СПЕКТРІ Li-ПОДІБНОГО КАЛЬЦІЮ

Резюме.

Комбінований релятивістське наближення квантового дефекту і релятивістська теорія збурень з оптимізованим одночастинковим нульовим наближенням використані для вивчення сил осциляторів радіаційних переходів з основного стану у рідбергівські стани у спектрі Li-подібного кальцію. Основна особливість нового підходу пов'язана з імплементацією оптимізованого релятивістського наближення квантового дефекту у межи енергетичного підходу. Виконано аналіз та порівняння отриманих результатів по силам осциляторів з наявними теоретичними та експериментальними даними і ряд значень сил осциляторів представлені, по-перше.

Ключові слова: квантового дефекту наближення, сили осциляторів, радіаційні переходи, Li-подібний кальцій

UDC 539.182

A. V. Glushkov, A. A. Svinarenko, V. B. Ternovsky, A. V. Smirnov, P. A. Zaichko

Odessa State Environmental University, 15, Lvovskaya str., Odessa, Ukraine
Odessa National Polytechnical University, 1, Shevchenko av., Odessa, Ukraine
e-mail: quantsvi@mail.ru

SPECTROSCOPY OF THE COMPLEX AUTOIONIZATION RESONANCES IN SPECTRUM OF HELIUM: TEST AND NEW SPECTRAL DATA

We applied a generalized energy approach (Gell-Mann and Low S-matrix formalism) combined with the relativistic multi-quasiparticle (QP) perturbation theory (PT) with the Dirac-Kohn-Sham zeroth approximation and accounting for the exchange-correlation, relativistic corrections to studying autoionization resonances in the helium spectrum, in particular, we predicted the energies and widths of the number of the Rydberg resonances. There are presented the results of comparison of our theory data for the autoionization resonance 3s3p 1P0 with the available experimental data and those results of other theories, including, method of complex rotation by Ho, algebraic approach by Wakid-Callaway, diagonalization method by Senashenko-Wague etc.

1. Introduction

Here we continue our investigations of studying the autoionization state and AR in spectra of many electron complex atoms and ions. Let us note [1] that theoretical methods of calculation of the spectroscopic characteristics for heavy atoms and ions are usually divided into a few main groups [1-21]. At first, one should mention the well known, classical multi-configuration Hartree-Fock method (as a rule, the relativistic effects are taken into account in the Pauli approximation or Breit hamiltonian etc.) allowed to get a great number of the useful spectral information about light and not heavy atomic systems, but in fact it provides only qualitative description of spectra of the heavy atoms and ions. Another more consistent method is given by the known multi-configuration Dirac-Fock (MCDF) approach. In the MCDF calculations the one- and two-particle relativistic effects and important exchange-correlation corrections are usually taken into account practically, however the total accounting is not possible. In this essence it should be given special attention to very complex correlation effects, such as a continuum pressure and energy dependence of the inter electron interaction.

In this paper we applied a new relativistic approach [11-15] to relativistic studying the autoionization characteristics of the helium atom. The new elements of the approach include the combined the generalized energy approach and the gauge-invariant QED many-QP PT with the Dirac-Kohn-Sham (DKS) "0" approximation (optimized 1QP representation) and an accurate accounting for relativistic, correlation and others effects. The generalized gauge-invariant version of the energy approach has been further developed in Refs. [12,13]. Below we present new data on the energies and widths of the 2s,p, 3s,p ^{1}P, double excited AR for configurations ns^2 , np^2 , $3d^2\,{}^1$G, $4d^2\,{}^1$G, $5d^2\,{}^1$G, $4f^2\,{}^1$I , N snp $^{1,3}L^{\pi}$ and 3lnl′ $^{1,3}L^{\pi}$.

2. Relativistic approach in autoionization spectroscopy of heavy atoms

In refs. [11-15, 17-20] it has been in details presented, so here we give only the fundamental aspects. In relativistic case the Gell-Mann

and Low formula expressed an energy shift ΔE through the QED scattering matrix including the interaction with as the photon vacuum field as the laser field. The first case is corresponding to definition of the traditional radiative and autoionization characteristics of multielectron atom. The wave function zeroth basis is found from the Dirac-Kohn-Sham equation with a potential, which includes the ab initio (the optimized model potential or DF potentials, electric and polarization potentials of a nucleus; the Gaussian or Fermi forms of the charge distribution in a nucleus are usually used) [5]. Generally speaking, the majority of complex atomic systems possess a dense energy spectrum of interacting states with essentially relativistic properties. Further one should realize a field procedure for calculating the energy shifts ΔE of degenerate states, which is connected with the secular matrix *M* diagonalization [8-12]. The secular matrix elements are already complex in the second order of the PT. Their imaginary parts are connected with a decay possibility. A total energy shift of the state is presented in the standard form:

$$\Delta \mathrm{E} = \mathrm{Re}\,\Delta E + i\,\mathrm{Im}\,\Delta E \qquad \mathrm{Im}\,\Delta E = -\Gamma/2\,, \quad (1)$$

where Γ is interpreted as the level width, and the decay possibility $\mathrm{P} = \Gamma$. The whole calculation of the energies and decay probabilities of a non-degenerate excited state is reduced to the calculation and diagonalization of the *M*. The *jj*-coupling scheme is usually used. The complex secular matrix *M* is represented in the form [9,10]:

$$M = M^{(0)} + M^{(1)} + M^{(2)} + M^{(3)}. \qquad (2)$$

where $M^{(0)}$ is the contribution of the vacuum diagrams of all order of PT, and $M^{(1)}$, $M^{(2)}$, $M^{(3)}$ those of the one-, two- and three-QP diagrams respectively. $M^{(0)}$ is a real matrix, proportional to the unit matrix. It determines only the general level shift. We have assumed $M^{(0)} = 0$. The diagonal matrix $M^{(1)}$ can be presented as a sum of the independent 1QP contributions. For simple systems (such as alkali atoms and ions) the 1QP energies can be taken from the experiment. Substituting these quantities into (2) one could have summarized all the contributions of the 1QP diagrams of all orders of the formally exact QED PT. The optimized 1-QP representation is the best one to determine the zeroth approximation. In the second order, there is important kind of diagrams: the ladder ones. These contributions have been summarized by a modification of the central potential, which must now include the screening (anti-screening) effect of each particle by two others. The additional potential modifies the 1QP orbitals and energies. Let us remind that in the QED theory, the photon propagator D(12) plays the role of this interaction. Naturally, an analytical form of D depends on the gauge, in which the electrodynamic potentials are written. In general, the results of all approximate calculations depended on the gauge. Naturally the correct result must be gauge invariant. The gauge dependence of the amplitudes of the photoprocesses in the approximate calculations is a well known fact and is in details investigated by Grant, Armstrong, Aymar-Luc-Koenig, Glushkov-Ivanov [1,2,5,9]. Grant has investigated the gauge connection with the limiting non-relativistic form of the transition operator and has formulated the conditions for approximate functions of the states, in which the amplitudes are gauge invariant (so called Grant's theorem). These results remain true in an energy approach as the final formulae for the probabilities coincide in both approaches. In ref. [16] it has been developed a new version of the approach to conserve gauge invariance. Here we applied it to get the gauge-invariant procedure for generating the relativistic DKS orbital bases (abbreviator of our method: GIRPT).

A width of a state associated with the decay of the AR is determined by square of the matrix element of the interparticle interaction $\Gamma \infty |V(\beta_1\beta_2, \beta_3 k)|^2$. The total width is given by the expression:

$$\Gamma(n_1^0 j_1^0, n_2^0 j_2^0; J) = \frac{2\pi\varepsilon}{K_0} \sum_{\beta_1\beta_2} \sum_{\beta_1'\beta_2'} C^J(\beta_1\beta_2) \times$$

$$\times C^J(\beta_1'\beta_2') \sum_{\beta\,\beta_K} V_{\beta_1\beta_2;\beta\,\beta_K} V_{\beta_K\beta\,;\beta_1'\beta_2'} \qquad (3)$$

where the coefficients C can be determined bas follows:

$$C^J(\beta_1\beta_2) = C^J(n_1 j_1 n_1^0 j_1^0; n_2 j_2 n_2^0 j_2^0)\times$$

$$\times A(j_1 m_1; j_2 m_2; JM) \tag{4a}$$

$$A(j_1 m_1, j_2 m_2 JM) = (-1)^{j_1 - j_2 + M}\begin{pmatrix} j_1 & j_2 & J \\ m_1 & m_2 & -M \end{pmatrix}\sqrt{2J+1} \tag{4b}$$

$$C^J(n_1 j_1 n_1^0 j_1^0; n_2 j_2 n_2^0 j_2^0) = N(n_1^0 j_1^0, n_2^0 j_2^0)\times$$

$$\times[\delta(n_1^0 j_1^0 n_1 j_1)\delta(n_2^0 j_2^0 n_2 j_2) + \tag{4c}$$

$$+(-1)^{j_1+j_2+J+1}\delta(n_1^0 j_1^0 n_2 j_2)\delta(n_2^0 j_2^0 n_1 j_1)]$$

$$N(n_1^0 j_1^0; n_2^0 j_2^0) = \begin{cases} \frac{1}{\sqrt{2}} & n_1^0 j_1^0 = n_2^0 j_2^0 \\ 1 & n_1^0 j_1^0 \neq n_2^0 j_2^0 \end{cases} \tag{4d}$$

The matrix element of the relativistic interparticle interaction

$$V(r_i r_j) = exp(i\omega_{ij} r_{ij})\cdot(1-\alpha_i\alpha)/r_{ij} \tag{5}$$

(here α_1 –the Dirac matrices) in (3) is determined as follows:

$$V_{\beta_1\beta_2;\beta_4\beta_3} = \sqrt{(2j_1+1)(2j_2+1)(2j_3+1)(2j_4+1)}\times$$

$$\times(-1)^{j1+j2+j3+j4+m1+m2}\times$$

$$\times\sum_{a\mu}(-1)^{\mu}\begin{pmatrix} j_1 & j_3 & a \\ m_1 & -m_3 & \mu \end{pmatrix}\begin{pmatrix} j_2 & j_4 & a \\ m_2 & -m_4 & \mu \end{pmatrix}\times \tag{6}$$

$$\times Q_a(n_1 l_1 j_1 n_2 l_2 j_2; n_4 l_4 j_4 n_3 l_3 j_3),$$

$$Q_a = Q_a^{\text{Qul}} + Q_a^{\text{B}}\ . \tag{7}$$

Here Q_a^{Qul} and Q_a^{B} is corresponding to the Coulomb and Breit parts of the interlparticle interaction (5). It is worth to remind that the real part of the interaction matrix element can be expanded in terms of Bessel functions [5,8]:

$$\frac{\cos|\omega|r_{12}}{r_{12}} = \frac{\pi}{2\sqrt{r_1 r_2}}\sum_{\lambda=0}(\lambda)J_{\lambda+1/2}(|\omega|r_<)\times$$

$$\times J_{-\lambda-1/2}(|\omega|r_>)P_\lambda(\cos\mathbf{r}_1\mathbf{r}_2) \tag{8}$$

The Coulomb part Q_λ^{Qul} is expressed in the radial integrals R_λ, angular coefficients S_λ as follows:

$$\text{Re}\,Q_\lambda^{\text{Qul}} \sim \text{Re}\{R_l(1243)S_\lambda(1243)+$$

$$+R_\lambda(\tilde{1}24\tilde{3})S_\lambda(\tilde{1}24\tilde{3})+$$

$$+R_\lambda(1\tilde{2}4\tilde{3})S_\lambda(1\tilde{2}4\tilde{3})+$$

$$+R_\lambda(\tilde{1}\tilde{2}4\tilde{3})S_\lambda(\tilde{1}\tilde{2}4\tilde{3})\} \tag{9}$$

where, for example, $\text{Re}Q_\lambda(1243)$ is as follows:

$$\text{Re}\,R_\lambda(1243) = \iint dr_1 r_1^2 r_2^2 f_1(r_1) f_3(r_1) f_2(r_2)\times$$

$$\times f_4(r_2) Z_\lambda^{(1)}(r_<) Z_\lambda^{(1)}(r_>) \tag{10}$$

Here f is the large component of radial part of the 1QP state Dirac function and function Z is :

$$Z_\lambda^{(1)} = [2/|\omega_{13}|\alpha Z]^{\lambda+1/2} J_{\lambda+1/2}(\alpha|\omega_{13}|r)/[r^\lambda\Gamma(\lambda+3/2)] \tag{11}$$

The angular coefficient is defined by standard way as above [3]. The calculation of radial integrals $\mathbf{Re}R_\lambda(1243)$ is reduced to the solution of a system of differential equations:

$$\left.\begin{aligned} y_1' &= f_1 f_3 Z_\lambda^{(1)}(\alpha|\omega|r) r^{2+\lambda}, \\ y_2' &= f_2 f_4 Z_\lambda^{(1)}(\alpha|\omega|r) r^{2+\lambda}, \\ y_3' &= [y_1 f_2 f_4 + y_2 f_1 f_3] Z_\lambda^{(2)}(\alpha|\omega|r) r^{1-\lambda}. \end{aligned}\right\} \tag{12}$$

In addition, $y_3(\infty)=\mathbf{Re}R_\lambda(1243)$, $y_1(\infty)=X_\lambda(13)$. The system of differential equations includes also equations for functions $f/r^{|æ|-1}$, $g/r^{|æ|-1}$, $Z_\lambda^{(1)}$, $Z_\lambda^{(2)}$. The formulas for the autoionization (Auger) decay probability include the radial integrals $R_\alpha(\alpha k\gamma\beta)$, where one of the functions describes electron in the continuum state. When calculating this inte-

gral, the correct normalization of the function ψ_k is a problem. The correctly normalized function should have the following asymptotic at $r \to 0$:

$$\left.\begin{matrix} f \\ g \end{matrix}\right\} \to (\lambda\omega)^{-1/2} \begin{cases} \left[\omega + (\alpha Z)^{-2}\right]^{-1/2} sin(kr+\delta), \\ \left[\omega - (\alpha Z)^{-2}\right]^{-1/2} cos(kr+\delta). \end{cases} \quad (13)$$

When integrating the master system, the function is calculated simultaneously:

$$N(r) = \left\{\pi\omega_k \left[f_k^2 \left[\omega_k + (\alpha Z)^{-2}\right] + g_k^2 \left[\omega_k + (\alpha Z^{-2})\right]\right]\right\}^{-1/2} \quad (14)$$

It can be shown that at $r \to \infty$, $N(r) \to N_k$, where N_k is the normalization of functions f_k, g_k of continuous spectrum satisfying the condition (9). Other details can be found in refs.[10-13,16-20] as well as description of the "Superatom" and Cowan PC codes, used in all computing.

3. Results and conclusions

In figure 1 there are presented the fragments of the He photoionization spectrum plus absorption (due to the data by NIST [22]). Spectral range includes the ARs, which are on average 35-40 eV above the first ionization potential (24.58eV).

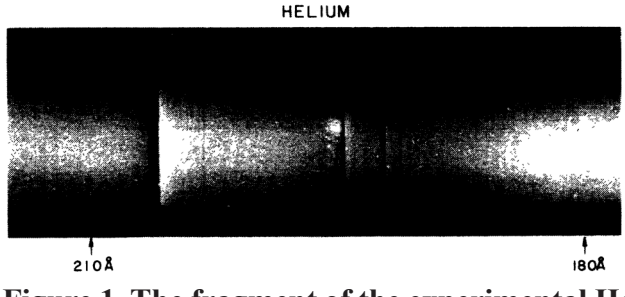

Figure 1. The fragment of the experimental He photoionization spectrum (210-180A)

One of the first members of the AR series is associated with the transition to double the permitted level excited 2s2p $^1P_1^0$. Generally there are identified two series of the resonances namely 2snp, 2pns, and both have a first member 2s2p and converge to 189.6A). In Table 1 we list the experimental data on energy and width (NBS, National Bureau of Standards) $^1P_0$, lying below the ionization threshold n=2, and theoretical results - one of the most accurate theory type Fano (Bhatia-Temkin: Th1) and our theory (Th2)[1,3], which shows the comparison is quite acceptable accuracy of our theory. Another important test of any theory - calculation parameters AS 3s3p $^1P_0$.

Table 1

The energy and width of the AR He $^1P_0$ (see text)

	Th.1	Th.2 (our data)	Exp. (NBS, NIST)
E	60.1444	60.1392	60.133±0.015 60.151±0.0103
Γ	0.0369	0.0374	0.038±0.004 0.038±0.002

In the Tables 2 and 3 we present the comparison of our data for the AR 3s3p $^1P_0$ with those of other theories, including, method of complex rotation by Ho, algebraic approach by Wakid-Callaway, diagonalization method by Senashenko-Wague, relativistic Hartree-Fock (RHF) methid by Nicolaides-Komninos, R-matrix method by Hayes-Scott, method of the adiabatic potential curves by Koyoma-Takafuji-Matsuzawa and Sadeghpour, L^2 technique with the Sturm decomposition by Broad- Gershacher and Moccia-Spizzo, the Feshbach method by Wu-Xi) and data measurements in laboratories: NIST (NBS; 2SO-MeV electron synchrotron storage ring (SURF-II)), Wisconsin Laboratory (Wisconsin Tantalus storage ring), Stanford Synchrotron Radiation Laboratory (SSRL), Berlin electron storage ring (BESSY), Daresbury Synchrotron Radiation Source (DSRS) [1,3,5,22-24].

On the one hand, there is sufficiently good accuracy of our theory, the secondly (bearing in mind that most of the listed methods are developed specifically for the study helium and can not be easily generalized to the case of the heavy multi-electron atoms) the definite advantage of the presented approach. Note that during translation for the units "Ry-eV" there was used the He ground-state energy value: E=- 5.80744875 Ry and the reduced Rydberg constant 1Ry = 13.603 876 eV.

Table 2a

Theoretical data for energy of the AR 3s3p $^1P_0$ (our data with those of other theories)

Method	Authors	E_r (Ry)
PT-REA	Our theory	-0.668802
Complex-rotation	Ho	-0.671252
Algebraic close coupling	Wakid-Callaway	-0.670
Diagonalization method	Senashenko-Wague	-0.6685
RHF	Nicolaides-Komninos	- 0.671388
R-matrix calculation	Hayes-Scott	-0.6707
Adiabatic potential curves	Koyoma etal	-0.6758
Adiabatic potential	Sadeghpour	-0.67558
L^2 tech.+Sturm	Broad-Gershacher	-0.67114
Feshbach method	Wu-Xi	-0.669 27
K-matrix L^2 basis-set	Moccia-Spizzo	-0.670 766

Table 2b

Theoretical data for width of the AR 3s3p $^1P_0$ (our data with with those of other theories)

Method	Authors	Γ/2 (Ry)
PT-REA	Our theory	0.006814
Complex-rotation	Ho	0.007024
Algebraic close coupling	Wakid-Callaway	0.00695
Diagonalization method	Senashenko-Wague	0.00548
RHF	Nicolaides-Komninos	-
R-matrix calculation	Hayes-Scott	0.00660
Adiabatic curves	Koyoma etal	-
Adiabatic potential	Sadeghpour	-
L^2 tech.+Sturm	Broad-Gershacher	0.00704
Feshbach method	Wu-Xi	0.00420
K-matrix L^2 basis-set	Moccia-Spizzo	0.00676

An interesting and valuable renewed data on Rydberg AR energies (in atomic units) of the double excited states $ns^2\ ^1S$ are listed in Table 4.

In whole an detailed analysis shows quite physically reasonable agreement between the presented theoretical and experimental results. But some difference, in our opinion, can be explained by different accuracy of estimates of the radial integrals, using the different type basis's (gauge invariance conservation or a degree of accounting for the exchange-correlation effects) and some other additional computing approximations.

Table 3

Theoretical and experimental data for energy and width of the AR 3s3p $^1P_0$ (our data with those of other best theories)

Method	E_r (eV)	Γ/2 (eV)
Theories		
Our data	69.9055	0.1854
Complex-rotation	69.8722	0.1911
MCHF	69.8703	-
R-matrix	69.8797	0.1796
Exp.		
NBS-I (1973)	69.919±0.007	0.132±0.014
Wisconsin(1982)	69.917±0.012	0.178±0.012
SSRL (1987)	69.917±0.012	0.178±0.012
BESSY (1988)	69.914±0.015	0.200±0.020
DSRS (2009)	69.880±0.022	0.180±0.015

Note: the He ground-state energy value: E=-5.80744875 Ry and the reduced Rydberg constant 1Ry = 13.603 876 eV.

Table 4

Predicted data for Rydberg AR energies (in atomic units) of the He double excited states $ns^2\ ^1S$ (our theory)

State	Energy	State	Energy
$6s^2$	0.08697	$10s^2$	0.03002
$7s^2$	0.06288	$11s^2$	0.02468
$8s^2$	0.04467	$12s^2$	0.01998
$9s^2$	0.03697	$13s^2$	0.01923
$14s^2$	0.01596	$18s^2$	0.00928
$15s^2$	0.01370	$19s^2$	0.00832
$16s^2$	0.01198	$20s^2$	0.00746
$17s^2$	0.01042	$21s^2$	0.00507

In our theory there are used gauge-optimized basis's of the relativistic and such basis has advantage in comparison with the standard DF type basis's.

In conclusion let us remind that in ref. [14] (see also [5,12]) it had been predicted a new optics and spectroscopy effect of the giant changing of the AS width in a sufficiently weak electric field (for two pairs of the Tm, Gd AR). Naturally any two states of different parity can be mixed by the external electric field. The mixing leads to redistribution of the autoionization widths. In a case of the heavy elements such as lanthanide and actinide atoms the respective redistribution has a giant effect. In the case of degenerate or near-degenerate resonances this effect becomes observable even at a moderately weak field.

We have tried to discover the same new spectral effect in a case of the He Rydberg autoionization states spectrum using the simplified version of the known strong-field operator PT formalism [5,14]. However, the preliminary estimates have indicated on the absence of the width giant broadening effect for the helium case, except for minor changes of the corresponding widths, which are well known in the standard atomic spectroscopy.

References

1. Grant I.P., Relativistic Quantum Theory of Atoms and Molecules. – Oxford, 2008. – 650P.
2. Luc Koenig E., Aymar M., Van Leeuwen R., Ubachs W., Hogervorst W.//Phys. Rev.A. – 1995. – Vol.52. – P.208-215.
3. Quiney H., Relativistic Quantum Mechanics of Atoms and Molecules//New Trends in Quantum Systems in Chemistry and Physics (Springer). – 2002. – Vol.6. – P.135–173.
4. Bell K.L., Berrington K., Crothers D., Hibbert A., Taylor K.T., BERTHA: 4-Component Relativistic Molecular Quantum Mechanics// Supercomputing, Collision Processes, and Application, Series: Physics of Atoms and Molecules (Springer). – 2002. – P.213–224.
5. Glushkov A.V., Relativistic Quantum Theory. Quantum, mechanics of Atomic Systems.-Odessa: Astroprint, 2008.-900P.
6. Safronova U.I., Safronova M.S., Third-order relativistic many-body calculations of energies, transition rates, hyperfine constants, and blackbody radiation shift in $^{171}Yb^{+}$//Phys. Rev. A. – 2009. – Vol.79. P. 022512.
7. Bieron J, Froese-Fischer C., Fritzsche S., Pachucki K., Lifetime and hyperfine structure of $^{3}D_{2}$ state of radium// J.Phys.B:At.Mol.Opt.Phys. – 2004. – Vol.37. – P.L305-311.
8. Ivanov L.N.,Ivanova E.P., Extrapolation of atomic ion energies by model potential method: Na-like spectra/ // Atom.Data Nucl. Data Tab. – 1979. – Vol.24. – P.95-121.
9. Bekov G.I., Vidolova-Angelova E., Ivanov L.N.,Letokhov V.S., Mishin V.I., Laser spectroscopy of low excited autoionization states of the ytterbium atom// JETP. – 1981. – Vol.80. – P.866-878.
10. Vidolova-Angelova E., Ivanov L.N., Autoionizing Rydberg states of thulium. Re-orientation decay due to monopole interaction// J.Phys.B:At.Mol.Opt.Phys. – 1991. – Vol.24. – P.4147-4158
11. Ivanov L.N., Letokhov V.S. Spectroscopy of autoionization resonances in heavy elements atoms// Com.Mod. Phys.D.:At.Mol.Phys. – 1985. – Vol.4. – P.169-184.
12. Glushkov A.V., Ivanov L.N., Ivanova E.P., Radiation decay of atomic states. Generalized energy approach// Autoioni-zation Phenomena in Atoms. – M.: Moscow State Univ. – 1986. – P.58-160.
13. Glushkov A.V., Ivanov L.N. Radiation decay of atomic states: atomic residue and gauge non-invariant contributions // Phys. Lett.A. – 1992. – Vol.170. – P.33-38.
14. Glushkov A.V., Ivanov L.N. DC Strong-field Stark-effect: consistent quantum-mechanical approach// J.Phys.B: At. Mol. Opt. Phys. – 1993. – Vol.26. – P.L379-386.

15. Glushkov A.V., Khetselius O.Yu., Svinarenko A.A., Relativistic theory of cooperative muon-gamma-nuclear processes: Negative muon capture and metastable nucleus discharge// Advances in the Theory of Quantum Systems in Chemistry and Physics (Springer). – 2012. – Vol.22. – P.51-70.
16. Glushkov A.V., Khetselius O.Yu., Loboda A.V., Svinarenko A.A., QED approach to atoms in a laser field: Multiphoton resonances and above threshold ionization//Frontiers in Quantum Systems in Chemistry and Physics (Springer). – 2008. – Vol.18. – P.541-558.
17. Glushkov A.V., Svinarenko A.A., Ignatenko A.V., Spectroscopy of autoionization resonances in spectra of the lanthanides atoms//Photoelectronics. – 2011. – Vol.20. – P. 90-94**.**
18. Svinarenko A.A., Nikola L.V., Prepelitsa G.P., Tkach T., Mischenko E., The Auger (autoionization) decay of excited states in spectra of multicharged ions: Relativistic theory//Spectral Lines Shape. – 2010. – Vol.16. – P.94-98
19. Svinarenko A.A., Spectroscopy of autoionization resonances in spectra of barium: New spectral data // Phototelectronics. – 2014. – Vol.23. – P.85-90.
20. Malinovskaya S.V., Glushkov A.V., Khetselius O.Yu., Svinarenko A., Bakunina E.V., Florko T.A., The optimized perturbation theory scheme for calculating interatomic potentials and hyperfine lines shift for heavy atoms in buffer inert gas//Int. Journ.of Quantum Chemistry. – 2009. – Vol.109. – P.3325-3329.
21. Khetselius O.Yu., Relativistic perturbation theory calculation of the hyperfine structure parameters for some heavy-element isotopes//Int. Journ. of Quantum Chemistry. – 2009. – Vol.109, N14. – P.3330-3335.
22. Madden R., Codling K., New autoionization atomic energy levels in He, Ne, Ar// Phys.Rev.Lett. 1963 – Vol.10. – P.516-520.
23. SakhoI., Konté K., Ndao A.S., Biaye M., Wagué A., Calculations of $(nl)^2$ and (3lnl') autoionizing states in two-electron systems/.// Physics Scripta. – 2010. – Vol.82. – P. 035301 (8pp)
24. Ho Y.K., Autoionizing $^1P^0$ states of He between the N=2 and 3 threshold of He^+ //Phys.Rev.A.1991. – Vol.44. – P.4154-4161.

This article has been received within 2015

UDC 539.183

A. V. Glushkov, A. A. Svinarenko, V. B. Ternovsky, A. V. Smirnov, P. A. Zaichko

SPECTROSCOPY OF THE COMPLEX AUTOIONIZATION RESONANCES IN SPECTRUM OF HELIUM: TEST AND NEW SPECTRAL DATA

Abstract.

We applied a generalized energy approach (Gell-Mann and Low S-matrix formalism) combined with the relativistic multi-quasiparticle (QP) perturbation theory (PT) with the Dirac-Kohn-Sham zeroth approximation and accounting for the exchange-correlation, relativistic corrections to studying autoionization resonances in the helium spectrum, in particular, we predicted the energies and widths of the number of the Rydberg resonances. There are presented the results of comparison of our theory data for the autoionization resonance 3s3p $^1P_0$ with the available experimental data and those results of other theories, including, method of complex rotation by Ho, algebraic approach by Wakid-Callaway, diagonalization method by Senashenko-Wague etc.

Key words: spectroscopy of autoionization resonances, relativistic energy approach, helium

УДК 539.183

А. В. Глушков, А. А.Свинаренко, В. Б. Терновский, А. В. Смирнов, П. А. Заичко

СПЕКТРОСКОПИЯ СЛОЖНЫХ АВТОИОНИЗАЦИОННЫХ РЕЗОНАНСОВ В СПЕКТРЕ ГЕЛИЯ: ТЕСТ И НОВЫЕ СПЕКТРАЛЬНЫЕ ДАННЫЕ

Резюме.

Обобщенный энергетический подход (S-матричный формализм Гелл-Мана и Лоу) и релятивистская теория возмущений с дирак-кон-шэмовским нулевым приближением и учетом обменно-корреляционных и релятивистских поправок применены к изучению автоионизационных резонансов в атоме гелия, в частности, предсказаны энергии и ширины ряда ридберговых резонансов. Представлены результаты сравнения данных нашей теории, в частности, для автоионизацийного резонанса 3s3p $^1P_0$ с имеющимися экспериментальными данными и результатами других теорий, в том числе, методом комплексного вращения Хо алгебраического подхода Wakid-Callaway, метода диагонализации Senashenko-Wague и т.д.

Ключевые слова: спектроскопия автоионизационных резонансов, релятивистский энергетический подход, гелий

УДК 539.183

А. В. Глушков, А. А.Свинаренко, В. Б. Терновський, А. В. Смирнов, П. О. Заїчко

СПЕКТРОСКОПІЯ СКЛАДНИХ АВТОІОНІЗАЦІЙНИХ РЕЗОНАНСІВ В СПЕКТРІ ГЕЛІЮ: ТЕСТ І НОВІ СПЕКТРАЛЬНІ ДАНІ

Резюме.

Узагальнений енергетичний підхід (S-матричний формалізм Гелл-Мана та Лоу) и релятивістська теорія збурень з дірак-кон-шемівським нульовим наближенням та урахуванням обмінно-кореляційних і релятивістських поправок застосований до вивчення автоіонізаційних резонансів у атомі гелію, зокрема, передбачені енергії та ширини ряду рідбергових резонансів. Представлені результати порівняння даних нашої теорії, зокрема, для автоіонізаційного резонансу $3s3p\ ^1P_0$ з наявними експериментальними даними і результатами інших теорій, у тому числі, методом комплексного обертання Хо, алгебраїчного підходу Wakid-Callaway, методу діагоналізації Senashenko-Wague і т.д.

Ключові слова: спектроскопія автоіонізаційних резонансів, релятивістський енергетичний підхід, гелій

UDC 621.315.592

N. S. Simanovych, Y. N. Karakis, M. I. Kutalova, A. P. Chebanenko, N. P. Zatovskaya

THE PROCESSES ASSOCIATED WITH THE BIFURCATION IN THE CURRENT-VOLTAGE CHARACTERISTICS

Odessa I. I. Mechnikov National University, Odessa, 42, Pastera str., tel. 765-32-16
e-mail: photoelectronics@onu.edu.ua.

The mechanisms leading to the intersection of the dark and light current-voltage characteristics and related phenomena has been considered. The possibility of participation in it as non-equilibrium carriers in the case of solar cells, and the contribution of the equilibrium charge when the temperature impact on the reference diode has been shown. A model explaining the observed features has been built

The intersection of the current-voltage characteristics (CVC) in the study of electrical characteristics of p-n-junctions suggests that in addition to the standard mechanisms of the CVC formation are present or additional process, depending on the applied voltage, or the formation of the diffusion and drift current differs from the "classic" model, or additional external exposure to radiation or temperature takes place. These reasons make the actual identification of additional mechanisms influencing the CVC formation.

1. The intersection of solar cells light and dark current-voltage characteristics

In the study of the solar cells based on CdS-Cu_2S heterojunctions [1] the crossing of the dark and light current-voltage characteristics under forward bias applied to the element (Fig.1) was observed. Similar was the appearance of the control volt-ampere characteristic of silicon solar cells FD6K of industrial manufacturing.

Crossing of the dark and light current-voltage characteristic of the photodiode seems quite paradoxical. It turns out that there is a bias voltage, where via structure the same current flows regardless of influence on it light or it is in the darkness. While it is known that irradiation creates new non-equilibrium carriers. Moreover, since for creation of the photodiodes are selected especially photosensitive materials, the concentration of nonequilibrium carriers Δn is much larger than the equilibrium concentration of carriers n_0, located in the semiconductor in the initial state before irradiation. At the same voltage light current must be much greater than the dark. Moreover, equilibrium carriers in the semiconductor before the lighting under the action of applied voltage are also involved in charge transfer and, accordingly, shall contribute to the light flowing current amount.

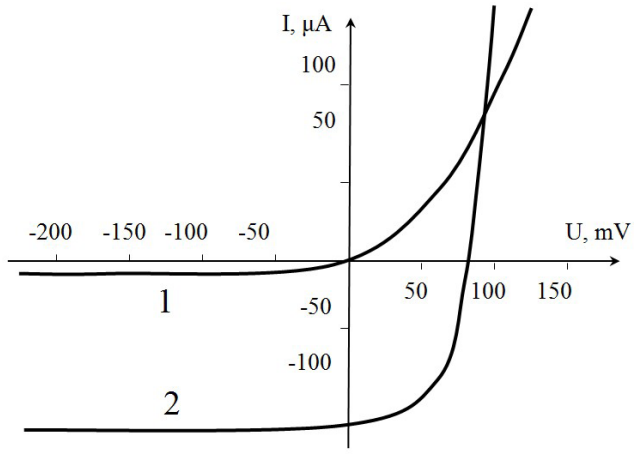

Fig. 1. Typical current-voltage characteristic in the dark (1) and under illumination (2) of investigated photodiode.

It should be noted that the effect of the current-voltage characteristic was observed only in the presence of a sufficiently large contact potential difference. The barrier height for the studied structures, defined as by the standard method from the capacitance-voltage characteristics [2], and by the cutoff of the straight section of direct branches of current-voltage characteristic at high voltages [3,4], was 0.6 eV for heterostructures and 0.4 eV in the case of silicon diodes. On the contrary, in the control experiments for germanium photocells FD-3 of the industrial manufacturing with a barrier height of 0.11 to 0.14 eV was not able to produce the intersection of light and dark current-voltage characteristics in the workspace of direct biases.

Thus, the model to explain the anomalous form of the CVC should be based on high altitude equilibrium barrier p-n junction.

At application of the reverse bias barrier height increases (Fig. 2, cipher 2) and current, as in the dark and at the light is formed by the drift of minority carriers, remaining essentially the same throughout the region of negative biases (left semiaxis, Fig.1). The effect of the light is reduced to the arise of additional nonequilibrium charge and a corresponding increase in the light-generated current. At the same time due to the spatially separated non-equilibrium carriers generates the additional internal field directed in accordance with the principle of Le Chatelier-Braun against the field barrier. As a result, the barrier height decreases slightly. In figure 2 this is shown by the dotted line. In order not to overload the zone diagram there shows only the changes of the bottom of the conduction band. Since the barrier height is significant, its small reduction has virtually no effect on the amount of the drift current.

If no other processes have not occurred, as the result of lighting the entire dark current-voltage characteristic must shift down the same distance at all points, and no intersection of the graphs could not happen. However, for direct branch (right semiaxis, Fig.1) it is not so.

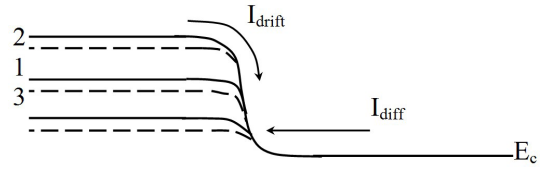

Fig. 2. The change of the barrier profile from the initial state (1) at the reverse (2) and direct (3) biases

At forward bias occurs two processes. First, the external voltage is now directed against the field barrier and, consequently, lowers its (in Fig. 2, cipher 3). Secondly the current transport mechanism changes. Now the current is formed due to diffusion of majority carriers from right to left, as shown in figure 2.

For a much lower barrier additional its reducing at light exposure is much more sensitive. Moreover, note that into the transfer process involves electrons with lower, much more populated levels.

At the same time due to the barrier height decrease the field electric intensity in junction decreases and competing drift current occurs less. These reasons lead to an additional increase in current at the light, and as a result, its value is more than dark one. Light current-voltage characteristic at the curtain biases lies above the dark.

At the same time at small direct biases, as seen in Fig. 1, at voltages that are lower than open-circuit voltage, the current remains negative. This is transfer region when the barrier is not enough strong lowered and current formation is carried predominantly by the same mechanisms as for backward branch. Plot of the light current-voltage characteristic lies below the plot of the dark current-voltage characteristic.

If at the beginning of the straight branch of the light current-voltage characteristic curve is below the dark current-voltage characteristic curve, and at the end of the straight branch the light current-voltage characteristic curve lies above the curve of the dark current-voltage characteristic, in accordance with the theorem of Bolzano-Cauchy necessarily exist a point of their intersection. From the above it is also clear that this can occur only for positive currents, that is, when voltages are greater than the open-circuit voltage.

Thus, the proposed model is based on the reducing of the barrier height at light and a corresponding diffusion current increase in the formed gap. This helps to explain the currents balance at the bifurcation point. Under illumination field patterns of the barrier, now at this point unchanged, the spatial parts of the nonequilibrium carriers. Drift current occurs(figure 2) from left to right. But this process includes feedback – at the expense of the field of free carriers, the barrier is reduced and the additional diffusion currier stream

forms – (figure 2) from right to left. At some forward bias, so the original height of the barrier in the dark, these two additional competing flux at light compensate each other. So for this voltage at the point of current-voltage characteristic intersection total current across the junction when the light is on not changed.

It becomes also clear why for photodiodes with a small initial barrier it is difficult to achieve the current-voltage characteristic crossing. Diffusion current even before lighting is too large. So the lightning may not considerably change its value.

The proposed model allows us to explain the bifurcation point coordinate dependence on the light intensity. If the luminous flux increases, a number of carriers separated by a barrier grow. It requires larger forward bias, the barrier height occurs less and its sagging at the light effect were more efficiently. Indeed, such behaviour has been identified for the CdS-Cu_2S heterostructure (Fig.3).

On the plot, are clearly seen two regions. So, the view according to Fig. 3 indicates the existence of two mechanisms of the volt-luxury characteristic formation at high and low light intensities.

It should be noted that the point of intersection always observed on the transitional region of schedule current-voltage characteristic between the exponential part, when works normal diode mechanisms and a linear ohmic region for large direct biases when the barrier is already compensated by the external field and the current is limited only by the diode base series resistance. This requires additional considerations.

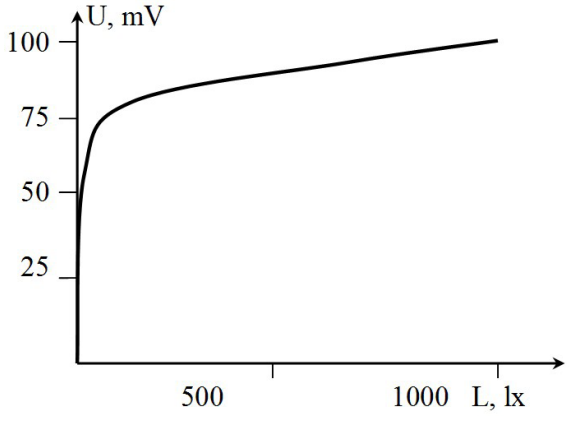

Fig. 3. The dependence of the coordinates of the current-voltage characteristics crossing point on light intensity.

If the diode series resistance in the dark and at the light has not changed, the ends of current-voltage characteristic plots would be parallel. However, the photocells consciously made of very sensitive materials. At lightning, the series resistance decreases. The slope of the linear part of the plot at limiting direct biases at the light increases. The curves intersect.

Most likely, both considered mechanism – the light barrier height reducing and series resistance decrease is carried out at the same time, ensuring by their mutual action the occurrence of the plot current-voltage characteristic intersection effect.

However, for the volt-luminous characteristic (Fig. 3) two presented mechanisms are competitors. As shown above, the barrier height reduction at lightening should lead to an increase the voltage in the point of branching. Bifurcation coordinate needs to shift to the right. If the slope of the linear part of the current-voltage characteristic with the light intensity increases, the bifurcation point should to shift to the left (Fig. 1), towards the smaller voltage values. The presence of such competition creates rather complicated, nonlinear type of plot (Fig. 3). At low light intensities the first mechanism prevails. Coordinate of the bifurcation point increases relatively quickly. At high light intensities contribution of the second, competing, mechanism increases. The voltage at the point of branching is increased more flat.

2. The intersection of the dark current-voltage characteristics

For standard reference diode D814G of industrial manufacturing in the area of stabilization, we observed the intersection of current-voltage characteristics measured at different temperatures (Fig. 4). Further raising the temperature above 60 ^{0}C led to the current-voltage characteristic formation mechanism change as far as in this temperature region in Germanium already is noticeable number of area-zone and above-barrier transitions carriers.

The intersection of the current-voltage characteristics creates a paradoxical situation. Before the diode bifurcation point the reverse current increases with temperature due to the saturation current I_s increase (in the figure arrow “down”).

In the case of stabilitrons, one of this condition is in principle enough in order to from geometrical considerations formed the intersection point. If the basic proportions of the current-voltage characteristic plot are stored, including the section of stabilization, when the current graph grows downwards at an angle, a simple it lowering with temperature must inevitably create the intersection. This requires that for high temperatures the transition on the section of stabilization was carried out at higher voltages, i.e., the standard horizontal "shelf" on the reverse branches of current-voltage characteristic was delayed.

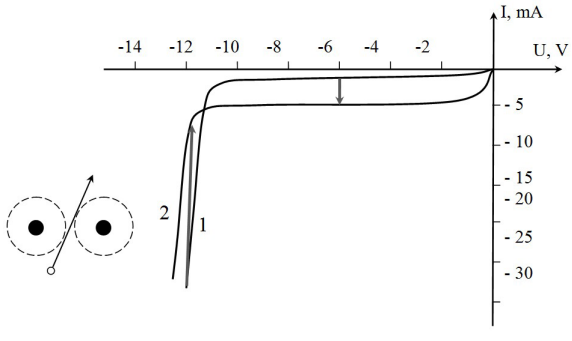

Fig. 4. Reverse current-voltage characteristics of the stabilitron, measured at different temperatures: (1) – 17 ^{0}C, (2) – 56 ^{0}C.

From a physical point of view it requires the construction of an adequate model, as the current formed after the bifurcation point in the diode at the same voltage decreases sharply. Moreover, this decrease was several times greater than the increase in the current at voltages before the bifurcation. This unusual manifestation is even more paradoxical if take into account that the processes leading to an increase in current I_s with temperature, of course, continue to be performed for the entire region of the applied voltage change.

Thus, it is necessary to fined the mechanism that is more powerful than the exponential increase with temperature in the carrier number and is able to imbibe this process. In addition, this model would explain the observed bifurcation point removal, during heating to the left in the region of higher biases. Or, what is the same, why with the temperature increasing increases the length of horizontal section of the current-voltage characteristic before the breakdown region.

To clarify this processes peculiarity lets consider influence of the temperature on the diode material crystal lattice. The usual carrier concentration in a semiconductor is of the order of 10^{16} – 10^{17} cm^{-3}, whereas the density of lattice sites ~ 10^{21} cm^{-3}. I.e. cell crystal lattice density is about 10^{20} cm^{-3}. This means that during the current formation carriers are not the total substance. Each one is in its crystalline cell and from each other they are separated by several orders of cells. The lattice points are charged relative to the electron by equal in magnitude but opposite in sign charge. Such points are much closer to each carrier. In other words, the current formation in the crystal structure mainly influences the individual interaction of the electron with the lattice points.

In the case of the reference diodes this mechanism is enhanced. One of the main processes of stabilization section formation, when the diode current is rising rapidly and the voltage remains practically unchanged, is the formation of carrier number avalanche multiplication. At the same time on one or more of the free path lengths, the carrier must pick up the energy in an external field equal or greater than the width of the forbidden zone. This allows it in the impact with another lattice point to knock out an additional electron. Therefore, the semiconductor material for the stabilitrone manufacture is chosen in such way as to ensure sufficient free carriers and the crystal structure points interaction - grid transition must be relatively small, and the capture cross section high [5].

With temperature increasing diode reverse current and the breakdown voltage increases. This is connected with the fact that the thermal scattering increases, the carrier free path reduces and to p-n-junction need to put more voltage for the charge carriers on a smaller path (equal to the length of free path) pick up kinetic energy sufficient for ionization [6]. Thus, with increasing temperature the length of the stationary section of the current-voltage characteristic ("shelves" on the current-voltage dependence) increases.

Simultaneously there is another process. With the temperature increasing the crystal lattice vibrations increases. As a result, their capture cross-sections increase. In conventional diodes it does not lead to any noticeable changes in current. However, in the reference diodes it is not so,

because the semiconductor material is chosen so that the magnitude of the capture cross section is comparable with the distance between the lattice points. In these conditions, even small changes in the capture cross-section diameters can significantly narrow "corridor" for flying carries (see inset in fig. 4). The frequency of interactions with the lattice points is greatly increased. This leads to a strong additional scattering of picked up in a field the carrier energy. The formation of avalanches becomes more difficult, the current on the stabilization section decreases (see Fig. 4). Moreover, because the interaction with the lattice for each carrier is individually, the total increase in the equilibrium charge concentration with temperatures increasing influence on this effect slightly. If the capture cross-section will increase so that will be closed down, avalanche generation, and hence the stabilization section will be impossible for any charge amount.

Thus, all the observed features of the reference diodes current-voltage characteristic due to the specific character of the material used have the same nature, determined by the increase lattice points fluctuatings with the temperature, and consequently increase in currier scattering.

Literature

1. Karakis Yu.N., Kutalava M.I., Zatovskaya N.P. "Optimization in conditions for CdS-Cu_2S heterophotocell shaping" // "Photoelectronics", № 21. Odessa, "Одеський національний університет" 2012. – P. 86 – 89.
2. Берман Л.С., Лебедев А.А. – Емкостная спектроскопия глубоких центров в полупроводниках // Ленинград, "Наука", 1981. – 176 с.
3. Лебедев А.И. Физика полупроводниковых приборов // М. Физматлит., 2008 .
4. Чебаненко А.П., Зубрицкий С.В., Каракис Ю.Н. – Методические указания к специальному практикуму "Физика полупроводниковых приборов Часть I. Полупроводниковые диоды". // Издательство Одесского национального университета. г. Одесса. 2015. – С. 1 – 62.
5. Горелик С.С., Дашевский М.Я. Материаловедение полупроводников и диэлектриков//М., "Мисис" 2003, 481 с.
6. Викулин И.М., Стафеев В.И. – Физика полупроводниковых диодов // М. "Радио и связь" 1990, 264 с.

This article has been received within 2015

UDC 621.315.592

N. S. Simanovych, Y. N. Karakis, M. I. Kutalova, A. P. Chebanenko, N. P. Zatovskaya

THE PROCESSES ASSOCIATED WITH THE BIFURCATION IN THE CURRENT-VOLTAGE CHARACTERISTICS

Resume

The mechanisms leading to the intersection of the dark and light current-voltage characteristics and related phenomena has been considered. The possibility of participation in it as non-equilibrium carriers in the case of solar cells, and the contribution of the equilibrium charge when the temperature impact on the reference diode has been shown. Models explaining the observed features has been built

Key words: bifurcation, process, characteristic.

УДК 621.315.592

Н. С. Симанович, Ю. М. Каракис, М. И. Куталова, А. П. Чебаненко, Н. П. Затовская

ПРОЦЕССЫ, СВЯЗАННЫЕ С БИФУРКАЦИЕЙ ВОЛЬТ-АМПЕРНЫХ ХАРАКТЕРИСТИК

Резюме.

Рассмотрены механизмы, приводящие к пересечению вольт-амперных характеристик и сопутствующие явления. Показана возможность участия при этом как неравновесных носителей в случае фотоэлементов, так и вклад равновесного заряда при температурном воздействии на опорные диоды. Построены модели, объясняющие наблюдаемые особенности.

Ключевые слова: бифуркация, процессы, характеристика.

УДК 621.315.592

Н. С. Сімanович, Ю. М. Каракіс, М. І. Куталова, А. П. Чебаненко, Н. П. Затовська

ПРОЦЕСИ, ЩО ПОВ'ЯЗАНІ З БІФУРКАЦІЄЮ ВОЛЬТ – АМПЕРНИХ ХАРАКТЕРИСТИК

Резюме.

Розглянуто механізми, що приводять до перетину вольт-амперних характеристик та явища, що їх супроводжують. Показано можливість участі при цьому як нерівноважних носіїв у випадку фотоелементів, так і внесок рівноважного заряду при температурному впливі на опорні діоди. Побудовано моделі, які пояснюють особливості що спостерігаються.

Ключові слова: бифуркація, процес, характеристика.

UDC 539.182

A. N. Shakhman

Odessa National Polytechnical University, 1, Shevchenko pr., Ukraine
e-mail: quantsha@mail.ru

RELATIVISTIC THEORY OF SPECTRA OF PIONIC ATOMS WITH ACCOUNT OF STRONG PION-NUCLEAR INTERACTION EFFECTS

It is presented a consistent relativistic theory of spectra of the pionic atoms on the basis of the Klein-Gordon-Fock with a generalized radiation and strong pion-nuclear potentials. There are presented data of calculation of the energy and spectral parameters for pioninc neon, cesium, holmium, thulium, ytterbium, lutetium, thallium, lead, and others, including the calculation of energy shifts, the widths of the levels due to the strong interaction with accounting for the the radiation (vacuum polarization), nuclear (finite size of a nucleus) and other corrections.

1. Introduction

In previous papers [1-3] we have developed a new relativistic method of the Klein-Gordon-Fock equation with the simplified pion-nuclear potential to determine transition energies in spectroscopy of light, middle and heavy pionic atoms with accounting for the strong interaction effects.

Here we generalize this theory in order to describe pion-nuclear interaction more consistently using generalized radiation and strong pion-nuclear potentials. As illustration there are presented data of calculation of the energy and spectral parameters for pioninc neon, cesium, holmium, thulium, ytterbium, lutetium, thallium, lead, and others, including the calculation of energy shifts, the widths of the levels due to the strong interaction with accounting for the the radiation (vacuum polarization), nuclear (finite size of a nucleus) and other corrections.

Following [1-3], let us remind that spectroscopy of hadron atoms has been used as a tool for the study of particles and fundamental properties for a long time. Exotic atoms are also interesting objects as they enable to probe aspects of atomic and nuclear structure that are quantitatively different from what can be studied in electronic or "normal" atoms. At present time one of the most sensitive tests for the chiral symmetry breaking scenario in the modern hadron's physics is provided by studying the exotic hadron-atomic systems. Nowadays the transition energies in pionic atoms are measured with an unprecedented precision and from studying spectra of the hadronic atoms it is possible to investigate the strong interaction at low energies measuring the energy and natural width of the ground level with a precision of few meV [1-13]. The strong interaction is the reason for a shift in the energies of the low-lying levels from the purely electromagnetic values and the finite lifetime of the state corresponds to an increase in the observed level width. The most known theoretical models to treating the hadronic (pionic, kaonic, muonic, antiprotonic etc.) atomic systems are presented in refs. [1-5,7,8]. The most difficult aspects of the theoretical modelling are reduced to the correct description of pion-nuclear strong interaction [1-3] as the electromagnetic part of the problem is reasonably accounted for.

2. Total relativistic theory of spectra of pionic atoms

As the basis's of a new method has been published, here we present only the key topics of an approach [1-3]. All available theoretical models

to treating the hadronic (kaonic, pionic) atoms are naturally based on the using the Klein-Gordon-Fock equation [2,5], which can be written as follows :

$$m^2c^2\Psi(x)=\{\frac{1}{c^2}[i\hbar\partial_t+eV_0(r)]^2+\hbar^2\nabla^2\}\Psi(x) \quad (1)$$

where c is a speed of the light, *h* is the Planck constant, and $\Psi_0(x)$ is the scalar wave function of the space-temporal coordinates. Usually one considers the central potential $[V_0(r), 0]$ approximation with the stationary solution:

$$\Psi(x)=\exp(-iEt/\hbar)\,\varphi(x), \quad (2)$$

where $\varphi(x)$ is the solution of the stationary equation:

$$\{\frac{1}{c^2}[E+eV_0(r)]^2+\hbar^2\nabla^2-m^2c^2\}\varphi(x)=0 \quad (3)$$

Here E is the total energy of the system (sum of the mass energy mc^2 and binding energy e_0). In principle, the central potential V_0 naturally includes the central Coulomb potential, the vacuum-polarization potential, the strong interaction potential.

The most direct approach to treating the strong interaction is provided by the well known optical potential model (c.g. [2]). Practically in all papers the central potential V_0 is the sum of the following potentials. The nuclear potential for the spherically symmetric density $\rho(r|R)$ is [6,13]:

$$V_{nucl}(r|R)=-((1/r)\int_0^r d\,r'^2\rho(r'|R)+\int_r^\infty d\,r'\rho(r'|R) \quad (4)$$

The most popular Fermi-model approximation the charge distribution in the nucleus $\rho(r)$ (c.f.[11]) is as follows:

$$\tilde{n}(r)=\tilde{n}_0/\{1+\exp[(r-c)/a)]\}, \quad (5)$$

where the parameter *a=0.*523 fm, the parameter *c* is chosen by such a way that it is true the following condition for average-squared radius:

$$<r^2>^{1/2}=(0.836\times A^{1/3}+0.5700)\text{fm}.$$

The effective algorithm for its definition is used in refs. [12] and reduced to solution of the following system of the differential equations:

$$V'nucl(r,R)=(1/r^2)\int_0^r d\,r'^2\rho(r',R)\equiv(1/r^2)y(r,R), \quad (6)$$

$$y'(r,R)=r^2\rho(r,R), \quad (7)$$

$$\tilde{n}'(r)=(\tilde{n}_0/a)\exp[(r-c)/a]\{1+\exp[(r-c)/a)]\}^2 \quad (8)$$

with the corresponding boundary conditions. Another, probably, more consistent approach is in using the relativistic mean-field (RMF) model, which been designed as a renormalizable meson-field theory for nuclear matter and finite nuclei [13].To take into account the radiation corrections, namely, the effect of the vacuum polarization we have used the generalized Ueling-Serber potential with modification to take into account the high-order radiative corrections [5,12].

The most difficult aspect is an adequate account for the strong interaction. On order to describe the strong p^-N interaction we have used the optical potential model in which the generalized Ericson-Ericson potential is as follows:

$$V_{\pi^-N}=V_{opt}(r)=-\frac{4\pi}{2\overline{m}}\left\{q(r)\nabla\frac{\alpha(r)}{1+4/3\pi\xi\alpha(r)}\nabla\right\} \quad (9)$$

$$q(r)=\left(1+\frac{m_\pi}{m_N}\right)\{b_0\rho(r)+b_1[\rho_n(r)-\rho_p(r)]\}+$$
$$+\left(1+\frac{m_\pi}{2m_N}\right)\{B_0\rho^2(r)+B_1\rho(r)\delta(r)\}, \quad (10)$$

$$\alpha(r)=\left(1+\frac{m_\pi}{m_N}\right)^{-1}\{c_0\rho(r)+c_1[\rho_n(r)-\rho_p(r)]\}+$$
$$+\left(1+\frac{m_\pi}{2m_N}\right)^{-1}\{C_0\rho^2(r)+C_1\rho(r)\delta(r)\}. \quad (11)$$

Here $\rho_{p,n}(r)$ – distribution of a density of the protons and neutrons, respectively, ξ – parameter ($\xi=0$ corresponds to case of "no correlation", $\xi=1$, if anticorrelations between nucleons); respectively isoscalar and isovector parameters b_0, c_0, B_0, b_1, c_1, C_0 B_1, C_1 –are corresponding to the s-wave and p-wave (repulsive and attracting potential member) scattering length in the combined spin-isospin space with taking into account the

absorption of pions (with different channels at p-p pair $B_{0(pp)}$ and *p-n* pair $B_{0(pn)}$), and isospin and spin dependence of an amplitude p-N scattering

$$(b_0\rho(r) \to b_0\rho(r) + b_1\{\rho_p(r) - \rho_n(r)\},$$

the Lorentz-Lorentz effect in the p-wave interaction. For the pionic atom with remained electron shells the total wave-function is a product of the product Slater determinant of the electrons subsystem (Dirac equation) and the pionic wave function. In whole the energy of the hadronic atom is represented as the sum:

$$E \approx E_{KG} + E_{FS} + E_{VP} + E_N; \qquad (12)$$

Here E_{KG} -is the energy of a pion in a nucleus (Z, A) with the point-like charge (dominative contribution in (12)), E_{FS} is the contribution due to the nucleus finite size effect, E_{VP} is the radiation correction due to the vacuum-polarization effect, E_N is the energy shift due to the strong interaction V_N.

The strong pion-nucleus interaction contribution can be found from the solution of the Klein-Gordon equation with the corresponding pion-nucleon potential.

3. Results and conclusions

In table 1 we present theoretical and experimental data for shift and widths (keV) provided by the strong pion-nuclear interaction for a number of pionic atoms. The shortened designation of the parameter sets for the strong p-N interaction potential: Tauscher -Tau1; Tauscher, -Tau2; Batty etal-Bat; Seki etal- Sek; de Laat-Konijin et al - Laat, this work -Sha. In our parameterization of the strong p-N interaction potential the most reliably defined (B_0,c_0,c_1,C_0) parameters are remained unchanged, and the parameters whose values differ greatly in different sets, in particular, b_1 (b_1 = -0.094) plus still not included ones ImB_1, ImC_1 have been optimized by calculating dependencies strong shifts for p-^{20}Ne, ^{24}Mg, ^{93}Nb, ^{133}Cs,^{175}Lu, ^{181}Ta, ^{197}Au, ^{208}Pb and further check that satisfies the smallest standard deviation of reliable experimental values.

Table 1

Theoretical and experimental data for shift and widths (keV) provided by the strong pion-nuclear interaction for a number of pionic atoms (see text)

ε_{4f},Γ_{4f}	Exp	H-like Func.	Tau1 $\xi = 0$	Tau2 $\xi = 1$
^{165}Ho: ε	0.29±0.01	0.21	0.25 0.27	0.24 0.26
^{169}Tm: ε	-	-	-	-
^{173}Yb: ε	-	-	-	-
^{175}Lu: ε	0.51±0.04	0.36	0.43	0.42
^{181}Ta: ε	0.56±0.04	0.47	0.57	0.54
^{197}Au: ε	1.25±0.07	-	1.21	1.14
^{208}Pb: ε	1.68±0.04	-	1.76	1.62
^{209}Bi: ε	1.78±0.06	-	1.94	1.80
^{165}Ho: Γ	0.21±0.02	0.08	0.13	0.12
^{169}Tm: Γ	-	-	-	-
^{173}Yb: Γ	-	-	-	-
^{175}Lu: Γ	0.27±0.07	0.14	0.23	0.22
^{181}Ta: Γ	0.31±0.05	0.16	0.31	0.30
^{197}Au: Γ	0.77±0.04	-	0.73	0.68
^{208}Pb: Γ	0.98±0.05	-	1.18	1.04
^{209}Bi: Γ	1.24±0.09	-	1.35	1.18

Table 1 (continuation)

Theoretical and experimental data for shift and widths (keV) provided by the strong pion-nuclear interaction for a number of pionic atoms (see text)

$\varepsilon_{4f}, \Gamma_{4f}$	Bat $\xi = 1$	Sek $\xi = 1$	Laat $\xi = 1$	Sha $\xi = 1$
^{165}Ho: ε	0.24	0.21	0.26	0.29
^{169}Tm: ε	-	-	-	0.38
^{173}Yb: ε	-	-	-	0.44
^{175}Lu: ε	0.41	0.36	0.46	0.50
^{181}Ta: ε	0.53	0.47	0.60	0.55
^{197}Au: ε	1.12	0.98	1.25	1.24
^{208}Pb: ε	1.58	1.39	1.68	1.65
^{209}Bi: ε	1.78	1.57	1.83	1.77
^{165}Ho: Γ	0.13	0.11	0.13	0.20
^{169}Tm: Γ	-	-	-	0.23
^{173}Yb: Γ	-	-	-	0.26
^{175}Lu: Γ	0.24	0.20	0.24	0.28
^{181}Ta: Γ	0.31	0.27	0.31	0.30
^{197}Au: Γ	0.69	0.58	0.67	0.75
^{208}Pb: Γ	1.03	0.86	0.98	0.97
^{209}Bi: Γ	1.17	0.99	1.10	1.22

Analysis shows that the data from Table 1 of all alternative theories (except the column «H-like Func», containing data calculation within variation theory with relativistic H-like functions; here there is very unsatisfactorily agreement with experimental data) are obtained on the basis of the Klein-Gordon-Fock equation with nuclear potential V_{pN} by Erickson-Erickson with different parametrization [2]. More precise calculation data are based on the theory of Klein-Gordon-Fock equation with nuclear potential V_{pN} with parameters Tau1, Tau2, Laat, Sha (see table 1). Our theory shows that more optimal parameterization V_{pN} can significantly improve a quality of determining characteristics of the pionic atoms, which are provided by the strong pion-nuclear interaction. This conclusion is confirmed by the data of computing quadrupole shift of the 4f level in spectra of some p^-A, in particular,^{165}Ho, ^{169}Tm, ^{173}Yb,^{175}Lu,^{209}Bi [2-7, 13], provided by the strong pion-nuclear interaction.

References

1. Shakhman A.N., Strong p-nucleat interaction effects in spectroscopy of hadronic atoms //Photoelectronics. – 2013. – Vol.22. – P.93-97
2. Serga I.N., Dubrovskaya Yu.V., Kvasikova A.S., Shakhman A.N., Sukharev D.E., Spectroscopy of hadronic atoms: Energy shifts// Journal of Physics: C Ser. (IOP). – 2012. – Vol.397. – P.012013 (5p.).
3. Kuznetsova A.A., Kvasikova A.S., Shakhman A.N., Vitavetskaya L.A., Calculating the radiative vacuum polarization contribution to the energy shift of 2p-2s transition in m-hydrogen// Photoelectronics. – 2012. – N21. – P.66-67.
4. Deslattes R., Kessler E., Indelicato P., de Billy L., Lindroth E. , Anton J., Exotic atoms// Rev. Mod. Phys. – 2003. – Vol.75. – P.35-70.
5. Backenstoss G., Pionic atoms//Ann.Rev. Nucl.Sci.-1970.-Vol.20.-P.467-510.
6. Menshikov L I and Evseev M K, Some questions of physics of exotic atoms// Phys. Uspekhi.2001 – Vol. 171. – P.150-184.
7. Scherer S, Introduction to chiral perturbation theory//Advances in Nuclear Physics, Eds. J.W. Negele and E.W. Vogt (Berlin, Springer). – 2003. – Vol.27.-P.5-50.
8. Schroder H., Badertscher A., Goudsmit P., Janousch M., Leisi H., Matsinos E., Sigg D., Zhao Z., Chatellard D., Egger J., Gabathuler K., Hauser P., Simons L., Rusi El Hassani A., The pion-nucleon scattering lengths from pionic hydrogen and deuterium//Eur.Phys.J. – 2001. – Vol. C21.-P.473
9. Lyubovitskij V., Rusetsky A., πp atom

in ChPT: Strong energy-level shift/ // Phys. Lett.B. – 2000. – Vol.494. – P.9-13.
10. Anagnostopoulos D., Biri S., Boisbourdain V., Demeter M., Borchert G. et al-PSI, Low-energy X-ray standards from pionic atoms/ //Nucl. Inst. Meth.B. – 2003. – Vol.205. – P.9-18.
11. Batty C.J., Eckhause M., Gall K.P., et al, Strong interaction effects in high Z- K^- atoms//Phys. Rev. C. – 1989. – Vol.40. – P.2154-2160.
12. Glushkov A.V., Gauge-invariant QED perturbation theory approach to calculating nuclear electric quadrupole moments, hyperfine structure constants for heavy atoms and ions/ Glushkov A.V., Khetselius O.Yu., Sukharev D.E., Gurnitskaya E.P., Loboda A.V., Florko T.A., Lovett L.// Frontiers in Quantum Systems in Chemistry and Physics (Berlin, Springer). – 2008. – Vol.18. – P.505-522.
13. Serot B. D., Advances in Nuclear Physics Vol. 16: The Relativistic Nuclear Many Body Problem/ Serot B. D., Walecka J. D. – Plenum Press, New York, 1986.

This article has been received within 2015

UDC 539.182

A. N. Shakhman

RELATIVISTIC THEORY OF SPECTRA OF THE PIONIC ATOMS WITH ACCOUNT OF STRONG PION-NUCLEAR INTERACTION EFFECTS

Abstract.

It is presented a consistent relativistic theory of spectra of the pionic atoms on the basis of the Klein-Gordon-Fock with a generalized radiation and strong pion-nuclear potentials. There are presented data of calculation of the energy and spectral parameters for pioninc neon, cesium, holmium, thulium, ytterbium, lutetium, thallium, lead, and others, including the calculation of energy shifts, the widths of the levels due to the strong interaction with accounting for the the radiation (vacuum polarization), nuclear (finite size of a nucleus) and other corrections.

Key words: strong interaction, pionic atom, relativistic theory

УДК 539.182

А. Н. Шахман

РЕЛЯТИВИСТСКАЯ ТЕОРИЯ СПЕКТРОВ ПИОННЫХ АТОМОВ С УЧЕТОМ ЭФФЕКТОВ СИЛЬНОГО ПИОН-ЯДЕРНОГО ВЗАИМОДЕЙСТВИЯ

Резюме.

Представлена последовательная релятивистская теория спектров пионных атомов на основе уравнения Клейна-Гордона-Фока с обобщенными радиационным и сильным пион-ядерным потенциалом. Выполнен расчет энергетических и спектральных параметров для пионных атомов неона, цезия, гольмия, тулия, иттербия, лютеция, таллия, свинца и других, включая расчет энергетических сдвигов, ширин уровней вследствие сильного взаимодействия с учетом радиационных (поляризация вакуума), ядерных (конечный размер ядра) и других поправок.

Ключевые слова: сильное взаимодействие, пионный атом, релятивистская теория

УДК 539.182

А. М. Шахман

РЕЛЯТИВІСТСЬКА ТЕОРІЯ СПЕКТРІВ ПІОННИХ АТОМІВ З УРАХУВАННЯМ ЕФЕКТІВ СИЛЬНОЇ ПІОН-ЯДЕРНОЇ ВЗАЄМОДІЇ

Резюме.

Представлена послідовна релятивістська теорія спектрів півоній атомів на основі рівняння Клейна-Гордона-Фока з узагальненими радіаційним і сильним півонія-ядерним потенціалом. Виконано розрахунок енергетичних і спектральних параметрів для піоних атомів неону, цезію, гольмію, тулія, ітербію, лютецію, талію, свинцю та інших, включаючи розрахунок енергетичних зрушень, ширин рівнів внаслідок сильної взаємодії з урахуванням радіаційних (поляризація вакууму), ядерних (кінцевий розмір ядра) та інших поправок.

Ключові слова: сильна взаємодія, піонний атом, релятивістська теорія

UDC 539.182

A. V. Ignatenko, E. L. Ponomarenko, A. S. Kvasikova, T. A. Kulakli

[1]Odessa State Environmental University, L'vovskaya str.15, Odessa-16, 65016, Ukraine
e-mail: quantflo@mail.ru

ON DETERMINATION OF RADIATIVE TRANSITIONS PROBABILITIES IN RELATIVISTIC THEORY OF DIATOMIC MOLECULES: NEW SCHEME

On the basis of new gauge-invariant scheme in the relativistic energy approach combined with the multi-body perturbation theory for diatomic molecules it is formulated a new theoretical scheme for calculating the probabilities of radiative transitions of molecules. It is analysed the possible way to take into account for the inter-electron correlation and correspondingly the non-gauge-invariant contributions in relativistic molecular theory.

1. The experimental and theoretical studying of the radiation transition characteristics of a whole number of many-electron systems such as atoms and diatomic molecules is of a great importance and interest from the point of view of as the quantum electronics and atomic physics as atmosphere, plasma physics and plasma diagnostics science [1-33]). The traditional problem of any theory of the multielectron systems is determination of the radiation transition probabilities (oscillator strengths). Naturally to present time there are many well developed methods in a relativistic theory of atoms and ions and non-relativistic theory of molecular systems [1-16]. The well known multi-configuration Hartree-Fock method (the relativistic effects are often taken into account in the Pauli approximation or Breit Hamiltonian etc) allowed to obtain the useful spectral data on light and not heavy systems. The multi-configuration Dirac-Fock (DF) method is the most reliable version of calculation for systems with a large number of electrons. In these calculations the effects are taken into account practically precisely [1-18]. The calculation program of Desclaux (the Desclaux program, Dirac package) is compiled with proper account of the one- and two-particle relativistic, a finiteness of the nucleus size etc. It should be given special attention to two very general and important computer systems for relativistic calculations of atomic and molecular properties developed in the Oxford group and known as GRASP ("GRASP", "Dirac"; "BERTHA", "QED", "Dirac") (see [1-5] and references there). Besides, the well known density functional theory (DFT), relativistic coupled-cluster approach and model potential approaches in heavy atoms and ions should be mentioned too [1-15].

Nevertheless, as a rule, detailed description of the method for studying role of the relativistic, gauge-invariant contributions, for molecular systems is lacking. Serious problems are connected with correct definition of the high-order correlation corrections etc. The further improvement of this method is connected with using the gauge invariant procedures of generating the electron orbitals basis's and more correct treating the correlation effects [1-5,16-21].

In refs. [5,17-22] it has been performed an analysis of approaches to description of the relativistic many-electron systems with accurate consistent treating the relativistic, exchange-correlation and other, based on the relativistic perturbation theory (PT) formalism.

In the relativistic theory of heavy diatomic molecules a main problem of using the Dirac equation as a zero approximation in molecular

calculations associated with the non-ability to divide the variables in difference of the standard non-relativistic Schrödinger equation.

In this paper on the basis of new gauge-invariant scheme in the relativistic energy approach combined with the multi-body perturbation theory for diatomic molecules it is formulated a new theoretical scheme for calculating the probabilities of radiative transitions of molecules. It is analysed the possible way to take into account for the inter-electron correlation and correspondingly the non-gauge-invariant contributions in relativistic molecular theory.

Naturally, one of the effective ways in relativistic molecular theory is in using the Breit-Pauli approximation [3-5].

2. Let us describe in brief the important moment of our theoretical approach. As usually, the wave functions zeroth basis is found from the Schrodinger (Dirac in the consistent version) equation solution with potential, which includes the core ab initio potential, electric potentials of nuclei and possibly exchange-correlation one-particle potentials. The last potential in part takes into account for contribution of the correlation corrections of the PT second and high orders (electrons screening, particle-hole interaction etc.) are accounted for.

For arbitrary diatomic molecule in the perturbation theory zeroth approximation the two-center centre Schrodinger equation is written in spheroidal coordinates, l,m,j

$$(\lambda = (r_A + r_B)/R, 1 \le \lambda < \infty,$$
$$\mu = (r_A - r_B)/R, -1 \le \mu \le 1,\ 0 \le \mu \le 2\pi)$$

and after a number of transformations results in the following form (look,for example, [5]):

$$[\frac{\partial}{\partial\lambda}\left((\lambda^2-1)\frac{\partial}{\partial\lambda}\right) - \frac{m^2}{\lambda^2-1} - p^2\lambda^2 +$$
$$+ R(Z_A + Z_B - 2e^{-kR\lambda})\lambda + A] \times \Lambda(\lambda) = 0$$
$$[\frac{\partial}{\partial\mu}\left((1-\mu^2)\frac{\partial}{\partial\mu}\right) - \frac{m^2}{1-\mu^2} + p^2\mu^2 -$$
$$- R(Z_A - Z_B)\mu - A] \times M(\mu) = 0 \qquad (3)$$

where A is a constant separation. The wave function is represented as:

$$\psi(\lambda,\mu,\varphi) = \Lambda(\lambda)M(\mu,\varphi) = \Lambda(\lambda)G(\mu)e^{\pm im\varphi}. \qquad (4)$$

and the one-electron energy: $E = -2p^2/R^2$

The perturbation theory operator is as follows:

$$H_{\rho T} = \sum_{\delta}\sum_{ij}\left[r_{ij}^{-1} - V_M(r_{i\delta})\right] \qquad (5)$$

where d,i,j are the summation indexes correspondingly at nuclei and electrons.

In [5] it was constructed for the perturbation theory formalism for secular operator matrix and there are analyzed the diagrams summation tools for secular operator matrix. The terms of this set are represemted as contributions on of the Feynman diagrams, which are usually classified on number of the end lines. According to such a classification the matrix element of the secular operator has a form [5]:

$$M_{\xi\mu} = M_{\xi\eta}^{(0)} + M_{\xi\eta}^{(1)} + \ldots + M_{\xi\eta}^{(i)}, \qquad (6)$$

where i is a total number of valence particles, $M^{(0)}$ – the vacuum diagrams contribution (without the end lines) $M^{(1)}$ – a contribution of the 1-particles diagrams (one pair o the end lines); $M^{(2)}$-contribution of the two-particle diagrams (two pair of the end lines) and so on. Contribution $M^{(1)}$ is equal to a sum of the one-particle energies e_i. In the first perturbation theory order one should compute only the contribution of the two-particle diagrams of the first order. In fact this correction is equal to interaction energy of the particles $\Delta E^{(1)}$ and can be expressed through the matrix elements of the usual type on the wave functions of the zeroth approximation. For the Coulomb operator r_{12}^{-1} one should use the Neumann expansions on the Legendre polynomials of the first and second kind and spherical harmonics. 3.

3. As the first step, the relativistic block of the theory may into account the main relativistic effects within the model based on the perturbation theory with the Breit-Pauli Hamiltonian, taking into account relativistic corrections of the a^2 corder (a-fine structure constant), in particular,

the term due to the dependence of mass on velocity (H_1 and h_1), Darwin correction (H_2 and h_2), the spin-orbit term $\begin{bmatrix} H_3 & H_4 \\ h_3 & h_4 \end{bmatrix}$ [5]. The further simplification is connected with using the Cowan-Griffin approximation [13], which takes into account only two first effects in molecular calculations, in particular, for the s states.

Let us further examine the multielectron molecule with one or two quasi-particles (valence electrons). In the case of the multi-electron system with molecular core of the closed electron shells one can use the model potential method namely the bare two centre potential $V_N + V_C$ with V_N describing the electric potential of the nucleue, V_C, imitating the interaction of the quasi-particle with the molecular core. Surely, the core two-centre potential V_C is related to the core electron density r_C in a standard way. The latter fully defines the one electron representation. Moreover, all the results of the approximate calculations are the functionals of the density $r_C(r)$. The key step is determinatiojn of the complex energy of a molecule (that is in a relativistic theory).

According to the energy approach [17-19] the probability is directly connected with imaginary part of electron energy of the system, which is defined in the lowest order of perturbation theory as follows (the a-n transition is studied):

$$\mathrm{Im}\Delta E(B) = -\frac{\hat{e^2}}{4\pi} \sum_{\alpha>n>f} V^{|\omega_{\alpha n}|}_{\alpha n \alpha n}; \qquad (5)$$

The matrix element in (5) is provided by the following determination:

$$V^{|\omega|}_{ijkl} = \iint dr_1 dr_2 \Psi^*_i(r_1)\Psi^*_j(r_2)\frac{\sin|\omega|r_{12}}{r_{12}}(1-\alpha_1\alpha_2)\Psi^*_k(r_2)\Psi^*_l(r_1) \qquad (6)$$

The separated terms of the sum in (5) represent the contributions of different channels and a probability of the dipole a-n transition is:

$$\Gamma_{\alpha_n} = \frac{1}{4\pi} \cdot V^{|\omega_{\alpha n}|}_{\alpha_n \alpha_n} \qquad (7)$$

Under calculating the matrix elements (5) one could use the angle symmetry of the two-centre task and write the expansion for potential $\sin|w|r_{12}/r_{12}$ on spherical functions as follows [2]. This expansion is corresponding to usual multipole one for probability of radiative decay.

Obviously that the expression (5) is corresponding to first order of the molecular perturbation theory or second order of the quantum electrodynamical perturbation theory. Correspondingly in the second (fourth) order of the perturbation theory there are appeared the exchange-correlation or exchange-polarization corrections which being under consideration are gauge- dependent (dE_{ninv}) [19].

Surely, all the results of the exact calculation of any physical quantity must be gauge independent . However, even most advanced theories of diatomic molecules can hardly take into account all types of exchange-polarization corrections, especially, so called multi-particle ones and also continuum pressure etc. In fact their non-account provides a non-conservation of a gauge invariance in molecular calculations.

The simple way to reconstruct gauge invariance of a theory is to consider the corresponding many-particle exchange-polarization diagrams and determine the next corresponding term in an expression for the imaginary part of electron energy of the system (look different schemes in Refs. [20-25]). Then the minimization of the functional Im dE_{ninv} leads to the integro-differential equation for the r_c (the DF or Dirac-Kohn-Sham-like equations for the electron density) that should be numerically solved. In result there is a possibility to obtain the optimal one-particle representation and respectively optimal basis of electron orbitals, which is further used in calculation of the radiative transition characteristics.

Unlike the many-electron atoms in the case of diatomic molecules, this approach is naturally much more difficult. However, taking into account the substantial progress in the development of relativistic molecular theories, including, radiative transitions, the problem could be solved in a particular in simplifying accompanying approaches.

References

1. Grant I.P., Relativistic Quantum Theory of Atoms and Molecules, Theory and Computation, Springer Series on Atomic, Optical, and Plasma Physics,

vol. 40 (Springer, Berlin, 2007), p. 587-626
2. Relativistic Electronic Structure Theory, Series: Theoretical and Computational Chemistry Series., vol.11, part1, ed. P. Schwerdtfeger (Springer, 2002); vol.12, part2, ed. P. Schwerdtfeger (Springer, 2004);
3. Wilson S., in Recent Advances in Theoretical Physics and Chemistry Systems, Series: Progress in Theoretical Chemistry and Physics, vol. 16, ed. by J. Maruani, S. Lahmar, S. Wilson, G. Delgado-Barrio (Springer, Berlin, 2007), p. 11-80.
4. K.L. Bell, K.A. Berrington, D.S.F. Crothers, A. Hibbert, K.T. Taylor, Bertha: 4-Component Relativistic Molecular Quantum Mechanics, in Supercomputing, Collision Processes, and Application, Series: Physics of Atoms and Molecules, (Kluwer, New York, 1999) pp. 213–224.
5. Glushkov A.V., Relativistic Quantum Theory. Quantum, mechanics of Atomic Systems. – Odessa: Astroprint, 2008. – 900P.
6. Aerts P.J.C., Nieuwpoort W.C. On the use of gaussian basis sets to solve the Hartree-Fock-Dirac equation. I. Application to one electron atomic systems// Chem. Phys. Lett. – 1985. – Vol.113, N2. – P.165-172.
7. Safronova U.I., Safronova M.S., Third-order relativistic many-body calculations of energies, transition rates, hyperfine constants, and blackbody radiation shift in $^{171}Yb^{+}$//Phys. Rev. A. – 2009. – Vol.79. – P.022512
8. Botham C., Martensson A.M., Sanders P.G. Relativistic effects in atoms and molecules. – Vancouver: Elseiver, 1981. – 545p.
9. Photonic, Electronic and Atomic Collisions. – Singapore: World Scientific Publ. Co. – 1997. – P.621-630
10. Laughlin C., Victor G.A. Model potential method//Adv. Atom. Mol. Phys. – 1988 – Vol.25. – P.163-194.
11. Luke S.K., Hunter G., McEachran R.P., Cohen M. Relativistic theory of H^{+}_{2}// Journ. of Chem. Phys. – 1969. –Vol.50. – P.1644-1654.
12. Pavlik P.I., Blinder S.M. Relativistic effects in chemical bonding: The H^{+}_{2} molecule// Journ. of Chem. Phys. – 1967. – Vol.44. – P.2749-2751.
13. Martin R.L. All electron relativistic calculation of AgH. An investigation of the Cowan-Griffin operator in a molecular species// Journ. of Phys. Chem. – 1983. – Vol.87. – P.2749-2751.
14. Fuentealba P., Stoll H. On the reliability of semiempirical pseudopotentials: simulation of Hartree-Fock and Dirac-Fock methods// J.Phys.B: At.Mol.Opt. Phys. – 1983. – Vol.16,N2. – P.L323-328.
15. Parpia F.A., Froese-Fischer C., Grant I., Generalized relativistic atomic structure package: GRASP//Comp. Phys. Commun. – 1996. – Vol.94, N2. – P.249-270.
16. Dietz K., Heb B.A. Single particle orbitals for configuration interaction derived from quantum electrodynamics// Phys.Scripta. – 1989. – Vol.39. – P.682-688.
17. Ivanova E.P., Ivanov L.N., Aglitsky E.V., Modern Trends in Spectroscopy of Multicharged Ions // Physics Rep. – 1988. – Vol.166, N6.-P.315-390.
18. Glushkov A.V., Ivanov L.N., Ivanova E.P.// Autoionization Phenomena in Atoms. – M.: Moscow State University. – 1986. – P.58-160;
19. Glushkov A.V., Ivanov L.N. Radiation Decay of Atomic States: atomic residue and gauge non-invariant contributions // Phys. Lett.A. – 1992. – Vol.170, N1. – P.33-38.
20. Glushkov A.V., Relativistic calculation of oscillator strengths in multicharged ions with single electron above closed shells core// Opt. Spectr. – 1992. – Vol.72. – P.542-547.
21. Glushkov A.V., Ambrosov S.V., Loboda A.V., Gurnitskaya E.P., Prepelitsa G.P.,

Consistent QED approach to calculation of electron-collision excitation cross-sections and strengths: Ne-like ions // Int. Journ.Quant.Chem. – 2005. – Vol.104, N4 . – P. **562-569**
22. Glushkov A.V., Lovett L., Khetselius O.Yu., Gurnitskaya E.P. et al, Gauge-invariant QED perturbation theory approach to calculating nuclear electric quadrupole moments, hyperfine structure constants for heavy atoms and ions// Fro-ntiers in Quantum Systems in Chemistry and Physics (Springer). – 2008. – Vol.18. – P.505-522.
23. Florko T.A., Theoretical determination of oscillator strengths of some transitions in rare-earth atom of Eu// Photoelectronics. – 2007. –N16. – P.98-101.
24. Florko T.A., Gurnitskaya E.P., Polischuk V.N., Seredenko S.S., Dipole transitions of rare earth atoms in inert medium in a weak electromagnetic field and quasimolecular term//Photoelectronics. – 2007. – N16. – P.26-32.
25. Frorko T.A., A theoretical determination of the radiative transition probabilities and oscillator strengths in spectra of the Ne-like multicharged ions// Photoelectronics. – 2010. – N19. – P.51-55.

This article has been received within 2015

UDC 539.182

A. V. Ignatenko, E. L. Ponomarenko, A. S. Kvasikova, T. A. Kulakli

ON DETERMINATION OF RADIATIVE TRANSITIONS PROBABILITIES IN RELATIVISTIC THEORY OF DIATOMIC MOLECULES: NEW SCHEME

Abstract.
On the basis of new gauge-invariant scheme in the relativistic energy approach combined with the multi-body perturbation theory for diatomic molecules it is formulated a new theoretical scheme for calculating the probabilities of radiative transitions of molecules. It is analysed the possible way to take into account for the inter-electron correlation and correspondingly the non-gauge-invariant contributions in relativistic molecular theory
Key words: radiative transitions, diatomic molecules, new relativistic approach

УДК 539.182

А. В. Игнатенко, Е. Л. Пономаренко, А. С. Квасикова, Т. А. Кулакли

ОБ ОПРЕДЕЛЕНИИ ВЕРОЯТНОСТЕЙ РАДИАЦИОННЫХ ПЕРЕХОДОВ В РЕЛЯТИВИСТСКОЙ ТЕОРИИ ДВУХАТОМНЫХ МОЛЕКУЛ: НОВАЯ СХЕМА

Резюме.
С использованием калибровочно-инвариантной схемы в рамках релятивистского энергетического подхода и многочастичной теории возмущений для двухатомных молекул сформулирована новая теоретическая схему определения вероятностей радиационных переходов двухатом-

ных молекул. Предложены и проанализированы возможные методики учета обменно-корреляционных и соответственно, калибровочно-неинвариантных вкладов в вероятность перехода в релятивистской молекулярной теории.

Ключевые слова: радиационные переходы, двухатомные молекулы, новая релятивистская схема

УДК 539.182

Г. В. Ігнатенко, Е. Л. Пономаренко, Г. С. Квасикова, Т. А. Кулакли

ПРО ВИЗНАЧЕННЯ ЙМОВІРНОСТЕЙ РАДІАЦІЙНИХ ПЕРЕХОДІВ У РЕЛЯТИВІСТСЬКІЙ ТЕОРІЇ ДВОАТОМНИХ МОЛЕКУЛ: НОВА СХЕМА

Резюме.

З використанням калібрувально-інваріантної схеми в рамках релятивістського енергетичного підходу і багаточастинкової теорії збурень для двохатомних молекул сформульована нова теоретична схему визначення ймовірностей радіаційних переходів двохатомних молекул. Запропоновані та проаналізовані можливі методики урахування обмінно-кореляційних і відповідно, калібрувально- неінваріантних внесків в ймовірність переходу в релятивістській молекулярній теорії.

Ключові слова: радіаційні переходи, двоатомні молекули, нова релятивістська схема

UDK 539.184

Yu. G. Chernyakova, L. A. Vitavetskaya, P. G. Bashkaryov, I. N. Serga, A. G. Berestenko

Odessa National Politechnical University, 1, Shevchenko av., Odessa, Ukraine
Odessa State Environmental University, 15, Lvovskaya str., Odessa, Ukraine
e-mail: nucvita@mail.ru

THE RADIATIVE VACUUM POLARIZATION CONTRIBUTION TO THE ENERGY SHIFT OF SOME LEVELS OF THE PIONIC HYDROGEN

Calculating the radiative contribution due to the vacuum polarization effect to energy value for some levels in pionic hydrogen atom including in particular the main Uehling-Serber and the high-order Källen-Sabry and Wichmann - Kroll corrections has been carried out using the modified Uehling-Serber potential. The values for some characteristic energy corrections to 1s, 2p, 3p, 4p states of the pion hydrogen (in particular, radiation contributions and contributions due to the finite size of the proton and pion are presented and compared with alternative data by Schlesser-Indelicato et al.

1. Introduction

It is well known that the development of a new theoretical approach to the description of spectral parameters pionic atoms in the excited states with precise accounting relativistic, radiation, nuclear, electron screening effects (look [1-18]) on the basis of Klein-Gordon-Fock (Dirac) equation and a development of a consistent relativistic theory of hyperfine structure of spectra represents one of actual fundamental problem of moden optics and spectroscopy of hadronic atomic systems. Especial problem is connected with précised calculating the radiative corrections to the transition energies of the low-Z exotic (pionic, kaonic, muonic) atoms, namely, hydrogen and deuterium. Naturally, it is provided by necessity of further developing the modern as atomic and as nuclear spectra theories. From the other side, one could mention that the detailed data about spectra of the exotic atomic systems (kaonic, pionic, muonic atoms) can be very useful under construction of the new X-ray standards. It is worth to remind about known achievements and a great importance of the theoretical muonic, hadronic chemistry and hadronic spectroscopy as well as the significant progress in the modern experimental technologies applying to hadronic atoms [1-15].

The standard Dirac approach is traditionally used as starting basis in calculations of the heavy ions [2]. The problem of accounting the radiative corrections, in particular, self-energy part of the Lamb shift and vacuum polarization contribution is mostly treated with using the expansions on the natural physical parameters *1/Z, aZ* (*a* is fine structure constant) [5,10]. It permits evaluations of the relative contributions of different expansion energy terms: non-relativistic, relativistic ones, as functions of Z. For high Z (Z is a nuclear charge) it should be necessary to account for the high-order QED corrections and the nuclear finite size correction etc [1-3,10-12,16]. Further improvement of this method in a case of the heavy ions is linked with using gauge invariant procedures of generating relativistic orbital basises and more correct treating nuclear and QED effects [1-3]. In a case of the low-Z exotic atomic systems such as an exotic hydrogen (deuterium) a great interest attracts estimation of the radiative, in particular, vacuum polarization, correction. In refs. [17-19] it has been proposed a precise scheme to calculating spectra of heavy systems with account of nuclear and radiative effects, based on the relativistic many-body perturbation theory (see also [3]) and advanced effective procedures for accounting the radiative corrections.

In this paper we present the results of calculating the QED contribution and first of all due to the vacuum polarization effect to energy shift for some levels energies of pionic hydrogen. The obtained results are compared with the calculation data by [2]. As theoretical model we have used relativistic models, presented in Ref. [20,21] (look [23-25]).

The master equation for describing thepionic atom dynamics is the Klein-Gordon-Fock equation, which is in atomic units as follows:

$$\left\{\alpha^2\left[E-V_c(r)\right]^2+\vec{\nabla}^2-\mu^2c^2\right\}\psi(r)=0, \quad (1)$$

де *m*-наведеная маса p^-, *E*- енергія піон, V_c–загальний потенціал, який, зокрема, включає кулонівський потенціал взаємодії p^- з ядром (з урахуванням скінченого розміру), узагальнений радіаційний потенціал, потенціал електронних оболонок.

where *m*- is a reduced mass, *E*- a pion energy V_c– total electromagnetic interaction which includes especially Coulomb interaction potential of p^- with a nucleus (with accounting for the finite size effect), radiation potential (including thr vacuum polarization potential) and possibly the potential of electron shells (for multi-electron pionic atom).

The total electromagnetic interaction potential:

$$V_c(r)=V_n(r)+U_R(r). \quad (1)$$

includes the electrical V_n and radiation (including polarization) U_R(r) potential of a nucleus with accounting the finite size correction. The expectation value of the radiative vacuum polarization operator gives the corresponding correction. In ref. [21] it is presented a consistent approach to determining radiation QED corrections (main among them, of course, is the correction the polarization of the vacuum; effect which is typical for a distance of Compton wavelength $\lambda_C^e=\hbar/m_ec=$ 386.16Fm; while the Bohr radius of a pion orbit $r_B^\pi=194n^2/Z$ Fm) to the energy states of pionic atom, which is based on using the Uehling-Serber potential with effective accounting for the Breit-Rosenthal-Crawford-Schawlow):

$$U_{PV}^{FS}(r)=-\frac{2\alpha^2}{3\pi}\int d^3r'\int_m^\infty dt\exp\left(-2t|r-r'|/\alpha Z\right)\times \quad (2)$$
$$\times\left(1+\frac{1}{2t^2}\right)\frac{\sqrt{t^2-1}}{t^2}\frac{\rho(r')}{|r-r'|},$$

and additional terms which take into account a contribution of the corrections of $[\alpha(Z\alpha)]^n$ order, in particular, the Källen-Sabry and Wichmann - Kroll corrections ($\alpha^2(\alpha Z)+\alpha(Z\alpha)^n$...).

A vacuum polarization potential without the Breit-Rosenthal-Crawford-Schawlow effect is usually represented as follows (in fact in the first PT order):

$$U(r)=-\frac{2\alpha}{3\pi r}\int_1^\infty dt\exp(-2rt/\alpha Z)\left(1+1/2t^2\right)\frac{\sqrt{t^2-1}}{t^2}\equiv \quad (3)$$
$$\equiv-\frac{2\alpha}{3\pi r}C(g),$$

$$g=\frac{r}{\alpha Z}. \quad (4)$$

The corresponding expectation value of this operator gives the corresponding vacuum polarization correction. In the scheme [20,21] this potential is approximated by quite precise analytical function (see details in refs. [12-16]). The most advanced version of the such potential ($C\circledR\widetilde{\widetilde{C}}$) is presented as follows:

$$\widetilde{\widetilde{C}}(g)=\widetilde{C}_1(g)\widetilde{\widetilde{C}}_2(g)/\left(\widetilde{C}_1(g)+\widetilde{\widetilde{C}}_2(g)\right), \quad (5)$$
$$\widetilde{\widetilde{C}}_2(g)=\widetilde{C}_2(g)\,f(g)\text{'}$$
$$\widetilde{C}_2(g)=-1.8801\exp(-g)/g^{3/2}$$
$$\widetilde{C}_1(g)=\text{h}(g/2)+1.410545-1.037837g\text{ ,}$$
$$f(g)=\left((1.1024/g-1.3361)/g+0.8027\right)$$

The using this formula permits one to decrease the calculation errors for this term down to ~0.1%. Error of usual calculation scheme is~10%.

Earlier we carried out the calculation of the vacuum polarization contribution to the energy shift of a number of the levels and transitions in kaonic and pionic nitrogen. One should keep in mind that the energy.

levels of exotic (pionic, kaomic etc) atoms are very sensitive to effects of QED, nuclear structure and recoil since the pion (kaon) is heavier than the electron. As usually the fundamental constants from the CODATA 1998 are used in the numerical calculations. We have evaluated the values for the QED contributions and other specific corrections to the energy 1s, 2p, 3p, 4p states of the pion hydrogen. In table 1 we present

the values (in meV) for some characteristic energy corrections to 1s, 2p, 3p, 4p states of the pion hydrogen (in particular, radiation contribtions and contributions due to the finite size of the proton and pion) estimated by the theory and Schlesser-Indelicato et al. [5] and our theory. The following abbreviations are used: correction on polarization of the vacuum of Uehling Serber (PV-US), the correction to the Breit interaction (BI), correction to a size radius (SR) of a proton and a pion, the higher-order corrections for a vacuum polarization Kallen-Sabry (PV-KS) and Wichman-Kroll (PV-WC). Analyzing the results, it should be noted that, in general between the theoretical results (actually the contributions of electromagnetic energy in the state or transition) obtained under various theories, in particular, our theory and the theory Schlesser-Indelicato et al. [5] there is a fairly good agreement that is easily explained in principle (as in the case of the conventional hydrogen atom) in a sense negligible role of radiation and nuclear finite-size corrections, Obviously it is of a great interest application of the presented scheme in computing QED corrections to levels energies in heavy pionic atoms.

Table 1

The values (in meV) some specific corrections to the energy 1s, 2p, 3p, 4p states of the pion hydrogen (QED contributions and contributions by the proton and pion SR) according to the theory Schlesser-Indelicato et al. [5] and our theory (see. Text)

QED	*F*	1s [5]	1s (our)
PV-US		-3240.802	-3240.799
BI	1/2 3/2	-178.461	-178.458
SR	p π^-	61.711 39.33	61.711 39.33
PV-KS		-24.365	-24.363
PV-WK		-4.110	-4.113
QED	*F*	2p [5]	2p (our)
PV-US		-35.795	-35.793
BI	1/2 3/2	-11.655 -4.048	-11.652 -4.046
SR	p π^-	0 0	0 0
PV-KS		-0.346	-0.343
PV-WK		-0.008	-0.010
QED	*F*	3p [5]	3p (our.)
PV-US		-11.407	-11.405
BI	1/2 3/2	-4.221 -1.967	-4.219 -1.965
SR	p π^-	0 0	0 0
PV-KS		-0.108	-0.105
PV-WK		-0.002	-0.003
QED	*F*	4p [5]	4p (our)
PV-US		-4.921	-4.918
BI	1/2 3/2	-1.943 -0.992	-1.940 -0.989
SR	p π^-	0 0	0 0
PV-KS		-0.046	-0.044
PV-WK		-0.001	-0.002

References

1. Lyubovitskij V., Rusetsky A., πp atom in ChPT: Strong energy-level shift// Phys. Lett.B. – 2000. – Vol.494. – P.9-13..
2. Mohr P.J., Energy Levels of H-like atoms predicted by Quantum Electrodyna-mics,10<Z<40//Atom.Dat.Nucl.Dat. Tabl. – 1983 – Vol.24,N2. – P.453-470.
3. Glushkov A.V., Relativistic quantum theory. Quantum mechanics of atomic systems, Odessa: Astroprint, 2008. – 700P.
4. Hayano R.S., Hori M., Horvath D., Widman E., Antiprotonic helium and CPT invariance//Rep. Prog. Phys. – 2007. – Vol.70. – P.1995-2065.
5. Schlesser S., Le Bigot E.-O., Indelicato P., Pachucki K., Quantum-electrodynamics corrections in pionic hydrogen// Phys.Rev.C. – 2011. – Vol.84. – P.015211 (8p.).
6. Gotta D., Amaro F., Anagnostopoulos D., Pionic Hydrogen//Precision Physics of

Simple Atoms and Molecules, Ser. Lecture Notes in Physics (Springer, Berlin / Heidelberg).-2008.-Vol.745.-P.165-186.
7. Mitroy J., Quantum defect theory for the study of hadronic atoms/ Mitroy J., Ivallov I.A.// J. Phys. G: Nucl. Part. Phys. – 2001. – Vol.**27. – P.**1421–1433
8. Deslattes R., Kessler E., Indelicato P., de Billy L., Lindroth E. , Anton J., Exotic atoms//Rev. Mod. Phys. – 2003. –Vol.75. – P.35-70.
9. Borie E., Lamb shift in muonic hydrogen// Phys.Rev. A. – 2005. – Vol.71. – P.032508-1-8.
10. Mohr P.J. Quantum Electrodynamics Calculations in few-Electron Systems// Phys. Scripta. – 1993. – Vol.46, N1. – P.44-52.
11. Klaft I.,Borneis S., Engel T., Fricke B., Grieser R., Huber G., Kuhl T., Marx D., Neumann R., Schroder S., Seelig P., Volker L. Precision laser spectroscopy of ground state hyperfine splitting of H-like $^{209}Bi^{82+}$// Phys.Rev.Lett. – 1994. – Vol.73. – P.2425-2427.
12. Glushkov A.V., Relativistic quantum theory. Quantum mechanics of atomic systems, Odessa: Astroprint, 2008. – 700P.
13. Khetselius O.Yu., Relativistic perturbation theory calculation of the hyperfine structure parameters for some heavy-element isotopes// Int. Journ. of Quantum Chemistry. – 2009. – Vol.109. – N14. – P. 3330-3335.
14. Backenstoss G., Pionic atoms//Ann.Rev. Nucl.Sci. – 1970. – Vol.20. – P.467-510.
15. Menshikov L I and Evseev M K, Some questions of physics of exotic atoms// Phys. Uspekhi.2001 – Vol. 171. – P.150-184.
16. Ivanova E.P., Ivanov L.N., Aglitsky E.V., Modern trends in spectroscopy of multicharged ions// Phys.Rep. – 1991. – Vol. 166. – P.315-390.
17. Glushkov A.V., Ambrosov S., Loboda A., Chernyakova Y.G., Khetselius O., Svinarenko A., QED theory of the superheavy elements ions: energy levels, radiative corrections, and hyperfine structure for different nuclear models// Nuclear Phys.A – 2004. – Vol. 734. – P.21-28.
18. Glushkov A.V., Khetselius O.Yu., Gurnitskaya E.P., Loboda A.V., Florko T.A., Sukharev D.E., Lovett L., Gauge-invariant QED perturbation theory approach to calculating nuclear electric quadrupole moments, hfs structure constants for heavy atoms and ions// Frontiers in Quantum Systems in Chem. and Phys. (Springer). – 2008. – Vol.18. – P.505-522.
19. Kuznetsova A.A., Vitavetskaya L.A., Chernyakova Yu.G., Korchevsky D.A., Calculating radiative vacuum polarization contribution to the energy shift of 3p-1s transition in pionic deuterium// Photo-electronics. – 2013. – Vol.22. – P.108-111
20. Serga I.N., Dubrovskaya Yu.V., Kvasikova A.S., Shakhman A.N., Sukharev D.E., Spectroscopy of hadronic atoms: Energy shifts// Journal of Physics: C Series (IOP, London, UK). – 2012. – Vol.397. – P.012013 (5p.).
21. Serga I.N., Relativistic theory of spectra of pionic atoms with account of the radiative and nuclear corrections// Photoelectronics. – 2013. – Vol.22. – P.71-75.
22. Kvasikova A.S., Ignatenko A.V., Florko T.A., Sukharev D.E., Chernyakova Yu.G., Photoeffect and spectroscopy of the hydrogen atom in the crossed dc electric and magnetic field// Photoelectronics. – 2011. – Vol.20. – P.71-75.
23. Kuznetsova A.A., Kvasikova A.S., Shakhman A.N., Vitavetskaya L.A., Calculating the radiative vacuum polarization contribution to the energy shift of 2p-2s transition in m-hydrogen// Photoelectronics. – 2012. – N21. – P.66-67.
24. Khetselius O.Yu., Turin A.V., Sukharev D.E., Florko T.A., Estimating of X-ray spectra for kaonic atoms as tool for sensing the nuclear structure// Sensor Electr. and Microsyst. Techn. - 2009. - N1. – P.30-35..
25. Serga I.N., Electromagnetic and strong interactions effects in X-ray spectroscopy of pionic atoms // Photoelectronics. – 2011. – Vol.20. – P.109-112.

This article has been received within 2015

UDK 539.184

Yu. G. Chernyakova, L. A. Vitavetskaya, P. G. Bashkaryov, I. N. Serga, A. G. Berestenko

THE RADIATIVE VACUUM POLARIZATION CONTRIBUTION TO THE ENERGY SHIFT OF SOME LEVELS OF THE PIONIC HYDROGEN

Abstract.

Calculating the radiative contribution due to the vacuum polarization effect to energy value for some levels in pionic hydrogen atom including in particular the main Uehling-Serber and the high-order Källen-Sabry and Wichmann - Kroll corrections has been carried out using the modified Uehling-Serber potential. The values for some characteristic energy corrections to 1s, 2p, 3p, 4p states of the pion hydrogen (in particular, radiation contributions and contributions due to the finite size of the proton and pion are presented and compared with alternative data by Schlesser-Indelicato et al.

Key words: pionic hydrogen, radiative corrections

УДК 539.184

Ю. Г. Чернякова, Л. А. Витавецкая, П. Г. Башкарьов, И. Н. Серга, А. Г. Берестенко

РАДИАЦИОННЫЕ ВКЛАДЫ ЗА СЧЕТ ЭФФЕКТА ПОЛЯРИЗАЦИИ ВАКУУМА В СДВИГ ЭНЕРГИИ РЯДА УРОВНЕЙ ПИОННОГО ВОДОРОДА

Резюме.

Проведен расчет радиационного вклада за счет эффекта поляризации вакуума в величину энергии ряда уровней в пионном водороде в том числе, в частности, основной вклад Юлинга-Сербера и вклады высоких порядков Каллена-Сабри и Вичманна-Кролла с использованием модифицированного потенциала Юлинга-Сербера. Приведены значения некоторых характерных энергетических поправок к энергии 1s, 2p, 3p, 4p состояний пионного водорода (в частности, радиационные поправки, поправки за счет конечного размера протона и пиона представлены и др.) и проведено их сравнение по сравнению с альтернативными данным Schlesser-Indelicato и др.

Ключевые слова: пионный водород, радиационные поправки

УДК 539.184

Ю. Г. Чернякова, Л. А. Вітавецька, П. Г. Башкарьов, І. М. Сєрга, А. Г. Берестенко

РОЗРАХУНОК РАДІАЦІЙНОГО ВНЕСКУ ЗА РАХУНОК ЕФЕКТУ ПОЛЯРИЗАЦІЇ ВАКУУМУ У ЗСУВ ЕНЕРГІЇ ДЕКОТРИХ РІВНІ ПІОННОГО ВОДНЮ

Резюме.

Виконано розрахунок радіаційного внеску за рахунок ефекту поляризації вакууму у величину енергії декотрих рівнів у піонному водні у тому числі, зокрема, основний внесок Юлінг-Сербер і вклади високих порядків Каллена-Сабрі і Вічманна –Кролла, з використанням модифікованого потенціалу Юлінга-Сербера. Наведені значення деяких характерних енергетичних поправок до енергії 1s, 2p, 3p, 4p станів піонного водню (зокрема, радіаційні поправки, поправки за рахунок кінцевого розміру протона і півонії представлені і ін.) І проведено їх порівняння в порівнянні з альтернативними даними Schlesser-Indelicato та ін.

Ключові слова: піонний водень, радіаційні поправки

UDC 539.182

V. V. Buyadzhi

Odessa State Environmental University, L'vovskaya str.15, Odessa-16, 65016, Ukraine
E-mail: vbuyad@mail.ru

LASER MULTIPHOTON SPECTROSCOPY OF ATOM EMBEDDED IN DEBYE PLASMAS: MULTIPHOTON RESONANCES AND TRANSITIONS

The consistent relativistic energy approach to atom in a realistic laser field, based on the Gell-Mann and Low S-matrix formalism, is applied to studying the resonant multiphoton transitions in atoms embedded in the Debye plasmas. There is considered a new scheme to calculating the multiphoton transitions characteristics, shifts and widths of multiphoton resonances. An approach is used for treating the three-photon transitions in krypton embedded in the Debye plasmas.

1. The physics of multiphoton phenomena is one of the very quickly developed branches of the modern optics and spectroscopy, photophysics. Studying of multiphoton phenomena in atoms, molecules ets has a great progress that is stimulated by development of new laser technologies (see Refs. [1-10]). The appearance of the powerful laser sources allowing to obtain the radiation field amplitude of the order of atomic field in the wide range of wavelengths results to systematic investigations of the nonlinear interaction of radiation with atomic and molecular systems [1-14].

At the same time a direct laser-nucleus interactions traditionally have been dismissed because of the well known effect of small interaction matrix elements [9-11]. Some exceptions such as an interaction of x-ray laser fields with nuclei in relation to alpha, beta-decay and x-ray-driven gamma emission of nuclei have been earlier considered. With the advent of new coherent x-ray laser sources in the near future, however, these conclusions have to be reconsidered.

At present time a great interest has been connected with studying atomic processes in plasma environments because of the plasma environment screening effect on the plasma-embedded atomic systems. One should remind that the screening effects have play a important and significant part in the investigation of plasma environments over the past several decades.

Different theoretical methods have been employed along with the Debye screening to study plasma environments.

The interaction of atoms with the external alternating fields, in particular, laser fields, has been the subject of intensive experimental and theoretical studied (see, for example, Refs. [1-8, 12-24]). A definition of the k-photon emission and absorption probabilities and atomic levels shifts, study of dynamical stabilization and field ionization etc are the most actual problems to be solved.

Above methods which are usually used one should mention such approaches as the standard perturbation theory (surely for low laser filed intensities), Green function method, the density-matrix formalism, time-dependent density functional formalism, direct numerical solution of the Schrödinger (Dirac) equation, multi-body multiphoton approach, the time-independent Floquet formalism etc (see [1-8,12-24] and Refs. therein).

Earlier the relativistic energy approach to studying the interaction of atom with a realistic strong laser field, based on the Gell-Mann and Low S-matrix formalism, has been developed. Originally, Ivanov has proposed an idea to describe quantitatively a behaviour of an atom in a realistic laser field by means studying the radiation emission and absorption lines and further the theory of interaction of an atom with the Lorenz laser pulse and calculating the corresponding

lines moments has been in details developed in Ref. [19-25]. It has been checked in numerical simulation of the multiphoton resonances shifts and widths in the hydrogen and caesium. Theory of interaction of an atom with the Gauss and soliton-like laser pulses and calculating the corresponding lines moments has been in details presented in Refs. [23,26,27].

Here the consistent relativistic energy approach to atom in a realistic laser field, based on the Gell-Mann and Low S-matrix formalism, is applied to studying the resonant multiphoton transitions in atoms embedded in the Debye plasmas. There is considered a new scheme to calculating the multiphoton transitions characteristics, shifts and widths of multiphoton resonances. An approach is used for treating the three-photon transitions in krypton embedded in the Debye plasmas

2. The relativistic energy approach in the different realizations and the radiation lines moments technique is in details presented in Refs. [19-30]. So, here we are limited only by presenting the master elements. In the theory of the non-relativistic atom a convenient field procedure is known for calculating the energy shifts dE of degenerate states. This procedure is connected with the secular matrix M diagonalization. In constructing M, the Gell-Mann and Low adiabatic formula for dE is used [20-23,31]. In relativistic theory, the Gell-Mann and Low formula dE is connected with electrodynamical scattering matrice, which includes interaction with as a laser field as a photon vacuum field. A case of interaction with photon vacuum is corresponding to standard theory of radiative decay of excited atomic states. Surely, in relativistic theory the secular matrix elements are already complex in the second perturbation theory (PT) order. Their imaginary parts are connected with radiation decay possibility. The total energy shift is usually presented in the form [23]:

$$\delta E = \mathrm{Re}\delta E + \mathrm{i}\ \mathrm{Im}\delta E\ ,$$

$$\mathrm{Im}\ \delta E = -\mathrm{P}/2, \qquad (1)$$

where P is the level width (decay possibility). Let us describe the interaction "atom-laser field" by the Ivanov potential [21,23]:

$$V(r,t)=V(r)\int d\omega f(\omega-\omega_0)\sum_{n=-\infty}^{\infty}\cos[\omega_0 t+\omega_0 n\tau] \qquad (2)$$

Here w_0 is the central laser radiation frequency, n is the whole number. The function f(w) is a Fourier component of the laser pulse. The condition $\int dw f^2(w)=1$ normalizes potential $V(rt)$ on the definite energy in the pulse. Usually one could consider the pulses with Lorentz shape (coherent 1-mode pulse): $f(w) = b/(w^2+D^2)$, Gaussian one (multi-mode chaotic pulse): $f(w) = b\exp[\ln 2(w^2/D^2)]$ and the soliton-like pulse: $f(t) = b\ ch^{-1}[t/D]$ (b -normalizing multiplier).

The master program results in the calculating an imaginary part of energy shift $\mathrm{Im}dE_a(w_0)$ for any atomic level as the function of the central laser frequency w_0. An according function has the shape of the resonance, which is connected with the transition a-p (a, p-discrete levels) with absorption (or emission) of the "k" number of photons. For this transition the following values are determined [20-23]:

$$\delta\omega(p\alpha|k)=\int' d\omega\ \mathrm{Im}\ \delta E_\alpha(\omega)(\omega-\omega_{p\alpha}/k)/N,\ ($$

$$\mu_m=\int' d\omega\ \mathrm{Im}\ \delta E_\alpha(\omega)\ (\varpi-\omega_{p\alpha}/k)^m/N,$$

where

$$\int' d\omega \mathrm{Im} E_\alpha$$

is the normalizing multiplier; w_{pa} is position of the non-shifted line for transition a-p, dw($pa|k$) is the line shift under k-photon absorption; $v_{pa}=w_{pa}+k\times dw(pa|k)$. The first moments m_1, m_2 and m_3 determine the atomic line centre shift, its dispersion and the asymmetry.

To find m_m, we need to get an expansion of E_a to PT series:

$$E_\alpha=\sum E_\alpha^{(2k)}(\omega_0).$$

One may use here the Gell-Mann and Low adiabatic formula for dE_a [20-23]. The consideration can be simplified by account of the k-photon absorption contribution in the first two PT orders. Besides, summation on laser pulse is exchanged by integration. The corresponding (l+2k+1)-times integral on (l+2k) temporal variables and r ($l=0,2$) (integral I_g) are calculated [19-23]. Finally, after some cumbersome transformations one can get the expressions for the line moments. The corresponding expressions for the Gaussian laser pulse are as follows:

$$\delta\omega(p\alpha \mid k) =$$

$$=\{\pi\Delta/(k+1)\mathrm{k}\}[E(p,\omega_{p\alpha}/k)\text{-}E(\alpha,\omega_{p\alpha}/k)], \quad (9)$$

$$\mu_2 = \Delta^2/\mathrm{k}$$

$$\mu_3=\{4\pi\Delta^3/[k(k+1)]\}[E(p,\omega_{p\alpha}/k)\text{-}E(\alpha, \omega_{p\alpha}/k)],$$

where

$$E(j,\omega_{p\alpha}/k)=0{,}5\sum_{p_i} V_{jpi}\, V_{pij}\,[\frac{1}{\omega_{jp_i}+\omega_{p\alpha}/k}+ + \frac{1}{\omega_{jp_i}-\omega_{p\alpha}/k}] \quad (10)$$

The summation in (10) is over all atomic states. Let us note that these formulas for the Gaussian pulse differ of the Lorenz shape laser pulse expressions [21-23]. For the soliton-like pulse it is necessary to carry out the numerical calculation or use some approximations to simplify the expressions [27].

In order to calculate (10), one should use the technique [28,29] of calculating sums of the QED PT second order, which has been earlier applied by us in calculations of some atomic and mesoatomic parameters [26,27,30-32].

Finally the computational procedure results in a solution of the ordinary differential equations system for above described functions and integrals. In concrete numerical calculations the PC "Superatom-ISAN" package is used. The construction of the operator wave functions basises within the QED PT, the technique of calculating the matrix elements in Egs. (9,10) and other details is are presented in Refs. [19-30].

3. In order to take into account the plasmas screening effect one could use the known Debye shielding model. As it is well known (c.f.[33-35] and refs there) in the classical theory of plasmas developed by Debye and Hückel, the interaction potential between two charged particles in a plasma is modelled by a Yukawa-type potential as follows:

$$\mathrm{V}(\mathrm{r_i}, \mathrm{r_j}) = (Z_a Z_b/|\mathrm{r_a}\text{-}\mathrm{r_b}|\}\exp(-\mu\cdot|\mathrm{r_a}\text{-}\mathrm{r_b}|), \quad (11)$$

where r_a, r_b represent respectively the spatial coordinates of particles A and B and Z_a, Z_b denote their charges. A difference between the Yukawa type potential and standard Coulomb potential is in account for the effect of plasma, which is modeled by the shielding parameter m [33]. The parameter m is linked with the plasma parameters such as the temperature T and the charge density n as follows $\mu \sim \sqrt{e^2 n / k_B T}$ where, as usually, e is the electron charge and k_B is the Boltzman constant. The density n is given as a sum of the electron density N_e and the ion density N_k of the k-th ion species having the nuclear charge q_k :. Let us remind [35] that under typical laser plasma conditions of T~ 1keV and n~ 10^{23} cm^{-3} the parameter m is of the order of 0,1 in atomic units. By introducing the Yukawa-type electron-nuclear attraction and electron-electron repulsion potentials, the electronic Hamiltonian for N-electron multicharged ion in a plasma is given in atomic units as follows:

$$H = \sum_i [\alpha p_i - \beta m^2 - Z\exp(-\mu r_i)/r_i] + \sum_{i>j} \frac{(1-\alpha_i\alpha_j)}{r_j}\exp(-\mu r_j) \quad (12)$$

A difference between the Hamiltonian (12) and analogous model Hamiltonian with the Yukawa potential of ref. [33] is in using the relativistic approximation, which is obviously necessary for adequate description of relativistic systems [35].

4. In ref. [36] there were presented the results of the numerical simulation for the three-photon resonant, four-photon ionization profile of atomic krypton (the 4p ® 5d[1/2]$_1$ and 4p ® 4d[3/2]$_1$ three photon Kr resonances are considered; intense uv (285-310 nm) laser radiation with intensity range 3´10^{12}-10^{14} W/cm^2 studied) in a free state (n in sense of the absence a plasmas environment). There have been determined the corresponding parameters of the 4p ® 5d[1/2]$_1$ (i) and 4p ® 4d[3/2]$_1$ (ii) three photon Kr resonances. The resonance shift is proportional to intensity with a width dominated by lifetime broadening of the excited state.

The numerical simulation [36] results for the 4p ® 5d[1/2]$_1$ (i) and 4p ® 4d[3/2]$_1$ (ii) three photon Kr resonances are as follows: (i) the shift $dw_0(pa|3)=aI$, a_{exp}=3.95 meV/(Tw×cm^{-2}) and width b_{exp}= 1.5 meV/(Tw×cm^{-2}); (ii) shift $dw_0(pa|3)=aI$, a_{exp}=8.1 meV/(Tw×cm^{-2}) and width b_{exp}=4.2 meV/(Tw×cm^{-2}). We have chosen the Debye length parameter values λ_D=50 (25) and the corresponding computed coefficients are as

follows: (i) a=3.76 meV/(Tw×cm^{-2} (a=3.2 meV/(Tw×cm^{-2}); (ii) a=7.8 meV/(Tw×cm^{-2}) (a=6.5 meV/(Tw×cm^{-2}).

The presented results show that Debye plasma environments have an effect on the multiphoton transitions. Nevertheless, one should keep in mind some important facts the (see, for example, [33,34]). It is clear the static screening result considered above is subject to the condition that the plasma is a thermodynamically equilibrium plasma and neglects the contributions from ions in plasma since electrons provide more effective shielding than ions.

Obviously with the changing the plasma conditions (parameters) in principle there can be taken a place a significant variations. Besides, one should remember about the conditions of applicability of the Debye approximation.

References

1. Batani D., Joachain C. J., eds. 2006 Matter in super-intense laser fields, AIP Serie, N.-Y.
2. Ivanova E. P. 2011 Phys.Rev.A 84 043829
3. Jaron-Becker A., Becker A., Faisal F. H. M 2004 Phys.Rev.A 69 023410
4. Plummer M, Noble C J 2003 J.Phys. B: At. Mol. Opt. Phys. 36 L219
5. van der Hart H. W., Lysaght M. A., Burke P. G. 2007 Phys.Rev.A 76 043405
6. Mercouris T., Nikolaides C. A. 2003 Phys. Rev. A 67 063403
7. Brandas E., Floelich P 1977 Phys. Rev. A 16 2207
8. Kwanghsi Wangt, Tak-San Hot, Shih-I Chu 1985 J.Phys. B: At. Mol. Opt. Phys. 18 4539; 2006 Phys.Rev.A 73 023403
9. Glushkov A. V., Ivanov L. N., Letokhov V. S. Nuclear quantum optics 1991 Preprint of Institute for Spectroscopy, USSR Academy of Sciences, Troitsk-N7
10. Bürvenich T. J., Evers J., Keitel C. H. 2006 Phys.Rev.Lett. 96 142501; 2006 Phys.Rev.C 74 044601
11. Shahbaz A., Müller C., Staudt A., Bürvenich T. J., Keitel C. H. 2007 Phys. Rev.Lett. 98 263901
12. Fedorov M. V. 1999 Physics-Uspekhi 169 66
13. Delone N. B., Kraynov V. P. 1998 Physics-Uspekhi 168 531
14. Belyaev V. S., Kraynov V. P., Lisitsa V. S., Matafonov A. P. Physics-Uspekhi 178 823
15. Zoller P. 1982 J.Phys. B: At. Mol. Opt. Phys. 15 2911
16. Lompre L-A., Mainfrau G., Manus C., Marinier J. P. 1981 J.Phys. B: At. Mol. Opt. Phys.14 4307
17. Khetselius O.Yu., 2012 J. of Phys.: Conf. Ser.. 397 012012; 2009 Phys.Scr. T.135 014023.
18. Landen O. L., Perry M. D., Campbell E. M. 1987 Phys.Rev.Lett. 59 2558
19. Ivanov L. N., Letokhov V. S. 1975 JETP 68 1748; 1985 Com. Mod. Phys. D4 169
20. Ivanov L. N., Ivanova E. P., Aglitsky E. V. 1988 Phys. Rep. 166 315
21. Glushkov A. V., Ivanov L. N., 1985 Preprint of ISAN, USSR Academy of Sci., Troitsk, N3.
22. Glushkov A. V., Ivanov L. N., Ivanova E. P., 1986 Autoionization Phenomena in Atoms, Moscow Univ. Press, Moscow, p 58
23. Glushkov A. V., Ivanov L. N. 1992 Phys. Lett. A 170 33.
24. Glushkov A. V., Ivanov L. N. 1992 Proc. of 3rd Seminar on Atomic Spectroscopy (Chernogolovka, Moscow reg.) p 113
25. Glushkov A, Ivanov L N 1993 J.Phys. B: At. Mol. Opt. Phys. 26 L179.
26. Glushkov A. V., Loboda A., Gurnitskaya E., Svinarenko A., 2009 Phys. Scripta T135 014022
27. Glushkov A. V., Khetselius O. Yu., Loboda A. V., Svinarenko A. A., 2008 Frontiers in Quantum Systems in Chem. and Phys., Ser. Progress in Theoretical Chemistry and Physics, vol. 18. ed. S Wilson, P. J., Grout, J., Maruani, G.; Delgado-Barrio, P Piecuch (Berlin: Springer) p 543
28. Ivanov L. N., Ivanova E. P., 1974 Theor. Math.Phys. 20 282
29. Ivanova E P, Ivanov L N, Glushkov A V, Kramida A E 1985 Phys. Scripta 32 512

30. Glushkov A V 2012 Advances in the Theory of Quantum Systems in Chemistry and Physics. Ser. Progress in Theoretical Chemistry and Physics, vol. 28, ed. by K Nishikawa, J Maruani, E Brandas, G Delgado-Barrio, P Piecuch (Berlin: Springer) p 131
31. Glushkov A V, Khetselius O Yu, Malinovskaya S V 2008 Europ. Phys. Journ ST 160 195.
32. Khetselius O Yu, 2009 Int. Journ. Quant. Chem. 109 3330 ;
33. Okutsu, H.; Sako, T.; Yamanouchi, K.; Diercksen, G.H.F. J. Phys. B: At. Mol. Opt. Phys. 2005, 38, 917-928; Badnell, N.R. Journ. Phys. CS. 2007, 88, 012070 (8p.).
34. Paul S., Ho Y.K., J. Phys. B: At. Mol. Opt. Phys. 2010, 43, 065701
35. Glushkov, A.V.; Malinovskaya, S.V.; Prepelitsa, G.P.; Ignatenko, A.V. et al Journ. Phys. CS. 2004, 11, 199–208; Int.J. Quant. Chem. 2011, 111,288-298.
36. Nakamura, N. ; Kavanagh, A.P. ; Watanabe, H. ; Sakaue, H.A. ; Li, Y.; Kato, D. ; Curell, F.J. ; Ohtani S. Journ. Phys. CS. 2007, 88, 012066 (6p.); Li, Y.; Wu, J. ; Hou, Y.; Yuan, J. J. Phys. B: At. Mol. Opt. Phys. 2008, 41, 145002 (8p.).
37. Buyadzhi V.V., Glushkov A.V., Lovett L., Photoelectronics. 2014, 23, 38-43.

This article has been received within 2015

UDC 539.182

V. V. Buyadzhi

LASER MULTIPHOTON SPECTROSCOPY OF ATOM EMBEDDED IN DEBYE PLASMAS: MULTIPHOTON RESONANCES AND TRANSITIONS

Abstract.

The consistent relativistic energy approach to atom in a realistic laser field, based on the Gell-Mann and Low S-matrix formalism, is applied to studying the resonant multiphoton transitions in atoms embedded in the Debye plasmas. There is considered a new scheme to calculating the multiphoton transitions characteristics, shifts and widths of multiphoton resonances. An approach is used for treating the three-photon transitions in krypton embedded in the Debye plasmas.

Key words: electromagnetic interactions, laser field, multiphoton resonances, plasmas

УДК 539.182

В. В. Буяджи

ЛАЗЕРНАЯ МУЛЬФОТОННАЯ СПЕКТРОСКОПИЯ АТОМОВ В ДЕБАЕВСКОЙ ПЛАЗМЕ : МНОГОФОТОННЫЕ ПЕРЕХОДЫ И РЕЗОНАНСЫ

Резюме.

Релятивистский энергетический подход к описанию спектроскопии атома в лазерном поле, основывающийся на S-матричном формализме Гелл-Манна и Лоу, применяется для изучения

резонансных многофотонных переходов атомов в дебаевской плазме. Предложена новая схема вычисления характеристик многофотонных переходов, энергий и ширин многофотонных переходов. Подход использован для описания трехфотонных переходов в криптоне в плазме Дебая.
Ключевые слова: электромагнитное, лазерное поле, многофотонные резонансы, плазма

УДК 539.182

В. В. Буяджи

ЛАЗЕРНА МУЛЬФОТОНА СПЕКТРОСКОПІЯ АТОМІВ У ДЕБАЄВСЬКІЙ ПЛАЗМІ: БАГАТОФОТОННІ ПЕРЕХОДИ І РЕЗОНАНСИ

Резюме.

Релятивістський енергетичний підхід до опису спектроскопії атома в лазерному полі, що грунтується на S-матричному формалізмі Гелл-Манна і Лоу, застосовується для вивчення резонансних багато фотонних переходів атомів в дебаєвській плазмі. Запропоновано нову схему обчислення характеристик багатофотонніих переходів, енергій і ширин багато фотонних переходів. Підхід використаний для опису трьох фотонних переходів у криптоні в плазмі Дебая.

Ключові слова: електромагнітна взаємодія, лазерне поле, багатофотонні резонанси, плазма

UDC 539.182

A. A. Kuznetsova

Odessa National Maritime Academy, Odessa, 4, Didrikhsona str., Odessa, Ukraine
e-mail: quantign@mail.ru

PENNING AND STOCHASTIC COLLISIONAL IONIZATION OF ATOMS IN AN EXTERNAL MAGNETIC FIELD: MODEL POTENTIAL SCHEME

The key physical aspects of the Penning and stochastic collisional ionization of atoms in an external magnetic field are considered and new model potential approach has been implemented in order to take into account an effect of magnetic field on multi-electron atom energy parameters and to compute the wave functions basis for next using in the collisional block. The corresponding Schrödinger equation for atom in a magnetic field and the Focker-Plank stochastic equation are solved within the standard differences-grid method.

1. Above a great number of different elementary atomic and molecular processes to be studied in collisions physics, physics and chemistry of plasma, gases and other mediums one should note such complicated phenomena as an ionization of excited atoms by means of the photon and electron impact, atom-atom or ion-atom collisions, inclufing these processes at presence of the external field. As a rule in any case an adequate treating these processes requires an accurate account of different exchange-correlation and even relativistic corrections [1-25]. Indeed to fulfill an accurate account of the inter electron correlation effects in the atomic collisions is very difficult as these effects and other ones are not adequately described within many simplified models. Situation changes dramatically under consideration of the different atomic collisional processes under availability of the external electromagnetic fields. Even more simple case of the external static electric or magnetic field is remained hitherto quantitatively undeceived. Several theoretical attempts were taken to make formulation of the consistent quantum theory for the atomic collisional processes in presence of the external magnetic field. [11-20].

Usually there are considered the key interatomic collisional processes, which are of a great interest for many applications, namely [1-4]:

$$A^*(nl)+B\rightarrow(A+B^+)+e \text{ or} \qquad (1)$$

$$A^*(nl)+B\rightarrow(A^+ +B)+e \text{ or} \qquad (2)$$

$$A^*(nl)+B\rightarrow AB^+ +e. \qquad (3)$$

As usually, in these formula A^* denotes the atom in an excited state, B^+ is the ionized atom. The first process (1) occurs and runs very effectively in a case when the excitation energy of the A atom is more than the ionization potential of the atom B. Here one can introduce the Penning process, which is corresponding to the situation when the atom A is in the metastable state. The process (3) is corresponding to the associative ionization. It takes a place when the dissociation energy of molecular ion AB^+ is more than the ionization potential of the excited atom [1,2].

The most widespread theoretical schemes for description of the cited processes (look, for example, [1-5,17-22]) are based on the computing the capture cross-section of collisional particles

by field of the wan der Waals interaction potential. Above other consistent methods one should mention a few versions of the rectilinear classical trajectories model too [1-3,20]. Besides, standard problems of adequate treating complex inter electron correlations, there are other difficulties in a correct description of collisional processes studied.

Remember that the above cited models do not account for any difference between the Penning process and resonant collisional processes. Though the Penning and stochastic collisional ionization of atomic systems remains a subject of intensive theoretical and experimental interest, however, at present time an available level of modelling these processes is still not satisfactory. The most important tasks include more accurate modelling of an external electromagnetic field on the corresponding Penning and stochastic collisional ionization processes. As for the last years a great interest has been renewed after discovery of the quantum chaos phenomenon in atomic systems in the static magnetic field [1-13,22], it is of a importance studying stochastic collisional ionization processes.

In series of papers [17, 22-24] the different aspects of new theoretical methods to the treating elementary atomic processes (1)-(3) in a presence of external electric and magnetic field were considered . In this paper we formulate a consistent, computationally effective model potential approach of accounting the external magnetic field effect in many-electron atomic system and further using in collisional problem.

2. Further we formulate the simple physical model of elementary collisional process with additional stochastic block. Let us remind the main moments of the elementary model for collisional process, in particular (1). A definition of complete cross section for the collisional process can be written as [24]:

$$\sigma = \int_0^{\infty} 2\pi\rho d\rho\{1-\exp[-\int_{-\infty}^{+\infty} G(R)dt]\} \qquad (4)$$

where $G(R)$ is a probability of the Auger effect $G(R)= 2p|V_{12}|^2 g_2$ (indexes 1and 2 are relating to states: A^*+B and $A+B^+ +e$; g is a density of the final states; V is operator of interaction between atoms).

In a case when ionization process is realized in the repulsive potential of interaction between atoms in the initial channel, the cross-section is :

$$\sigma = (4\pi f_W / v) \int_{R_{tm}}^{\infty} R^2 G(R)\sqrt{1-U(R)/E}\,dR \qquad (5)$$

Here v is the relative velocity of collision, R_{tm} is the minimally possible distance of rapprochement (the turning point); f_w is the probability that the process is permitted on full electron spin of system of the collisional atoms.

The important step is to account for a possibility of decay in the second and higher orders of perturbation theory on $V(R)$. Such approach may be used as for the Penning ionization description as for ionization through the wan-der-Waalse capture [3,5, 17,24].

Let us remind that in the perturbation theory second and higher orders it is introduced the matrix element: $\left\langle 1\left|V(R)G_{E_\infty}V(R)...V(R)\right|2\right\rangle$ insist of the simple matrix element $\left\langle 1\left|V(R)\right|2\right\rangle$ in expression for probability of collisional decay. Here [1> $\equiv$[A*+B> is the initial state, [2>$\equiv$[A+B$^+$+e> is the final state; G_E is the Green function (see below); $E\infty$ is an energy of quasi-molecule A*B under $R \to \infty$.

Further one can use for operator V(R) the standard expansion on non-reducible tensor operators:

$$V(R)= \sum_{l_1,l_2=1}^{\infty} V_{l_1 l_2}(n)/R^{l_1+l_2+1} \qquad (6)$$

$$V_{l_1 l_2}(n) = (-1)^{l_2}\sqrt{\frac{(2l_1+2l_2)!}{(2l_1)!(2l_2)!}}(C_{l_1+l_2}(n)\{Q_{l_1}^A \otimes Q_{l_2}^B\})$$

$$\mathrm{n}=\frac{R}{R} \qquad (7)$$

where $\hat{Q}_{lm}$ is an operator of the 2^l-pole moment of atom and C_{lm} (n) is the modified spherical function. If we suppose that atom A* is in the state with the whole moment J_i and projection on the quantization axe M_i; in the final state the corresponding quantum numbers are $J_f M_f$; The final expression for the full probability of the electron ejection is similar to expressions in different approximation is, for example, presented in ref. [17-24].

Above the theoretical consideration concerns the standard collisional process without accounting any stochastical (or chaotic) elements. In ref. [22,23] it has been considered the perspective for realization the stochastic collisional process for a case when the atom A in process (1) is highly excited (Rydberg state). This physical situation can be adequately treated within generalized theory of chaotic drift for the Coulomb electron in the external microwave field (see refs. [4-6,19-23]).

The function of distribution $f(n,t)$ of the Rydberg electron on space of effective quantum numbers n should be introduced. The equation of motion of the Rydberg electron has the well known form:

$$\partial f(n,t)/\partial t\, t = \partial/\partial n\, [\Theta(n-N_{min})D(R)n^3 \partial f(n,t)/\partial n] - \Theta(n-N_{max})G(n,R)f(n,t) \quad (8)$$

Here $Q(n-N_{min})$ is the Heviside function. It served here as additive multiplier in the coefficient of diffusion: Dn^3 and provides freeezing of the stochastic processes in region of the low lying states in accordance with the known Cirikov criterion: $N_{min}<n<N_{max}$. For the Rydberg states ($n>N_{max}$) a direct channel of ionization is opened and the electron ejection takes a place. It is important to note that process will be realized with more probability under availability of the external magnetic field. So the task is further resulted in implementation of an adequate theoretical model of an external magnetic field accounting or in more details the model for computing the corresponding electron wave functions of the Zeemane problem.

3. The next step is implementation of the model potential approach to multi-electron atom in a magnetic field into collisional problem. Let us remind that despite a long history since the discovery of the Zeemane effect and sufficiently great number papers on atomic systems in an external magnetic field, hitherto a majority of results are as a little acceptable for many applications as related only the hydrogen atom (look, for instance, [4-6,11-13]). The problem of the treating many-electron atom in a magnetic field remains very complicated especially in a case of the strong field. Below we implement a simple scheme to treating multi-electron atom in a static magnetic field. The purpose is to present the basis scheme for definition of the electron wave functions for further using in the collisional task.

The Hamiltonian of the many-electron atom in magnetic field is different from the operator of the hydrogen atom by the presence of the operator of electron-electron Coulomb interaction, which, of course, exacerbates the problem of separation of variables in the Schrödinger equation.

Because of the invariance of $\hat{H}$ in relation to rotations around the axe Oz (it is parallel to field B and crossing a nucleus of an atom), naturally z-component of the orbital moment $L_z=hM$ is the conserving variable. In the cylindrical coordinates with axe Oz||B with account of the trivial dependence of the wave function upon the rotation angle φ around the axe z ($\Psi \sim e^{M\varphi}$), one could write the corresponding equation in the form (in atomic units: $e=h=m=1$):

$$\{\frac{\partial^2}{\partial\rho^2}+\frac{1}{\rho}\frac{\partial}{\partial\rho}+\frac{\partial^2}{\partial z^2}-\frac{M^2}{\rho^2}-4\gamma^2\rho^2+ +\frac{4}{r}+V_c(r)+(\frac{E}{R_y}-\gamma M]\Psi(\rho,z)=0 \quad (9)$$

where $V_c(r)$ is the self-consistent model potential (analog of the Hartree-Fock potential). It can be, for example, chosen in the Green et al like form (look details in Ref. [5,16], which indeed well approximates the Hartree potential:

$$V=-\frac{(N_c-1)\Omega(r)}{r} \quad (10)$$

where the screening function is

$$\Omega(r)=1/[\exp(r/d_1-1)+d_2]$$

and $d_{1,2}$ are the known parameters of the model potential.

Naturally the equation (9) has not an analytical solution as the Coulomb interaction term with $r=(\rho^2+z^2)^{1/2}$, prevents to the variables separation. As usually the equation (9) can be in some approximation rewritten as follows:

$$Hy(r,z)=Ey(r,z) \quad (11)$$

$$H = -1/2(\partial^2/\partial\rho^2 + 1/\rho\partial/\partial\rho + \\ + \partial^2/\partial z^2 - m^2/\rho^2)$$
$$V(\rho,z) = -(\rho^2+z^2)^{-1/2} + (N_c - 1)\times \\ \Omega(\rho^2+z^2)^{-1/2} + 1/8\gamma^2\rho^2 + \gamma m/2, \quad (12)$$

Where, as usually, $g=B/B_o$ (B_o=2,3505×10^9). The potential $1/8\gamma^2\rho^2$ limits a motion in the direction, which is perpendicular to the *B* direction. In the region γ>>1 the electron motion along (or perpendicular) magnetic field is defined by the Coulomb interaction (by a size of the cyclotronic orbit $\lambda = (\hbar c/eM)^{1/2}$). The simplified circumstance is that the potential of the longitudinal Coulomb interaction can be received by way of the averaging the total Coulomb potential $e^2(\rho^2+z^2)^{-1/2}$ on the little radius of the transverse motion.

The one-particle energy for given values of magnetic field *B* is defined as:

$$\varepsilon_{B\mu} = (m_\mu + |m_\mu| + 2s_{z\mu} + 1)\gamma/2 - \varepsilon_\mu \quad (13)$$

where e*m* - one-particle energy (the field is absent), $S_z m$ is the spin projection on the axe z.

After the analytical integration on the angles, two-dimensional *(r,z)* Schrodinger equation (12) is solved by the finite difference method. One-electron function is represented in the form:

$$\Psi_\mu(\rho,\phi,z) = (2\pi)^{-1/2} e^{-im_\mu\phi}\psi_\mu(z,\rho) \quad (14)$$

where *m* is the number of electrons numbers, each of which is described by a certain value of the magnetic quantum number m_m. Note that unlike the hydrogen-like system for a multi-electron atom is an essential consideration of the effects of electron correlations and exchange. The numerical solution of the written equations can be performed on the basis of the differences-grid standard method. Really, according, for example, to [5],under the differences solving, an infinite region was replaced by rectangular area: 0<*r*< L_ρ, 0<z< L_Z by sufficienlt large size , in which there is constructed ь uniform grid with steps h_ρ, h_Z. On the outer boundary there are set conditions: $(\partial\Psi\partial n)_r = 0$. In the absence of a field, the wave function decreases at infinity like exp[-$(-2E)^{1/2}$ r]. In the presence of E must be replaced with the ionization energy of the stationary state in the lowest Landau level: (-E). A rough estimate for L:

L=15$(-2E)^{-1/2}$. Derivatives of *r are* approximated (2m + 1) -point symmetric difference schemes obtained by differentiating the interpolation formula of Lagrange. For the second derivative z used symmetric three-point difference scheme. The eigenvalues of the Hamiltonian are calculated based on the method of inverse iterations. The corresponding system of inhomogeneous equations solved by Thomas (look details, for example, in Ref. [5]). Naturally, the concrete realization of such a algorithms and its further implementation into collisional problem block requires significant computational work and will be considered in the next paper. Here let underline that using the simple model potential model simplifies all theory. Though, it is obvious that in a case of the stochastic collisional process, in particular, with Rydberg collided atoms, the model became more complicated to take into account the possible essential changing stochastic mechanism due to an effect of the external filed.

References

1. Chemistry of plasma, Eds. Smirnov B. M., Devdariani A.L. – Moscow, 1989. – Vol.15.
2. Kaplan I.G., Intermolecular interactions. – Moscow: Nauka, 1987. – 380P.
3. Nikitin E.E., Umansky S.Ya., Semiempiril methods of calculating the atomic interaction potentials. . Achievements of science and technique. Serie: Structure of molecules and chemical bond. – Moscow: VINITI, 1980. – Vol.4.-220P.
4. Letokhov V.S. Nonlinear selective photo processes in atoms and molecules. – M.: Nauka, 1983. – 408P.

5. Ruder H., Wunner G., Herold H., Geyer F. Atoms in Strong Magnetic Fields. – Berlin: Springer-Verlag, 1994. – 384p.
6. Glushkov A.V., Atom in electromagnetic field.-Kiev: TNT.-2005, 405P.
7. Lisitsa V.S., New in Stark and Zeemane effects for atom of hydrogen//UFN. – 1987. – Vol.153. – P.379-422.
8. Bodo E., Zhang P., Dalgarno A., Ultra-cold ion–atom collisions: near resonant charge exchange// New Journal of Physics. – 2008. – Vol. 10. – P.033024.
9. Jamieson M.J., Dalgarno A., Aymar M., Tharamel J., A study of exchange interactions in alkali molecular ion dimers with application to charge transfer in cold Cs.// J. Phys. B: At. Mol. Opt. Phys. – 2009. – Vol.42. – P.095203
10. Ivanov L.N., Letokhov V.S. Spectroscopy of autoionization resonances in heavy elements atoms// Com.Mod.Phys.D.:At.Mol.Phys. – 1985. – Vol.4. – P.169-184.
11. Dando P.A., Monteiro T.S. Atoms in Static Fields: Chaos or Difraction?// Photonic, Electronic, Atomic Collisions.-Singapore: World Sci.Pub. – 1997. – P.621-630.
12. Atoms and Molecules in Strong External Fields.Eds. Schmelher P., Schweizer W.-N.-Y.: Plenum Press, 1998. – 410p.
13. Glushkov A.V., Atom in electromagnetic field.-Kiev: KNT, 2005. – 400P.
14. Glushkov A.V., Ivanov L.N., DC Strong-field Stark-effect: New consistent quantum-mechanical approach // J.Phys. B: At. Mol. Opt. Phys. – 1993. – Vol.26. – P.L379-L386.
15. Glushkov A.V., Lepikh Ya.I., Fedchuk A.P., Ignatenko A.V., Khetselius O.Yu., Ambrosov S.V , Wannier-Mott excitons and atoms in a DC electric field: photoionization, Stark effect, resonances in the ionization continuum// Sensor Electr. and Microsyst. Techn.-2008. – N4. – P.5-11.
16. Masnow-Seeuws F., Henriet A., Two-electron calculations for intermediate Rydberg states Na_2: quantum defects/ //J.Phys.B.At.Mol.Phys. – 1988 –Vol.21 – P.L338-346.
17. Ambrosov S.V. New optimal scheme for gases and isotopes optically discharged separation with Penning and stochastic collisional ionization// Phys. Aerodisp. Syst. – 2003. – N40. – P.340-352.
18. Manakov N.L., Ovsyannikov V.D., Ostrovsky V.N., Yastrebov V.N. Influence of long-acting forces on the Penning-ionization//Opt. Spectr. 1984.-Vol.56,-P.222-226.
19. Bezuglov N.N., Borodin B.M., Kazansky A.K. et al, Analysis of stochastic equations of the Focker-Plank with valuable boundary conditions in elementary process of collisional ionization//Opt. Spectr.– 2001.-Vol.89.-P.25-33.
20. Photonic, Electronic and Atomic Collisions. Eds. Aumar F., Winter H.-Singapore: World Scientific.-2007.-650P.
21. Ambrosov S.V., Ignatenko V.M., Korchevsky D.A., Kozlovskaya V.P., Sensing stochasticity of atomic systems in crossed electric and magnetic fields by analysis of level statistics for continuous energy spectra//Sensor Electronics and Microsyst.Techn. – 2005. – N2. – P.19-23.
22. Mikhailenko V.I., Kuznetsova A.A., Penning and stochastic collisional ionization of atoms in an external electric field // Sensor Electr. and Microsyst. Techn. – 2009. – N4. – P.12-17.
23. Mikhailenko V.I., Kuznetsova A.A., Prepelitsa G.P., Ignatenko A.V., The Penning and stochastic collisional ionization of atoms in an external magnetic field// Photoelectronics.-2010.-N19.-P.89-92.
24. Svinarenko A., Mikhailenko V.I., Kuznetsova A., Dynamics of radiative transitions between Stark sublevels for non-hydrogenic atoms in dc electric field //Sensor Electr. & Microsyst. Tech.-2010.-N1.-P.4-9.

This article has been received within 2015

UDC 539.182

A. A. Kuznetsova

PENNING AND STOCHASTIC COLLISIONAL IONIZATION OF ATOMS IN AN EXTERNAL MAGNETIC FIELD: MODEL POTENTIAL SCHEME

Abstract.

The key physical aspects of the Penning and stochastic collisional ionization of atoms in an external magnetic field are considered and new model potential approach has been implemented in order to take into account an effect of magnetic field on multi-electron atom energy parameters and to compute the wave functions basis for next using in the collisional block. The corresponding Schrödinger equation for atom in a magnetic field and the Focker-Plank stochastic equation are solved within the standard differences-grid method.

Key words: Penning and stochastic collisional ionization, magnetic field, model potential approach

УДК 539.182

А. А. Кузнецова

ПЕННИНГОВСКАЯ И СТОХАСТИЧЕСКАЯ СТОЛКНОВИТЕЛЬНАЯ ИОНИЗАЦИЯ АТОМОВ ВО ВНЕШНЕМ МАГНИТНОМ ПОЛЕ: СХЕМА НА ОСНОВЕ МОДЕЛЬНОГО ПОТЕНЦИАЛА

Резюме.

Рассмотрены ключевые физические аспекты пеннинговской и стохастической столкновительной ионизации атомов во внешнем магнитном поле и сформулирован новый подход к решению задачи учета влияния внешнего магнитного поля на энергетические параметры многоэлектронных атомов и вычисления базиса волновых функций для последующего использования в столкновительном блоке. Соответствующее уравнение Шредингера для атома в магнитном поле и стохастическое уравнение Фоккера-Планка решаются в рамках стандартном конечно-разностного метода сеток.

Ключевые слова: пеннинговская, стохастическая столкновительная ионизация, магнитное поле, подход на основе модельного потенциала

УДК 539.182

Г. О. Кузнецова

ПЕННІНГІВСЬКА ТА СТОХАСТИЧНА ЗА РАХУНОК ЗІТКНЕНЬ ІОНІЗАЦІЯ АТОМІВ У ЗОВНІШНЬОМУ МАГНІТНОМУ ПОЛІ: СХЕМА НА ОСНОВІ МОДЕЛЬНОГО ПОТЕНЦІАЛА

Резюме.

Розглянуті ключові фізичні аспекти пеннінговской і стохастичною зіткнень іонізації атомів у зовнішньому магнітному полі і сформульований новий підхід до вирішення завдання врахування впливу зовнішнього магнітного поля на енергетичні параметри багатоелектронних атомів і обчислення базису хвильових функцій для подальшого використання в блоці зіткнення. Відповідне рівняння Шредінгеру для атома в магнітному полі і стохастичне рівняння Фоккера-Планку вирішуються в рамках стандартного скінченно-різницевого методу сіток.

Ключові слова: пеннінгівська, стохастична за рахунок зіткнень іонізація,магнітне поле, підхід на основі модельного потенціалу

UDC 539.183

A. S. Kvasikova

[1]Odessa State Academy of Technical Regulation and Quality, 15, Kovalskaya str., Odessa, 65020, Ukraine
e-mail: quantkva@mail.ru

ON PROBABILITIES OF THE VIBRATION-NUCLEAR TRANSITIONS IN SPECTRUM OF THE RuO_4 MOLECULE

There are firstly presented theoretical data on the vibration-nuclear transition probabilities in a case of the emission and absorption spectrum of the nucleus of ruthenium 186Re ($E^{(0)}_{\gamma}$ = 186.7 keV) in the molecule of RuO_4, estimated on the basis of consistent quantum-mechanical approach to cooperative electron-γ-nuclear spectra (a set of the vibration-rotational satellites in a spectrum of molecule) of multiatomic molecules.

From physical viewpint it is obvious that any alteration of the molecular state must be manifested in the quantum transitions, for example, in a spectrum of the γ-radiation of a nucleus (see for example [1-22]). In result of the gamma nuclear transition in a nucleus of a molecule there is arised a set of the electron-vibration-rotation satellites, which are due to an alteration of the state of the molecular system interacting with photon. The known example is the Szilard-Chalmers effect which results to molecular dissociation because of the recoil during radiating gamma quantum with large energy (c.f. [1-5]).

In series of works [11-22] it has been carried out detailed studying the co-operative dynamical phenomena due the interaction between atoms, ions, molecule electron shells and nuclei nucleons. There have been developed a few advanced approaches to description of a new class of dynamical laser-electron-nuclear effects in molecular spectroscopy, in particular, a nuclear gamma-emission or absorption spectrum of a molecule.

A consistent quantum- mechanical approach to calculation of the electron-nuclear g transition spectra (set of vibration-rotational satellites in molecule) of a nucleus in the multiatomic molecules has been earlier proposed [13,14] and generalizes the well known approach by Letokhov-Minogin [8]. Earlier there were have been obtained estimates and calculations of the vibration-nuclear transition probabilities in a case of the emission and absorption spectrum of nucleus ^{191}Ir ($E^{(0)}_{g}$ = 82 keV) in the molecule of IrO_4 , ^{188}Os ($E^{(0)}_{g}$ = 155 keV in OsO_4 and other molecules were listed.

In this paper there are firstly presented theoretical data on the vibration-nuclear transition probabilities in a case of the emission and absorption spectrum of the nucleus of ruthenium ^{97}Ru in the molecule of RuO_4, estimated on the basis of the simplified version [18,19] of the consistent quantum-mechanical approach to cooperative electron-g-nuclear spectra (a set of the vibration-rotational satellites in a spectrum of molecule) of multiatomic molecules.

As the method of computing is earlier presented in details, here we consider only by the key topics following to Ref. [18] The aim is to compute parameters of the gamma transitions (a probability of transition) or spectrum of the gamma satellites because of changing the electron-vibration-rotational states of the multi-atomic molecules under gamma quantum radiation (absorption). Here it is considered a case of the five-atomic molecules (of XY_4 type; T_d).

Hamiltonian of interaction of the gamma radiation with a system of nucleons for the first nucleus can be expressed through the co-ordinates of nucleons r_n' in a system of the mass centre of the one nucleus [14,18]:

$$H(r_n) = H(r_n^{'}) \exp(-k_{\gamma} u) \qquad (1)$$

where k_g is a wave vector of the gamma quantum; u is the shift vector from equality state (coinciding with molecule mass centre) in system of co-ordinates in the space. The matrix element for transition from the initial state "a" to the final state "b" is presented as usually:

$$< \Psi_b^* \mid H \mid \Psi_a > \bullet < \Psi_b^* \mid \hat{a}^{-k_{\gamma} u} \mid \Psi_a > \qquad (2)$$

where a and b is a set of quantum numbers, which define the vibrational and rotational states before and after interaction (with gamma- quantum). The first multiplier in eq. (2) is defined by the gamma transition of nucleus and is not dependent upon the internal structure of molecule in a good approximation. The second multiplier is the matrix element of transition of the molecule from the initial state "a" to the final state "b":

$$M_{ba} \propto \Psi_b^*(r_e) \mid \Psi_a(r_e) > \bullet$$
$$\bullet < \Psi_b^*(R_1, R_2) \mid e^{-k_{\gamma} R_1} \mid \Psi_a(R_1, R_2) > \qquad (3)$$

The expression (3) gives a general formula for calculating the probability of changing the internal state of molecule during absorption or emitting g quantum by a nucleus. It determines an intensity of the corresponding g-satellites. Their positions are fully determined as follows:

$$E_{\gamma} = E_{\gamma}^0 \pm R + \hbar k_{\gamma} v \pm (E_b - E_a) \qquad (4a)$$

Here M is the molecule mass, v is a velocity of molecule before interaction of nucleus with g quantum; E_a and E_b are the energies of the molecule before and after interaction; E_g is an energy of nuclear transition; R_{om} is an energy of recoil:

$$R_{om} = [(E_g^{(o)}]^2 / 2Mc^2. \qquad (4b)$$

Obviously only single non-generated normal vibration (vibration quantum $\hbar\omega$) is excited and initially a molecule is on the vibrational level $v_a = 0$. If denote a probability of the excitation as $P(v_b, v_a)$ and use expression for shift u of the g-active nucleus through the normal co-ordinates, then an averaged energy for excitation of the single normal vibration is as follows [8,14,18]:

$$\overline{E}_{\text{vib}} = \sum_{v=0}^{\infty} \hbar\omega\left(v + \tfrac{1}{2}\right)\overline{P}(v,0) - \hbar\infty/2 =$$
$$= \sum_{v=0}^{\infty} \hbar\omega\left(v + \tfrac{1}{2}\right)P(v,0) - \hbar\omega/2 =$$
$$= \sum_{v=0} \hbar\omega\left(v + \tfrac{1}{2}\right)\frac{z^v}{v!}e^{-z} - \frac{\hbar\omega}{2} = \frac{1}{2}R\left(\frac{M-m}{m}\right), \qquad (5)$$

where

$$z = (R/\hbar\omega)[M - m/m]\cos^2\vartheta,$$

and m is the mass of g-active nucleus, ϑ is an angle between nucleus shift vector and wave vector of g-quantum and line in $\overline{E}_{\text{vib}}$ means averaging on orientations of molecule (or on angles ϑ). To estimate an averaged energy for excitation of the molecule rotation, one must not miss the molecule vibrations as they provide non-zeroth momentum $L = k_v u \sin\vartheta$, which is transferred to a molecule by g-quantum. In supposing that a nucleus is only in the single non-generated normal vibration and vibrational state of a molecule is not changed $v_a = v_b = 0$, one could evaluate an averaged energy for excitation of the molecule rotations as follows:

$$\overline{E}_{\text{rot}} = \left\langle \overline{B^2} \right\rangle = B^2 \left\langle u^2 \right\rangle \overline{\sin^2\vartheta} =$$
$$= \tfrac{1}{2} R(B/\hbar\omega)[(M-m)/m] \qquad (6)$$

As for multi-atomic molecules it is typical $B/\hbar\omega \sim 10^{-4}$-$10^{-2}$, so one could miss the molecule rotations and consider g-spectrum of a nucleus in the molecule mass centre as a spectrum of the vibration-nuclear transitions.

A shift u of the g-active nucleus can be expressed through the normal co-ordinates $Q_{s\sigma}$ of a molecule:

$$u = \frac{1}{\sqrt{m}} \sum_{s\sigma} b_{s\sigma} Q_{s\sigma} \qquad (7)$$

where m is a mass of the g- active nucleus; components of the vector b_{sF} of nucleus shift due to the F-component of "s" normal vibration of a

molecule are the elements of matrix b [2]; it realizes the orthogonal transformation of the normal co-ordinates matrix Q to matrix of masses of the weighted Cartesian components of the molecule nuclei shifts q.

According to eq.(1), the matrix element can be written as multiplying the matrix elements on molecule normal vibration, which takes contribution to a shift of the g- active nucleus:

$$M(b,a) =$$

$$= \prod_s \left\langle v_s^{\,b} \,|\, \prod_\sigma \exp(-ik_\gamma b_{s\sigma} Q_{s\sigma} / \sqrt{m}) v_s^{\,a} \right\rangle. \quad (8)$$

It is obvious that missing molecular rotations means missing the rotations which are connected with the degenerated vibrations. Usually wave functions of a molecule can be written for non-degenerated vibration as:

$$| v_s \rangle = \Phi_{v_s}(Q_s), \quad (9)$$

for double degenerated vibration in the form:

$$|v_s\rangle = (v_s+1)^{-1/2} \sum_{v_s \sigma_1, v_s \sigma_2, v_s \sigma_3} \Phi_{v_{s\sigma_1}}(Q_{s\sigma_1}) \Phi_{v_{s\sigma_2}}(Q_{s\sigma_2}) \quad (10)$$

(where $v_{s\sigma_1} + v_{s\sigma_2} = v_s$) and for triple degenerated vibration as follows:

$$|v_s\rangle = \left(\frac{2}{(v_s+1)(v_s+2)}\right)^{1/2} \times$$

$$\times \sum_{v_s \sigma_1, v_s \sigma_2, v_s \sigma_3} \Phi_{v_{s\sigma 1}}(Q_{s\sigma_1}) \Phi_{v_{s\sigma_2}}(Q_{s\sigma_2}) \Phi_{v_{s\sigma_3}}(Q_{s\sigma_3}) \quad (11)$$

where

$$v_{s\sigma_1} + v_{s\sigma_2} + v_{s\sigma_3} = v_s .$$

In the simple approximation function $\Phi_{v_{s\sigma}}(Q_{s\sigma})$ can be chosen in a form of the linear harmonic oscillator one. More exact calculating requires a numerical determination of these functions. Taking directly the wave functions $\left| v_s^a \right\rangle$ and $\left| v_s^b \right\rangle$, calculating the matrix element (8) is reduced to a definition of the matrix elements on each component F of the normal vibration.

Below we present the accurate data on the vibration-nuclear transition probabilities in a case of the emission and absorption spectrum of the nucleus of ruthenium ^{97}Ru ($E^{(0)}_g$ = 215 keV) in the molecule of RuO_4. As a molecule has the only normal vibration of the given symmetry type, then the corresponding values of b_{ss} can be found from the well known Eccart conditions, normalization one and data about the molecule symmetry.

For several normal vibrations of the one symmetry type, a definition of b_{ss} requires solving the secular equation for molecule $|GF\text{-}lE|=0$ [23-26]. There have been used the results of advanced theoretical calculating electron structure of the molecule within an advanced relativistic scheme of the X_α- scattered waves method (see description in Refs.[23,26]).

In table 1 we present the results of calculating probabilities of the first several the vibration-nuclear transition probabilities in a case of the emission and absorption spectrum of the nucleus of ruthenium ^{97}Ru ($E^{(0)}_g$ = 215 keV) in the molecule of RuO_4.

Table 1

The vibration-nuclear transition probabilities in a case of the emission and absorption spectrum of the nucleus of ruthenium ^{97}Ru in the molecule of RuO_4,

Vibration transition $v_3^{\,a}, v_4^{\,a} - v_3^{\,b}, v_4^{\,b}$	$\overline{P}(v_3^{\,a}, v_4^{\,a} - v_3^{\,b}, v_4^{\,b})$ This work
0,0 – 0,0	0.74
1,0 – 0,0	0.014
0,1 – 0,0	0.067
1,0 – 1,0	0.68
0,1 – 0,1	0.61

References

1. Letokhov V S, 1977 Laser Spectroscopy, Academic Press, N.-Y.
2. Law J and Campbell J L,1982 *Phys. Rev.C* 25 514.

3. Amudsen P. A. and Barker P. H., 1994 *Phys.Rev.C* 50 2466
4. L. Wauters, N. Vaeck, M. Godefroid, H var der Hart and M Demeur, 1997 *J.Phys.B*. 30 4569.
5. Shahbaz A., Müller C., Staudt A, Bürvenich T J, Keitel C H 2007 *Phys.Rev. Lett.* 98 263901
6. Fedorov M. V. 1999 *Phys.-Uspekhi* 169 66
7. Letokhov V. S., 1974 *Phys. Lett.A* 46 257.
8. Letokhov V. S. and Minogin V. G., 1985 *JETP.* 69(5) 1568.
9. Ivanov L. N., Letokhov V. S. 1975 *JETP* 68 1748;
10. Ivanov L. N. and Letokhov V. S. 1988 *Com. Mod. Phys.* D 4 169
11. Glushkov A V and Ivanov L N 1992 *Phys. Lett.* A 170 33
12. A. V. Glushkov, O. Yu. Khetselius, Malinovskaya S V, 2008 *Europ. Phys. Journ ST* 160 195.
13. A. V. Glushkov, O. Yu. Khetselius, Malinovskaya S. V., 2008 *Molec.Phys.* 106 1257.
14. Glushkov A. V., Khetselius O. Yu., Malinovskaya S. V., 2008 *Frontiers in Quantum Systems in Chem. and Phys., Ser. Progr. in Theor. Chem. and Phys.*, vol. 18. ed. S Wilson, P J Grout, J Maruani, G; Delgado-Barrio, P Piecuch (Berlin: Springer) p 523
15. Glushkov A. V., 2012 *J. of Phys.: Conf. Ser.*. 397 012011
16. Glushkov A. V., Malinovskaya S. V., Svinarenko A. A. and Chernyakova Yu. G., 2004 *Int. J. Quant. Chem.* 99 889.
17. Glushkov A. V., Loboda A., Gurnitskaya E., Svinarenko A. 2009 *Phys. Scripta* T135 014022
18. Glushkov A.V., Kondratenko P.A., Lopatkin Yu.M., Buyadzhi V.V., Kvasikova A.S., 2014 *Photoelectronics.* 23 142-146
19. Glushkov A.V., Kondratenko P.A., Buyadzhi V.V., Kvasikova A.S., Shakhman A., Sakun T.N., 2014 Journal of Physics: C Series (IOP, London,UK). 548 012025.
20. Glushkov A., Ivanov L., Ivanova E., 1986 *Autoionization Phenomena in Atoms*, Moscow Univ. Press, Moscow, p 58
21. Khetselius O.Yu., 2012 *J. of Phys.: Conf. Ser.* 397 012012;
22. Khetselius O.Yu., 2009 *Phys.Scr.* T.135 014023.
23. Glushkov A, 1993 Journ.Struct. Chem. 34(1) 3.
24. Glushkov A.V. and Malinovskaya S.V., 1988 *Russian J.Phys.Chem.* 62(1) 100.
25. G Simons and R G Parr, 2002 Quantum Chemistry, Academic Press, N-Y.
26. V. N. Gedasimov, A. G. Zelenkov, V. M. Kulakov, V. A., Pchelin, M. V. Sokolovskaya, A. A. Soldatov, L. V. Chistyakov, 1984 *JETP.* 86 1169; A. A. Soldatov, 1983 Preprint of I.V.Kurchatov Institute for Atomic Energy IAE-3916, Moscow

This article has been received within 2015

UDC 539.183

A. S. Kvasikova

ON PROBABILITIES OF THE VIBRATION-NUCLEAR TRANSITIONS IN SPECTRUM OF THE RuO_4 MOLECULE

Abstract.

There are firstly presented theoretical data on the vibration-nuclear transition probabilities in a case of the emission and absorption spectrum of the nucleus of ruthenium ^{97}Ru in the molecule of RuO_4, estimated on the basis of consistent quantum-mechanical approach to cooperative electron-γ-nuclear spectra (a set of the vibration-rotational satellites in a spectrum of molecule) of multiatomic molecules.

Key words: electron-γ-nuclear transition spectrum, multiatomic molecules

УДК 539.183

А. С. Квасикова

О ВЕРОЯТНОСТИ КОЛЕБАТЕЛЬНО-ЯДЕРНЫХ ПЕРЕХОДОВ В СПЕКТРЕ МОЛЕКУЛЫ RuO_4

Резюме.

Впервые представлены теоретические данные о вероятностях колебательно-ядерных переходов в случае испускания и поглощения гамма-кванта ядром рутения ^{97}Ru в молекуле RuO_4, полученные на основе последовательного квантово-механического подхода к расчету электронно-гамма-ядерного спектра (система колебательно-вращательных спутников в спектре молекуле) в многоатомных молекулах.

Ключевые слова: спектр электрон -γ- ядерных переходов, многоатомные молекулы

УДК 539.183

Г. С. Квасикова

ПРО ІМОВІРНОСТІ КОЛИВАЛЬНО-ЯДЕРНИХ ПЕРЕХОДІВ В СПЕКТРІ МОЛЕКУЛИ RuO_4

Резюме.

Вперше представлені теоретичні дані про ймовірності колебательно-ядерних переходів у разі випускання і поглинання гамма-кванта ядром рутенію ^{97}Ru в молекулі RuO_4, отримані на основі послідовного квантово-механічного підходу до розрахунку електронно гамма-ядерного спектру (система колебательно-обертальних супутників в спектрі молекулі) в багатоатомних молекулах.

Ключові слова: спектр електрон -γ- ядерних переходів, багатоатомні молекули

UDC 539.182

T. A. Florko, A. V. Glushkov, Yu. M. Lopatkin, S. V. Ambrosov, V. P. Kozlovskaya

1Odessa State Environmental University, L'vovskaya str.15, Odessa-16, 65016, Ukraine
2Sumy State University, 2, Rimsky-Korsakov Street, 40007, Sumy, Ukraine
e-mail: quantflo@mail.ru

ON INTENSITY OF EMISSION OF THE METALS ATOMS IN A HYDROGEN-OXYGEN FLAME IN A PRESENCE OF A MAGNETIC FIELD

An intensity of emission for the alkali atoms (potassium and rubidium) in the hydrogen-oxygen flame under action of a magnetic field is theoretically estimated with using quantum defect approximation in operator perturbation theory for atomic systems in external magnetic field. New estimates for the intensities of emission of the lines for K (D1: $4^2P_{1/2} - 4^2S_{1/2}$ and D2: $4^2P_{3/2} - 4^2S_{1/2}$) and Rb (1: $5^2P_{3/2} - 5^2S_{1/2}$ and 2: $6^2P_{3/2} - 5^2S_{1/2}$) are presented. The maximum value of the magnetic effect for D2 line of K atom for σ - polarization is equal 1.65, for π -polarization— 1,24. For Dl line the maximum value is equal 1,36 for both polarizations.

In this paper we present renewed theoretical estimates for intensity of emission of the alkali atoms (potassium and rubidium) in the hydrogen-oxygen flame under action of a magnetic field. To take into account the magnetic field effect we use simplified model based on the operator perturbation theory for atomic systems in external magnetic field. New estimates are listed for the intensities of emission of the lines for K (D1: $4^2P_{1/2} - 4^2S_{1/2}$ and D2: $4^2P_{3/2} - 4^2S_{1/2}$) and Rb (1: $5^2P_{3/2} - 5^2S_{1/2}$ and 2: $6^2P_{3/2} - 5^2S_{1/2}$). The maximum value of the magnetic effect for D2 line of K atom for σ - polarization is equal 1.65, for π -polarization— 1,24. For Dl line the maximum value is equal 1,36 for both polarizations. Let us remind that an effect of external field on the spectral parameters for atoms and ions in the flame is of a great interest as in the modern chemical physics and physics of combustion as atomic optics and spectroscopy [1-10].

Among the effects that require further theoretical and experimental research related phenomenon is increasing the intensity of the glow of atoms in a strong magnetic field in the complete absorption at the line center. *The known* example is the excess luminosity of sunspots in the rays λ, Ca^+, on the luminosity of the solar disk, which is apparently due to the effects of environmental enlightenment in a magnetic field of about 4.5 kE.

In series of papers by Hayashi et al (look for example, [1]) it has been investigated the fluorescence additives of inorganic salts in flames at atmospheric pressure and was found the effect of external magnetic field H on the intensity of the luminescence of the intermediate particles. For the OH radical in a magnetic field of 18 kE luminescence intensity increased by 14%, and for the sodium atom - by 2.5 times. Sodium salts were introduced into the dispersing aqueous solutions of flame under a stream of nitrogen. The experimentally measured magnetic effect, i.e. the ratio of I(H)/I(0) luminescence intensity in a magnetic field H to the intensity of the glow without a magnetic field. Hayashi et al have shown that such salts $NaCl$ magnetic effect increases with the concentration (s) of the salt in solution, and salts of the type $NaNO2$, on the contrary, the magnetic effect decreases. Sorokin and others [1] concerning the effect of the magnetic field on the intensity of the luminescence of alkali metals sodium and cesium in the flames. Appropriate aerosol stream is saturated nitrogen vapor salts $NaCl$, $CsCl$.

It was studied an influence of the magnetic field strength of 10 kE on the luminescence intensity of the resonance lines of sodium (D1: $3^2P_{1/2} - 3^2S_{1/2}$ and D2: $3^2P_{3/2} - 3^2S_{1/2}$). The range of variation of pressure sodium $10^{-5} - 5.10^{-4}$ Torr. For the line D2 in the case of σ - polarization maximum value of the magnetic effect is equal to 2, and in the case of π- polarization - 1.5. In the case of lines D1 maximum value is 1.6 and is the same for both polarizations. For cesium atom measurements were taken at two wavelengths of transitions (1: $6^2P_{3/2} - 6^2S_{1/2}$ and 2: $7^2P_{3/2} - 6^2S_{1/2}$). In refs. [2,3] there were presented first theoretical estimates for the effect of a magnetic field on the intensity of the luminescence of alkali metals: sodium and cesium (salts $NaCl$, $CsCl$) in a hydrogen - oxygen flame intensity magnetic field of 10 kE. There were listed preliminary data for the intensity of the luminescence lines of sodium (D1: $3^2P_{1/2} - 3^2S_{1/2}$ and D2: $3^2P_{3/2} - 3^2S_{1/2}$) and cesium lines (1: $6^2P_{3/2} - 6^2S_{1/2}$ and 2: $7^2P_{3/2} - 6^2S_{1/2}$). The maximum value of the magnetic effect of the D2 line of the sodium atom in the case of σ - polarization is equal to 1.9, and in the case of π - polarization - 1.45, and for the line D1 maximum value is 1.5.

In order to get more precise data it is necessary to use more consistent model for treating an effect of a magnetic field on the intensity of the luminescence of alkali metals. Here we use such a model and apply it to studying emission intensities for alkali atoms in the hydrogen - oxygen flame under availability of the magnetic field (strength 10 kE) for the lines D1: $4^2P_{1/2} - 4^2S_{1/2}$, D2: $4^2P_{3/2} - 4^2S_{1/2}$ in potassium and D1: $5^2P_{3/2} - 5^2S_{1/2}$ D2: $6^2P_{3/2} - 5^2S_{1/2}$)in the caesium.

Naturally, the intensity *I* of the *i-j* transition is connected with the concentration of atoms (standardly determined by the appropriate dissociation constant, see. [2.4]) and correspondingly the line strength S is defined as follows:

$$S = 3\hbar e^2 g_1 f_{i-j} / 2m\omega_0 \ . \qquad (1)$$

Here $\omega_0 = E_i - E_j$ - the frequency of the tran sition, and f_{i-j} -is the radiative transition *i-j* oscillator strength. In approximation of the "length" form *D* transition operator an oscillator strength is defined by the following expresssion:

$$f_{i-j} = 2m/\hbar^2 \left(E_i - E_j\right) \left| \left\langle \Psi_j \left| D \right| \Psi_i \right\rangle \right|^2 . \qquad (2)$$

Naturally the intensity σ - component is proportional to the square of the standard *3j*- symbols:

$$\begin{pmatrix} ...J...1.....J' \\ -M.\ 1....M-1 \end{pmatrix} \begin{pmatrix} ...J.....1.....J' \\ -M.\ -1.....M+1 \end{pmatrix}$$

and for the π – component it has:

$$\begin{pmatrix} ...J.....1.....J' \\ -M.\ 0.....M \end{pmatrix}.$$

The key moment of the model is determination of the wave functions. Here the wave functions of the states were found from the numerical solution of the Schrodinger equation for alkali atom in a magnetic field using the simplified quantum defect approximation version of the operator perturbation theory method [11]. Such a model is more correct with the usual H-like approximation, nevertheless it is more simplified in comparison with the model potential approach (look analysis regarding different models in Refs. [6-8,12-14]).

In Table 1 we present our data which illustrate an influence of the magnetic field H in the luminescence intensity of D2 line of the potassium atom in the σ - and π - polarizations depending on the partial pressure of potassium atoms. In the first case, the maximum value of the magnetic effect of I(H)/I(0) is equal to 1.65, and in the second - 1.24.

In the case of line D1 potassium atom calculated value of the maximum magnetic effect - 1,36. Let us not that the preliminary estimate of this value in [3] is 1.4.

For the rubidium atoms the magnetic field increases the intensity of emission line (1) in ~1.5 times. Analysis shows that the obtained renewed estimates are in physically reasonable (at least qualitative) agreement with experimental data.

Table 1

The influence of magnetic field on the intensity of the sodium atom D2 line in the s- and p-polarization as a function of the partial pressure of sodium atoms in flames: I(H)/I(0) - the ratio of the luminescence intensity in the magnetic field strength H of the luminescence intensity without magnetic field; p is the partial pressure (0 $^{-5}$ Torr).

$I(H)/I(O)\backslash p$	6	12	18	24	30
σ - polarization	1,04	1,27	1,65	1,59	1,28
π - polarization	0,98	1,10	1,24	1,22	0,68

References

1. Sorokin N.I., Dultsev E.N., Bazhin N.M. The influence of magnetic field on the intensity of luminescence of alkali metal atoms in a hydrogen-oxygen flame // Chemical Physics. – 1988. – T.7, № 1. – P. 100-103.
2. Kuklin I.V., Kozlovskaya V.P. The calculation of the intensity of luminescence of alkali metal atoms in a hydrogen-oxygen flame in the presence of a magnetic field// Physics aerodisperse systems. – 2001. – Vol38. - P.273-276.
3. Kozlovskaya V.P., The theoretical determination of the intensity of luminescence of alkali metal atoms in a hydrogen-oxygen flame in the presence of a magnetic field// Physics of Aerodisp. Systems. – 2003. – Vol.40 – P.322-326.
4. Kasabov G.A., Eliseev V.V. Spectroscopic tables low-temperature plasma. - M .: Atomizdat, 1973. - P.160.
5. Sobelman I.I. Introduction to the theory of atomic spectra. – M .: Nauka, 1977. – P.213.
6. Kleppner D., Chun-Ho I., Welch G. R. In: Irregular Atomic Systems and Quantum Chaos/ Ed. J.C.Gay (Kluwer,N-Y.,1990).
7. Benvenuto F., Casati G., Shepelyansky D.L. Rydberg Stabilization of atoms in strong fields: “magic” mountain in chaotic sea // Z. Phys. B. – 1994. – Vol.94. – P.481-486.
8. Dupret K., Zakrzewski J., Delande D. Resonances in the Diamagnetic Rydberg Spectrum: Order and Chaos // Europhys. Lett. – 1995. – Vol.31, №5-6. – P.251-256.
9. Glushkov A.V., Ivanov L.N. DC Strong-Field Stark-Effect: consistent quantum-mechanical approach // J.Phys. B: At. Mol. Opt. Phys. – 1993. – Vol. 26, №16. – P.L379-L386.
10. Glushkov A., Malinovskaya S., Ambrosov S., Shpinareva I., Troitskaya O., Resonances in quantum systems in strong external fields: Consistent quantum approach// J. of Techn. Phys.1997.-Vol. 38.-P.215-218.
11. Rusov V.D., Glushkov A.V., Vaschenko V.N., Korchevsky D.A., Ignatenko A.V. Stochastic dynamics of the atomic systems in the crossed electric and magnetic field: the rubidium atom recurrence spectra//Bulleten of Kiev National Univ.Ser. Phys. – Math. – 2004. – № 4. – P.433-438.
12. Fedchuk A.P., Glushkov A.V., Le-pikh Ya.I., Ignatenko A.V., Kvasikova A.S., Atom of hydrogen and wannier-mott exciton in crossed electric and magnetic fieldst// Photoelectronics. – 2014. – Vol.23. – P.176-181.
13. Kuklina I.V., Shevchuk V.G. H-like and He-like Systems in Superstrong magnetic field: Numeral Calculation // Uzhgorod Univ. Scientific Herald. Ser. Phys. – 2000. – Vol.8, №2. – P.361-364.
14. Ambrosov S.V., Ignatenko V.M., Korchevsky D.A., Kozlovskaya V.P., Sensing stochasticity of atomic systems in crossed electric and magnetic fields by analysis of level statistics for continuous energy spectra//Sensor Electronics and Microsyst.Techn. – 2005. – N2. – P.19-23.

15. Mikhailenko V.I., Kuznetsova A.A., Prepelitsa G.P., Ignatenko A.V., Penning and stochastic collisional ionization of atoms in an external magnetic field// Photoelectronics. – 2010. – N19. – P.89-92.

This article has been received within 2015

UDC 539.182

T. A. Florko, A. V. Glushkov, Yu. M. Lopatkin, S. V. Ambrosov, V. P. Kozlovskaya

ON INTENSITY OF EMISSION OF THE METALS ATOMS IN A HYDROGEN-OXYGEN FLAME IN A PRESENCE OF A MAGNETIC FIELD

Abstract.

An intensity of emission for the alkali atoms (potassium and rubidium) in the hydrogen-oxygen flame under action of a magnetic field is theoretically estimated with using quantum defect approximation in operator perturbation theory for atomic systems in external magnetic field 10 кЕ. New estimates for the intensities of emission of the lines for K (D1: $4^2P_{1/2} - 4^2S_{1/2}$ and D2: $4^2P_{3/2} - 4^2S_{1/2}$) and Rb (1: $5^2P_{3/2} - 5^2S_{1/2}$ and 2: $6^2P_{3/2} - 5^2S_{1/2}$) are presented. The maximum value of the magnetic effect for D2 line of K atom for σ - polarization is equal 1.65, for π -polarization— 1,24. For Dl line the maximum value is equal 1,36 for both polarizations

Key words: intensity of emission, alkali metals, hydrogen-oxygen flame, magnetic field

УДК 539.182

Т. А. Флорко, А. В. Глушков, Ю. М. Лопаткин, С. В. Амбросов, В. П. Козловская

О ИНТЕНСИВНОСТИ СВЕЧЕНИЯ АТОМОВ ЩЕЛОЧНЫХ МЕТАЛЛОВ В ВОДОРОДНО-КИСЛОРОДНОМ ПЛАМЕНИ В ПРИСУТСТВИИ МАГНИТНОГО ПОЛЯ

Резюме.

Дана теоретическая оценка эффекта влияния магнитного поля (10 кЭ) на интенсивности свечения атомов щелочных металлов: калия и рубидия в водородно- кислородном пламени с использованием приближения квантового дефекта в операторной теории возмущений для атомов во внешнем магнитном поле. Рассчитаны интенсивности свечения линий *K* (Dl: $4^2P_{1/2} - 4^2S_{1/2}$ и D2: $4^2P_{3/2} - 4^2S_{1/2}$) и линий *Rb* (1: $5^2P_{3/2} - 5^2S_{1/2}$ и 2: $6^2P_{3/2} - 5^2S_{1/2}$). Максимальная величина магнитного эффекта для линии D2 атома калия в случае σ- поляризации равна 1.65, в случае π- поляризации — 1.24, для линии D1 максимальное значение составляет 1.36 и одинаково для обеих поляризаций.

Ключевые слова: интенсивность излучения, щелочные металлы, водородно-кислородное пламя, магнитное поле

УДК 539.182

Т. О. Флорко, О. В. Глушков, Ю. М. Лопаткін, С. В. Амбросов, В. П. Козловська

ПРО ІНТЕНСИВНІСТЬ СВІЧЕННЯ АТОМІВ ЛУЖНИХ МЕТАЛІВ У ВОДНЄ-КИСЕНЕВОМУ ПЛАМЕНІ У ПРИСУТНОСТІ МАГНІТНОГО ПОЛЯ

Резюме.

Одержана теоретична оцінка ефекту впливу магнітного поля (10 кЕ) на інтенсивності світіння атомів лужних металів: калію і рубідію в воднево кисневому полум'ї з використанням наближення квантового дефекту в операторної теорії збурень для атомів у зовнішньому магнітному полі. Розраховані інтенсивності свічення ліній К (Dl: $4^2P_{1/2} - 4^2S_{1/2}$ та D2: $4^2P_{3/2} - 4^2S_{1/2}$) і *Rb* (1: $5^2P_{3/2} - 5^2S_{1/2}$ і 2: $6^2P_{3/2} - 5^2S_{1/2}$). Максимальна величина магнітного ефекту для лінії D2 атому *K* у випадку σ - поляризації складає 1.65, а у випадку π- поляризації – 1.24 , а для лінії D1 максимальне значення складає 1.36 і є однаковим для обох поляризацій.

Ключові слова: інтенсивність випромінювання, лужні метали, водне-кисневе полум'я, магнітне поле

Інформація для авторів наукового збірника «Photoelectronics»

В журналі «Фотоелектроніка» друкуються статті, які містять відомості про наукові дослідження та технічні розробки у напрямках

- фізика напівпровідників;
- гетеро- та низьковимірні структури;
- фізика мікроелектронних приладів;
- лінійна та нелінійна оптика твердого тіла;
- оптоелектроніка та оптоелектронні прилади;
- квантова електроніка;
- сенсорика

Журнал «Фотоелектроніка» видається англійською мовою. Рукопис подається автором у двох примірниках англійською мовою. До рукопису додається дискета з текстовим файлом і малюнками. Електронна копія матеріалу може бути надіслана до редакції електронною поштою.

Електронна копія статті повинна відповідати наступним вимогам:

1. Електронна копія (або дискета) матеріалу надсилається одночасно з твердою копією тексту та малюнків.
2. Для тексту припустимі наступні формати – MS Word (rtf, doc).
3. Малюнки приймаються у форматах – EPS, TIFF, BMP, PCX, JPG, GIF, CDR, WMF, MS Word I MS Giaf, Micro Calc Origin (opj). Малюнки, виконані пакетами математичної та статистичної обробки повинні бути конвертовані у вищевказані графічні формати.

Рукописи надсилаються на адресу:

Відп. секр. М. І. Куталовій,
вул. Пастера, 42, фіз. фак. ОНУ, м. Одеса,
e-mail: photoelectronics@onu.edu.ua.

До рукопису додається:

Експертний висновок – висновок експертної комісії про можливість відкритої публікації даної роботи (для авторів з України).

1. Коди PAC та УДК. Допускається використання декількох шифрів, що розділяються комою. У випадку, коли автором (авторами) не буде вказано жоден шифр, редакція журналу встановлює шифр статті за своїм вибором.
2. Прізвище (а) та ініціали автора (їв).
3. Установа, повна поштова адреса, номер телефону, номер факсу, адреса електронної пошти для кожного з авторів
4. Назва статті
5. Резюме об'ємом до 200 слів пишеться англійською.

Текст повинен друкуватися шрифтом 14 пунктів через два інтервали на білому папері формату А4. Назва статті, а також заголовки підрозділів друкуються прописними літерами і відзначаються напівжирним шрифтом.

Рівняння необхідно друкувати у редакторі формул MS Equation Editor. Статті з вписаними від руки рівняннями до друку не приймаються. Необхідно давати визначення величин, що з'являються в тексті вперше.

Таблиці повинні бути виконані у відповідних табличних редакторах або представлені у текстовому вигляді з використанням роздільників (крапка, кома, кома з крапкою, знак табуляції).

Посилання на літературу повинні друкуватися через два інтервали, нумеруватись в квадратних дужках (у нормальному положенні) послідовно у порядку їх появи в тексті статті. Необхідно на літературу, яка вийшла з друку не раньше 2000 року. Для посилань використовуються наступні формати:

Книги. Автор(и) (ініціали, потім прізвища), назва книги курсивом, видавництво, місто і рік видання. (При посиланні на главу книги, вказується назва глави, назва книги курсивом, номери сторінок). Приклад J A Hall, Imaging tubes, Chap 14 ш The Infrared Handbook, Eds W W Wolfe, O J' Zissis.pp 132-176, ERIM, Arm Arbor, MI (1978).

Журнали (Часописи). Автор(и) (ініціали, потім прізвища), назва статті, назва журналу курсивом (використовуються абревіатури тільки для відомих журналів), номер тому і випуску, номер сторінок і рік видання. Приклад N Blutzer and A S Jensen, Current readout of infrared detectors // Opt Eng 26(3), pp 241-248 (1987). Посилатись необхідно на літературу, яка вийшла з друку не раніше 2000 року.

Підписи до малюнків і таблиць друкуються у рукописі після літературних посилань через два інтервали.

Ілюстрації будуть скануватися цифровим сканером. Приймаються до друку тільки високоякісні ілюстрації. Підписи і символи повинні бути вдруковані. Не приймаються до друку негативи, слайди, транспаранти.

Рисунки повинні мати відповідний до формату журналу розмір не більше 160х200 мм. Текст на рисунках повинен виконуватись шрифтом 10 пунктів. На графіках одиниці виміру вказуються через кому (а не в дужках). Усі рисунки (ілюстрації) нумеруються в порядку їх розміщення в тексті. Частини рисунків нумеруються (а), (б) і т. ін. Не допускається вносити номер і підпис безпосередньо в рисунок. Верхні частини рисунків повинні бути позначені стрілкою.

Рецензія на статтю, підпис авторів рецензіїї повинен бути завізован .

Резюме об'ємом до 200 слів пишеться англійською, українською та російською мовами Перед текстом резюме відповідною мовою вказуються УДК, назва статті, прізвища та ініціали всіх авторів.

Информация для авторов
Научного сборника «Photoelectronics »

В сборнике «Фотоэлектроника» печатаются статьи , которые содержат сведения о научных исследованиях и технических разработках в направлениях

* физика полупроводников;
* гетеро- и низкоразмерные структуры;
* физика микроэлектронных приборов;
* линейная и нелинейная оптика твердого тела;
* оптоэлектроника и оптоелектронные приборы;
* квантовая электроника;
* сенсорика.

Сборник «Photoelectronics» издаётся на английском языке. Рукопись подается автором в двух экземплярах на английском и русском языках. К рукописи прилагаются дискета с текстовым файлом и рисунками Электронная копия материала может быть прислана в редакцию по электронной почте.

Электронная копия статьи должна отвечать следующим требованиям:

1. Электронная копия материала присылается одновременно с твердой копией текста и рисунков.

2. Для текста допустимые следующие форматы - MS Word (rtf, doc).

3. Рисунки принимаются в форматах - EPS, TIFF, BMP, PCX, JPG, GIF, CDR, WMF, MS Word И MS Giaf, Micro Calc Origin (opj). Рисунки, выполненные пакетами математической и статистической обработки должны быть конвертируемые в вышеуказанные графические форматы.

Рукописи присылаются в адрес:

Отв. секр. Куталовій М.И., ул. Пастера, 42, физ. фак. ОНУ, г.Одесса, 65026

E-mail: wadz@mail.ru, тел. 0482 – 726 6356 .

Аннотации статей сб.”Photoelectronics” находятся на сайте:http://photoelectronics.onu.edu.ua

К рукописи прилагается

1 Коды PAC и УДК. Допускается использование нескольких шифров, которые разделяются запятой. В случае, когда автором (авторами) не будет указан ни один шифр, редакция журнала устанавливает шифр статьи по своему выбору.

2. Фамилия (а) и инициалы автора (ел).

3 Учреждение, полный почтовый адрес, номер телефона, номер факса, адреса электронной почты для каждого из авторов

4.Название статьи

5.Резюме объемом до 200 слов пишется на английском, русском языках, и (для авторов из Украины) – на украинском.,после текста резюме печатаются Ключевые слова.

Текст должен печататься шрифтом 14 пунктов через два интервала на белой бумаге формата А4. Название статьи, а также заголовки подразделов печатаются прописными буквами и отмечаются полужирным шрифтом.

Уравнения необходимо печатать в редакторе формул MS Equation Editor. . Необходимо давать определение величин, которые появляются в тексте впервые.

Таблицы Должны быть выполнены в соответствующих табличных редакторах или представленные в текстовом виде с использованием разделителей (точка, запятая, запятая с точкой, знак табуляции).

Ссылки на литературу должны печататься через два интервала, нумероваться в квадратных

дужках (в нормальном положении) последовательно в порядке их появления в тексте статьи. Ссылаться необходимо на литературу, которая издана начиная с 2000 года. Для ссылок используются следующие форматы:

Книги. Автор(и) (инициалы, потом фамилии), название книги курсивом, издательство, город и год издания. (При ссылке на главу книги, указывается название главы, название книги курсивом, номера страниц). Пример J A Hall, Imaging tubes, Chap 14 ш The Infrared Handbook, Eds W W Wolfe, O J' Zissis. 2000,, ERIM, Arm Arbor, MI .pp 132-176,

Журналы (Журналы). Автор(и) (инициалы, потом фамилии), название статьи, название журнала курсивом (используются аббревиатуры только для известных журналов), номер поэтому и выпуска, номер страниц и год издания. Пример N Blutzer and A S Jensen, Current readout of infrared detectors // Opt Eng 2000,26(3), pp 241-248

Иллюстрации будут сканироваться цифровым сканером. Принимаются в печать только высококачественные иллюстрации. Подписи и символы должны быть впечатаны. Не принимаются в печать негативы, слайды, транспоранты. Графики и рисунки печатаются в тексте статьи.

Рисунки должны иметь соответствующий к формату журнала размер не больше 160х200 гг. Текст на рисунках должен выполняться шрифтом 12пунктов. На графиках единицы измерения указываются через запятую (а не в скобках). Все рисунки (иллюстрации) нумеруются в порядке их размещения в тексте. Не допускается вносить номер и подпись непосредственно на рисунках.

Резюме объемом до 200 слов пишется на английском, русском языках. и на украинском (для авторов из Украины). Перед текстом резюме соответствующим языком указываются УДК, фамилии и инициалы всех авторов, название статьи, ключевые слова..

Information for contributors of «Photoelectronics» articles

"Photoelectronics" Articles publishes the papers which contain information about scientific research and technical designs in the following areas:

- Physics of semiconductors;
- Physics of microelectronic devices;
- Linear and non-linear optics of solids;
- Optoelectronics and optoelectronic devices;
- Quantum electronics;
- Sensorics.

"Photoelectronics" Articles is defined by the decision of the Highest Certifying Commission as the specialized edition for physical-mathematical and technical sciences and published and printed at the expense of budget items of Odessa I.I. Mechnikov National University.

«Photoelectronics» Articles is published in English. Authors send two copies of papers in English. The texts are accompanied by 3.5» diskette with text file, tables and figures. Electronic copy of a material can be sent by e-mail to the Editorial Board and should meet the following requirements:

1.The following formats are applicable for texts – MS Word (rtf, doc).

2. Figures should be made in formats – EPS, TIFF, BMP, PCX, JPG, GIF, WMF, MS Word I MS Giaf, Micro Calc Origin (opj). Figures made by packets of mathematical and statistic processing should be converted into the foregoing graphic formats.

The papers should be sent to the address:

Kutalova M.I., Physical Faculty of Odessa I.I. Mechnikov National University, 42 Pastera str, 65026 Odessa, Ukraine, e-mail: wadz@mail.ru, tel. +38-0482-7266356. Information is on the site:

http://www.photoelectronics.onu.edu.ua

The title page should contain:

1. Codes of PACS
2. Surnames and initials of authors
3. TITLE OF PAPER
4. Name of institution, full postal address, number of telephone and fax, electronic address

An abstract of paper should be not more than 200 words. Before a text of summary a title of paper, surnames and initials of authors should be placed.

Equations are printed in MS Equation Editor.

References should be printed in double space and should be numbered in square brackets consecutively throughout the text. References for literature published in 2000-2009 years are preferential.

Illustrations will be scanned for digital reproduction. Only high-quality illustrations will be taken for publication. Legends and symbols should be printed inside. Neither negatives, nor slides will be taken for publication. All figures (illustrations) should be numbered in the sequence of their record in text.

For additional information please contact with the Editorial Board.

Верстка – О. І. Карличук

Підп.до друку .07.2015. Формат 60×84/8. Ум.-друк.арк. 18,14. Тираж 300 прим.
Замов. № ____

Видавець і виготовлювач
«Одеський національний университет імені І. І. Мечникова»
Свідоцтво ДК № 4215 від 22.11.2011 р.

65082, м. Одеса, вул. Єлісаветинська, 12, Україна
Тел.: (048) 723 28 39, e-mail: druk@onu.edu.ua